IAEA Nuclear Energy Series

No. NP-T-1.9

Design Features and Operating Experience of Experimental Fast Reactors

IAEA
International Atomic Energy Agency

IAEA NUCLEAR ENERGY SERIES PUBLICATIONS

STRUCTURE OF THE IAEA NUCLEAR ENERGY SERIES

Under the terms of Articles III.A and VIII.C of its Statute, the IAEA is authorized to foster the exchange of scientific and technical information on the peaceful uses of atomic energy. The publications in the **IAEA Nuclear Energy Series** provide information in the areas of nuclear power, nuclear fuel cycle, radioactive waste management and decommissioning, and on general issues that are relevant to all of the above mentioned areas. The structure of the IAEA Nuclear Energy Series comprises three levels: **1 — Basic Principles and Objectives; 2 — Guides; and 3 — Technical Reports.**

The **Nuclear Energy Basic Principles** publication describes the rationale and vision for the peaceful uses of nuclear energy.

Nuclear Energy Series Objectives publications explain the expectations to be met in various areas at different stages of implementation.

Nuclear Energy Series Guides provide high level guidance on how to achieve the objectives related to the various topics and areas involving the peaceful uses of nuclear energy.

Nuclear Energy Series Technical Reports provide additional, more detailed, information on activities related to the various areas dealt with in the IAEA Nuclear Energy Series.

The IAEA Nuclear Energy Series publications are coded as follows: **NG** — general; **NP** — nuclear power; **NF** — nuclear fuel; **NW** — radioactive waste management and decommissioning. In addition, the publications are available in English on the IAEA's Internet site:

http://www.iaea.org/Publications/index.html

For further information, please contact the IAEA at PO Box 100, Vienna International Centre, 1400 Vienna, Austria.

All users of the IAEA Nuclear Energy Series publications are invited to inform the IAEA of experience in their use for the purpose of ensuring that they continue to meet user needs. Information may be provided via the IAEA Internet site, by post, at the address given above, or by email to Official.Mail@iaea.org.

DESIGN FEATURES AND OPERATING EXPERIENCE OF EXPERIMENTAL FAST REACTORS

The following States are Members of the International Atomic Energy Agency:

AFGHANISTAN
ALBANIA
ALGERIA
ANGOLA
ARGENTINA
ARMENIA
AUSTRALIA
AUSTRIA
AZERBAIJAN
BAHRAIN
BANGLADESH
BELARUS
BELGIUM
BELIZE
BENIN
BOLIVIA
BOSNIA AND HERZEGOVINA
BOTSWANA
BRAZIL
BULGARIA
BURKINA FASO
BURUNDI
CAMBODIA
CAMEROON
CANADA
CENTRAL AFRICAN REPUBLIC
CHAD
CHILE
CHINA
COLOMBIA
CONGO
COSTA RICA
CÔTE D'IVOIRE
CROATIA
CUBA
CYPRUS
CZECH REPUBLIC
DEMOCRATIC REPUBLIC OF THE CONGO
DENMARK
DOMINICA
DOMINICAN REPUBLIC
ECUADOR
EGYPT
EL SALVADOR
ERITREA
ESTONIA
ETHIOPIA
FIJI
FINLAND
FRANCE
GABON
GEORGIA
GERMANY
GHANA
GREECE
GUATEMALA
HAITI
HOLY SEE
HONDURAS
HUNGARY
ICELAND
INDIA
INDONESIA
IRAN, ISLAMIC REPUBLIC OF
IRAQ
IRELAND
ISRAEL
ITALY
JAMAICA
JAPAN
JORDAN
KAZAKHSTAN
KENYA
KOREA, REPUBLIC OF
KUWAIT
KYRGYZSTAN
LAO PEOPLE'S DEMOCRATIC REPUBLIC
LATVIA
LEBANON
LESOTHO
LIBERIA
LIBYA
LIECHTENSTEIN
LITHUANIA
LUXEMBOURG
MADAGASCAR
MALAWI
MALAYSIA
MALI
MALTA
MARSHALL ISLANDS
MAURITANIA
MAURITIUS
MEXICO
MONACO
MONGOLIA
MONTENEGRO
MOROCCO
MOZAMBIQUE
MYANMAR
NAMIBIA
NEPAL
NETHERLANDS
NEW ZEALAND
NICARAGUA
NIGER
NIGERIA
NORWAY
OMAN
PAKISTAN
PALAU
PANAMA
PAPUA NEW GUINEA
PARAGUAY
PERU
PHILIPPINES
POLAND
PORTUGAL
QATAR
REPUBLIC OF MOLDOVA
ROMANIA
RUSSIAN FEDERATION
RWANDA
SAUDI ARABIA
SENEGAL
SERBIA
SEYCHELLES
SIERRA LEONE
SINGAPORE
SLOVAKIA
SLOVENIA
SOUTH AFRICA
SPAIN
SRI LANKA
SUDAN
SWAZILAND
SWEDEN
SWITZERLAND
SYRIAN ARAB REPUBLIC
TAJIKISTAN
THAILAND
THE FORMER YUGOSLAV REPUBLIC OF MACEDONIA
TOGO
TRINIDAD AND TOBAGO
TUNISIA
TURKEY
UGANDA
UKRAINE
UNITED ARAB EMIRATES
UNITED KINGDOM OF GREAT BRITAIN AND NORTHERN IRELAND
UNITED REPUBLIC OF TANZANIA
UNITED STATES OF AMERICA
URUGUAY
UZBEKISTAN
VENEZUELA
VIETNAM
YEMEN
ZAMBIA
ZIMBABWE

The Agency's Statute was approved on 23 October 1956 by the Conference on the Statute of the IAEA held at United Nations Headquarters, New York; it entered into force on 29 July 1957. The Headquarters of the Agency are situated in Vienna. Its principal objective is "to accelerate and enlarge the contribution of atomic energy to peace, health and prosperity throughout the world''.

IAEA NUCLEAR ENERGY SERIES NO. NP-T-1.9

DESIGN FEATURES AND OPERATING EXPERIENCE OF EXPERIMENTAL FAST REACTORS

INTERNATIONAL ATOMIC ENERGY AGENCY
VIENNA, 2013

COPYRIGHT NOTICE

Marketing and Sales Unit, Publishing Section
International Atomic Energy Agency
Vienna International Centre
PO Box 100
1400 Vienna, Austria
fax: +43 1 2600 29302
tel.: +43 1 2600 22417
email: sales.publications@iaea.org
http://www.iaea.org/books

Printed by the IAEA in Austria
November 2013
STI/PUB/1585

IAEA Library Cataloguing in Publication Data

Design features and operating experience of experimental fast reactors. — Vienna : International Atomic Energy Agency, 2013.
p. ; 30 cm. — (IAEA nuclear energy series, ISSN 1995–7807 ; no. NP-T-1.9)
STI/PUB/1585
ISBN 978–92–0–136410–4
Includes bibliographical references.

1. Fast reactors — Design and construction. 2. Fast reactors — Cooling. 3. Breeder reactors — Cooling. 4. Liquid metal cooled reactors. I. International Atomic Energy Agency. II. Series.

IAEAL 13–00849

FOREWORD

One of the IAEA's statutory objectives is to "seek to accelerate and enlarge the contribution of atomic energy to peace, health and prosperity throughout the world". One way this objective is achieved is through the publication of a range of technical series. Two of these are the IAEA Nuclear Energy Series and the IAEA Safety Standards Series.

According to Article III.A.6 of the IAEA Statute, the safety standards establish "standards of safety for protection of health and minimization of danger to life and property". The safety standards include the Safety Fundamentals, Safety Requirements and Safety Guides. These standards are written primarily in a regulatory style, and are binding on the IAEA for its own programmes. The principal users are the regulatory bodies in Member States and other national authorities.

The IAEA Nuclear Energy Series comprises reports designed to encourage and assist R&D on, and application of, nuclear energy for peaceful uses. This includes practical examples to be used by owners and operators of utilities in Member States, implementing organizations, academia, and government officials, among others. This information is presented in guides, reports on technology status and advances, and best practices for peaceful uses of nuclear energy based on inputs from international experts. The IAEA Nuclear Energy Series complements the IAEA Safety Standards Series.

The IAEA has begun an initiative to help coordinate Member State efforts in the field of fast neutron nuclear reactors. This initiative is primarily targeted at the preservation of knowledge in the areas of design, construction and operation, for both experimental and power fast reactors. The ultimate goal of this activity is to establish a comprehensive, international inventory of fast reactor data and knowledge, which will be an essential resource for the future development and deployment of fast reactor technology.

In this project, carried out within the framework of the Department of Nuclear Energy's Technical Working Group on Fast Reactors (TWG-FR), the IAEA supports and coordinates data retrieval and interpretation efforts in Member States, and ensures collaboration with other international organizations.

The main objective of this report is to compile and document key aspects of fast reactor engineering development and experience, as a part of the IAEA's ongoing efforts in knowledge preservation and data retrieval. More specifically, the aim is to generalize R&D activities and experience with experimental facilities and reactors for providing engineering options for liquid metal cooled fast reactors.

The IAEA acknowledges the contributions and support of the members of the IAEA TWG-FR in the preparation of this report. The IAEA officers responsible for this publication were A. Rinejski, A. Stanculescu, Y. Yanev and S. Monti of the Department of Nuclear Energy.

EDITORIAL NOTE

This report has been edited by the editorial staff of the IAEA to the extent considered necessary for the reader's assistance. It does not address questions of responsibility, legal or otherwise, for acts or omissions on the part of any person.

Although great care has been taken to maintain the accuracy of information contained in this publication, neither the IAEA nor its Member States assume any responsibility for consequences which may arise from its use.

The use of particular designations of countries or territories does not imply any judgement by the publisher, the IAEA, as to the legal status of such countries or territories, of their authorities and institutions or of the delimitation of their boundaries.

The mention of names of specific companies or products (whether or not indicated as registered) does not imply any intention to infringe proprietary rights, nor should it be construed as an endorsement or recommendation on the part of the IAEA.

The IAEA has no responsibility for the persistence or accuracy of URLs for external or third party Internet web sites referred to in this book and does not guarantee that any content on such web sites is, or will remain, accurate or appropriate.

CONTENTS

1. INTRODUCTION

Nuclear power currently provides about 17% of the world's electricity, primarily from thermal water cooled reactors. In parallel with the development and construction of these thermal reactors, several Member States have undertaken research and development (R&D) programmes on fast reactors cooled by a liquid metal, in most cases sodium.

Growing energy needs and concern for the environment currently drive the demand for large scale and low impact energy sources; by the same token, radioactive waste control is gaining importance. Therefore, national and international research on advanced fast neutron critical and hybrid subcritical systems for electricity production and for actinide transmutation is increasing. The members of the Generation IV International Forum (GIF) signed an agreement on international collaboration in R&D of innovative nuclear energy systems. Six reactor concepts were selected, among them three fast neutron systems: two liquid metal cooled fast reactors (LMFRs) (sodium and lead), and one gas cooled fast reactor (GFR). The technological goals are defined in the broad areas of sustainability, safety, radioactive waste burning, reliability, economics and proliferation resistance.

LMFRs have been under development for more than 50 years, and several countries currently have important development programmes. Fourteen experimental fast reactors with a thermal power of up to 400 MW(th) and six commercial size prototypes with an electrical output ranging between 250 and 1200 MW(e) have been constructed and operated. Four reactors — one prototype and one commercial size reactor with a thermal efficiency of up to 43% (the highest value in nuclear power practice) and two experimental reactors — are currently in operation. Two reactors, the Prototype Fast Breeder Reactor (PFBR) (500 MW(e) in India) and a commercial size reactor (~900 MW(e) in the Russian Federation), are under construction.

Great strides have been made in fast reactor technology, encouraging future development. The closed fuel cycle has been demonstrated and an effective breeding ratio has been experimentally confirmed. In total, fast reactors have gained nearly 400 reactor-years of operating experience. Fuel burnup in excess of 130 000 MW · d/t has been reached in several reactors, and major steps towards commercial fast reactor designs have been made.

The worldwide investment already made in the development and demonstration of LMFR technology exceeds US$50 billion [1.1]; these efforts have significantly improved the understanding of LMFR technology. The achievements of past R&D activities have been effectively used to develop fast reactor systems with advanced engineering characteristics and economics; a well validated way forward to commercial utilization of fast reactors has been established. This is generally consistent with today's studies in Member States, and it indicates that the goal of competitive fast reactors may be within reach.

During the 1980s–1990s, mostly for political and economic reasons, fast breeder reactor (FBR) development declined, particularly in countries characterized by advanced market economics, relatively slow growth in primary energy consumption and good availability of oil and gas. This resulted in the premature shutdown of some prototypes and many test fast reactors, and in a slowing down or closing of important fast reactor development programmes and the retirement of many of the key developers.

In this connection, the IAEA stepped forward with its initiative to preserve the knowledge gained in fast reactor technology development until the need for sustainability and economic criteria create the necessary conditions for a large scale deployment of FBRs. The IAEA has served as a place for accumulation and exchange of information during almost the whole period of LMFR development. The activities of the Technical Working Group on Fast Reactors (TWG-FR) and of the International Nuclear Information System (INIS) have made it possible to collect and summarize basic scientific and technological knowledge, including knowledge about the choice and mastery of fast reactor coolant and systems for fast reactor heat rejection and heat conversion to electricity. Countries that plan to embark on their own fast reactor development programme will be able to analyse the successful design approaches, components, systems and working parameters. They will therefore be able to avoid considering disregarded project solutions and designs.

An important objective of this report is to present the properties and some criteria for comparison and choice of liquid metal coolants, a detailed description of the heat transfer systems and major design features, and the operating experience of experimental facilities and fast reactors which have been shut down. The detail of treatment varies for the different aspects and, to some extent, with the availability of source information and the general applicability of design features. Some background conceptual thinking is also included in this report.

The report presents the history, the state of the art and an overview of fast reactor cooling, heat transport and heat conversion system development. Section 3 provides basic information on liquid metal coolants: comparison, choice, properties, development and mastery. Comparatively detailed data are presented for the following liquid metal coolants: lead, lead–bismuth (PbBi), lithium, mercury, potassium, sodium and sodium–potassium (NaK). Sections 4–6 outline design features and operating experience of experimental facilities and fast reactors with mercury, NaK alloy, and sodium and PbBi alloy coolants. Section 7 presents some important issues concerning sodium and heavy metal coolant technology. In the final section, the report identifies the progress achieved and some issues to be resolved in sodium and heavy metal coolant technology.

REFERENCE TO SECTION 1

[1.1] MOUROGOV, V., JUHN, P.E., KUPITZ, J., RINEISKII, A., Liquid-metal-cooled-fast reactor (LMFR) development and IAEA activities, Energy **23** 7/8 (1998) 637–648.

2. FAST REACTOR COOLANTS AND HEAT REMOVAL AND HEAT TRANSPORT SYSTEMS: HISTORY OF DEVELOPMENT AND OVERVIEW

From an early stage of nuclear reactor development, it was recognized that nuclear energy utilization would be sustainable if based on a mix of thermal spectrum reactors burning the limited available nuclear fuel and FBRs that could produce more nuclear fuel than they would consume, for use in thermal reactors.

The appropriate choice of the reactor core coolant is of great significance for achieving high breeding performance. The choice also determines the main design approaches of FBRs and the technical and economic characteristics of the fast reactor nuclear power plant. Avoidance of excessive moderation of the neutron flux was a fundamental requirement for a fast reactor coolant. Therefore, liquids containing chemical elements of low atomic weight, particularly hydrogen, were avoided as breeder reactor coolants. Thus water and organic compounds were unacceptable. As fast reactor coolants, high pressure gases such as helium and CO_2 were studied. Helium cooled fast reactor designs have been pursued as alternative options in Europe and the United States of America (USA). A variety of commercial scale (500–1500 MW(e)) designs were studied and several large scale experiments demonstrating key aspects of the technology were conducted or in advanced stages of planning. These included critical experiments in the Zero Power Reactor (ZPR) facility, fuel irradiations at EBR-II and at the Mol reactor in Belgium, a core flow loop at Oak Ridge National Laboratory (ORNL) and decay heat removal and fuel melting studies at Los Alamos and Argonne National Laboratory (ANL) in the USA. The General Atomics helium cooled fast reactor offered the potential for low doubling times and high breeding ratios. For this reason, the outlet gas temperature was limited to 350°C. This, plus a coolant pressure of about 8.5 MPa, yielded comparatively low plant thermal efficiency[1].

From the very beginning, the outstanding advantage of LMFRs was considered to be their ability to provide a high breeding ratio, thus allowing the effective use of uranium and thorium resources, as well as the excellent thermal properties. It should be noted that thorium breeding is possible with both fast and thermal spectra, but the breeding ratio for early light water reactor (LWR) designs is very close to unity or lower.

Additional advantages result from such LMFR features as the ability of some of them (in particular those with sodium coolant) to tolerate the use of standard structural materials and the possibility of achieving an internal breeding ratio greater than unity (both sodium and lead cooled reactors). The latter feature makes possible core design for long term operation without fuel reloading. Liquid metal coolants are also attractive because they provide means for achieving a comparatively high coolant temperature and therefore a high thermal efficiency, resulting in lower fuel and capital costs.

2.1. ATTEMPTS TO USE SODIUM COOLANT IN AREAS OTHER THAN FAST REACTORS

As noted in Ref. [2.1], in 1958–1963, design studies[2] were undertaken using sodium as a coolant in traditional (non-nuclear) boilers: sodium heated by burning fossil fuel in a furnace was employed to transport heat to a steam boiler located in the vicinity of a turbine. This resulted in a considerable decrease in the length of the steam/water pipelines connecting the boiler and the turbine. However, this option was abandoned because of the too complicated sodium handling for traditional power engineering.

The sodium graphite thermal reactor Hallam (240 MW(th), 75 MW(e)) was constructed and put into operation in the USA. The graphite moderator was clad in stainless steel. There were problems with the cladding; corrosion and stress cracking led to the failure of the cladding cans. Correcting the failure would have been expensive, so the plant was prematurely closed down. (Construction started in 1958; the plant operated from 1962 to 1964; decommissioning was completed in 1969. Currently the site houses a fossil fuel plant.)

---

[1] The high thermal efficiency gas cooled fast reactor system is one of six Generation IV systems selected for cooperative R&D by the GIF.

[2] At St Petersburg (formerly Leningrad) Centralnyj Kotlo-Turbinnyj Institut (Central Boiler-Turbine Institute).

The goal of the Solar Power Plant (SPP, 500 kW(e)) at Almeria, Spain, with sodium coolant, was to demonstrate the feasibility of electrical power generation by the conversion of direct solar radiation into thermal energy, and then, by conventional methods, into electrical power. The SPP consisted mainly of a heliostat field which reflected solar radiation into the receiver, which absorbed and transferred the thermal energy to the sodium fluid. The sodium fluid (70 t) was used for heat transportation and heat accumulation fluid as well. The energy was used to drive a conventional steam power generation system.

One of the most significant sodium fire accidents was at the Almeria SPP in August 1986. The accident occurred during the repair of a valve when about 14 t of sodium at 225°C was spilled in the plant room over a period of half an hour. The sodium burned in the atmosphere, and the temperature reached an estimated 1200°C. It caused considerable damage (the metallic beams became distorted and a hole was blown in the roof), and the facility was closed down. The Almeria accident was one of the reasons that spray fires must now be taken into account in the safety analyses of nuclear power plants. The Almeria accident accelerated R&D and code development with respect to spray fires.

The investment already made worldwide in the development, mastery and demonstration of LMFR technology exceeds $50 billion. Research during recent decades has significantly improved the understanding of LMFR technology issues. The achievements of past research activities have been effectively used to develop a system of structural analysis methods, which were used to evaluate the design solutions for advanced fast reactors. It is predicted that the LMFRs that are currently being designed will be able to achieve a very high degree of availability. As a benefit of these previous investments in sodium cooled reactor technology, the majority of the R&D needs for future plants are related to performance rather than to viability of the system. A well validated way forward to the commercial utilization of fast reactors has been established. This way is generally consistent with that of other studies and indicates that the goal of competitive fast reactors may be within reach [2.2].

2.2. INDIRECT CYCLE WITH SODIUM REACTOR COOLANT

The nuclear reactor is primarily a heat source. As background for the engineering aspects of reactor design, it is important to consider the path of heat transport from the thermodynamic and engineering viewpoints. As with conventional heat sources, one of the most practical means of converting heat to electrical energy is by use of the Rankine thermodynamic cycle. In a classic nuclear power plant, reactor heat is transferred from the fuel elements to a coolant and then to a steam generator, to produce steam. Work is produced by expending the steam in a turbine generator.

The turbine exhaust steam is then condensed and recycled. Heat extracted during the condensation process is rejected to the environment. Thus, the energy moves from the heat generation at high temperature in the fuel elements regressively downward on the temperature scale until the environment is reached. Along the way, a portion (35–45%) of the original energy is converted to useful work by steam expansion in the turbine that is almost thermodynamically reversible.

Although in the early period of fast reactor development several heat transport systems and variants thereof were under development, only one — the indirect three circuit cycle (Fig. 2.1) — has been mastered for experimental use and then used for power fast reactor application. A primary heat transport system (PHTS) removes heat from the reactor core and transfers it to an intermediate heat transport system (IHTS) (containing virtually no radioactive sodium). From the secondary circuit, this heat is transferred to a steam generator system (SGS) to produce superheated steam, which drives a turbogenerator.

The system used in fast reactors for transferring energy from the reactor core to the turbine requires high heat removal reliability. An intermediate link (secondary coolant loops) between the sodium cooled reactor core and the steam generator (SG) is generally used to prevent the release of radioactive sodium in the event of a SG tube rupture.

Other advantages of the intermediate loop system are the following:

— Hydrogenous materials are kept out of the reactor, minimizing the possibility of increasing the emergency reactivity insertion.
— The reactor containment structure can be designed for a lower pressure since it does not have to protect against the energy release of a sodium–water reaction.

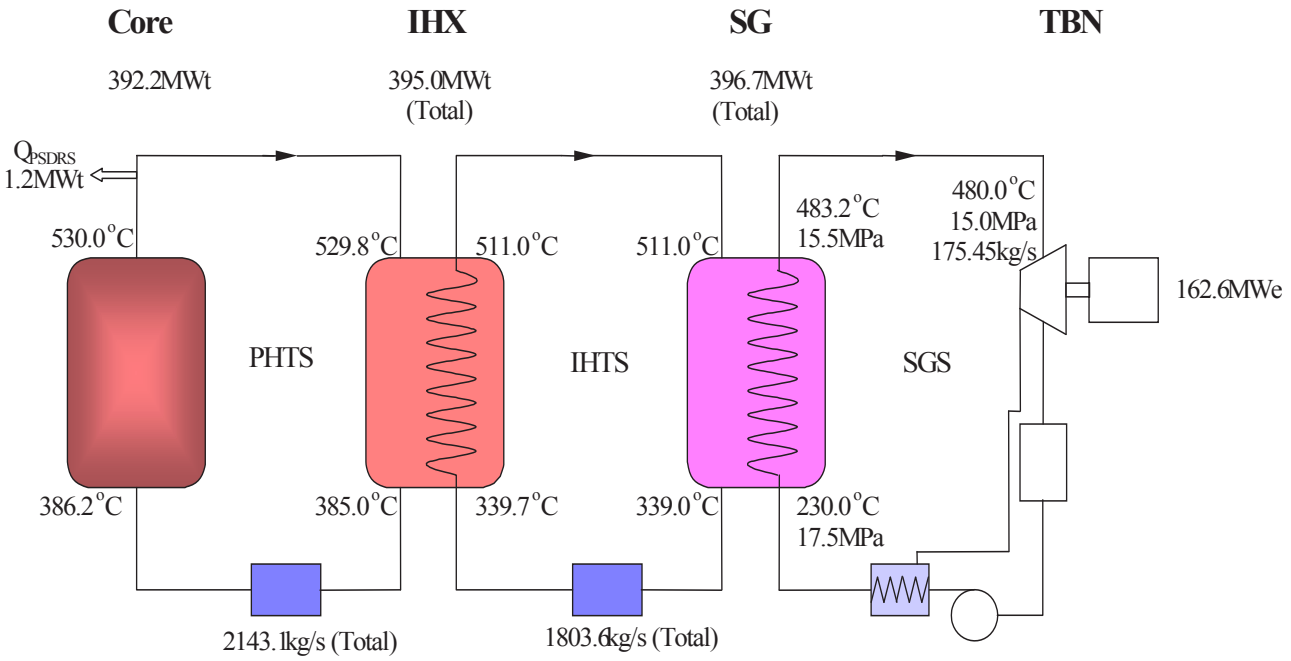

FIG. 2.1. Typical sodium cooled fast reactor heat transport/conversion system: primary, secondary and tertiary circuits (KALIMER-150, Republic of Korea) [2.3].

— Each secondary loop is completely separate; the sodium can be drained out of any one secondary loop without jeopardizing heat removal in the reactor with a passive safety system.

Because sodium has a comparatively high boiling temperature, the cooling system can operate at almost atmospheric pressure and therefore the vessels and heat exchanger tubes can have thin walls. As noted, sodium is also non-corrosive to structural materials used in the reactor. These unique characteristics of a sodium cooled system give rise to long lifetime and superior reliability, operability and maintainability, contributing to low life cycle costs. As result, the cost of a tree circuit combined system with optimal design is not much greater than that of a two circuit LWR system.

The total heat transfer surface and weight of the intermediate heat exchangers (IHXs) and the SGs in a fast reactor are less than those of the SGs in a pressurized water cooled reactor (Table 2.1), because of a higher temperature difference across the heat exchanger (possible with the liquid metal systems) and higher heat transfer coefficients owing to the better heat transfer properties of sodium.

Sixteen LMFRs of various designs, all using a liquid metal coolant and the three circuit thermal scheme, have been built and operated with varying degrees of success. Standouts have been the EBR-II experimental fast reactor at the National Reactor Testing Station in Idaho in the USA (60 MW(th)/15 MW(e)), which ran successfully for 30 a, and the BN-350 (250 MW(e)+100 000 t/d fresh water) in the former USSR (run for 25 a). Superphénix (1200 MW(e)) in France, and PFR (250 MW(e)) in the United Kingdom were prematurely shut down for non-technical reasons. The experimental reactors BOR-60 (Russian Federation) and FBTR (India) are still successfully running [2.3]. The BN-600 power reactor in the Russian Federation was connected to the grid in April 1980. Reactor operation is stable: its load factor is 75–77%, with the turbine efficiency being ~43%.

Phénix in France (250 MW(e)) was operated for about 100 000 h at a temperature of 560°C (the reactor hot structures) with a thermal efficiency of 45.3%, the highest value in nuclear power practice; the average burnup was increased from 50 to 100 GW·d/t, with maximum burnup exceeding 150 GW·d/t. These levels were reached with eight cores of fuel with 166 000 fuel pins. The plutonium produced in Phénix was used for fuel fabrication for its core. The cumulative amount of fast reactor fuel reprocessed in France is about 30 t. A breeding ratio of 1.16 was experimentally confirmed in Phénix. From 2003, the Phénix reactor power was limited to 350 MW(th), 145 MW(e), and the reactor was operated with two primary/secondary loops instead of three. Two fast reactors — BN-800 (~ 900 MW(e)) in the Russian Federation and PFBR (500 MW(e)) in India — are under construction [2.3].

TABLE 2.1. AP-600 AND BN-600 TYPE NUCLEAR STEAM SUPPLY SYSTEM TECHNICAL DATA

Item	AP-600 [2.4]	BN-600 type FR [2.3]
Power, per loop, MW(th)	970	760
Coolant inlet/outlet temperature, at reactor vessel, °C	279.5/315.6	382/550
Coolant inlet/outlet temperature, at steam generator (SG), °C	315.6/279.5	525/345
Steam temperature/pressure, °C/MPa	272.7/5.74	500/13.7
Power plant thermal efficiency, net %	35	40
SG heat transfer surface, m^2	6 986	2 088
Intermediate heat exchanger (IHX) heat transfer surface, m^2	—	2 444
(SG + IHX) heat transfer surface, m^2	6 986	4 532
Number of heat exchanger tubes per SG (dimensions)	6 307 (ø17.5/15.5 mm)	1 663 (ø16.4/12.2 mm)
Number of heat exchanger tubes per IHX (dimensions)	—	5 022 (ø17.1/15.1 mm)
Number of heat exchanger tubes per (SG + IHX)	6 307	6 685
SG shell outer diameter/length, mm	4 500/21 051	1 573/30 000
IHX shell outer diameter/length, mm	—	2 400/14 000
SG transport, t	365.5	98.3
IHX transport, t	—	105
SG+IHX weight, t	365.5	203.3

TABLE 2.2. FAST REACTOR JSFR-1500 AND PRESSURIZED WATER REACTOR APWR-1500: MAIN DESIGN CHARACTERISTICS [2.4, 2.5]

Item	JSFR	APWR
Power output, MW(th)/MW(e)	3 530/1 500	4 466/1 538
Pressure in reactor vessel (RV), MPa	0.17 (argon)	16.0
RV outside diameter/height, m	10.7/21.2	5.8/13.6
Thickness of RV wall, mm	30	255
Thickness of piping wall, mm	16–18	25–130
Number of loops	2	4
RV weight, t	465	590
IHX/pump weight, t	576 (2 units)	—
Steam generator (SG) weight, t	1 200 (2 units)	1 760 (4 units)
Plant component total weight, t/t per MW(e)	2 241/1.5	2 350/1.56
Building volume, m^3/m^3 per MW(e)	150 000/18 000	360 000/70 000

Some countries — for example, Japan — have made certain progress recently in fast reactor commercialization. A Japan Atomic Energy Agency (JAEA) sodium cooled fast reactor (JSFR) is characterized by the use of a compact, two loop, large scale heat transport system. The primary system consists of the IHX/pump and large diameter piping. The primary piping penetrates the roof deck of the reactor vessel ('top-entry system'). Therefore, a compact

plant layout has been achieved. Based on these results, the Japanese developers, in the framework of extensive feasibility studies, compared key economic parameters of generation III+ advanced pressurized water reactors (APWRs) and JSFR (FOAK), using input data, some of which are presented in Table 2.2.

Researchers believe that both the overnight cost and the busbar cost can be comparable to, or even lower than, those of future LWRs. Thus the compact loop type JSFR concept has great potential to meet the aim of economic competitiveness in spite of using the three circuit heat transfer scheme. Some experts believe that the true potential of sodium cooled reactors has not yet been fully explored.

Full industrial development of fast reactors is not yet complete. It is simply too early in the prototype stage of development to provide a more general view of LMFR technology and economic characteristics. Other reactor technologies, including water cooled reactors, had achieved high reliability and lower generating costs by the time their respective large scale introduction took place. It cannot be said that this will not happen in the case of the LMFRs.

2.3. INDIRECT CYCLE WITH TWO CIRCUIT SYSTEM AND HEAVY METAL COOLANT, BINARY CYCLE

As pointed out in Ref. [2.1], lead and PbBi alloy do not chemically react with air or water. Therefore, in principle, a PbBi and lead cooled reactor does not need an intermediate circuit between the primary coolant and the steam supply system (Fig. 2.2).

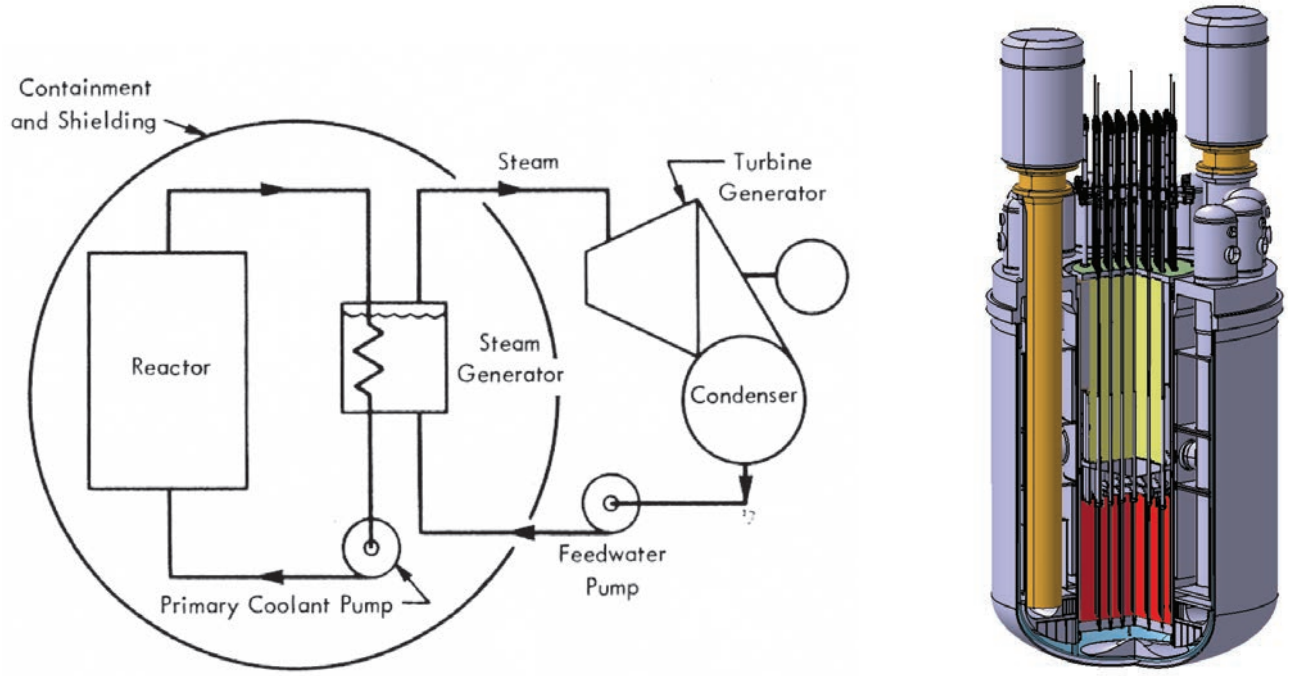

FIG. 2.2. Heavy metal coolant two circuit system, SVBR-75/100 pool type reactor [2.3] (two primary pumps, 12 SG modules — inside reactor vessel).

The elimination of an intermediate circuit is a prime factor in producing potential cost reductions over sodium cooled systems. However, it is known that there have been severe incidents with PbBi cooled reactors owing to water/steam leaks caused by corrosion damage of the heat exchange tubes that occurred in one of the first submarine SGs [2.6]. As a result of one leak, some areas of the reactor core were plugged by products of water and PbBi interaction, causing meltdown of the core. This incident showed that the elimination of the intermediate circuit between the primary coolant (PbBi, lead) and the water/steam is questionable and requires additional R&D.

The development of corrosion resistant structural materials is apparently the main problem in PbBi and, even more, lead cooled reactor technology.

The γ radioactivity induced in the lead and PbBi coolants is low so that the coolant circuit can be accessed after a shutdown period of about 24 h. However, the formation of α radioactive ^{210}Po from bismuth, and to a lesser extent from lead, poses problems because of ^{210}Po migration from the coolant to the cover gas and formation of aerosols. ^{210}Po is volatile, so that any leakage from the cover gas poses a serious hazard to the plant operators and the environment. In the early stages of development, the formation of deposits of lead oxide and other impurities posed problems.

The design and operating experience of the propulsion reactors with PbBi coolant has been used to develop the SVBR-75/100 reactor design in the Russian Federation. Its power is 280 MW(th)/75 MW(e), and the main thermal parameters are as follows: the primary coolant core outlet/inlet temperature is 439/275°C; the steam parameters are 3.24 MPa and 238°C; and the thermal efficiency is rather low.

In an indirect two circuit cycle the primary coolant from the core flows to a SG. A leak in the SG could result in an at least three problems:

— Spillage of water into the reactor;
— Release of radioactivity into the steam system;
— Primary coolant–water interaction.

The primary system would have to be designed to withstand high pressure water entry.

An indirect two circuit heat transport system was used for submarine heavy liquid metal cooled reactors where space and weight requirements dominate. Some experts maintain that the concern about leaks between the heavy metal and the water may preclude the elimination of an intermediate circuit. It seems that, conceptually, PbBi and lead heat transport systems could be attractive if the high corrosion activity inherent to heavy metals, long term materials compatibility and other problems were resolved.

The mercury cycle was studied in the past, and a two circuit mercury–water/steam system was evaluated. Mercury was vaporized and superheated in the reactor to a maximum temperature of 500–540°C and was condensed in a condenser boiler to produce 12.5 MPa superheated steam. Double-wall tubes in the SG minimized leakage [2.5]. The poor nuclear properties and toxicity of mercury preclude its general acceptance as a reactor coolant. The binary sodium–mercury system is shown in Fig. 2.3. In this system, sodium serves as a primary reactor coolant transferring its heat to mercury (Hg) in a boiler.

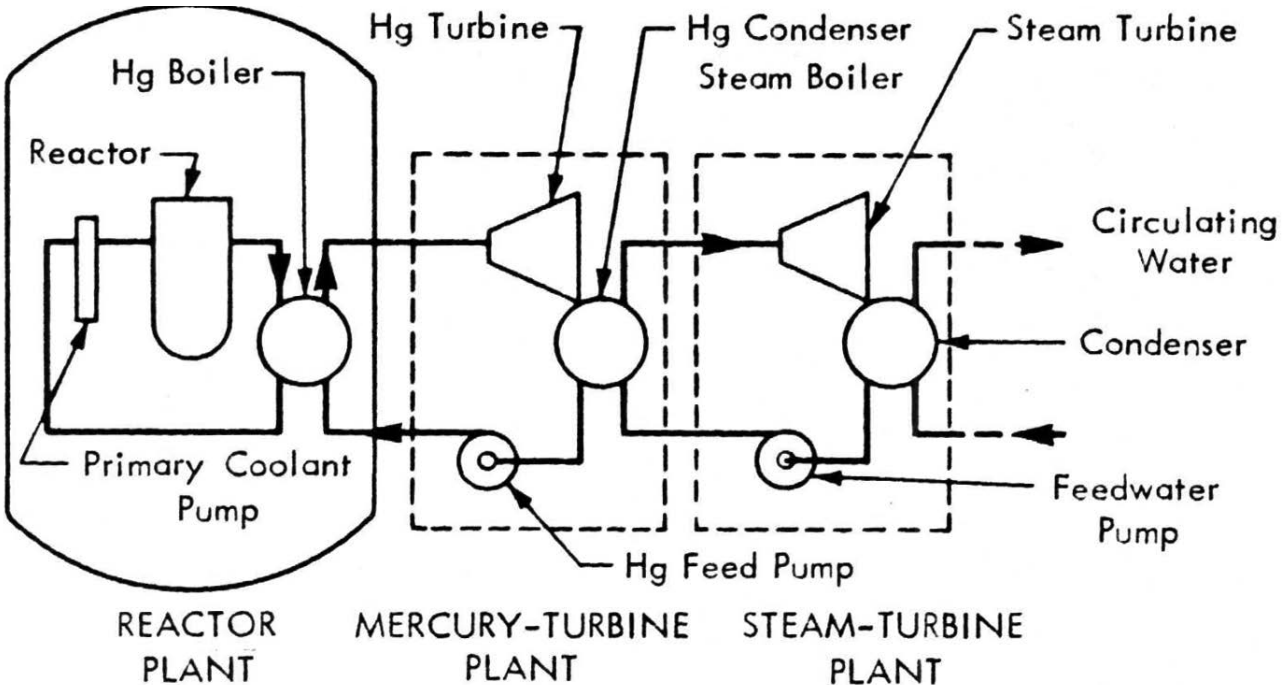

FIG. 2.3. Sodium cooled reactor binary thermodynamic system [2.5].

The mercury vapour operated a turbine and was then condensed in a steam boiler, producing steam to operate a steam turbine. It was concluded that the sodium cooled reactor with a binary thermodynamic system might be attractive if higher sodium temperatures are achieved in the future.

2.4. DIRECT CYCLE WITH WATER AS COOLANT AND WORKING MEDIUM

A simplest method for transferring heat from the reactor to the turbine is to vaporize and reheat the coolant, which removes heat from the reactor core, and to use the vapour to drive the turbine (Fig. 2.4).

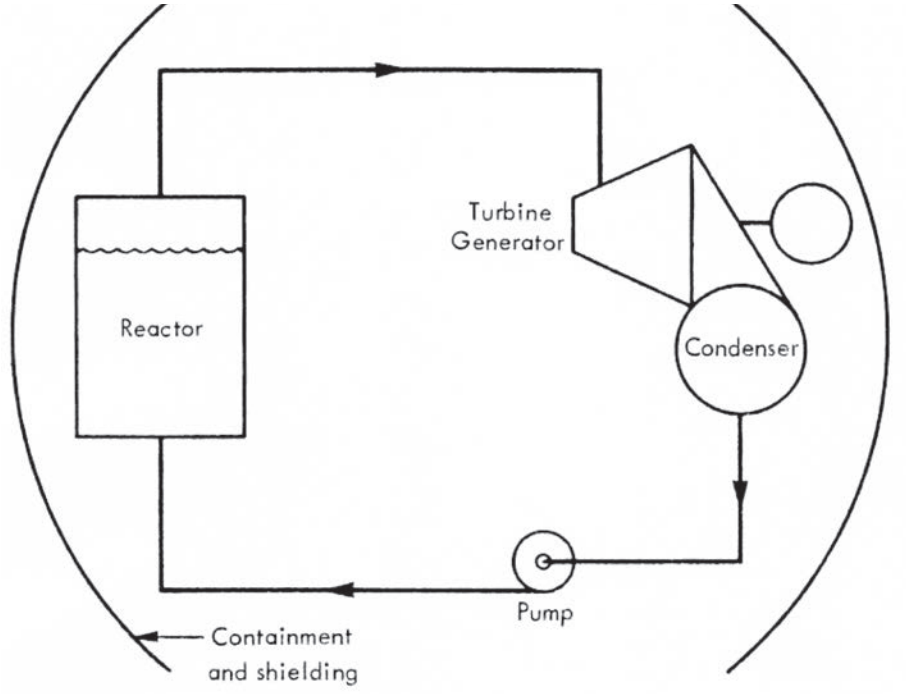

FIG. 2.4. Direct cycle heat transport system.

A Loeffler scheme steam cooled fast reactor (Fig. 2.5) with a power of 840 MW(th)/306 MW(e) and a thermal efficiency of ~36%, in which the steam is produced at 9.8 MPa and 507°C, has been studied [2.5]. About one third of the steam from the reactor is directed to the turbine; the remainder is directed (through a desuperheater) to vaporize the feedwater (250°C) in a Loeffler boiler. Saturated steam from the boiler (9.6 MPa, 320°C) is returned to the reactor (10.7 MPa, 325°C) by a steam circulator/compressor. The high recirculation ratio, the problems related to the low leakage circulator, the low thermal efficiency owing to the high required pumping power (10% of the total electric output), and the low breeding ratio were the drawbacks of this design.

A Loeffler boiler is necessary for generating inlet steam. The reactor requires steam blowers instead of feedwater pumps. Problems include emergency core cooling owing to fast reactor high power density and positive reactivity coefficient [2.7].

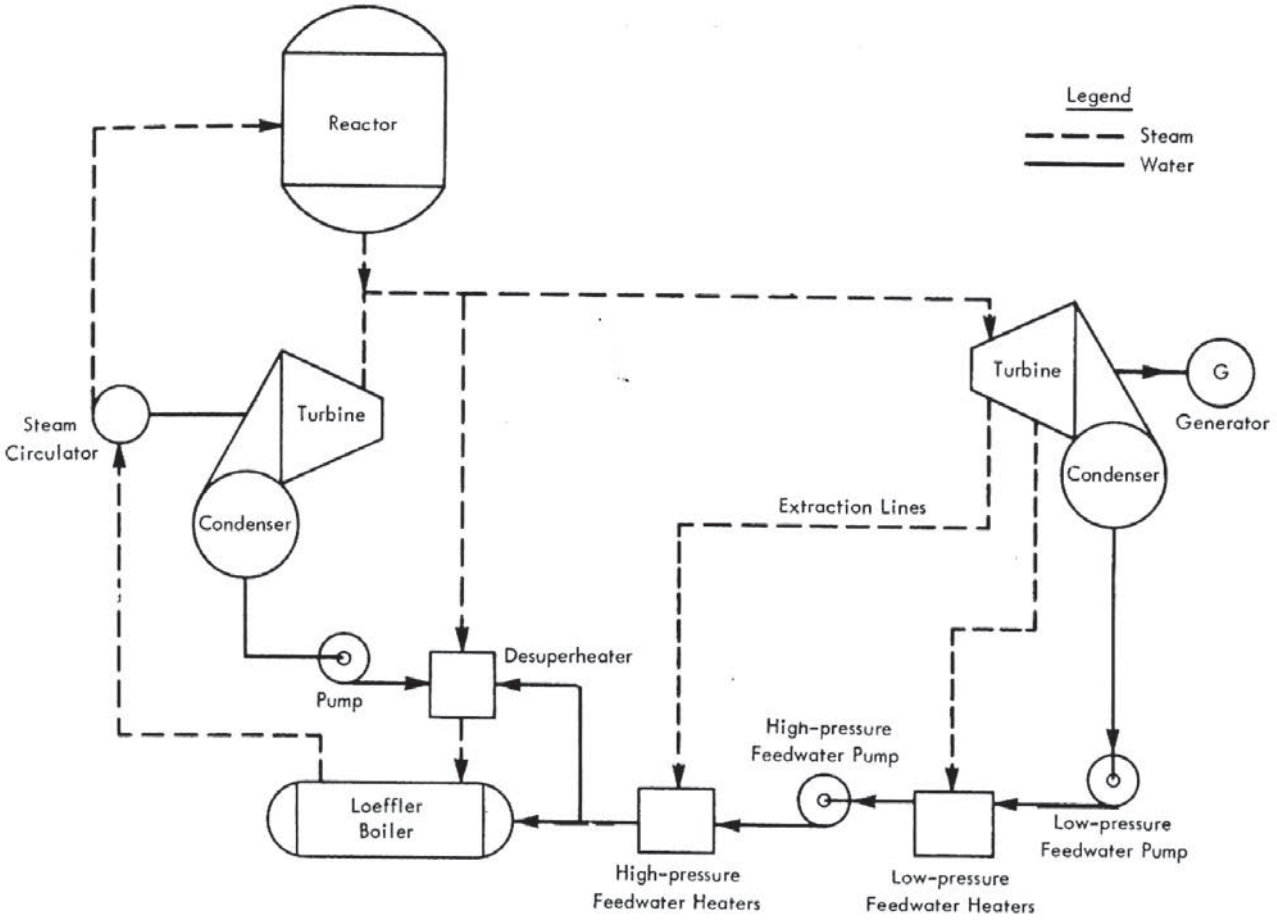

FIG. 2.5. Direct cycle steam cooled fast reactor [2.5].

REFERENCES TO SECTION 2

[2.1] INTERNATIONAL ATOMIC ENERGY AGENCY, Comparative Assessment of Thermo-physical and Thermo-hydraulic Characteristics of Lead, Lead-Bismuth and Sodium Coolants for Fast Reactors, IAEA-TECDOC-1289, IAEA, Vienna (2002).

[2.2] INTERNATIONAL ATOMIC ENERGY AGENCY, Status of Liquid Metal Cooled Fast Reactor Technology, IAEA-TECDOC-1083, IAEA, Vienna (1999).

[2.3] INTERNATIONAL ATOMIC ENERGY AGENCY, Fast Reactor Database, 2006 update, IAEA-TECDOC-1531, IAEA, Vienna (2006).

[2.4] INTERNATIONAL ATOMIC ENERGY AGENCY, Status of Advanced Light Water Cooled Reactor Designs, IAEA-TECDOC-968, IAEA, Vienna (1997).

[2.5] CHASE, W.L., "Heat transport system", in Fast Reactor Technology: Plant Design, YEVICK, J.G., AMOROSI, A. (Eds), The MIT Press, Cambridge, MA (1966).

[2.6] OSIPENKO, L., GILTSOV, L., MORMOL, N., Atomnaia podvodnaia epopea. A/O Borges, Moscow (1994) 208–209 (in Russian).

[2.7] OKA, Y., "Review of high temperature water and steam cooled reactor concepts", Int. Cong. on Advanced Nuclear Power Plants (ICAPP), 2002, Hollywood, FL (2002).

3. LIQUID METAL COOLANTS: PROPERTIES, COMPARISON, CHOICE

3.1. THE CRITERIA FOR LIQUID METAL COOLANT CHOICE

The idea to use a liquid metal as a fast reactor coolant goes back to the very earliest days of atomic energy development and was even considered for the very first nuclear plants in the USA and USSR. In the 1950s and 1960s, mercury, potassium, NaK eutectic, sodium, lithium, lead and PbBi alloy were studied as FBR coolants. The choice of the liquid metal coolant for fast reactors was governed by the following general criteria [3.1]:

(1) *Heat transfer and heat transport properties.* The coolant should yield high heat transfer coefficients and should possess a reasonably high heat capacity.
(2) *Corrosion and chemical activity.* The coolant should have low chemical affinity for the container walls, fuel cladding and all solid surfaces that it contacts, as well as a chemical inertness and compatibility with the working fluids in the case of leaks. Insoluble compounds or reaction products that might cause plugging should be kept to a minimum.
(3) *Boiling point.* The normal boiling point of the coolant should be well above its range of operating temperatures. This will preserve the liquid coolant properties without the need for high pressures and the penalty of increased container wall thicknesses. Coolants with a high boiling point can be operated at a high temperature to produce superheated steam of high pressure.
(4) *Decomposition.* The coolant should be stable in a high temperature and radiation environment.
(5) *Melting point.* For small, simple systems that can be sufficiently preheated, melting points up to about 315°C are acceptable. For filling complicated and large systems, a much lower melting point is preferred.
(6) *Radioactivity.* Ideally a coolant should develop no gamma activities from in-vessel radiation. If it does, these activities should preferably have short half-lives and low energies. Alpha and beta activities can easily be shielded, but must be contained.
(7) *Nuclear properties.* Since coolant normally occupies more than 30% of the core volume, its nuclear properties are very important. Its moderating power should be low. It is desirable that the temperature coefficient of reactivity be negative. The coolant should have low cross-sections of absorption and inelastic scattering.
(8) *Cost.* Except for the metals that have a low cost per unit volume, such as sodium, the inventory cost of liquid metal coolant can be substantial; generally, however, it is only a small fraction of the total plant investment.

The choice of a coolant depends on a compromise, since no known coolant excels in all criteria. Factors 1 through 4 and 7 make liquid metals the foremost choice as primary coolants. However, other coolants may be feasible if the requirements are relaxed. For example, if the power density is sufficiently low, gas or steam cooling may be a possible alternative to liquid metal cooling [3.1].

3.2. COMPARISON OF LIQUID METAL COOLANTS

Table 3.1 lists pertinent properties at 1000°F (~540°C) of 15 potential fast reactor coolants. Featured below are several ‘evaluation parameters’, useful in the preliminary selection of a coolant.

A low capture and non-moderation are the main requirements of neutronic qualities of a coolant to optimize the breeding and to minimize the void reactivity effect. To assess the suitability of coolant in a LMFR, some expressions were introduced in Ref. [3.2]:

(1) The neutronic transparency of the coolant:

$$I_1 = \rho \cdot Cp \cdot \Delta T_{eff} / \Sigma_a$$

(2) The moderation induced by elastic scattering:

$$I_2 = \rho \cdot Cp \cdot \Delta T_{eff} / \xi \Sigma_s$$

where

ρ is the coolant density, kg/m^3;
Cp is the specific heat, J/kg·K;
ΔT_{eff} is the effective liquid range, K;
Σ_a is the macroscopic absorption cross-section, cm^{-1};
Σ_s is the macroscopic scattering cross-section, cm^{-1};
ξ is the average gain of lethargy per collision.

As pointed out in Ref. [3.2], the effective liquid range goes from the melting point to the lowest value between the boiling point and an upper bound of the temperature limit imposed by the use of typical steels (in Ref. [3.2] the value 700°C was chosen).

The higher the values of I_1 and I_2, the better the potential of the candidate as a fast reactor core coolant: a high value for I_1 means little loss of neutrons in the coolant, a high value for I_2 means capability of keeping a hard neutron spectrum. I_1 and I_2 indicators for primary coolants of interest are shown in Table 3.2.

(3) The pumping power required for the heat removal is an important economic consideration. For a given coolant temperature rise, the pumping power is proportional to the following grouping, assuming the heat output, geometry and temperature differential are the same in all cases [3.1]:

$$\mu^{0.2} / (\rho^2 c_p^{2.8})$$

where

μ is the viscosity, lb/ft/h;
ρ is the density, lb/cu.ft;
Cp is the specific heat, Btu/lb/°F.

A low value for this grouping indicates a low pumping requirement.

TABLE 3.1. PROPERTIES OF LIQUID METAL COOLANTS [3.1]

	Bismuth	Gallium	Lead	Lithium (nat.)	Mercury	Potassium	Rubidium	Sodium	Tin	Zinc	Na (56%) K (44%)	Na (22%) K (78%)	Pb (44.5%) Bi (55.5%)	Sulphur	Phosphorus
General physical properties															
Atomic number	83	31	82	3	80	19	37	1I	50	30				16	15
Atomic weight	209	69.72	207.21	6.94	200.61	39.100	85.48	22.997	1J8.70	65.38	30.082	35.557	208.2	32.066	31
Density, lb/cu ft	608	359	650	29.9	826	44.6	84.4	51.4	421	428	47.4	46.3	625.5	102.5 (732°F)	84.9 (436°F)
Viscosity, lb/ft/h	2.664	1.836	4.1	0.82	2.76	0.41	0.415	0.55	2.736	6.192	0.47	0.43	2.88	680 (732°F)	<1
Surface tension, lb/ft	0.0247	NA	0.0293	0.0238	0.0307	0.0057	0.0022	0.0101	0.0347	0.0535	0.0071	0.0078	NA	0.00294	NA
Electrical resistivity, μ ohm/cm	142.78	NA	104	36	108.3	48	60	29	55.54	35.22	61	71	129.85	173 (732°F)	NA
Vapour pressure, mm Hg	Neg.	Neg.	Neg.	Neg.	9300	62	139	9	Neg.	Neg.	26	45	Neg.	310.2 (732°F)	227.5 (436°F)
Thermal properties															
Melting point, °F	520	85.86	621	357	–37.97	146	102	208.1	449	787	66.2	12	257	246	111.5
Boiling point, °F	2691	3601	3159	2428	675	1402	1270	1618	4118	1663	1518	1443	3038	832	536
Specific heat, Btu/lb/°F	0.0369	0.082	0.0346	0.996	0.0326	0.182	0.0877	0.301	0.0639	0.1165	0.2485	0.209	0.035	0.248 (732°F)	NA
Thermal conductivity, Btu/h/ft F	8.95	18.0	8.84	27.6	5.8	21.2	13.2	37	19.0	33.2	16.4	15.05	8.05	0.0952	NA
Heat of fusion, Btu/lb	21.6	34.49	10.60	185.9	5.0	25.5	11.0	48.7	26.1	43.92	NA	NA	NA	25.8 (15°C)	9.06 (15°C)
Heat of vaporization, Btu/tb	367.74	1825	368.3	8349	1.25.	853	363	1718	1031	755.1	NA	NA	NA	121.2	254 (15°C)
Prandtl number (cp μ/k)	0.011	0.0083	0.016	0.0295	0.0154	0.0035	0.00276	0.0044	0.0095	0.022	0.0071	0.0060	0.0125	1771	<1
Change of volume on fusion, % solid volume	–3.32	–3.1	3.6	1.5	3.6	2.41	2.5	2.5	2.6	6.9	2.5	2.5	0.0	NA	NA

TABLE 3.1. PROPERTIES OF LIQUID METAL COOLANTS [3.1] (cont.)

	Bismuth	Gallium	Lead	Lithium (nat.)	Mercury	Potassium	Rubidium	Sodium	Tin	Zinc	Na (56%) K (44%)	Na (22%) K (78%)	Pb (44.5%) Bi (55.5%)	Sulphur	Phosphorus
Nuclear properties															
Fast activation cross-section, mb	0.6	28.0	3.1	0.03	89.0	0.59	46.0	0.87	14.0	13.0	0.80	0. 64	3.5	1.4	3
Non-elastic scattering cross-section at 2 MeV, b	0.53	NA	0.64	<1	2	4 (3,7 MeV)	NA	<1	1	1	NA	NA	0.58	NA	NA
n, γ daughter half-life	None	14.1 h	None	None	48 days	12.4 h	19 days	15 h	112 days	None	See K, Na	See K, Na	None	None	None
n, γ daughter activity, MeV	None	0.84, 0.60, 3.35	None	None	0.28	0.32,1.51	1.1	2.775, 1.368	0.39	None	NA	NA	None	None	None
ζ, average log energy decrement	0.0096	0.0287	0.0097	0.2643	0.0100	0.0507	0.0234	0.0852	0.0169	0.0305	NA	NA	NA	0.0616	0.064
General properties															
Cost, $/lb (as of 1960)	2.25	675	0.12	11	2.82	3.66	390	0.17	1.00	0.13	0.60	0.80	See Pb, Bi	0.08	0.09
Container material	Cr-Mo steel	Graphite	Carbon steel	Cb-Zr	Ferrous metals	304 5S	304 SS	304 SS	Quartz	Graphite	304 SS	304 SS	Cr-Mo steel	Graphite	NA
Reaction with uranium	Soluble	Soluble	Slight soluble	Slight	Soluble	Slight[a]	Slight[a]	Slight[a]	Sl soluble	Sl soluble	Slight	Slight	Sl. soluble	Reacts	Reacts
Reaction with plutonium	Soluble	Soluble	Slight soluble	Slight	Soluble	Slight[a]	Slight[a]	Slight[a]	Alloys	NA	Slight	Slight	Sl. soluble	Reacts	Reacts
Toxicity	Slight	Slight	High	Moderate	High	High	Moderate	High	None	None	High	High	High	Slight	Moderate
Fire or explosion hazard	Slight	None	Moderate as dust	High	None	High	High	High	Slight as dust	Moderate	High	High	Moderate as dust	Slight	High

TABLE 3.1. PROPERTIES OF LIQUID METAL COOLANTS [3.1] (cont.)

	Bismuth	Gallium	Lead	Lithium (nat.)	Mercury	Potassium	Rubidium	Sodium	Tin	Zinc	Na (56%) K (44%)	Na (22%) K (78%)	Pb (44.5%) Bi (55.5%)	Sulphur	Phosphorus
Evaluation parameters															
$\mu^{0.2}$ ($\rho^2 Cp^{2.8}$), pumping power criterion	0.034	0.009	0.039	0.00109	0.0261	0.050	0.107	0.0097	0.015	0.003	0.0189	0.0316	0.024	0.0174	NA
S (specific activity), curies/g 1000 MW(th) reactor	0.17	2.3			0.28	0.11	2.6	0.20	0.95	1.17	0.16	0.11	0.09	0.80	
$(T_b-T_m)/T_w$ temperature range ratio	1.49	2.41	1.74	1.40	0.94	0.86	0.80	0.97	2.51	0.60	0.99	0.98	1.91	0.90	0.47

Note: All data are for a temperature of 1000°F (~540°C), unless otherwise specified.

CONVERSION OF ENGINEERING UNITS TO CGS UNITS [3.1]:

Latent heat	1 Btu/lb (mass) = 0.5556 cal/g
Surface tension	1 lb (force)/ft = 1.459×10^4 dynes/cm
Density (ρ)	1 lb (mass)/cu ft = 0.01602 g/cm^3
Specific heat (Cp)	1 Btu/lb (mass)/°F = 1 cal/g/°C
Viscosity (μ)	1lb (mass)/ft/h = 4.134×10^{-3} g/cm/s
Thermal conductivity	1 Btu/h/°F = 4.134×10^{-3} cal/s/cm/°C

[a] Due to impurities.

TABLE 3.2. I_1 AND I_2 INDICATORS FOR PRIMARY COOLANTS OF INTEREST [3.2]

Coolant	I_1	I_2
Sodium (Na)	6.69×10^6	4.08×10^4
Lead (Pb)	3.21×10^6	2.04×10^5
Lithium (^{7}Li)	4.73×10^8	6.63×10^4

(4) The buildup of induced activity in the primary coolant is of major importance since it affects the amount of shielding required. The specific activity for isotopes formed from initial ingredients (in curies per gram) is given by the expression [3.1]:

$$S = \frac{1}{K} \sum_{ij} f_i \frac{N_0 \varphi_j \sigma_{ij}}{A_w} \frac{\tau_r}{\tau_0} (1 - e^{-0.693\,\theta/\theta_i})$$

where:

S is the specific activity, Ci/g;
f_i is the atomic fraction of *i*th isotope in coolant;
N_0 is Avogadro's number (atoms/gram mole of coolant) = 0.60248×10^{24};
φ_j is the neutron flux in the *j*th energy interval, neutrons·cm^{-2}·s^{-1};
σ_{ij} is the microscopic reaction cross-section for *i*th isotope and *j*th energy interval, m^2/nucleus;
A_w is the atomic weight (grams/gram mole) of coolant;
τ_r is the coolant residence time in the neutron flux during one cycle, s;
τ_o is the cycle time for coolant, s;
θ is the irradiation time, s;
θ_i is the half-life of *i*th isotope, s;
K is a constant = 3.7×10^{10} dis · Ci^{-1} · s^{-1}.

In Table 3.1, the specific activity is estimated in curies per gram of coolant for a 1000 MW(th) reactor. Exact values depend on reactor design details. For coolants having little or no induced (gamma) activity, e.g. lead and lithium, activation of the contained impurities takes on added importance.

(5) A measure of the useful temperature range of the liquid coolant is given by the expression:

Tb – Tm/Tw

where *Tb, Tm,* and *Tw* are the absolute temperatures at the coolant boiling point, melting point and the reactor outlet, respectively. High values of this ratio are desirable [3.1].

3.3. PHYSICAL AND CHEMICAL PROPERTIES OF LIQUID METAL COOLANTS

Data are presented for the following liquid metal coolants: lead, lithium, mercury, potassium, sodium, NaK and PbBi. The coolant in a fast reactor occupies a large fraction of the core volume. For neutron economy and other reasons, it is a prime nuclear prerequisite for the coolant to be a relatively poor moderator. Liquid metals are comparatively poor moderators and thus are well suited for use as fast reactor coolants. Some moderation occurs, however, because elastic and inelastic neutron collisions with coolant, structural and fuel atoms degrade the energy of the neutrons. The amount of moderation caused by a particular coolant depends upon the coolant volume, the macroscopic elastic and inelastic scattering cross-section, and the value of the average logarithmic energy loss per elastic collision.

3.3.1. Coolant activation

Although liquid metals have relatively small capture cross-sections for the fast neutrons, some of them can nevertheless become highly activated when used as the primary coolant in a high flux power reactor. Consequently, if the coolant is circulated outside the primary shield area, additional shielding is required for piping, pumps and heat exchangers, and maintenance problems are increased. The activation of the reactor coolant depends upon its cross-section as a function of energy, the reactor flux level, flux spectrum, coolant cycle time and the half-life of the isotope formed [3.1].

The liquid metal coolants can be divided into two basic categories of induced activity: the high activity coolants sodium, potassium and NaK, and the low activity coolants lead, lithium, and PbBi and mercury.

3.3.1.1. Comparatively high activity coolants: sodium, potassium

Liquid sodium, potassium and NaK alloy coolants are nearly identical with regard to their induced activities and shield requirements. All three substances have comparable capture cross-sections for fast neutrons. The radioisotopes formed, ^{24}Na and ^{42}K, both have about the same half-life and both emit gamma ray photons of fairly high energy. In addition, all three of these coolants undergo (n, 2n) reactions with fast neutrons to form either ^{22}Na or ^{38}K. Although the cross-section for the (n, 2n) reaction is small compared with the capture cross-section, it can be an important consideration in the case of sodium. Here, the longer lived ^{22}Na isotope becomes the principal activity after long decay periods, and therefore it is important for maintenance consideration [3.1].

3.3.1.1.1. Sodium ‘operational’ radioactivity

The natural isotope of sodium is ^{23}Na (abundance 100%). Neutron capture processes in sodium ((n, γ) reaction resulting in 1.4 MeV γ-quanta emission) lead to formation of the ^{24}Na isotope with a half-life of 15 h, while sodium is flowing through the core. Besides, there is an (n, 2n) threshold reaction producing ^{22}Na with a 2.6 a half-life. ^{22}Na emits 1.3 MeV γ-quanta; ^{22}Na is also a positron emitting nuclei, producing 0.5 MeV gammas, and its activity is proportional to the thermal power of the reactor plant.

Neutrons are not practically generated by sodium radionuclides with half-lives exceeding 2.6 a, even after 50 a of exposition to intensive fast neutron flux. ^{24}Na is the main isotope, giving rise to the requirement of protection against γ radiation. Approximately 10 d after reactor shutdown, the primary circuit activity is mainly determined by ^{22}Na. This feature, along with the fact that sodium interacts chemically with water and air, results in a three circuit reactor power plant design, including:

— The primary circuit containing radioactive sodium heated up in the core;
— The secondary non-radioactive sodium circuit coupled with the primary circuit by the IHX;
— The tertiary water circuit producing steam for electricity generation.

Within the primary circuit, the radioactive coolant is protected against air by the steel barriers and argon cover gas. The radioactive sodium of the primary circuit is separated from the non-radioactive sodium of the secondary circuit by the steel tubes of the IHX.

The operating experience of different reactors has shown that the coolants separated by the wall of the heat exchanging component of the reactor heat removal circuit (SG in PWRs, turbine condenser in BWRs and IHX in LMFRs) should be the same, to ensure nuclear plant safety and reliability (or should at least be highly compatible with each other in order to avoid plugging of the core flow channels by the products of coolant interaction). The increase in the total cost of a nuclear power plant owing to the application of identical coolants in the primary and the secondary circuits and the use of a tertiary water/steam circuit is insignificant, since standard operation and maintenance of the SG, water circuit and turbine plant are applied. Separation of the reactor cooling system and heat to energy transfer system by an intermediate circuit also provides efficient passive core cooling.

Operating experience gained on LMFRs, such as BN-350, Phénix, PFR and BN-600, has proven that sodium is practically non-corrosive to stainless steel, and the impurities, mainly oxygen and carbon, are maintained at an acceptably low level by the cold traps installed in the bypass of the main coolant circuit. Hazardous radioactive isotopes (caesium, tritium, strontium and iodine) are retained by sodium.

The primary sodium activity in the reactor under operation, mainly determined by ^{24}Na (BN350 reactor, Kazakhstan), is about 10 Ci per kilogram of sodium [3.3]; after the reactor has been shut down for decommissioning, the residual activity of ^{22}Na is ~1×10^{-4} Ci per kilogram of sodium [3.4].

If any component of the primary sodium circuit is to be removed from the reactor for the purpose of repair/maintenance, sodium sticking to the surface must be removed because of the:

— Chemical reaction of sodium with oxygen and moisture in air;
— Radioactivity of sodium.

The process of radioactive sodium removal has been selected for reasons of safety, effective cleaning of different components, economics, etc.

Cover gas is another source of LMFR radioactivity. Primary gas activity is, to a considerable extent, determined by the impurities in sodium and activation of ^{40}Ar and ^{41}Ar. As a result of the (n, p) reaction, radioactive ^{23}Ne with a short half-life of 38 s is produced from ^{23}Na [3.5].

3.3.1.1.2. Sodium residual radioactivity

As was pointed out in Ref. [3.6], the amount of long lived radioactivity generated in sodium by neutrons is negligible. Activation of sodium reaches an equilibrium state in about ten years of the first cycle of its use and will never exceed this level. The long lived radionuclides furnished by fission products, sodium impurities and corrosion activation products are chemical elements alien to sodium that make possible its external contamination at the reactor plant decommissioning stage. Two strategies have been considered for the disposal of contaminated sodium:

— Separation of radioactive products from sodium, reuse of the purified sodium and conversion of the concentrated waste into an inert form for a permanent repository;
— Retention of radioactive sodium on the plant site for later use.

Analysis has shown that the sodium coolant of a 1 GW(e) LMFR after 50 a of operation and ~50 a of retention may be exempted for free use in industry or returned to the environment [3.6].

3.3.1.2. Low activity coolants: Lead, bismuth, mercury, lithium

Although both lead and mercury have relatively high capture cross-sections they have low activity. Most of the captures occur in the ^{208}Pb and ^{199}Hg isotopes to produce ^{209}Pb, a weak beta emitter, and ^{200}Hg, a non-radioactive isotope. The macroscopic capture cross-sections (in the fast spectrum) are relatively small for ^{204}Pb and ^{198}Hg, and even these captures are not extremely troublesome, since the radioactive ^{205}Pb has relatively low induced activities and emits gamma radiation of low energy, and ^{199}Hg is stable. An additional advantage is that external shielding requirements for lead and mercury are reduced because both metals have high densities and afford considerable gamma shielding [3.1].

Lithium is classified as a low activity coolant because its activation cross-section (^{7}Li) is small and because its activity consists entirely of beta particles from the decay of the ^{8}Li radioisotope. Beta particles are easily stopped by all materials, and the only problem is the bremsstrahlung X radiation that results when the 12 MeV beta radiation is absorbed. A coolant shield utilizing materials of low atomic number would greatly minimize the deceleration radiation problem [3.1].

3.3.1.2.1. Lead and lead–bismuth ‘operational’ radioactivity

The natural isotope of bismuth is ^{209}Bi (abundance ~100%). Neutron capture results in the formation of ^{210}Po by the following reaction:

$$^{209}Bi(n,\gamma)^{210}Bi \xrightarrow[5.0d]{\beta^-} {}^{210}Po \xrightarrow[138.8d]{\alpha} {}^{206}Pb_{st}$$

The small amount of ^{209}Po is formed from ^{210}Po by (n, 2n) reaction. ^{210}Po is an alpha emitter with a half-life of 138 d, and ^{209}Po decays in a similar way with a half-life of 120 a. Polonium is volatile at coolant operating temperatures, with some amount of it migrating to the cover gas, where it forms aerosols [3.7, 3.8]. Leaks of cover gas or coolant may cause contamination problems, and maintenance of components requires special measures to protect personnel.

Even in the case of lead coolant, the problem of polonium contamination exists because of ^{209}Bi formation by neutron capture in ^{208}Pb (abundance 52.3%) [3.9]:

$$^{208}Pb(n,\gamma)^{209}Pb\xrightarrow[0.14d]{\beta^-}{}^{209}Bi(n,\gamma)^{210}Bi\xrightarrow[5.0d]{\beta^-}{}^{210}Po\xrightarrow[138.3d]{\alpha}{}^{206}Pb$$

Although the rate of production of ^{210}Po by this two step process is much lower (1000 times lower), the fraction of polonium migration out of the coolant is higher (perhaps by ~100 times) because of the higher coolant temperature.

In Ref. [3.9] it is pointed out that in the reactor cooled by PbBi, the polonium activity value is determined by the reaction on the ^{209}Bi isotope, and the equilibrium activity is ~10 Ci/kg. As for the lead cooled reactor (5×10^{-4}% Bi), the polonium activity is determined by the reaction on both the ^{209}Bi and ^{208}Pb isotopes and may reach 5×10^{-4} Ci/kg by the end of the reactor service life.

The authors of Ref. [3.9] have noted that such PbBi coolant activity gives rise to problems even under normal operating conditions. They consider that in the case of a cover gas leak rate of 0.01% of its volume per day, release of ^{210}Po to the central hall may (if the gas circuit is not cleaned of polonium) cause it to exceed by 200-fold its maximum permissible concentration (MPC) [3.5]. To ensure that the MPC value is not exceeded for personnel in the central hall, it is necessary to comply with very strong requirements for leak-tightness of the reactor cover gas circuit.

3.3.1.2.2. Lead and lead–bismuth residual radioactivity

Experts in nuclear technology believe that the selection of a coolant for future nuclear facilities with a fast neutron spectrum should take into account the management and disposal of the radioactive waste arising from decommissioning of the nuclear power plant. According to specialists in the field, the post-operational characteristics of a reactor plant including spent coolant waste should be considered to be as highly important as those related to the operational stage. The primary circuit coolant of the nuclear power plant could be one of the main potential sources of radioactive waste.

The long term residual activities of sodium, PbBi and lead coolants of fast reactors are compared in Ref. [3.6]. It was found, that the specific α activity of a typical PbBi coolant is determined by the ^{210m}Bi (half-life = 3.6×10^6 a) generated in the ^{209}Bi (n, γ) ^{210m}Bi reaction. The long lived β activity of ^{208}Bi (half-life = 3.65×10^5 a) is produced in the ^{209}Bi (n, 2n) ^{208}Bi reaction.

The most important contributor to the specific long lived residual radioactivity of lead coolant is the ^{205}Pb (half-life = 1.51×10^7 a) generated in the ^{204}Pb (n, γ) ^{205}Pb reaction. The specific β activity of the pure lead coolant is significantly lower than that of PbBi. Activation of the PbBi and lead coolants will increase in every stage of recycling, if recycling is possible in principle [3.6].

Thus, the residual activity of PbBi and lead coolants is expected to last as long as millions of years. As is pointed out in Ref. [3.6], purification of PbBi and lead coolants from the long lived radionuclides of bismuth and lead (if it is possible) would be too expensive.

In the summary provided in Ref. [3.6], it was concluded that sodium coolant appears to be the most appropriate for realization of the goal of low waste among the three liquid metal coolants (sodium, lead, PbBi) considered.

3.3.2. Liquid metal boiling phenomenon

One of the characteristics of liquid metals is their high saturation temperatures at atmospheric pressure. They are of potential interest in boiling reactors because high temperatures can be reached without high pressures. Operation at low pressure, however, results in a large specific volume of the vapour. Hence the vaporization of a small fraction of the volume of liquid can yield a very large volume of vapour and lead to significant changes in

the flow behaviour of the fluid. Limited experience with boiling mercury flowing in tubes [3.10] has shown that boiling mercury void fractions and pressure drops can be calculated with the methods developed for water, despite the fact that the flow patterns are quite different for the two fluids.

Boiling on a heated surface can occur in different ways depending on:

— Whether or not the coolant temperature exceeds the saturation temperature (saturated or sub-cooled boiling);
— The magnitude of the temperature difference between the heated wall and the liquid (nucleate, mixed or film boiling);
— The method of circulation of the fluid (pool, natural circulation or forced convection boiling) [3.1].

Whereas almost all combinations of the above conditions have been investigated for water, much less information is available for liquid metals. All data available at present pertain to the experiments performed with the coolant at saturation temperature. Most tests have been run under pool boiling conditions and only a few in natural convection or in forced circulation.

The experimental temperature differences between a heated wall and a saturated liquid metal cover the range from nucleate boiling to film boiling. In nucleate boiling the temperature of the wall only slightly exceeds the fluid temperature; bubbles grow on the surface and cause an intense local agitation of the coolant, which promotes the transfer of heat and yields high heat transfer coefficients. When the temperature difference becomes larger, a point is reached where the surface is almost covered with bubbles, and a maximum heat flux (critical heat flux) is obtained. At this point the liquid cannot reach the surface as easily, and the heat transfer coefficient decreases with further increases in temperature driving force (mixed or unstable film boiling). A further increase in temperature difference causes a complete vapour layer to form at the surface, which becomes physically isolated from the bulk liquid (film boiling).

The transfer of heat does not occur by direct contact with the liquid but by conduction and radiation through the vapour layer. Since this layer has a low thermal conductivity, the heat transfer coefficient drops considerably in film boiling. In liquid metals the contact between the liquid and the wall can be lost not only by the presence of a vapour film but also by poor wetting conditions which decrease or prevent actual contact between the liquid and the wall. Thus, film boiling and the corresponding low values of heat transfer coefficient can also be found at low temperature differences if the liquid does not wet the wall. Wetting has been shown [3.10] to have little effect on pressure drop, but the wetting characteristics of the coolant must be determined before boiling heat transfer coefficients can be predicted. Improving the wetting characteristics of the fluid (e.g. addition of sodium (0.1%), or magnesium (0.02%) and titanium (0.0001%), to mercury) increases the heat transfer coefficient by a large factor [3.1].

3.3.2.1. Sodium boiling phenomenon in tube bundles

The achievable positive reactivity ramp rate upon sodium boiling depends both on the total reactivity vested in the coolant and on the rate at which it can be boiled away.

Historically, the desire to lower the amplitude of the positive coolant void in a fast spectrum reactor was driven by concerns about extremely high rates of sodium voiding. These concerns had several origins. First were the observations in controlled experiments that high superheat (up to ~260°C) in the liquid sodium could be attained before any vapour was formed. This would have implied that once vapour began forming, the entire superheated coolant inventory in the core could void almost instantaneously without further heat addition. Second was the potential for vapour explosions wherein extremely high temperature fuel suddenly breached through cladding and mixed intimately with liquid sodium [3.11]. Finally, any case of rapid voiding could result in high positive reactivity ramp rates which might act faster than the negative feedbacks could respond and would take the core into the super prompt critical range.

However, experimental data on boiling in the tube bundles have since shown that the in-core sodium boiling process in fact does not reach high superheat, but rather comprises a series of local pressurization and flow reversals which voids part of an assembly for a short period of time. Detailed analyses have shown substantial spatial and temporal incoherence in the boiling process, with incoherent chugging and a few assemblies ‘leading’ the rest of the core. This behaviour reduces the achievable run out potential as a safety concern. The trade-offs have reduced the reactivity insertion ramp rate — even for cores with several dollars of positive sodium void reactivity — to values less than several tens of dollars per second. Such ramp rates allow time for negative reactivity feedbacks to

act. In the case of the vapour explosion potential, the temperature and energy content reached by the fuel prior to fuel–coolant mixing itself depends on the ramp rate as well as on the physical properties of cladding and fuel and on the scenario, i.e. whether sodium is present or already voided upon cladding breach. Thus, as pointed out in Ref. [3.11], "one cannot a priori rule out the potential need to reduce the coolant void worth as the means to limit the ramp rate".

3.3.3. Coolant reactivity coefficient

The influence of the coolant on critical mass and reactor stability is determined from the coolant reactivity coefficient. This coefficient consists of three components resulting from the effect of the coolant on neutron leakage, spectrum and absorption.

The coolant scatters neutrons and reduces leakage from the core. This component, the leakage component, of the coolant reactivity coefficient is positive. Its importance decreases with core size. In small reactors it is often the dominant effect. Of the liquid metal coolants, the leakage component is most important for lead and mercury because of their large scattering cross-sections.

The spectral component of the coolant reactivity coefficient arises because elastic and inelastic neutron collisions with coolant atoms soften the spectrum and affect reactivity through a change in the effective probability of fission absorption. This component can be either positive or negative depending upon the reactor composition, i.e. the type and amount of fissile, fertile and structural material in the core. The spectral component is more important for lithium, sodium and mercury than for the other liquid metal coolants.

Neutron absorption, a negative reactivity effect, is very small for sodium, potassium, NaK and lead, but it becomes quite important for lithium and mercury, both of which have relatively large capture cross-sections for fast neutrons. The value (sign and magnitude) of the coolant reactivity coefficient depends upon the importance of each component and is a strong function of reactor design as well as the choice of coolant [3.1].

3.3.3.1. Sodium void reactivity effect

Large conventional LMFR cores show a significant reactivity increase, if a coolant loss occurs by boiling or gas intrusion. Since this positive reactivity effect is very important for the overall behaviour of LMFRs from a safety point of view, many attempts have been undertaken worldwide to reduce the sodium void reactivity effect (SVRE).

Sodium has a comparatively high boiling point (~1000°C) at coolant pressure within the reactor core. Therefore, some experts consider that in the LMFR, an increase of the coolant temperature should initiate an expansion of the absorber rod guide structure of the fuel in the axial direction and of the core grid plate in the radial direction, resulting in negative reactivity coefficients counteracting the positive sodium void coefficient in large LMFRs. At the same time, taking into account that the cooling disruptions and sodium boiling might be on a time scale much shorter than the time scale of the passive negative feedback, there is a strong incentive to reduce the positive sodium void coefficient in large LMFRs.

One proposal to reduce the SVRE was made by the Russian Institute of Physics and Power Engineering, in which the core upper axial blanket is replaced by a sodium plenum consisting of sodium filled wrapper tubes. In this case, the enhanced axial neutron leakage would result in a strong negative reactivity effect in the event of sodium voiding which would compensate for a large fraction of the positive SVRE in the core region. The IAEA and the EC joint benchmark programme assessed the capability of reducing the SVRE of such an innovative core design. It was shown that overall SVRE for the reference 2100 MW(th) mixed oxide (MOX) fuel core might be close to zero. This method of reducing the SVRE has been adopted in the BN-800 reactor design in the Russian Federation.

However, investigations were needed to determine differences in severe accident responses in order to estimate the feedback to overall safety that could be achieved by a reduction in the SVRE value for the MOX fuel reactor core. Therefore, recognizing the importance of such an innovative LMFR core design, a comparative study of severe accidents for a BN-800 type reactor with a reduced sodium void coefficient was jointly undertaken by the IAEA and the EC during 1994–1998 [3.12]. The consequences of the accidents considered in this comparative exercise depend on the design details given in the case set-up and on the level of detail of theoretical analyses.

Thus, conclusions can only be drawn related to the specific cases considered in this exercise and deduced from results of the specific calculations.

The main advantages of the specified innovative BN-800 type core design are in providing for an additional inherently activated safety margin of preventing fuel pin failure or local boiling in the domain of operational and severe transients to be considered in the design basis. These features complement the large margin to fuel pin failure already achieved with the hollow pellet fuel pin design and a cladding material providing ductility even under high dose loads. Evaluation of the impact of the specified core design features on the core behaviour during operational transients and stability analyses were not part of this exercise. This would have required other theoretical approaches to evaluate the problems potentially involved. In the beyond design basis accident domain, which has extremely low probability and should be categorized as residual risk, some clear advantages of the innovative core design have been identified.

3.3.4. Effect of coolant on critical mass and on the temperature coefficient

With the exception of lithium, the liquid metal coolants contribute relatively little to the total reactivity. In large plutonium fuelled fast reactor cores, the sodium worth is positive, providing a reduction in critical mass. On the other hand, a reactor whose coolant has a negative reactivity coefficient requires an increase in critical mass to compensate for the coolant. In a large mercury cooled fast reactor [3.1], the coolant reactivity coefficient is negative, and thus a 2% increase in critical mass is required. Compared with other liquid metals, lithium has an appreciable effect on critical mass because of its strong absorption and neutron energy degrading properties.

In considering the coolant temperature coefficient, the leakage effect tends to make the coefficient negative, the absorption term tends to be positive, and the spectral term is either positive or negative depending on the reactor spectrum and composition.

Lead, sodium, potassium and NaK are less likely to give rise to positive coolant temperature coefficients of reactivity than are the other liquid metal coolants because of their smaller effect on the spectrum and their small capture cross-sections. For these coolants, the negative leakage component is most likely to be dominant in all but the largest reactors.

Almost all small experimental sodium cooled fast reactors have negative coolant temperature coefficients of reactivity. In these reactors the positive absorption component is insignificant compared with the spectral and leakage components, both of which are negative. However, the tendency in power fast reactor design is toward larger cores, increased concentrations of fertile (threshold fission) material, and the use of ^{239}Pu rather than ^{235}U as the fuel. These factors tend to make the leakage term less important and the spectral term more positive [3.1]. The net result is that the spectral component may be positive and larger in absolute magnitude than the negative leakage term, and thus a positive sodium temperature coefficient will exist.

Natural lithium has very strong absorption for fast neutrons. Consequently the absorption component of its temperature coefficient is strongly positive, and the sign of its net temperature coefficient depends upon the sign and magnitude of its spectral component, since its leakage term is comparatively small. The strong positive absorption component of lithium can be eliminated by using lithium from which the ^{6}Li isotope has been removed, since its absorption cross-section is almost entirely due to the (n, α) reaction in this isotope.

Mercury also has a very strong neutron absorption and energy degrading properties. However, its energy degradation is mainly by inelastic scattering at high energies, and this tends to make the spectral component of the coolant temperature coefficient positive in reactors that have a significant amount of the threshold fission or fertile material in the core. In a large fast breeder mercury cooled reactor, the coolant temperature coefficient of reactivity will probably be positive no matter what fissile material is used [3.1].

3.3.5. Coolant interaction with metals

The interaction of solids and liquid metals can be one of direct chemical attack, dissolution or chemical reaction with liquid metal impurities such as oxygen. Direct chemical reaction is rare. Dissolution is pertinent and can usually be detected only in a non-isothermal system. Impurities are important in corrosion of metals, thus test results should be carefully evaluated. The following sections discuss the reaction of liquid sodium, NaK, lithium, lead, PbBi, and mercury with metals.

3.3.5.1. Metals versus sodium, potassium and sodium–potassium alloy

When its initial carbon content is low, sodium decarburizes carbon steel by a diffusion mechanism. On the other hand, stainless steel carburizes when the carbon present in the sodium exceeds an equilibrium value. The equilibrium value for uncarburized 304 stainless steel at 1200°F is reported to be 15–18 parts per million (ppm) of carbon in sodium.

Mass transfer occurs in a flowing non-isothermal liquid metal system at a rate that is dependent upon the maximum temperature and the temperature difference. The mass transfer of common structural materials in sodium or NaK systems is probably solution rate limited rather than diffusion limited. The limiting process has not been qualitatively or quantitatively confirmed for Inconel–sodium or Inconel–NaK systems. Oxygen and water vapour form oxides, which increase mass transfer, although mass transfer in reasonably clean systems with less than 50 ppm of oxygen does not usually become important until the coolant temperature rises above 1100–1200°F.

Figure 3.1 is a bar diagram indicating the resistance of various materials to sodium and NaK. In general, ferrous metal welds are not attacked preferentially by sodium and NaK.

Comprehensive studies have been performed and reliable industrial experience has been gained on material corrosion in sodium. Corrosion intensity in sodium is significantly lower than that in water or lead based coolants [3.13]. In sodium, as well as in other liquid metals, the corrosion rate depends on many factors (temperature level, coolant velocity, impurity content, temperature difference, time, etc.). When evaluating corrosion rate, the majority of researchers took into account only the most important contributing factors.

Empirical equations for the corrosion rate were most commonly derived for 316 steel at a coolant velocity of >4 m/s and an oxygen content of ≤10 ppm. The most reliable results were obtained in Ref. [3.14] for corrosion rate K, $mg \cdot cm^{-2} \cdot h^{-1}$, which can be expressed as follows [3.4]:

$$K = 0.61\left(C_o\right)^{1.5} \exp\left(-\frac{18000}{RT}\right)$$

It was found that chromium alloyed and austenitic steels have high corrosion resistance. The equivalent corrosion rate of two steels such as HT-9 and Fe9Cr1Mo was measured after their exposure during 4000 h at 600 and 650°C temperature, 6 m/s flow velocity and 1 ppm oxygen content. The results of measurements are given in Table 3.3 [3.4, 3.15–3.18].

TABLE 3.3. CORROSION RATE OF STEELS IN SODIUM

Material	Equivalent corrosion rate, μmm/a	
	600°C	650°C
HT-9	1.15	3.1
9Cr1Mo	0.7	2.3

The operating experience of a number of LMFRs has shown that sodium is practically non-corrosive with respect to stainless steel, with the content of impurities, mainly oxygen and carbon, being held at an acceptably low level by the cold traps.

3.3.5.2. Metals versus lead, bismuth and lead–bismuth [3.19–3.26]

Lead, bismuth and sodium have been studied since the 1940s. The Russian Academician Alexander Leipunskiy at the Institute of Physics and Power Engineering considered mercury, lead and sodium (but adopted sodium) for fast reactors (following ANL) and PbBi for submarines (substantial experience since the 1950s, including accidents). In the early stages of development, the formation of deposits of lead oxide and other impurities posed problems. Careful control of the purity of the coolant was required to avoid the formation of such deposits. It was necessary to develop corrosion resistant steels and to pretreat the surfaces of components, and to use special inhibitors in the PbBi coolant. More extensive studies were required for lead coolant to demonstrate the corrosion resistance of structural material.

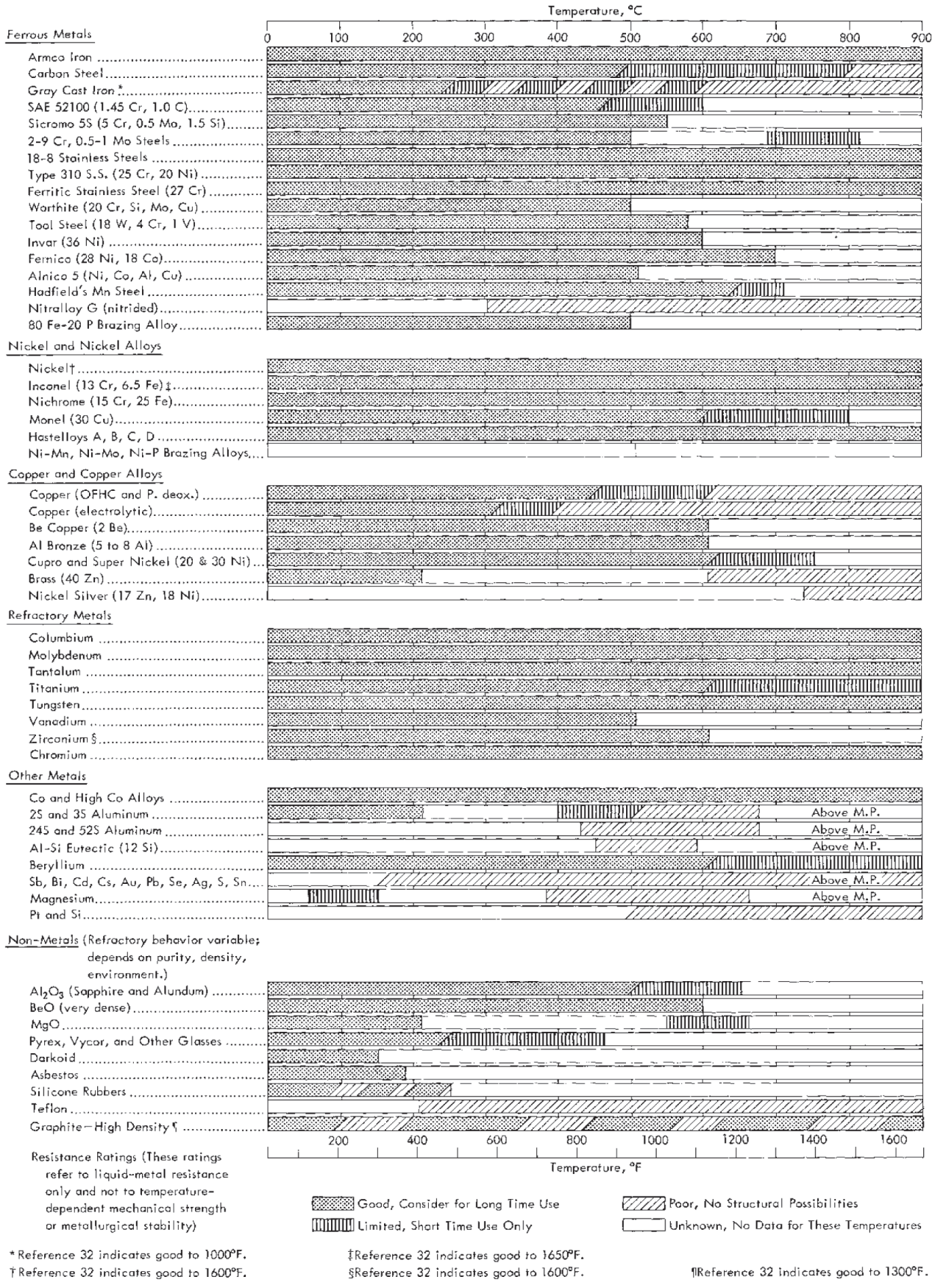

FIG. 3.1. Resistance of materials to sodium and sodium–potassium [3.1].

The development of corrosion resistant structural materials is apparently the main problem in lead cooled reactor technology. Lead exhibits a strong erosion/corrosion effect on structural materials: material dissolving, embrittlement (loss of elasticity of a material, making it brittle), mass transfer and inter-granular penetration of lead.

The most resistant to lead are the refractory metals followed by chromium steels and austenitic steels, being less resistant because of the high solubility of the incorporated nickel. Stabilization of austenitic steels by Ti, Nb and Mo enhances their resistance to lead.

The main type of corrosion damage in liquid lead, bismuth and PbBi is the dissolution of structural materials (steels) and their components in these coolants. The kinetics of dissolution processes can be of a different nature. For example, in some cases the dissolution is localized on boundaries of grain, causing interstructure infiltration of liquid metal (lead, PbBi) into steel.

The basic kind of corrosion damage that is the most dangerous for structural materials both in PbBi and in lead coolants is local corrosion of materials appearing as separate corrosion/erosion centres ('pitting'). Local leaks or defects through corrosion damage of structural elements may appear at temperatures over 550°C after holding for some one hundred hours under the following conditions: imbalance of alloying elements and impurities in steel, poor quality of metal, absence of coolant quality control and non-optimal coolant flow regimes.

The principal solutions ensuring high corrosion resistance of structural materials in heavy liquid metal coolant were found using oxygen dissolved in the coolant. It has been shown as a result of long term studies that this corrosion resistance essentially depends on the concentration of dissolved oxygen.

Upon reaching a certain level of concentration of dissolved oxygen, the corrosion process is stopped due to the formation of a protective oxide film on the steel surface. At high temperatures, an indispensable condition of corrosion inhibition is the presence of silicon in steel as an additional alloying element. The silicon content in steel varies within a range of 1–3.5% depending on the type of steel.

Oxide films formed on the steel surface prevent it from interaction with liquid lead. Since breakdown of oxide films is possible during operation, precautions must be taken for maintaining their thickness and density.

Thus, steel corrosion in molten lead can be significantly slowed down by the oxide film formed on the steel surface. The main technological problem is maintaining such oxygen content in the coolant, which, on the one hand, would provide stability of oxide film (Fe_2O_4) on the steel surfaces, but, on the other hand, would preclude generation of lead oxide (PbO) in the coolant, which could result in the circuit slagging.

There are some ranges of oxygen content dissolved in lead that meet these two conditions, for example, the ~5×10^{-6} to 10^{-3} wt% range. The oxygen content in lead can be controlled by injecting gaseous oxygen or dissolving solid PbO. The required oxygen content in lead can be maintained in two ways:

(1) Bubbling of an argon, hydrogen and water vapour mixture or gaseous oxygen through molten lead;
(2) Lead oxide filling through the same system by which the molten lead is pumped.

In order to change the oxygen content and remove surplus PbO, reactions with water vapour or hydrogen can be used. To determine the oxygen content in the molten lead (similarly to PbBi technology development), a galvanic cell can be used. The problem of hyper thermal corrosion resistance of structural materials was overcome by the development of preliminary protective coatings for the working steel surfaces. In particular, the most important structural units of the circuit, e.g. fuel rod cladding and SG tubes, are covered by these coatings at the final stage of their manufacture. Additional barriers are also formed directly on the inner surfaces of the liquid metal circuit under the effect of the coolant in the early stage of the reactor operation.

The best results using preliminary oxidation of circuit components were achieved by application of media with low partial pressure of oxygen, namely PbBi-O, H_2O+H_2 and CO_2. These methods, first of all, make it possible to avoid the critical kinetic stage of preliminary passivation of the uncoated surfaces of steel structures of the circuit. Moreover, they prove to extend the range of permissible decrease of oxygen concentration in the coolant.

Therefore, the basic factors ensuring high corrosion/erosion resistance of structural materials in heavy liquid metal coolant (lead, PbBi) are as follows:

— Application of silicon alloyed steels;
— Passivation by oxygen using special regime of coolant;

— Use of additional corrosion barriers such as oxide films formed on the working surfaces of circuit components under reactor startup conditions.

In the reaction of PbO reduction, water vapours are efficiently removed from the circuit. Small amounts of moisture act as a diluted oxidizer, preventing reduction conditions for oxide films on the steel surface.

Parameters of all these processes have to be developed with the necessary control of hydrogen content in cover gas and oxygen activity in liquid lead.

Preliminary studies have shown that, in principle, the possibility exists to develop the technology mentioned, but it should be noted that conditions of experiments did not correspond to those of real operation.

The tests performed on the experimental and industrial facilities showed that the corrosion rate for chromium steels in PbBi alloy is 6–60 mg/m^2 per hour at 450–500°C. This can vary with temperature, coolant velocity, oxygen content and other parameters. In lead, this value is about 0.026 mg/m^2 per hour at 600°C with no mass transfer. According to the latest data [3.25, 3.26]:

— Corrosion resistance of ordinary austenitic and ferritic steels (316L and T-91 type) in the heavy metal coolant flow is experimentally confirmed up to temperatures of 450–500°C. The duration of tests reached 7 000–10 000 h.
— Corrosion resistance of silicon-containing steels in lead flow has been experimentally confirmed up to a temperature of 650°C at a test duration of 16 000 h. In PbBi flow, the corrosion resistance is confirmed up to a temperature of 600°C at a test duration of more than 25 000 h. The tests are ongoing. The results obtained and the level of the heavy metal coolant technology achieved allow a new engineering stage of development of fast reactors with heavy metal coolant.
— The increase of corrosion resistance of materials in the heavy metal coolant may be achieved due to new nanostructure barriers on the steel surface. Such types of barrier can be created in the future by application of ‘pulsed electron beam modification’ technology.

PbBi technology has made much progress; silicon alloyed ferritic-martensitic steels have been developed. This technology has been studied for lead, and steels have been tested for 15 000 h since the late 1980s.

3.3.5.3. Metals versus lithium [3.1]

Tests indicate that lithium is more aggressive in its corrosive attacks on most metals than either sodium or NaK alloys, although the questionable purity of the lithium used in most tests may make the results somewhat misleading. Among the contaminants commonly dissolved in lithium, or mechanically dispersed in it as lithium compounds, are nitrogen, oxygen, chlorine, hydrogen, calcium, aluminium, iron, silicon, sodium and carbon. Few data exist on corrosion as a function of the amount of contamination of lithium by these impurities.

Lithium nitride, which is readily formed by the reaction of nitrogen with liquid or solid lithium, is a very reactive compound. No metal or ceramic material has been found to be resistant to molten nitride, although it has been tested with all the common metals and with their oxides, nitrides and silicides, as well as with porcelain.

Oxygen is more often present in solid lithium as a hydroxide than as an oxide. Molten lithium hydroxide is very corrosive and, again, no refractory or metal has been found to be suitable for its containment. When heated above its melting point, 455°C (851°F), the hydroxide tends to decompose to form oxide.

Lithium hydroxide or oxide can combine with many refractories and in this way can either remove protective oxide films from metals or, in some cases, add to the thickness of the films. The hydroxide also attacks metals, including those which form acidic ions, such as iron and platinum. Molten lithium chloride attacks iron and copper. This compound is generally found in commercial lithium, although some lithium is chloride free. Lithium hydride, which is likely to be present in molten lithium that has been exposed to moisture or to hydrogen, is reactive with metals and ceramics at high temperatures.

Most of the reported corrosion tests used commercial lithium of questionable, and certainly not consistent, purity. Many of these tests were carried out in containers of a dissimilar metal, and mass-transfer effects obscured the results. In some cases the lithium was first freed from oil by treatment with petroleum ether and then passed through a sintered stainless steel filter. In other cases no attempt was made to free the lithium from inorganic contaminants or from traces of protective oil.

Oak Ridge National Laboratory has conducted experiments on the purification of lithium by means of filtration, vacuum distillation and gettering with active metals, such as titanium, zirconium and yttrium [3.1]. Filtration through stainless steel filters at 250°C did not reduce the nitrogen or oxygen content of lithium. Vacuum distillation at 650°C and 10^{-4} mm Hg was also ineffective in removing nitrogen or oxygen. Titanium and zirconium were very effective in removing nitrogen from lithium at 816°C but were not effective in removing oxygen. Titanium gettering was used in test batches to produce lithium with an oxygen content of less than 10 ppm. Preliminary studies of yttrium in lithium at 816°C show that yttrium is more effective than titanium or zirconium in reducing the oxygen content of lithium. Tests with yttrium turnings in lithium at 816°C resulted in lithium with less than 100 ppm each of oxygen and nitrogen.

Attempts to melt most commercial lithium in quartz result in almost immediate failure of the container. Quartz appears to have good resistance to pure lithium at temperatures up to 285°C but not to lithium oxide or nitride. At higher temperatures the materials react to form lithium silicide. Glass has no resistance to attack by commercial lithium at 150°C, although lithium has been vacuum distilled in glass containers under carefully controlled conditions.

Porcelain and other silicates are attacked by liquid lithium. Molten lithium penetrates magnesia but does not otherwise attack it, whereas molten lithium attacks most other oxides of structural metals and also attacks carbides, silicides, rubber and plastics.

3.3.5.4. Metals versus mercury [3.1]

Mercury can attack materials by chemical combination, by alloy formation and by dissolution. The resistance of the material to wetting by mercury is a factor in its resistance to degradation by the above mentioned modes of attack; if the material is not wetted by mercury, it will not be affected by the mercury.

The rates and degrees of all three modes of attack by mercury are temperature dependent. In dynamic systems where mercury contacts its containment material at a high temperature and then is transported to and cooled in another section of the system, mass transport and precipitation of the containment material in the cooler portion of the system can be appreciable, even with low (a few parts per million) solubility of the containment material in mercury.

Some of the pioneering work on the determination of the resistance of engineering materials to mercury at elevated temperatures was performed in the USA [3.1] in connection with the development of the mercury vapour turbine by the General Electric Company [3.1]. Investigations of the mercury corrosion of numerous metals, alloys and non-metals have been made by a number of national laboratories and by private research organizations under federal government contracts.

In some short term corrosion tests [3.1] performed in mercury at 900°F, Ta, W, TiC, WC and Mo + 0.5wt% Ti showed no measurable attacks, and low-carbon steels and 400 series stainless steels showed very slight attacks, about 2 on a scale using 100 as a maximum attack rating. The 300 series stainless steels showed about 7 for the severity of corrosion, as did the low-carbon steels; in comparison, nickel alloys (Ni >20%) and nichrome had about three times as great a corrosion attack, with a rating of about 45. The metals showing the poorest resistance to mercury corrosion of all the metals tested, with a corrosion attack rating of about 88, were titanium, platinum, manganese, magnesium, aluminium and zirconium. It has been found [3.1] that low alloy steels containing 4–6 wt% chromium, 0.5 wt% molybdenum and 1–2 wt% silicon have better resistance to attack by mercury than do the low carbon steels.

This suggests the possibilities of using duplex materials consisting of a low carbon or low alloy steel layer (for the contacting surface) metallurgically bonded to an austenitic stainless steel or a nickel based alloy to provide the elevated temperature strength or mercury service up to 650°C.

In thermal convection loop tests it was found that the corrosion of the ferrous based alloys by mercury could be significantly reduced by dissolving small amounts of titanium in the mercury. The explanation of the corrosion inhibition mechanism was that the titanium reacted with the nitrogen and carbon in the ferrous materials and formed a thin film of TiC and TiN on the surface, which served as a barrier between the mercury and the container material.

Much work has been done on the resistance of engineering materials to attack by mercury. Considerable work is in progress, but much more has to be performed, particularly on the effect of impurities in mercury on its

corrosion of materials and on the purposeful addition of certain impurities to mercury to inhibit its corrosion of its containment material.

3.3.6. Sodium interaction with water and air

Sodium is chemically reactive. Hot sodium reacts vigorously with water and catches fire when it comes into contact with air, emitting dense clouds of white sodium peroxide smoke. According to the results of the materials engineering investigation, sodium coolant has good corrosion characteristics.

Sodium is an electropositive metal. Various chemical reactions between sodium and water are possible under proper conditions. Since it is ahead of hydrogen in electric tension, Na displaces H_2 out of water with the production of hydroxide: NaOH. When interacting with dry hydrogen, sodium forms NaH, which is soluble in sodium [3.4]:

$$2Na(s) + H_2(g) \rightarrow 2NaH(s) + 57.4 \text{ kJ/mol}$$

At a temperature of 420°C, NaH is decomposed with the release of hydrogen. This fact should be taken into account when a gas-tight vessel is heated.

When sodium interacts with a small amount of oxygen, Na_2O is produced, whereas its burning in air results in Na_2O_2:

$$4Na(s) + O_2(g) \rightarrow 2Na_2O(s) + 416 \text{ kJ/mol}$$

$$4Na(l) + O_2(g) \rightarrow 2Na_2O(s) + 436 \text{ kJ/mol}$$

$$2Na(s) + O_2(g) \rightarrow 2Na_2O_2(s) + 499 \text{ kJ/mol}$$

In the molten sodium, only Na_2O is stable, while Na_2O_2 dissociates as follows:

$$Na_2O_2 + 2Na \rightarrow 2Na_2O$$

When sodium interacts with water, some reactions occur and, depending on the reaction temperature, impurities of different composition will be present in the sodium.

Hydroxide is produced by the following reaction at 200–300°C:

$$2Na + 2H_2O \rightarrow 2NaOH + 142 \text{ kJ/mol}$$

Oxide as well as hydroxide is produced at 350–400°C:

$$2Na + NaOH \rightarrow 2Na_2O + NaH$$

$$2Na + H_2 \rightarrow 2NaH$$

At T > 420°C, hydride dissociates and the reaction goes escaping intermediate stages:

$$2Na + H_2O \rightarrow Na_2O + H_2$$

A burning reaction is characterized by a zone of small flames at the sodium–air interface, formation of Na_2O on the sodium surface and vigorous emission of high density white oxide fumes. However, this burning causes relatively low heat release, ~ 420 kJ/mol by Na_2O or 500 kJ/mol by Na_2O_2. This is equivalent to about 10 kJ (~2 kcal) per gram of sodium burned, being approximately equal to that for one gram of sulphur, one third of a gram of magnesium or aluminium, and less than one quarter of a gram of gas/oil. With the same volume of fuel, sodium burning results in an energy release equal to 50% of that for sulphur, 30% of that for gas/oil, 25% of that

for magnesium and slightly over 10% of that for aluminium. In a system where sodium can come into contact with water, provisions should be made for pressure relief and the prevention of hydrogen ignition.

Perhaps there is only one disadvantage inherent in the LMFR coolant liquid sodium, namely that it interacts chemically with air and water/steam. Therefore, providing integrity of the sodium circuits is the most important requirement to observe in the LMFR design, construction and operation tests.

The solution to the problem of the reliable elimination of coolant leaks is determined by the application of experimentally and analytically proved design, structural materials, manufacture and installation, as well as of quality control at all stages of LMFR component manufacture. Technological procedures and approaches, as well as quality criteria, should strictly correspond to the related regulatory documents.

The attempt to use sodium in on-ground solar batteries has failed. The large facility at Almeria, Spain, used sodium to transfer heat from the solar battery to water and steam. Seventy tonnes of sodium was used to transport the solar energy, which the mirror concentrated on a boiler to the SG, which turned a 500 kW(e) generator. On 18 August 1986, in order to work on the sodium circuit, the operators cooled the piping to freeze the sodium at ambient temperature and then cut the circuit. However, a problem occurred with the formation of the solid sodium plug, and pressurized sodium spewed through the cut that had been made, splashing off the nearby steel structures and causing a fire in the hall. Failure to observe special requirements for maintenance of the sodium components resulted in large amounts of sodium (14 t at 225°C) pouring out and burning in the atmosphere; the temperature reached an estimated 1200°C in approximately 15 minutes. Considerable damage was caused to the components, the metallic beams became distorted and a hole was blown in the roof, and the facility was closed down. This accident had large repercussions, giving rise to LMFR design modifications (both for operational reactors and for those under development) aimed at the confinement of possible leaks and the protection of components and building structures against sodium fire. This accident accelerated R&D and code development with respect to spray fires.

3.3.7. Coolant interaction with shielding materials

3.3.7.1. Graphite

Protection of fabricated graphite (used in fast reactors, for example, as shielding material) blocks from direct contact with molten sodium under reactor operating conditions is essential. Sodium in the temperature range of 320–540°C is initially non-wetting to graphite; but, in a matter of minutes, this condition changes and the sodium attacks the graphite. The result is graphite swelling and, in some cases disintegration of the graphite. Linear expansion of the order of 1% has been observed in 100 h at 540°C. The initial attack is grain-boundary penetration and pour filling, probably accompanied by inter-lamellar compound formation. Vacuum deposition, electroplating, electroforming, flame spraying and vapour decomposition of a metal halide have been used for deposition of chromium, nickel, zirconium, zirconium carbide, tungsten carbide, silicon carbide, silicon nitride and molybdenum disilicide on graphite test specimens. Although these coatings do protect the graphite from sodium attack, failure occurs owing to pinholes in the coating. Even if a pore-free coating were attainable on small laboratory specimens, it is doubtful that the same technique would result in a pore-free structure on a graphite block of large dimensions.

Corrosion (i.e. weight loss) of graphite by liquid sodium occurs at significant rates only when a ‘sink’ is available to remove the carbon that enters the sodium. In circulating sodium in contact with graphite, mass-transfer effects have been observed that result in carbon removal from the hot regions and deposition in the colder regions. Appreciable graphite corrosion rates have also been observed in isothermal systems where carburization of the container material occurred. At sufficiently high temperatures, carbon enters the sodium and produces carburization of stainless steel and zirconium surfaces without physical contact between these metals and the graphite. In experiments where nickel was the container material and the only metal present, negligible corrosion of the graphite occurred. Since nickel does not carburize, no ‘sink’ was provided for removal of the carbon. The equilibrium carbon content in the sodium contained in these nickel capsules proved to be a function of operating temperature; it was approximately 2000 ppm after operation at 750°C and zero after operation at 525°C.

The mechanism by which carbon enters the sodium has not been firmly established. Suggested mechanisms are (i) the true solution of carbon in sodium and (ii) the formation of Na_2C_2, which decomposes at lower temperatures. However, no Na_2C_2 was observed in any of the capsule tests.

Carburization of stainless steel was not observed below 550°C but was noticeable at 600°C and increased with higher temperatures. Zirconium also showed carburization at 750°C but not at 600°C or below.

Tests have shown that corrosion and dimensional stability of irradiated graphite in liquid sodium are significantly worse than for un-irradiated graphite under similar conditions. Hot graphite immersed into cooler liquid sodium may be fractured by thermal shock. It appears that wetting, in addition to a sufficient temperature difference between the solid and the liquid, is a necessary condition for this type of failure [3.1].

3.3.7.2. Concrete

Only sketchy information is available on the effect of liquid metals on concrete. Preliminary results from drop-wise or spray tests indicate a random surface granulation of a limited depth. Reported accidents involving a large amount of hot (800°F) sodium and a small amount of exposed concrete surface, however, resulted in gross granulation and bulk failure of the concrete. In the latter cases the water of hydration apparently reacted with the liquid metal involved [3.1].

3.3.7.3. Serpentine

Serpentine is an asbestos mineral, i.e. a hydrous magnesium silicate, with the formula $3MgO2SiO_2 \cdot 2H_2O$. The water of hydration in serpentine amounts to about 13.5 wt%. A remarkable characteristic of this substance is that it has the ability to retain its bound water to a much higher temperature than is normally the case with hydrated molecules. The rock has a lump density of between 2.55 and 2.65 g/cm^3 (160–165 lb/cu ft). It can be piled

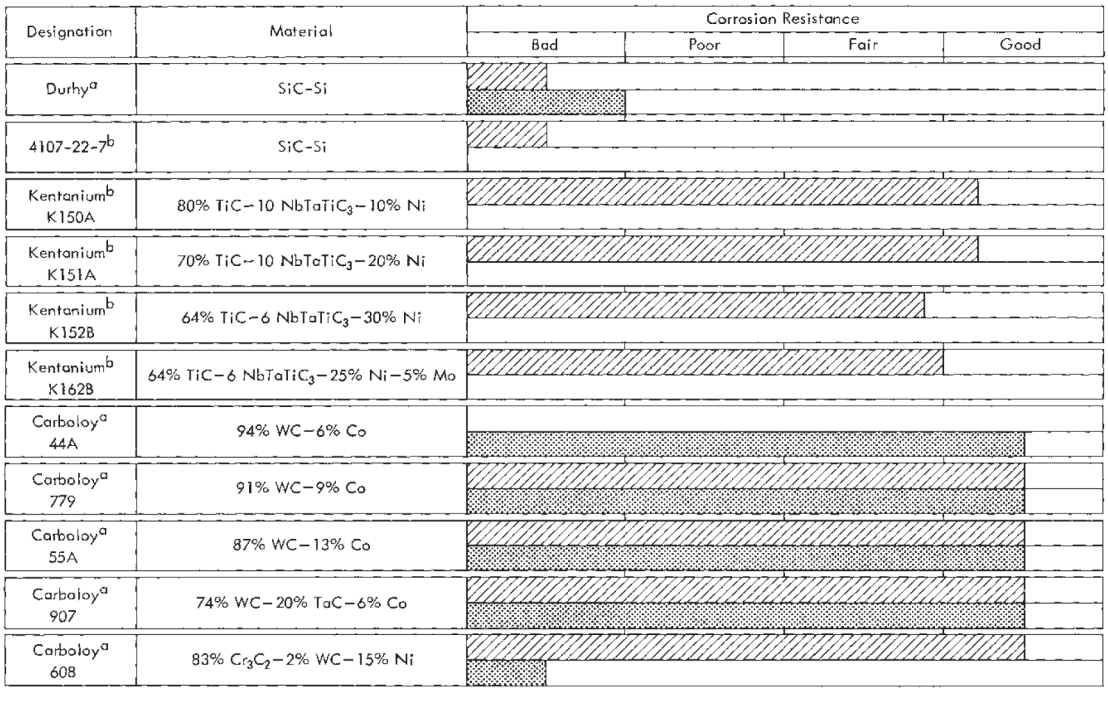

Na

Pb

[a]Static Test
[b]Seesaw Test
Hot Zone: 1500°F
Cold Zone: 1150°F

Type of Data	Arbitrary Corrosion Ratings and Data Range Bases			
	Bad	Poor	Fair	Good
Depth of attack, mils*	3	2	1	0
Weight change, %†	6	4	2	0
Dimensional change, %	3	2	1	0

* Measured in metallographic examinations.
† Determined by direct measurement and/or by calculations based on the material(s) found in the test medium by chemical analyses.

FIG. 3.2. Corrosion resistance of cermet to sodium and lead [3.1].

loosely to a density of from 80 to 110 lb/cu ft. It can be easily crushed and tamped as a fine powder to a density of about 130 lb/cu ft. A little is known of the effect of liquid metals on serpentine [3.1].

3.3.7.4. Isolation materials

In general, insolation materials do not hold up well in a liquid metal environment. Most reported test data show attack in varying degrees. Many specimens which cured at 540°C with no colour change showed drastic changes at 510°C due to the action of sodium. As noted in Ref. [3.1], the materials that showed the least disintegration and the greatest preservation of mechanical properties were superex paste and eagle-pitcher mineral wool. The uncured superex block did not hold up as well as superex paste, presumably because of the presence of water of crystallization. After the blocks were cured, their behaviour was similar to that of the paste. The refractory clays show the greatest degree of destruction. The time element is of vital importance, since a long period of contact with liquid sodium presumably results in complete destruction of every specimen tested [3.1].

3.3.7.5. Ceramic and cermet materials

Cermet and ceramics show generally good resistance to corrosion by liquid metals. The ceramics, essentially inert to chemical reaction, show good corrosion resistance to mercury, sodium and NaK, with less resistance to lithium. Figure 3.2 gives an indication of the corrosion resistance of various cermet and ceramics to sodium and lead [3.1].

REFERENCES TO SECTION 3

[3.1] FRIENDLEND, A.J., "Coolant properties, heat transfer, and fluid flow in liquid metals", in Fast Reactor Technology: Plant Design (YEVICK, J.G., AMOROSI, A. (Eds)), The MIT Press, Cambridge, MA (1966).

[3.2] PILARSKI, S., "Optimization of fast breeder reactors employing innovative Liquid metal coolants", Proc. of Global 2007 — Advanced Nuclear Fuel Cycles and Systems, Boise, Idaho, September 2007.

[3.3] INTERNATIONAL ATOMIC ENERGY AGENCY, Status of Liquid Metal Cooled Fast Breeder Reactors, Technical Reports Series No. 246, IAEA, Vienna (1985).

[3.4] INTERNATIONAL ATOMIC ENERGY AGENCY, Comparative Assessment of Thermophysical and Thermohydraulic Characteristics of Lead, Lead-Bismuth and Sodium Coolants for Fast Reactors, IAEA-TECDOC-1289, IAEA, Vienna (2002).

[3.5] "Standard of Radiation Safety of the Russian Federation" (NRB-96), Moscow, 1996.

[3.6] OUSANOV, V.I., et al., "Long-lived Radionuclide of Sodium, Lead-bismuth and Lead Coolants at Fast Reactors", Atomnaia Energia, **87** 9 (1999) 204–210.

[3.7] MOYE, H.V., "Polonium", Oak Ridge, Tennessee, July, 1956.

[3.8] "Polonium, Handbook of Inorganic and Organic and Metal Chemistry", 8th ed. Suppl., V.1, Springer, Berlin (1990).

[3.9] ORLOV, V.V., et al., Presentation at the International Seminar on "Cost Competitive, Proliferation Resistant, Inherently and Ecologically Safe Fast Reactor and Fuel Cycle for Large Scale Power", MINATOM, Moscow, 2000.

[3.10] KUTATELADZE, S.S., BORISHANSKII, V.M., NOVIKOV, I.I., FEDYNSKII, O.S., "Liquid-metal heat transfer media", At. Energ., Suppl. **2** (1958).

[3.11] WADE, D.C., "Recent innovation in IFR safety research", paper presented at Int. Meeting on Advanced Reactor Safety, 1994, Pittsburgh, USA.

[3.12] INTERNATIONAL ATOMIC ENERGY AGENCY, Transient and Accident Analysis of BN-800 Type LMFR with Near Zero Void Effect, IAEA-TECDOC-1139, IAEA, Vienna (2000).

[3.13] BALANDIN, Yu.F., et al., Proc. of Conference "XX Years of Atomic Energy", **2** Obninsk (1974) 16–27.

[3.14] THORLEY, A.W., TYZACK, G., "Liquid Alkali Metals", BNES, London (1973) 257.

[3.15] KRAEV, N.D., ZOTOV, V., Kernenergie, **8** 21 (1978) 244.

[3.16] ANAATATMULA, R.P., et al., Trans. ANS, **50** (1986) 259.

[3.17] POPLAVSKIY, V.M., A.KOZLOV, F., "Safety of sodium-water steam-generators", Energoatomizdat, Moscow (1990).

[3.18] EFIMOV, I.A., et al., Special Meeting IAEA-WGFR/7 (1975) 163–172.

[3.19] BALANDIN, Yu. F., MARKOV, V.G., "Materials for systems with liquid metal coolants", Atomizdat, Moscow (1961) (in Russian).

[3.20] BRAIENT, K.L., BENERDHET, S.K., "Fragility Steels and Alloys", Metallurgia, Moscow (1988) (in Russian).

[3.21] ALI-KHAN, J., in Material Behaviour and Physical Chemistry Liquid Metals Systems", H. V. Borgetedt (Ed.), Plenum Press (1962).
[3.22] CATHCART, J.V., MANLY, V.D., Corrosion, **12** 2 (1956).
[3.23] WEEKS, J.R., Nucl. Eng. & Design, **15** 2 (1971) 363–372.
[3.24] ORLOV, V.V., "Nuclear power based on fast reactors. A new start", Proc. of a Russian-U.S. Workshop on Future of the Nuclear Security Environment in 2015, November 2007, Vienna, Austria.
[3.25] ROUSSANOV, A., et. al., "Corrosion resistance of structure materials in lead coolant with reference to reactor installation", paper presented at the International Seminar on Cost, Competitive, Proliferation Resistant Inherently and Ecologically Safe Fast Reactor and Fuel Cycle for Large Scale Power, MINATOM, Moscow (2000) 65–67.
[3.26] TOSHINSKIY, G.I., et al., "SVBR technology features and the requirements to reactor core materials and coolants", 3rd International Scientific and Technical Conference on Development of Nuclear Power Industry Based on Closed Fuel Cycle with Fast Reactors: Innovative Technologies and Materials, ROSATOM, Moscow, 11–12 November, 2009.

4. DESIGN AND OPERATION OF EXPERIMENTAL FACILITIES

4.1. CLEMENTINE

4.1.1. Design features and parameters

This low power, mercury cooled experimental fast neutron facility, operating at 25 kW(th), was constructed to [4.1, 4.2]:

— Demonstrate the feasibility of operating with plutonium fuel and to serve as an experimental fast neutron facility and with a mercury–water cooling system;
— Serve as a critical facility for investigating the effect of configuration on criticality;
— Provide a source of un-moderated neutrons for physics studies;
— Study and evaluate the feasibility of controlling fast neutron systems;
— Provide information relevant to the use of plutonium as a fuel for FBRs.

Clementine was the world's first liquid metal cooled and ^{239}Pu fuelled fast reactor. Although it served primarily as a source of fast neutrons for experimental purposes, it also demonstrated the feasibility of plutonium as a fast reactor fuel. A cross-sectional view of the reactor is shown in Fig. 4.1.

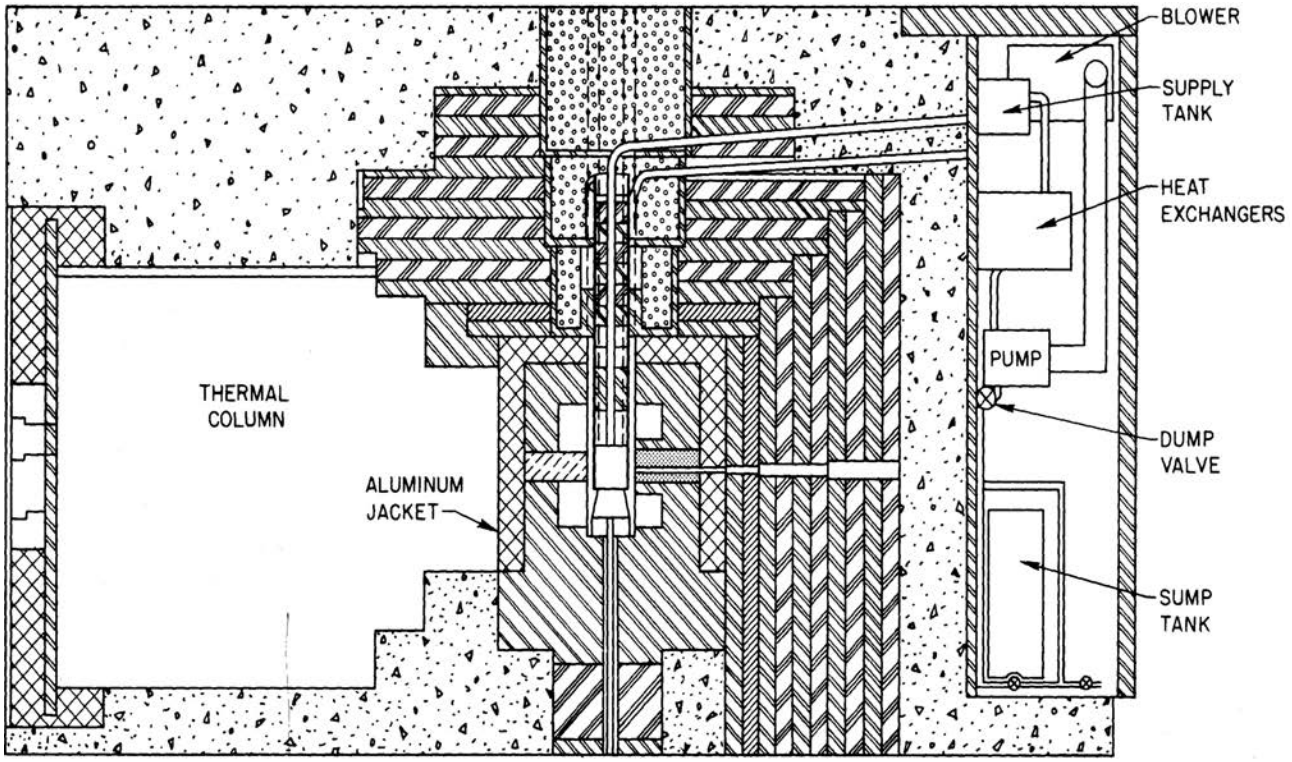

FIG. 4.1. Clementine cross-section through reactor shield [4.3].

A 46 in. long, 6.2 in. OD, and 6.00 in. ID mild steel cylinder served as the core container. The fuel cage rested on the bottom of this cylinder. Immediately above the case and filling the space to the top of the pot, or vessel, was a removable reflector and shield plug. This plug contained a number of layers of various materials, all in a steel cylinder having an l/4 in. wall thickness. A side shield, consisting of a permanent assembly of lamination and concrete, also served as a supporting and retaining wall for the reactor parts. A summary of the design data for Clementine is given in Table 4.1.

TABLE 4.1. CLEMENTINE DESIGN PARAMETERS [4.3]

Item	Value
Reactor data	
Thermal power, kW	25
High energy flux, neutrons·cm^{-2}·s^{-1}	4.3×10^{12}
Hg flow, gal/min	2.4
Hg velocity in core, ft/s	0.16
Core dimensions	
Length, in.	5.5
Diameter, in.	5.9
Inlet temperature, °F	100
Outlet temperature, °F	250
Pu temperature, °F	275
Fuel data	
Fuel	Delta-phase Pu
Fuel clad material	Nickel
Thickness of cladding, in.	0.003
Fuel diameter, in.	0.647
Fuel length, in.	5.5
Fuel can ID, in.	0.652
Fuel can OD, in.	0.692
Fuel rod swaged to OD, in.	0.686
Fuel rod triangular spacing, in.	0.718
Control	
Regulating control	Uranium reflector
Safety	B^{10} poison
Coolant system	
Volume Hg, cu ft	0.64
Volume Hg, lb	540
Cover gas pressure, psig	50
Pressure drop in cooling system components, psi	6.4
Efficiency of Hg pump 7.7 psi head, 2.4 gal/min and 11 amps, %	2

The reactor and shielding formed a rectangular block-like structure. In addition to the 35 plutonium fuel rods in steel cladding, the central active core contained 20 reflector rods containing natural uranium, having the same dimensions and cladding as the reactor core fuel rods. A 6 in. thick reflector blanket of natural uranium surrounded the core.

A l/4 in. thick aluminium jacket, containing water cooling tubes, removed the heat generated in the uranium blanket. The core and blanket were surrounded by a 6 in. steel reflector and a 4 in. thickness of lead shielding. The top shielding was made of a series of blocks which could be removed to give access to the reactor. The 5.9 in. diameter core contained 55 fuel and blanket elements, as shown in Fig. 4.2.

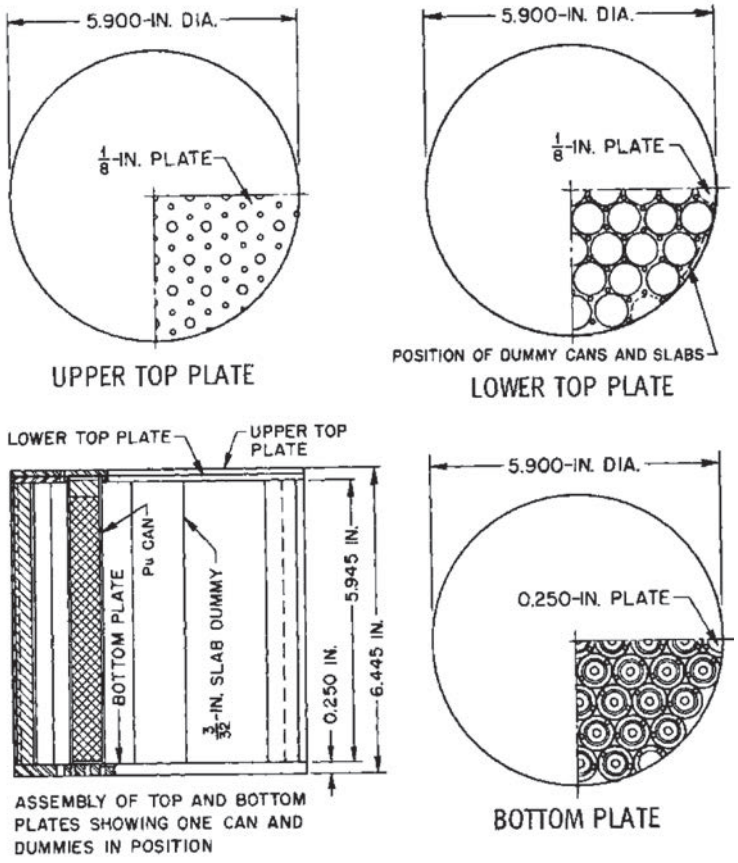

FIG. 4.2. Clementine core cross-section and elevation [4.3].

The fuel rods, of delta phase plutonium, were 0.647 in. in diameter and 5.5 in. long, as shown in Fig. 4.3. They were clad with type 1020 steel, 0.02 in. thick, and assembled in a vertical lattice.

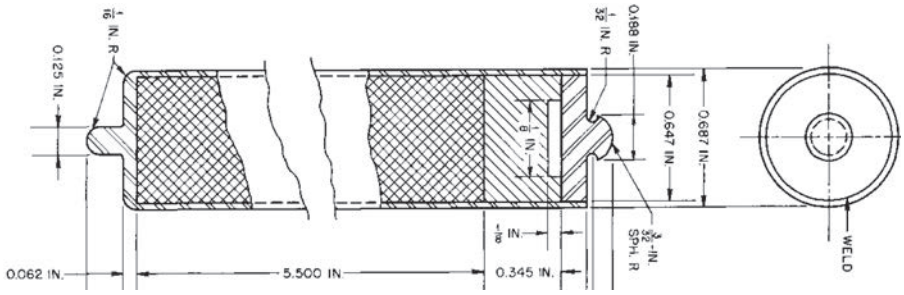

FIG. 4.3. Clementine fuel element [4.3].

The reactor was the first reactor to demonstrate reaction control via control of delayed neutrons; this was more of a function of being one of the very early reactors rather than a special design feature. Control was accomplished by several means. The uranium blanket could be raised and lowered. ^{238}U is a good neutron reflector, so the position of the blanket controlled the number of neutrons available to the reaction. When the blanket was raised, more neutrons were reflected back into the core, causing a greater number of fissions and consequently greater power output. Additionally there were two shutdown/control rods composed of natural uranium and boron which was enriched in the ^{10}B isotope. ^{10}B is a very effective neutron poison that could be inserted to control and shut down the reaction.

Shutdown of the reactor involved simultaneously dropping the uranium blanket and inserting the two control rods into the centre, which absorbed neutrons and poisoned the reaction.

A flow sheet of the mercury coolant system is shown in Fig. 4.4.

Since the reactor was primarily a research facility, with 25 kW(th) at full power, the heat removal requirements were quite modest. The mercury coolant was pumped by an eddy current type of electromagnetic pump at a rate of 2.4 gal/min through the core and then through a mercury to water heat exchanger. In the two heat exchangers, mercury flowed through a helical coil of 7/8 in. ID steel tubing inside a solid water cooled copper cylinder.

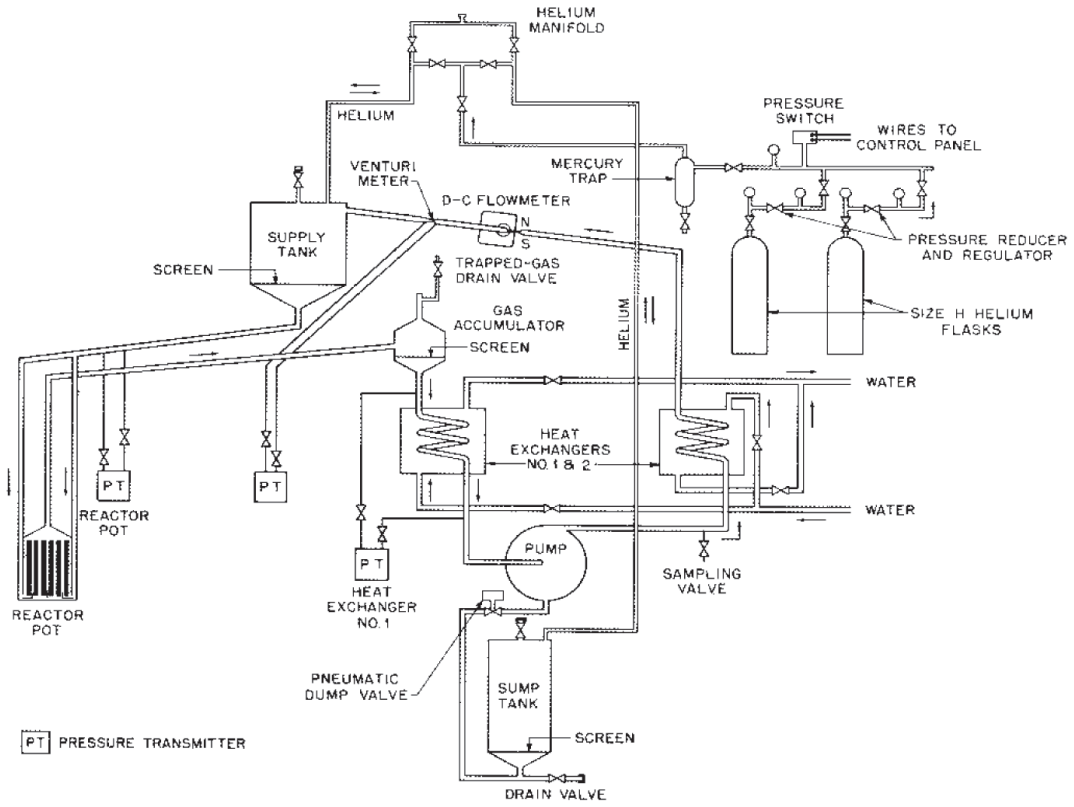

FIG. 4.4. Clementine reactor: mercury–water cooling system [4.3].

4.1.2. Operation

Construction of the Clementine reactor was formally proposed in November 1945, approval was given the following month, and design work began immediately. Construction began in September 1946, and the first critical assembly of the reactor was made at an incomplete stage of construction on 21 November 1946; nuclear measurements were performed at a power level of approximately one watt without further construction until February 1947. Construction efforts resumed during February 1947 and continued intermittently until January 1949. In March 1949, the system was brought to full operating power at 25 kW(th). For historical accuracy, Clementine enjoys the distinction of being the world's first LMFR.

The information obtained was valuable in establishing the feasibility of fast reactor operation, including the demonstration of control by delayed neutrons. Although the operating temperatures were too low for power production, the reactor was intended for research and it did demonstrate the feasibility of plutonium as a fuel for fast power reactors.

After about six years of operation of the plant, Clementine was finally shut down in December 1952, as it became evident that a plutonium rod had ruptured, and plutonium was entrained into the mercury coolant. Inasmuch as the primary objectives of the experiment had been realized, it was decided to dismantle the reactor, and this was completed by June 1953.

The experience and data provided by operating the Clementine reactor were very useful for both military and civilian applications. One of the notable achievements of the Clementine project included measurements for the total neutron cross-sections of 41 elements to a 10% accuracy. Additionally, Clementine provided invaluable

experience in the control and design of fast neutron reactors. It was also determined that mercury was not an ideal cooling medium for this type of reactor due to its poor heat transfer characteristics and other concerns.

4.2. EXPERIMENTAL BREEDER REACTOR I (EBR-I)

4.2.1. Plant design features and parameters

The Experimental Breeder Reactor I (EBR-I) was based on the concepts originating from Enrico Fermi and Walter Zinn in late 1944. By the autumn of 1945, the EBR-I power plant concept and design were fairly well advanced, and early in 1946 a formal proposal was made to build a FBR. The approach to the technology was simple: to minimize the fraction of neutrons lost by parasitic capture to the coolant, moderator and fuel; to maximize productive captures in massive uranium blankets; to prove the feasibility of breeding; and to establish the engineering feasibility of liquid metal coolants. The nominal thermal/electrical power was about 1000/200 kW.

The research and development programme was prepared early in 1945, and construction was approved in November 1945. The reactor was cooled by NaK alloy. Design and construction occupied the years from 1948 to 1951. The reactor consisted of three principal regions: a core, a light inner blanket that surrounded the core axially and radially, and a denser, cup-shaped outer blanket (Figs 4.5 and 4.6). Criticality with the Mark-I core was reached in August 1951.

On 20 December 1951, EBR-I produced the first usable amounts of electricity to be generated from a nuclear power fast reactor: enough to power four light lamps and, the next day, enough to run the entire EBR-I building — a milestone achievement. It was the first fast reactor to transform nuclear heat into electrical energy. The design effort of this reactor was pioneering in nature at that time.

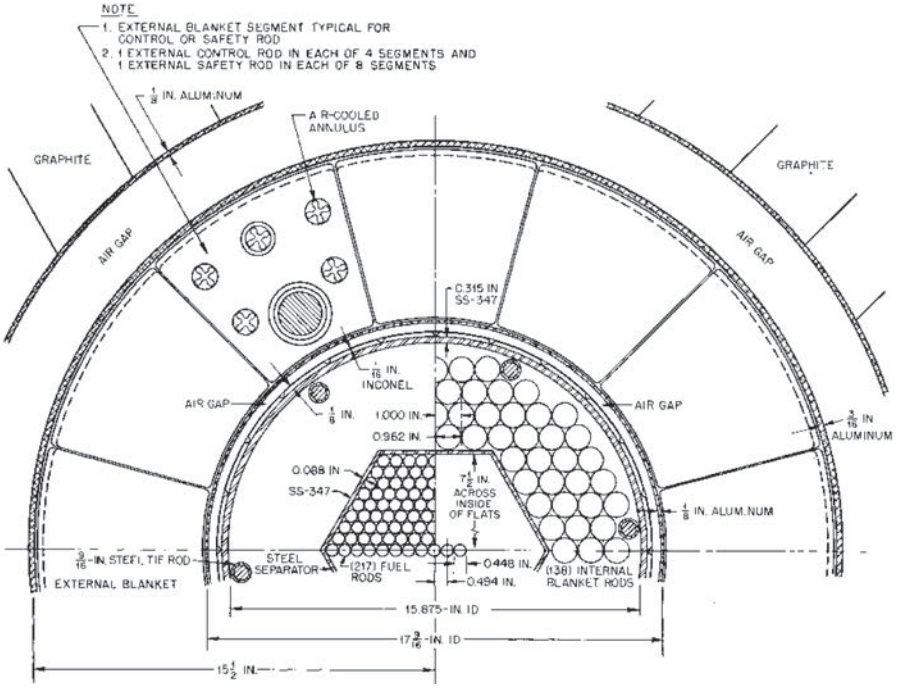

FIG. 4.5. EBR-I horizontal cross-section [4.3].

The EBR-I was constructed: to prove the validity of the breeding principle; to provide measurable quantities of high purity ^{239}Pu; to demonstrate the control characteristics of a fast neutron system; and to accumulate operating experience with the components of the cooling system, to prove the use of liquid metal coolants for reactor cooling and heat transfer. As a model, a nominal power level of the order of 1 MW(th) was chosen. The

highly enriched ^{235}U alloy (core I–III, surrounded by a natural ^{238}U blanket) and ^{239}Pu (core IV, surrounded by a depleted ^{238}U blanket) fuels were used.

For the Mark-I core, the power density was 170 kW/L. Initial plans called for a conservative design that would permit operation at power levels greater than 1 MW. Heat generation in the outer blanket proved to be greater than anticipated, however, and limited the operating power.

The Mark-II core horizontal cross-section is shown in Fig. 4.5.

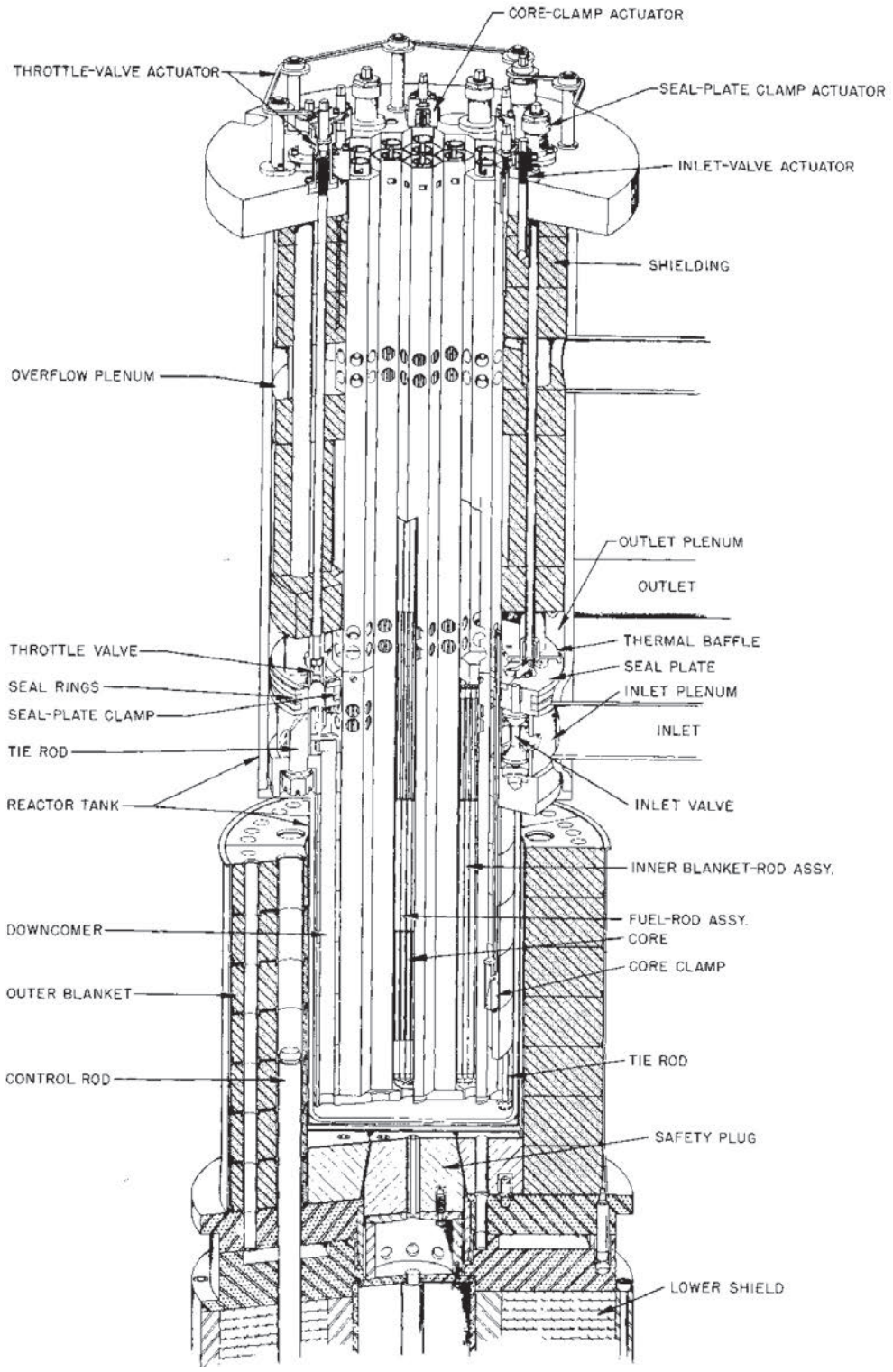

FIG. 4.6. EBR-I Mark-III inner tank assembly, vertical cross-section [4.3].

The inner fuel rods, 0.448 in. in outside diameter, were separated without spacer ribs by 0.046 in. The Mark-I core used spacer ribs. Enriched fuel was used in the middle of each rod, and natural uranium was used at the top and bottom to form an axial blanket. An inner blanket consisted of natural uranium slugs, 15/16 in. in diameter and 20 1/4 in. long, jacketed in 0.022 in. thick stainless steel. The core itself and the inner blanket were cooled by circulating NaK alloy.

The Mark-III core was designed primarily to investigate fast reactor stability. A cutaway view of the Mark-III inner tank assembly is shown in Fig. 4.6. A tube sheet at the bottom of the structure receives, supports and locates the nozzles of the rod assemblies. A seal plate above the outlet plenum restricts the bypass leakage occurring between the tank and the outlet edge of the seal plate. Restriction is accomplished by a system of two alloy seal rings expandable at high temperature. Seal plate shoes located between the inner edge of the seal plate and the blanket assemblies restrict bypass leakage.

The coolant, in series flow, enters the annular inlet plenum located immediately below the seal plate and flows into the outer ring of 12 blanket assemblies. At the bottom of the blanket assemblies, the flow is reversed 180°, directed upward through the seven fuel assemblies, through the outlet holes at the top, and then radially outward through the perforated portion of the blanket assemblies into the outlet plenum. The coolant, in parallel flow, flows into a lower annular plenum located immediately above the mounting plate. Here the coolant is distributed to the 12 downcomers through which it flows to the lower plenum. Upward flow through fuel and blanket assemblies is partitioned by a series of throttle valves.

The actual flow through the core, both in series and parallel, is less than the flow indicated through the metering of the primary inlet. Of a nominal metered flow of 290 gal/min, approximately 16% (47 gal/min) is bypassed as leakage and for seal plate cooling in series flow. The remaining 84% passes through the blanket and core. For a metered flow of 278 gal/min in parallel flow, approximately the same fraction, 84%, passes through the core; the remaining 16% passes through the blanket. Coolant from the blanket outlet cools the seal plate.

An air cooled outer blanket is located outside the reactor tank. It consists of 84 keystone shaped natural uranium bricks, each weighing 100 lb, clad with stainless steel 0.020 in. thick. This section is movable and contains the control rods. The moving parts are kept outside the liquid metal. The air cooling of the blanket proved to be the limitation on the operating power available for the reactor. Surrounding the external blanket is a graphite reflector, 19 in. thick, followed by 9 ft of concrete shielding. Six experimental beam holes pierce the concrete shield and graphite reflector.

The reactor vessel, or tank, is double walled and extends through the reactor shield. The section of the reactor vessel surrounding the reactor core has an inside diameter of 15.87 in. and a length of 28 in. Above this small section the vessel increases in diameter and is filled with shielding material, mostly steel sodium.

The whole reactor vessel rests on the shoulder formed by the change in diameter; thus the reactor core itself projects below the point of support as a smooth cylinder. The small-diameter part of the reactor tank consists of a stainless steel vessel of 5/16 in. wall thickness, made by deep drawing. It is surrounded by a second tank made of Inconel, 1/16 in. thick, which fits snugly on ribs formed in the Inconel. The upper portion of the reactor vessel also is double walled. The gas space between the two walls provides some thermal insulation and provides a method for testing vessel integrity. In the event that the inner vessel should develop a leak, the outer vessel would prevent complete loss of sodium.

A summary of the heat transport system data is given in Tables 4.2 and 4.3, and its arrangement is shown schematically in Figs 4.7 and 4.8.

TABLE 4.2. EBR-I HEAT TRANSPORT SYSTEM PARAMETERS [4.3]

Item	Value
Intermediate heat exchanger	
Overall length, ft	14.67
Shell outside diameter, in.	17
Type	Double-pass shell and tube
Tubes	
Number	102
Type	Hairpin
Material	‘A’ nickel

TABLE 4.2. EBR-I HEAT TRANSPORT SYSTEM PARAMETERS [4.3] (cont.)

Item	Value
Outside diameter, in.	0.75
Gauge	16
Outside area of tubes, sq. ft	495
Log mean temperature difference, °C	11
Overall heat transfer coefficient, Btu · h^{-1} · sq. ft^{-1} · $°F^{-1}$	400
Heat exchanger tube in superheater, boiler and economizer	
Effective length, ft	9.563
Outside diameter, in.	2.625
Inside diameter, in.	2
Superheater	
Number of heat exchangers	4
Arrangement	Series with counter-current flow
Total inside area of tube, sq. ft	20
Shell size, in. (IPS)	5
Shell-side cross-sectional flow area, sq. in.	14.6
NaKvelocity, ft/s	6.15
Steam velocity, average, ft/s	58.8
Economizer	
Number of heat exchangers	9
Arrangement	Series with counter-current flow
Total inside tube area, sq. ft	45
Shell size, in. (IPS)	5
Shell-side cross-sectional flow area, sq. ft	14.6
NaKvelocity, ft/s	6.15
Water velocity in annulus around l in. OD baffle, ft/s	3.43
Boiler	
Number of heat exchangers	18
Arrangement	Parallel with counter-current flow
Total inside tube area, sq. ft	90
Shell-side cross-sectional flow area per tube, sq. in.	1.98
Shell size, in. (IPS)	3
Sodium–potassium velocity, ft/s	2.51

TABLE 4.3. EBR-I STEAM GENERATOR DESIGN AND OPERATING CHARACTERISTICS [4.4]

Physical design and geometry			
Unit type	Forced circulation boiler		
No. components per unit:			
Economizer	9 (in series)		
Evaporator	18 (in parallel)		
Superheater	4 (in series)		
Steam drums	1		
	Economizer	Evaporator	Superheater
Shell-side geometry:			
Fluid contained	NaK	NaK	NaK
Materials	SS	SS	SS
Tube-side geometry:			
Fluid contained	Water	Steam	Steam
Type of tube	Three-layer composite	Drawn and diffusion bonded	
Material	Nickel OD; Copper—nickel ID		

TABLE 4.3. EBR-I STEAM GENERATOR DESIGN AND OPERATING CHARACTERISTICS [4.4] (cont.)

Physical design and geometry			
No. per component	1		1
Outside diameter, in.	2 5/8	2 5/8	2 5/8
Individual wall thickness[a], in.	1/16 – 1/8 – 1/8	1/16 – 1/8 – 1/8	1/16 – 1/8 – 1/8
Pattern	Single tube	Single tube	Single tube
Pitch, in.	Centred in shell	Centred in shell	Cantered in shell
Thermal and fluid data per component			
Heat transferred, Btu/h	1 432 000	4 560 000	368 000
Effective surface area, sq. ft	5	5	5
Effective tube length, ft	9.56	9.56	9.56
Liquid metal data:			
Temperature, °F			
In			583
Out	419		
Flow rate, lb/h	124 700	6 930	124 700
Fluid velocity, ft/s	6.15	2.51	6.15
Water and steam data:			
Temperature, °F			
In	214		
Out			529
Steam pressure, psig			423
Flow rate, lb/h	3630	202	3630
Fluid velocity, ft/s	3.43		58.8

[a] Dimensions for each layer of composite wall.

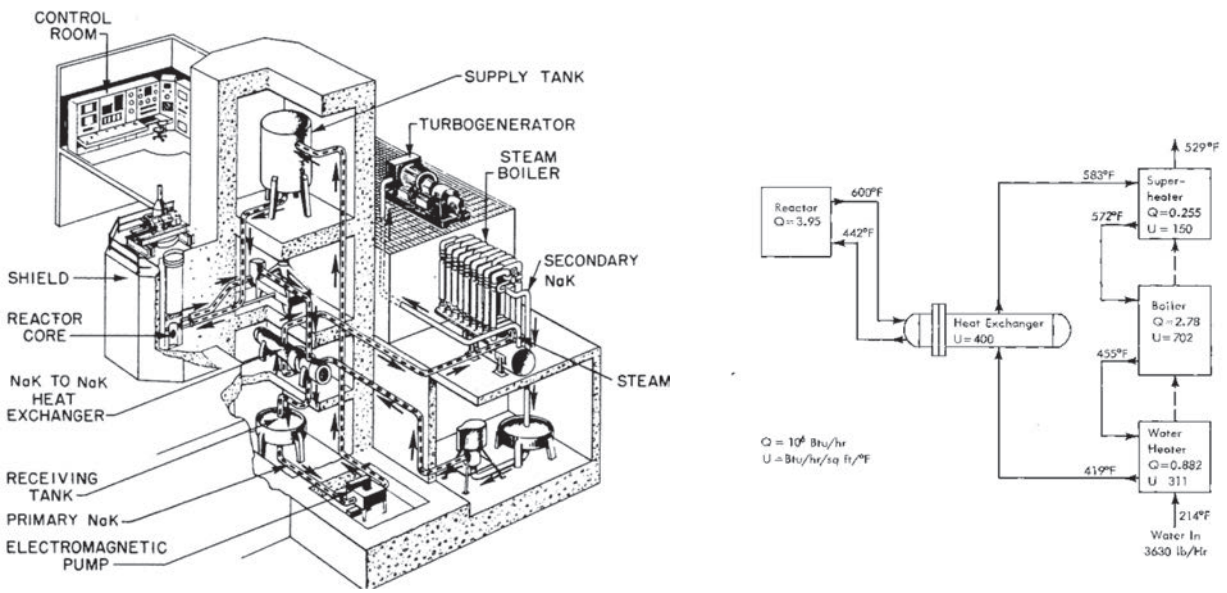

FIG. 4.7. EBR-I plant arrangement and flow diagram [4.4].

The primary NaK flow through the reactor (291 gal/min) is from an elevated, constant level tank. The flow proceeds down through the inner blanket, up through the core and out of the reactor. The coolant then flows through the IHX, returns to a receiving tank and is then pumped continuously by an electromagnetic pump to the constant-head tank. As indicated in Figs 4.7 and 4.8, and Table 4.3, the EBR-I SG is divided into an economizer, an evaporator and a superheater.

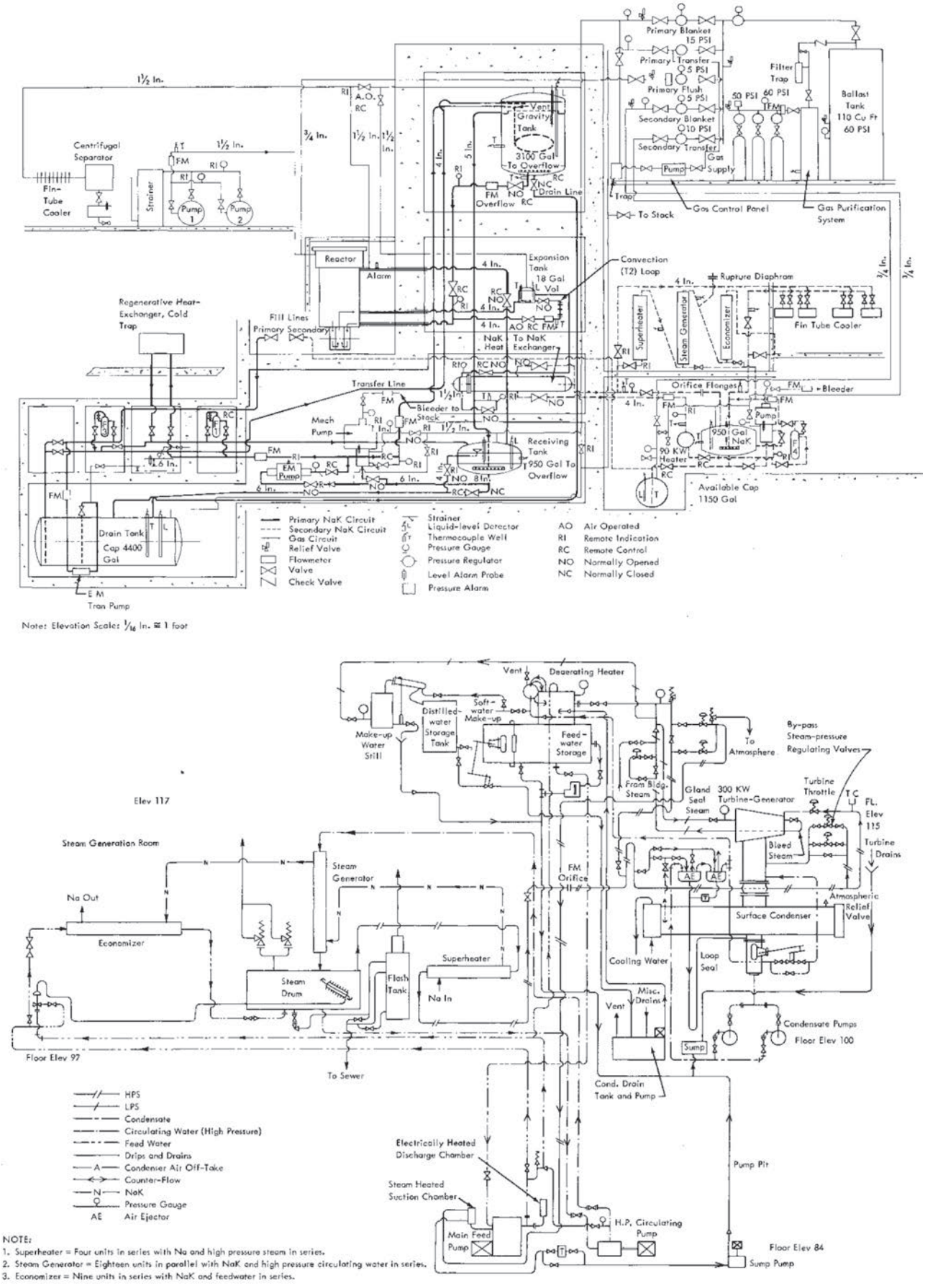

FIG. 4.8. EBR-I heat removal and balance of plant (BOP) systems [4.3].

In EBR-I the NaK-to-NaK IHX was of a conventional shell and tube design, with all joints welded and with primary flow passing through the tubes. The secondary flow on the shell side was double pass, and the tubes were bent in a hairpin shape. The actual values of the heat transfer coefficient were lower than calculated, apparently because the primary side was not running full. There was a continuous amount of blanket gas drawn into the NaK coolant stream from the reactor outlet free surface. Since the flow was downward in the primary side of the IHX, some amount of surface was blanketed by gas.

NaK passage through these units is in a counter-current to the flow of water and steam. Heat transfer tubes in each component are similar and consist of a composite assembly of inner nickel, intermediate copper and outer nickel tubes (Fig. 4.9).

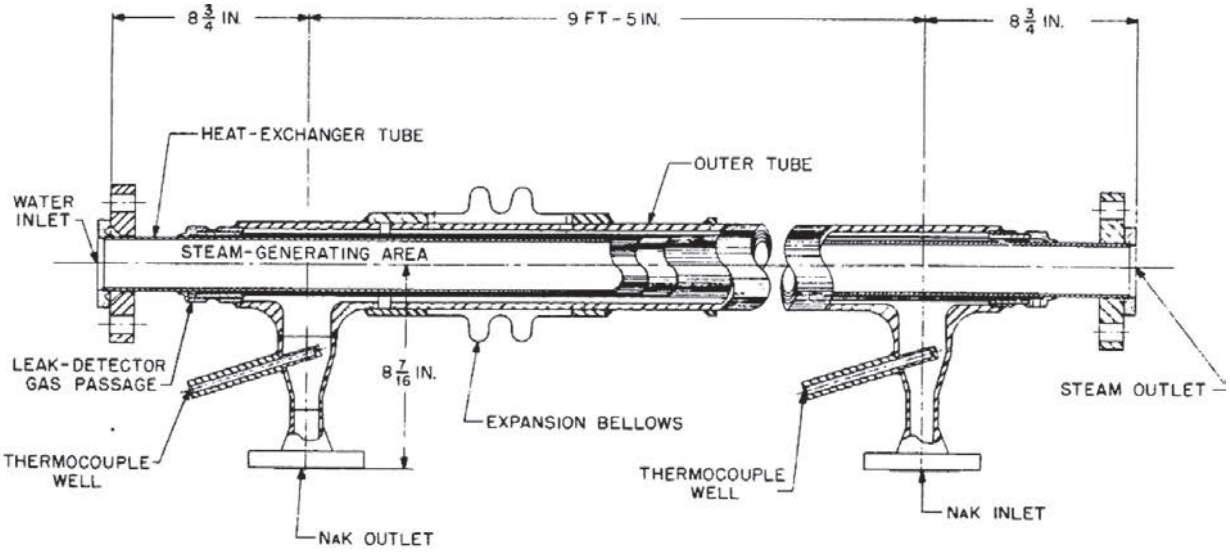

FIG. 4.9. EBR-I steam generator tube [4.4].

These tubes were assembled by mechanically drawing them together and thermally diffusion bonding them for good heat transfer between the tubes. Total wall thickness of the tube is 5/16 in., of which 3/16 in. is nickel. An outer stainless steel tube makes up the shell of the heat exchanger, and a bellows is used to allow for differential thermal expansion. Thus, each heat exchanger is of a 'single tube in a shell' type, where NaK flow is on the shell side and water or steam is in the tube.

The vertical forced circulation falling, film type SG limits the quantity of water in the system and increases the heat transfer rate. The heat exchangers are in a vertical position. The water film is established by a baffle at the top inner surface of the internal tube. The film runs to the bottom, where excess water and generated steam are piped into a drum. Steam is led through a separator in the drum out to the superheater, which consists of horizontal heat exchangers with NaK in the shell side. The economizer is a horizontal unit and serves to heat the feedwater from the de-aerating tank to steaming temperature before injection into the boiler drum.

Values were calculated for the heat transfer coefficient in the economizer by dividing the nine tubes in series unit into two parts, the first five tubes in nucleate boiling and second four tubes in film boiling. The values were 508 and 204 $Btu \cdot h^{-1} \cdot sq.\ ft^{-1} \cdot {}^{\circ}F^{-1}$, respectively. Temperature differentials in the second section were very low for boiling heat transfer; the gas blanket (characteristics of film boiling) is responsible for the poor values obtained. The reactor vessel, or tank, is double walled and extends through the reactor shield. The section of the reactor vessel surrounding the reactor core has an inside diameter of 15.87 in. and a length of 28 in. Above this small section the vessel increases in diameter and is filled with shielding material, mostly steel.

4.2.2. Operating experience

In the course of its life, EBR-I operated with four different fuel loadings. The first core, Mark-I, was fuelled with cylindrical slugs of fully enriched uranium metal contained in stainless steel tubes. The Mark-II core was installed in 1954. A series of kinetic experiments led to its meltdown on 20 November 1955. The Mark-I and Mark-II cores were similar with the exception of some changes in spacing ribs and composition.

Valuable information was derived from the operation of the Mark-I core. Measurement of the breeding to conversion ratio demonstrated conclusively the feasibility of breeding. Also, the theoretical prediction was confirmed that the neutronic behaviour of both fast and thermal systems below prompt criticality should be identical. During operation of the first core experiments, U–Zr alloy fuel was shown to be more resistant to irradiation induced swelling.

The Mark-I core was operated from 1951; it was found that radiation levels around the reactor were higher than had been anticipated. An additional 30 in. of concrete shielding was provided, and operation was resumed. In June 1952 a leak of NaK to NaK was discovered in the primary heat exchanger, and the reactor was shut down for repair. During the shutdown, 16 fuel elements were removed for examination and were replaced by new elements. More than 1500 MW(th) hours of operation had been accumulated by 15 April 1953.

During the four year period, EBR-I had essentially trouble-free operation. The operation of EBR-I demonstrated, among other things, that breeding was a technically achievable objective, with a measured conversion ratio of 1.01 + 0.05, and that the use of liquid metal coolant (NaK alloy in this case) was compatible with breeding economy as well as being metallurgically and mechanically feasible. Since ^{235}U fuel was utilized for the Mark-I, Mark-II and Mark-III cores, breeding in plutonium recycling will only be demonstrated with operation of the Mark-IV core. Breeding based on the ^{235}U fuel was demonstrated in the first cores. The EBR-I operation and theoretical determinations show that neutron behaviour below prompt criticality is the same in both fast and thermal reactors.

Under normal operating conditions the reactor was very stable and did not exhibit either a prompt positive temperature coefficient or a resonance. Under purposely imposed and drastically abnormal operating conditions, anomalies were observed: resonance consisting of oscillations in power level appeared during experiments in which the coolant flow rate was drastically reduced; and a prompt positive temperature coefficient appeared during startups undertaken with reduced coolant flow. Even under conditions where the net positive coefficient appeared, the reactor could be operated safely. Oscillator tests demonstrated the presence of instability.

In November 1955, the Mark-II core of the EBR-I partially melted during the last of a series of experiments designed to study its behaviour when put on positive periods with reduced or zero coolant flow. The accident occurred under extremely abnormal operating conditions purposely imposed on the reactor for the experiment and recognized to involve a risk of fuel melting. Two of the normally operative safety mechanisms, the flow interlock (which automatically shuts down the reactor if substantially full coolant flow is not maintained) and the period scram meter interlock (which automatically shuts down the reactor if the period becomes too short), were purposely disconnected. The coolant flow was stopped completely.

A certain fixed amount of reactivity was put into the reactor with the control rods, and the reactor was started up on short enough periods so that temperature differentials would be established in the fuel slugs. The prompt positive temperature coefficient previously observed appeared, and, as the power increased, the reactivity increased, thus further shortening the period. It was planned to scram the reactor when the period reached 0.27 seconds and the temperature of the fuel reached 932°F. When the period reached 1 second, the operator mistakenly activated the slow acting motor driven control rods instead of the faster acting scram rods. By the time the scram was initiated, the period had reached 0.3 seconds. The temperature overshot occurred, so that the uranium became heated above 1328°F, roughly the temperature at which the uranium–iron eutectic forms. The centre of the core melted, forming the eutectic. After the manually operated scram button was pressed (in less than 2 seconds), the reactor shut down and the meltdown stopped. The automatic power-limitation circuits also operated.

As a result of the accident, melting occurred in 40–50% of the EBR-I core. No explosive force developed. None of the remainder of the reactor, including the inner blanket and the reactor vessel, was damaged. A negligible amount of radioactive material reached the atmosphere through temporary thermocouple wire seals. Neither the operating personnel nor any other persons were injured in any way. Evacuation steps were precautionary. Operating personnel returned to the reactor building after a minor amount of surface decontamination. The core assembly was removed from the reactor by use of a temporary hot cell and shipped to ANL for disassembly and examination. Observations during disassembly and subsequent simulated meltdown experiments indicated that the porous structure formed in the core could have resulted from the vaporization of entrained NaK.

The full potential of breeding in a fast spectrum is realized only when plutonium is utilized as the fuel in the core, rather than ^{235}U. The EBR-I Mark-IV core, loaded in 1962, represented the first use of plutonium in the USA for the full core of a fast breeder power reactor. Operation of this reactor facility with the plutonium loading had as its objective the determination of general operating characteristics, the measurement of breeding gain, and the determination of radiation effects and nuclear parameters.

An alloy of plutonium with 1.25 wt% aluminium was used in the core. Slugs of this material, 0.232 in. in diameter and 2.121 in. long, were contained in Zircaloy-2 fuel tubes 0.299 in. in outside diameter with a 0.021 in. wall thickness. Three full-length ribs served to centre the slug in the jacket tube. Each fuel rod contained a 3.552 in. long lower depleted uranium blanket slug, four plutonium-alloy fuel slugs totalling 8½ in., and a single 7.745 in. long upper blanket depleted uranium slug. A 0.0125 in. NaK layer bonded the cladding to the fuel. A number of rods had 0.08 in. diameter zircaloy thermocouple tubes attached. Blanket rods were similar to those used in the fuel section; depleted uranium slugs were substituted for the plutonium alloy.

At shutdown, the Mark-III core had operated for 3220 MW·h. The Mark-III core was completely unloaded by 8 November 1962, and the Mark-IV loading went critical on 27 November 1962, with 27.1 kg of ^{239}Pu in 327 fuel rods. The initial loading consisted of 60 fuel rods in the central subassembly. Ten subsequent loadings — four of 42 rods each, two of 24 each, two of 18 each, one of 8, and a final one of 7 rods — were made to reach criticality. Foil irradiation runs at low power were carried out in early 1963 to determine the constants necessary for calculation of the breeding ratio. After transfer function runs at low and moderate power indicated that the reactor was quite stable, the system was gradually brought up to a power of 900 kW(th) in April 1963. The experiments showed that the breeding ratio of a plutonium fuelled system can significantly exceed that of a ^{235}U system. In the series of intensive foil activation experiments, a value of BR = 1.27±0.08 was measured.

The first fast reactor ever constructed was the EBR-I at the Idaho National Engineering and Environmental Laboratory (INEEL). It operated from 1951 to 1963 and was shut down on 30 December 1963. Following completion of the Mark-IV tests in 1964, EBR-I was shut down, decommissioned and, in 1966, declared a national historic landmark under the stewardship of the US Department of the Interior. Total power produced by the Mark-IV loading was 577 MW·h.

The reactor was secured subcritical by 1.75% Δk/k with the controls in their most reactive position and the reactor temperature at 30°C. Surveillance of the reactor blanket gas is to be maintained during this indefinite, extended shutdown period. Fifty irradiated Mark-III fuel rods have been shipped from the facility for reprocessing, thus completing the removal of irradiated Mark-II fuel.

EBR-I's initial purpose was to prove Enrico Fermi's fuel breeding principle, a principle that showed a nuclear reactor producing more fuel atoms than consumed. The operation of EBR-I demonstrated that breeding was a technically achievable objective, with a measured conversion ratio of 1.01 + 0.05, and that the use of liquid metal coolant was compatible with breeding economy as well as being metallurgically and mechanically feasible [4.1–4.4].

4.3. LOS ALAMOS MOLTEN PLUTONIUM REACTOR EXPERIMENT

4.3.1. Design features and parameters

The concept of using molten plutonium as fuel for a FBR system evolved from investigations carried out at the Los Alamos Scientific Laboratory after the dismantling of Clementine in 1953. Parallel to this effort, a homogeneous reactor concept was developed where the fissile material was dissolved in an aqueous system. The principal problem in the development of the Los Alamos Molten Plutonium Reactor Experiment (LAMPRE) was the design and fabrication of capsules that could provide adequate containment. Material choices were eventually narrowed to various tantalum alloys or to 'super-pure' tantalum. The fuel used in the first loading consisted of a mixture, 90 at.% plutonium and 10 at.% iron. Excess carbon in the form of elemental carbon and carbides was added to inhibit corrosive attack of the tantalum [4.1, 4.2].

This then led to the concept of using plutonium in the molten state as fuel for a FBR which was realized in LAMPRE, where the fuel was contained in capsules. The decision was made to build a reactor fuelled with molten plutonium in which the fuel would be contained in cylindrical capsules[1]. Development of LAMPRE began in the 1950s, and the facility was built in the early 1960s at Technical Area (TA) 35 in Los Alamos, NM.

The reactor went dry critical early in 1961 and reached its designed power level of 1 MW a short time later. The resulting specialization in plutonium fuelled FBRs, on the one hand, and the homogeneous concept, on the other, logically led to the concept of using plutonium in the molten state as a fuel for a fast breeder system.

[1] A zirconium hot trap protected tantalum (capsule material) in the core [4.1].

An early reactor design, for example, called for the plutonium fuel to be contained in a cylindrical vessel through which tubes carrying sodium coolant would flow in a typical calandria arrangement. The need for additional information regarding the behaviour of the container and fuel materials, however, led to the decision to first build a molten plutonium fuelled reactor in which the fuel would be contained in cylindrical capsules with the sodium coolant flowing outside.

This arrangement, used in LAMPRE, had been readily adapted to the testing of a variety of fuel and container material combinations. The limitations of this location fixed the reactor power at 1 MW(th). A second core loading was installed in April 1962. Since that time the reactor has been used primarily as a testing facility for materials intended to contain the highly corrosive fuel alloy and as a basic physics test unit for exploring the feasibility of using a molten plutonium fuel.

A plan view of the reactor installation and an elevation view are shown in Figure 4.10. A summary of LAMPRE design core parameters is given in Table 4.4.

TABLE 4.4. LAMPRE CORE PARAMETERS [4.3]

Item	Value
Capsule material/size, in.	
Inside diameter, in.	Ta-9.1/0.376
Wall thickness, in.	0.025
Length, in.	8
Core capacity, No. of capsules	199
No. of capsules for criticality (calculated)	143
Capsule spacing, pitch, in.	0.497
Core composition, vol.%:	
Fuel	51.5
Na	33.5
Ta	15.0
Fuel height, in.	6
Fission gas volume height, in.	2
Thermal power, MW(th)	1
Average fuel temperature, °C	637
Maximum fuel temperature, °C	870
Na inlet temperature, °C	450
Na outlet temperature, °C	563
Na flow rate, gal/min	133
Central to edge power ratio	1.8
Axial power ratio	1.8
Cylindrical radius, in.	~3.1
Cylindrical height, in.	~6.4
Fuel alloy mass, kg	~24.99
Core volume, L	~3.06
Central median fission energy, MeV	~1
Prompt-neutron lifetime, s	8.9×10^{-9}

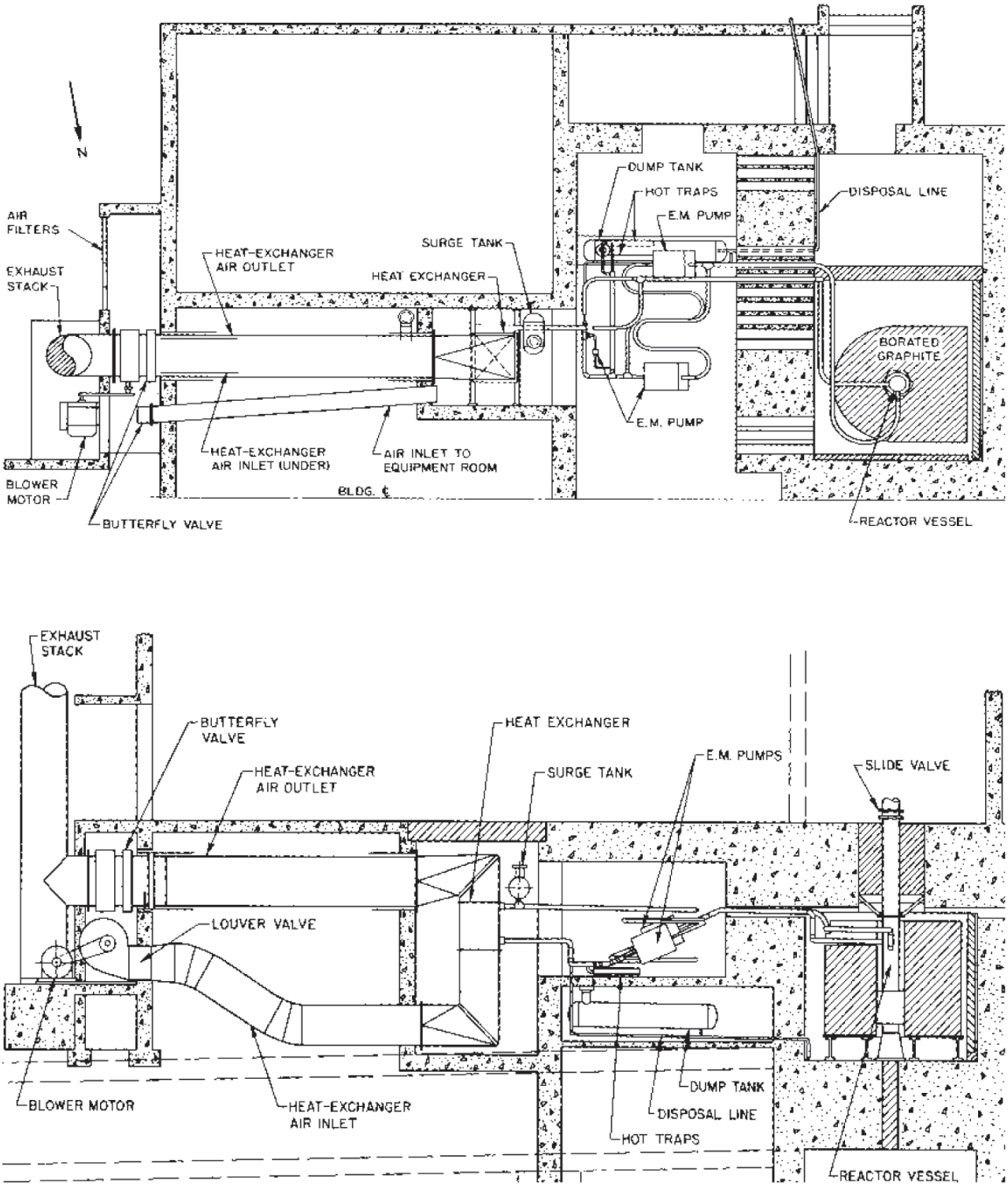

FIG. 4.10. LAMPRE plan and elevation views [4.3].

Component design was based on the need for installation in the existing cell facilities. No secondary sodium coolant system was used. The heat generated was transferred to the air and exhausted up a stack. Although thermal performance specifications are high, specific power and power density were not intended as representative of optimum values for a larger power reactor system.

The core consists of approximately 140 fuel capsules filled with plutonium–iron alloy and surrounded by approximately 60 stainless steel reflector pins of similar design. A cross-section of the core region and a vertical section of the core are shown in Fig. 4.11.

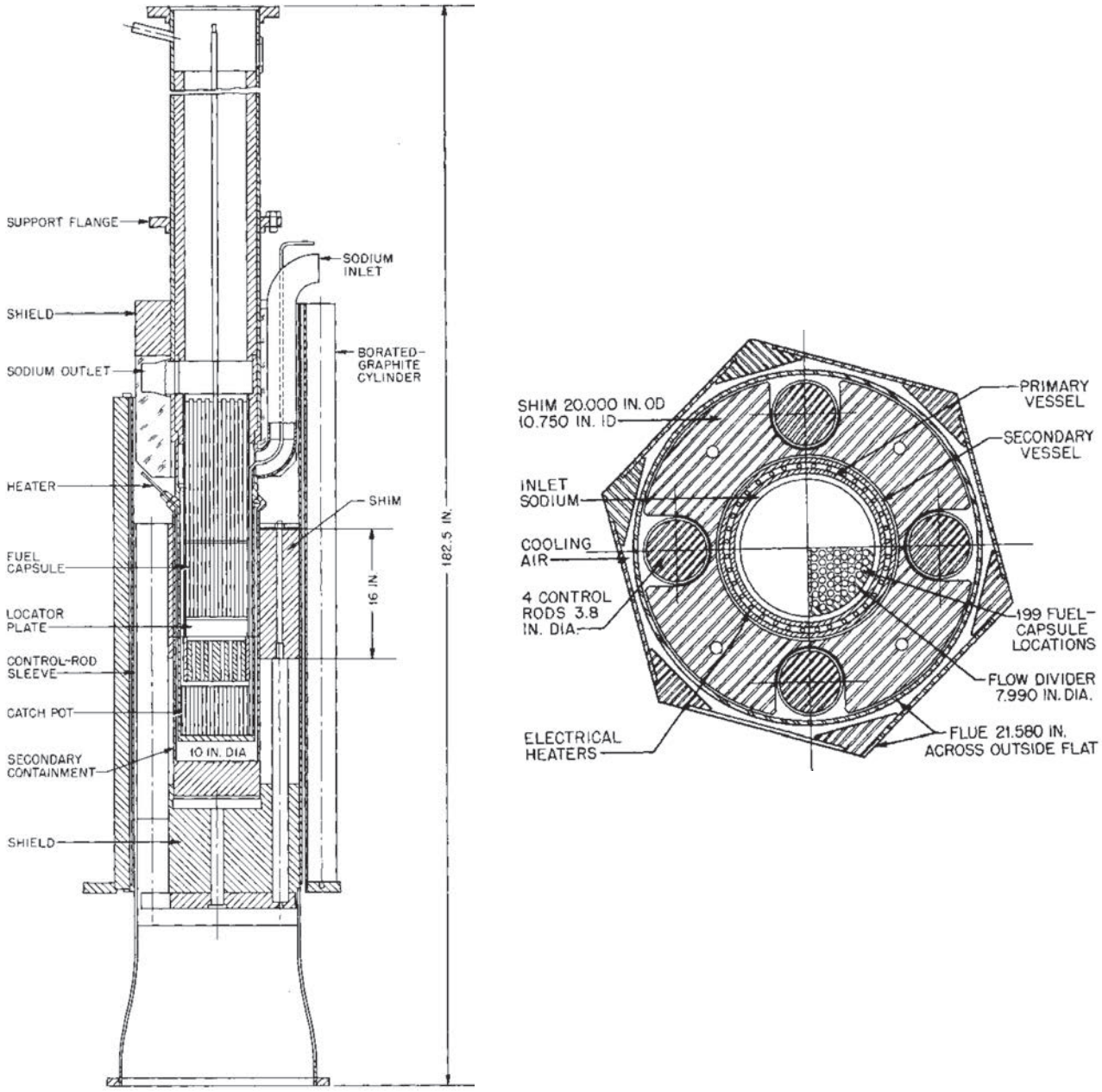

FIG. 4.11. LAMPRE vertical and horizontal cutaway [4.3].

An annular movable stainless steel reflector is contained in an inner vessel outside the core. It is 20 in. in outside diameter by 10 3/4 in. in inside diameter and 16 in. long. Final control can be obtained by moving four control rods, each consisting of a nickel cylinder 3.8 in. in diameter and 16 in. long, which moves vertically in the stainless steel reflector.

Coolant (sodium) flows down through a 3/8 in. annulus between the vessel and the flow divider. The coolant stream reverses in a plenum at the bottom of the flow divider. The sodium then flows through a bottom reflector, consisting of an Armco iron cylinder 6 7/8 in. in diameter by 6 in. high. Flow continues through a locater–plate assembly, then finally past the fuel capsules, through a top reflector region, and into the outlet plenum.

The core arrangement contains several safety features. Double-wall construction of the reactor vessel, with no pipes entering the lower part, prevents accidental drainage of coolant. A catch pot and a diluent plug are designed to contain any fuel in a non-critical geometry in the event of a leak from the core. The Armco iron diluent plug will dissolve in molten fuel to form an alloy with a higher melting point. As dissolution continues, the resulting alloy will solidify.

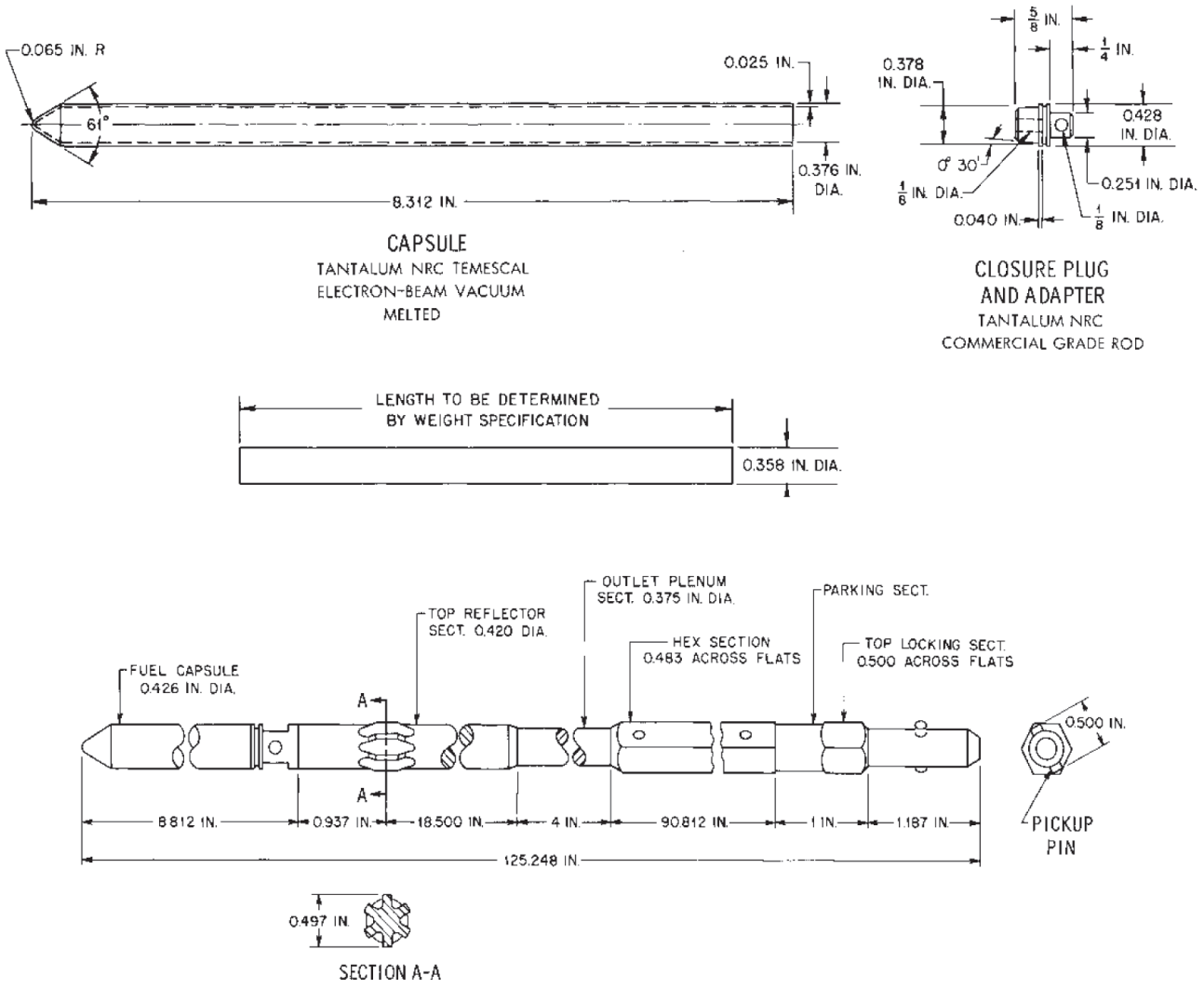

FIG. 4.12. LAMPRE fuel capsule and fuel subassembly [4.3].

A single fuel capsule, or pin, is used in each complete element (Fig. 4.12). The components of the capsule assembly shown are the thimble, fuel slug, closure plug and adaptor. Capsule fuel thimbles were constructed of various tantalum types, depending upon the desired materials test. A typical thimble, fabricated from tantalum-0.1 wt.% tungsten, is 0. 426 in. in outside diameter and 8.312 in. in overall length with an inside diameter tapered from 0.376 in. at the top to 0.362 in. at the cone end. Solid plutonium–iron alloy fuel slugs, 0.358 in. in diameter and of variable length depending on the fuel weight required (but averaging 6.33 in.), were machined immediately before assembly into the thimbles.

The remainder of the assembly includes a 90 in. shielding section and a so-called capsule handle, constructed of Armco 17-4 stainless steel, which is used to insert and withdraw the fuel capsules from the core and also to maintain radial core configuration.

The sodium coolant system is shown in schematic form in Fig. 4.13. Two parallel train electromagnetic conduction pumps, each rated at 100 gal/min at 20 psi head, are used for circulating sodium to the reactor.

Heat is removed directly from this primary circulating system to air in a finned section heat exchanger which exhausts up a stack. The coolant loop, constructed of 2 in. and 3 in. type 316 stainless steel pipe, includes a number of accessory components, such as flowmeters, a heating transformer for raising the temperature of the flowing sodium to the melting point of the fuel, three getter hot traps, and a fill and dump tank system.

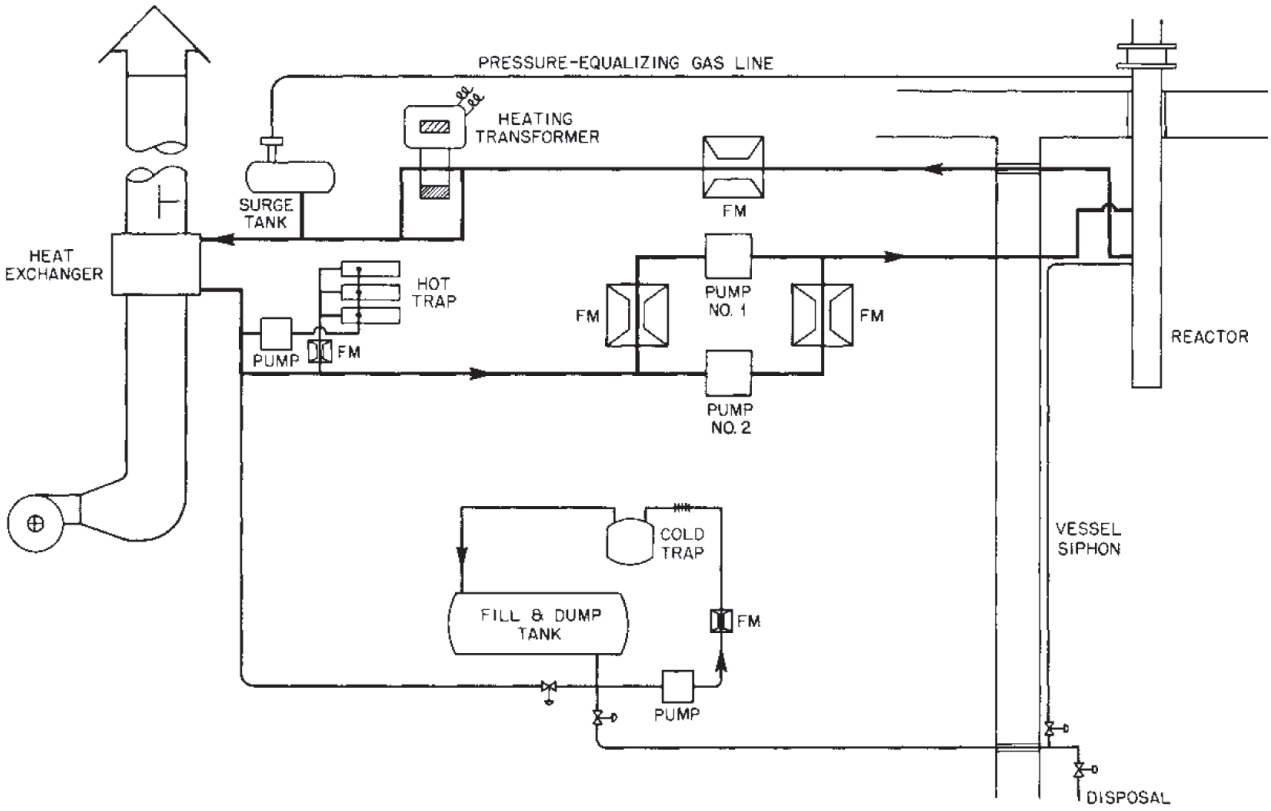

FIG. 4.13. LAMPRE sodium air cooling system [4.3].

4.3.2. Operation

As was noted, the LAMPRE reactor was designed as a facility for the study of molten plutonium fuels and their respective containers and for the investigation of operating problems that might be unique to the fluid nature of the fuel. The reactor started in 1961 with dry critical and low power operation. It was brought up to its designed power of 1 MW in early 1961. In April 1962, the reactor was reloaded with a Mark-II core. After capsule failure in September 1962, which permitted 75 g of plutonium–iron fuel to enter the coolant, the power level was temporarily limited to 500 kW.

Although bubbles of fission product gases tend to rise to the surface of the fuel, some separation of large portions of the fuel regions apparently results in reactivity changes with time. In the Mark-I loading, solid additives of carbon or plutonium carbide used to inhibit corrosive attack of the tantalum capsule by the fuel at high temperatures were believed to interfere with the release of the accumulated gas and hence to accentuate this reactivity loss. Although approximately ten dollars of reactivity was lost in the Mark-I loading, there was at no time any indication of instability caused by the froth or low density portion of the fuel. In the Mark-II loading, the disengagement of evolved gases is cleaner, with a smaller reactivity loss resulting as a function of integrated power. During operation, the dynamic characteristics of the reactor were evaluated. Temperature coefficients, power coefficients and reactor transfer functions were measured. Substantial negative temperature coefficients provide a high degree of operational stability.

LAMPRE fuel consists of 24 kg of a plutonium alloy, 90 at.% plutonium, 10 at.% iron. The rather unusual density characteristics of this alloy can lead to a plug during solidification, since the lower density solid material will tend to float to the top of the remaining fluid portion. In the initial loading, the presence of a few hundred parts per million (ppm) of carbon in the plutonium fuel alloy was believed to be effective in reducing the inter-granular attack on tantalum. Subsequent tests, however, indicated that fuel made with pure iron is less corrosive than fuel with added impurities.

The pure system likewise has the advantage of reducing the formation of a froth region, with resulting reactivity loss. The fuel alloy used in the Mark-I and Mark-II cores has a high plutonium concentration and is not particularly suitable for high performance reactors because of heat removal limitations. Attention has therefore

been given to ternary alloys, i.e. plutonium–cobalt–cerium and plutonium–copper–cerium, which permit plutonium concentrations from 2 to 4 g/cm^3 at operating temperatures. Some test capsules containing the former alloy have been irradiated in the LAMPRE core.

LAMPRE was built and operated to demonstrate the feasibility of using molten plutonium alloys as a fuel material for fast reactors, evaluate the relative merits of various binary and ternary plutonium alloys, and investigate the compatibility of molten plutonium alloys with various containment materials.

Operation with the second core continued uneventfully until September 1962, when a capsule failure released approximately 75 g of fuel material into the coolant. A few months later, two additional releases were noted. In all three cases fuel was released rapidly under pressure (145–370 psi). Although the coolant system was contaminated, there was no evidence of gaseous fission products in the operating area. In all cases defective capsules were identified and removed.

After the capsule failure in September 1962 and the entry of plutonium–iron fuel into the coolant, the reactor power was limited. A second phase of more advanced experiments was planned but not realized, because the liquid plutonium fuel programme was cancelled by the US Government in 1965 in view of the foreseeable breakthrough of MOX fast reactor fuel [4.1–4.6].

REFERENCES TO SECTION 4

[4.1] SMITH, R.R., CISSEL, D.W., "Fast reactor operation in the United States", paper prepared for the Int. Symposium on Design, Construction, and Operating Experience of Demonstration LMFBRs, Bologna (1978).

[4.2] SMITH, R.R., CISSEL, D.W., "Past and present role of fast breeder reactors in the United States of America", ibid.

[4.3] SESONKE, A., YEVICK, J.G., "Description of fast reactors", in Fast Reactor Technology: Plant Design (YEVICK, J.G., AMOROSI, A., Eds), The MIT Press, Cambridge (1966).

[4.4] CHASE , W.L., "Heat-transport systems", in Fast Reactor Technology: Plant Design (YEVICK, J.G., AMOROSI, A., Eds), The MIT Press, Cambridge (1966).

[4.5] INTERNATIONAL ATOMIC ENERGY AGENCY, Status of Liquid Metal Cooled Fast Breeder Reactors, Technical Reports Series No. 246, IAEA, Vienna (1985).

[4.6] PETERSON, R.E., CUBITT, R.L., "Operation of the plutonium-fuelled fast reactor LAMPRE, Fast Reactors", Topical Meeting, American Nuclear Society, Report ANS-101 (1967).

5. DESIGN AND OPERATING EXPERIENCE OF EXPERIMENTAL AND SEMI-INDUSTRIAL FAST REACTORS

5.1. BR-5

5.1.1. Plant arrangement, coolant system

BR-5 (Bystryi (fast) reactor 5 MW(th)) was the first reactor in the world to use sodium as a coolant and plutonium oxide as a fuel [5.1] (see Figs 5.1 and 5.2). This reactor was developed primarily to gain experience in operating a multi-loop, sodium cooled reactor and to test fuel elements and equipment for subsequent reactors.

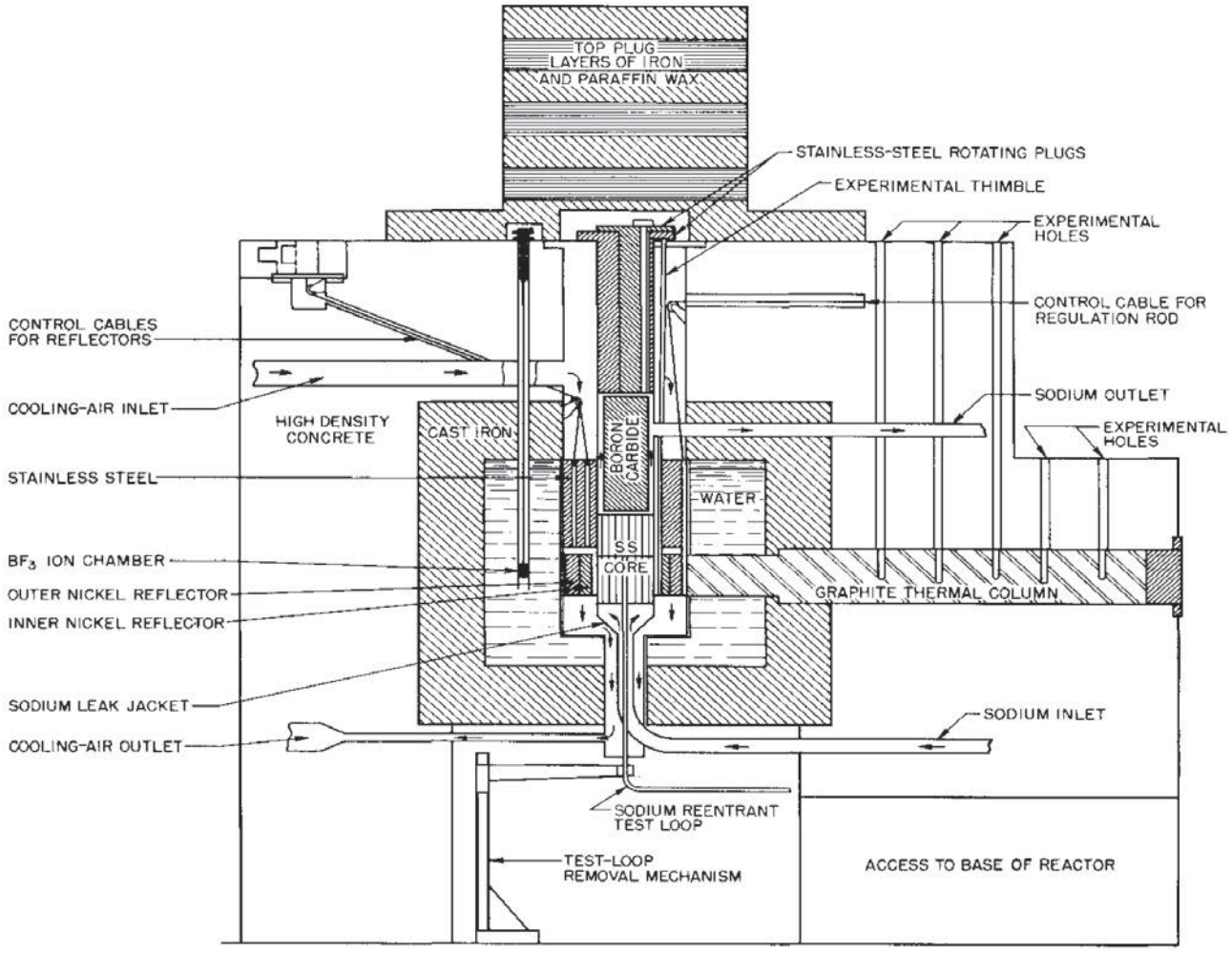

FIG. 5.1. BR5/10 general arrangement [5.1].

The BR-5 predecessor — BR-I (100 W(th)) — was constructed in 1955 as a ~zero energy assembly; it was fuelled with plutonium and was used to investigate fast reactor physics. The BR-I reactor was replaced in 1956 by BR-2, a mercury cooled reactor fuelled with plutonium metal with a core volume of 1.7 L, which was operated to 100 kW(th) and was shut down in 1958. The BR-2 provided facilities for physics experiments and irradiation of materials in fast-neutron fluxes up to 10^{14} neutrons · cm^{-2} · s^{-1} and provided experience in operating at temperatures to 60°C. The BR-2 was dismantled, and parts, such as shielding, were used for construction of it successor — the BR-5 reactor.

The experimental FBR BR-5 provided data on the technological aspects of sodium cooled fast neutron reactors for use in the design of future reactors: the engineering BOR-60 and semi-commercial BN350. The BR-5 had a power of 5 MW(th) and had sodium outlet temperatures of 500°C.

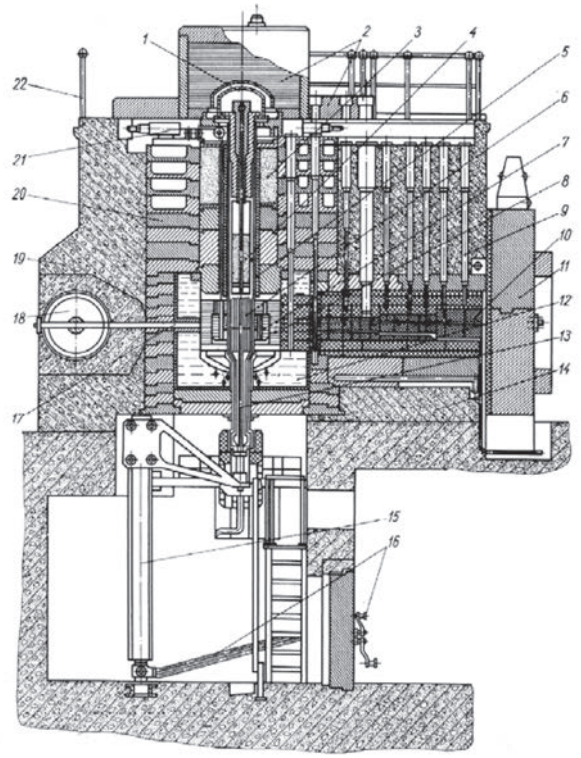

1 - Gas-tight cap of the central tube; 2 – Upper shield; 3 – Concrete plate; 4 – Rotating plate; 5 – Vessel shell;
6 – Core; 7 – 8 – Reflectors; 9 – Experimental channel; 10- Thermal column; 11- Thermal column gate;
12 - Water tank; 13 – Central experimental loop; 14 – Lower shield; 15 – Reloading machine of the central loop;
16 – Control of reloading; 17 – Neutron beam channel; 18 – Channel gate; 19-Concrete shield;
20-Cast-iron shielding; 21-Control and safety drive mechanism.

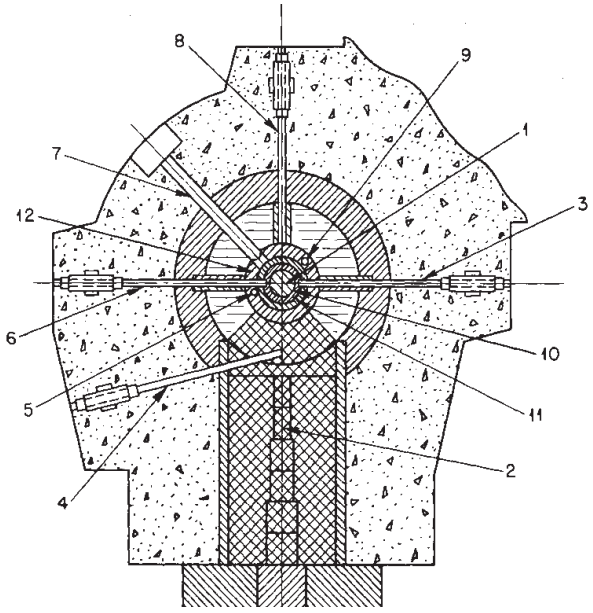

1-Reactor; 2-Thermal column; 3,4,6,7,8-Horizontal beam hole; 5,9-Vertical beam hole;
10-Inner movable cylinder reflector; 11-Outer movable cylinder reflector; 12-Stationary nickel reflector.

FIG. 5.2. BR-5/BR-10 general arrangement; vertical cross-section (top) and plan view (bottom) [5.2].

The R&D programme was prepared early in 1956 and was aimed at burnup data on PuO_2 and other fuel types (mono-carbides and mono-nitrides), to obtain experience in operation of radioactive sodium systems and to irradiate various structural materials. Since it was not considered necessary to obtain further data on breeding gain, the BR-5 design was simplified by omitting the axial and radial blankets of natural or depleted uranium. The general arrangement of the reactor is shown in Figs 5.1 and 5.2.

The core consists of 88 hexagonal fuel subassemblies, surrounded by two rows of blanket subassemblies. Each fuel subassembly contains 19 stainless steel clad pins, which are filled with plutonium oxide pellets and sealed after they have been charged with helium gas (Fig. 5.3).

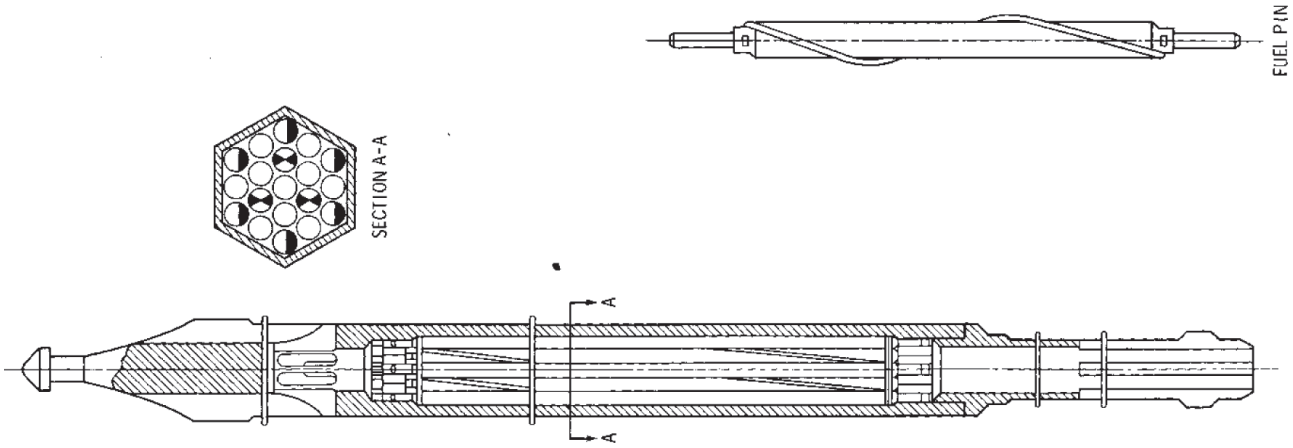

FIG. 5.3. BR-5 fuel pin and subassembly [5.3].

The pins are ~0.5 cm in outside diameter, the fuel is about 0.4 cm in diameter, and the cladding is 0.04 cm thick. The pins are separated by spiral wire spacers. The subassemblies are supported at the bottom by a perforated plate.

The core subassemblies and a ring of tubes loaded with natural uranium are enclosed in a stainless steel 'vessel'. There is no top plate, and no positive lateral restraint is provided at either the centre or the top. Sodium flows upward through the core from a single inlet at the bottom of the central sodium tube to a single outlet above the core, which supplies two cooling circuits.

Movement of an inner and outer cylindrical reflector is used to control the reactor. The inner nickel cylinder (~5 cm thick) is raised or lowered by cables; the outer nickel cylinder has two movable sections that provide fine control. In addition, two control rods operating in the outer cylinder provide shim adjustment. Emergency shutdown can be accomplished by an electromagnetic release of these two cylinders. Heat generated in the reflector is removed by air. Start-up instrumentation is located in the water tank outside the reflector (see Fig. 5.2).

Two temperature coefficients of reactivity were measured in BR-5, one relative to the inlet temperature and the second relative to the outlet temperature (power coefficient). These agreed with predictions and were both negative. The fuel elements supported in a lower support plate are free to move at the top to take up any tolerances in the lower plate. The pins within the subassemblies are welded together at the bottom. Alternate pins are wound spirally with stainless steel wires, which act as spacers. Bowing of pins or subassemblies tends to cause the tubes of the outer elements to move outward to reduce reactivity. An increase in coolant flow has a similar effect.

The reactor was designed not only to permit sample radiation under fast flux conditions but also to allow the insertion of special fuel subassemblies in the core in place of normal elements. A 1 in. diameter re-entrant tube in the centre of the core, designed for testing fuel elements, is cooled with a separate NaK cooling system. In this central loop a peak flux of 10^{15} neutrons $\cdot$ cm^{-2} $\cdot$ s^{-1} is available. A flux of one-half this value is available in the exposure holes at the edge of the core.

The coolant system is split into two 100 mm diameter primary loops, as shown in Fig. 5.4. The system is designed so that leakage, if there is any, is through the gland into the system. Heat is transferred from the primary loops by two IHXs to two secondary loops.

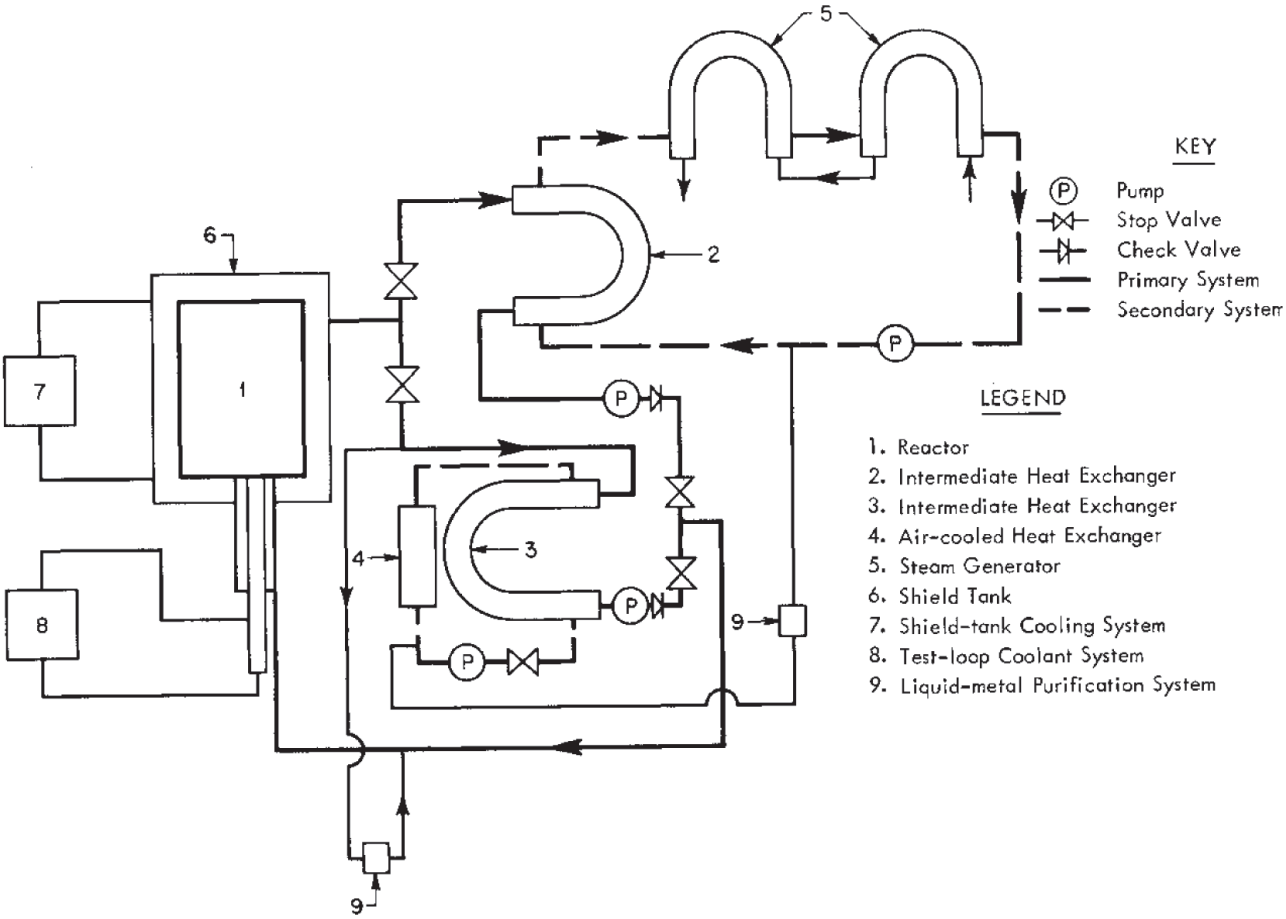

FIG. 5.4. BR-5 sodium primary and secondary systems (SG — at the early stage of operation) [5.3].

One of these NaK filled secondary loops was provided with a SG having duplex tubes. Mercury was used as the heat transfer substance in the space between the inner and the outer tube. There were big difficulties in operating — owing to mercury contact with sodium/water. Apart from this, the double wall tubes with a stagnant heat transfer medium significantly affected heat transfer. The SG was replaced by an air cooled IHX. An air cooled IHX and a blower were used to reject the heat in the other loop through a ~25 m stack. Residual heat after shutdown was also removed in this loop by natural convection.

5.1.2. Operating experience, cleaning and decontaminating of the primary circuit

The reactor started up at zero power in July 1958. During the period from July 1958 to January 1959, the assembly of the primary loop was completed and startup modifications were accomplished. In January 1959, the reactor was started up with sodium coolant. From January to July 1959, the reactor operated to 1000 kW(th). On 21 July 1959, the full power of 5000 kW(th) was reached. Later the reactor was operated at various levels up to 5000 kW(th) for a 450°C sodium outlet temperature. The temperature of the sodium in the primary loop was raised to 500°C in December 1960. During 1960–1961, the reactor was used for experimental purposes. The following operations were carried out:

— Determination of the effect on reactivity of circulating sodium;
— Measurement of the temperature and power coefficients;
— Determination of spatial neutron energy distribution and heat generation;
— Measurement of neutron flux in experimental channels and in sections of the reactor;
— Determination of radioactivity effects and safety aspects;
— Calibration of control rods.

The mechanical pump life was mainly determined by ball bearing capability; it averaged 8000 h. Replacement of primary equipment including cold traps usually started a week after shutdown, i.e. after sodium gamma decay. The cold traps in the primary system were replaced four times during four years of operation.

By October 1960, with about 2.5% maximum plutonium burnup, the leakage of fission products into the sodium became pronounced. By September 1961, the caesium activity in the sodium was 70% of total caesium plus Na^{22} activity after Na^{24} decay. Fuel burnup had reached 5%. The reactor was unloaded, and the subassemblies were steam cleaned. During cleaning, some of the subassemblies showed a considerable increase in steam condensate activity owing to increased failure of fuel pin cladding. Steam cleaning was discontinued, and a leak test with an ionization chamber was then used to check each subassembly to measure fission gas activity. Of the 81 subassemblies tested, 8 had been washed with steam; of the remainder, 63 showed normal sodium impurity activity and 10 had a gas activity higher by a factor of 1000. Examination of the 5% burnup pins showed longitudinal cracks in the cladding due to fuel swelling. The cracks showed up where the clearance between cladding and fuel was very small.

After fuel removal the primary system was drained, cleaned with steam at several pounds per square inch gauge and about 130°C injected into filled lines, and removed from the low point. The system was kept at about 150°C prior to steam injection. About 9 t of steam was used, and no violent reactions occurred. Contamination of the primary system was reduced by 50%.

The system was then filled with pure water twice, with no circulation, and drained. There was no decrease in activity. Each section of the primary system except a nickel basket in the reactor was then cleaned with a solution of 5% nitric acid at about 75°C for three successive flushes to reduce the activity two- to threefold in one of the sections. Two sections of the primary system were further subjected to a 0.5% $KMnO_4$ solution flush for 24 h at about 70°C, a 5% nitric acid and 1% oxalic acid mixture flush for 3–4 h at 75°C, and a pure water flush for 1 h at about 70°C.

These three flushes were repeated five times. Activity was reduced to a value low enough that repair work could begin. A total of 21 flushes per section were used, including the steam flush. This indicates the possible consequences of plating out of fission products on system components. Radiochemical analysis showed plutonium, zirconium, and caesium as the residual activity. After the final drain, the primary system was dried by vacuum and heat. Following repairs, the system was filled with distilled sodium. The reactor was placed back in operation in March 1962 after a six month shutdown. Eighty per cent of the original fuel subassemblies were placed back in the reactor. By the end of 1964 a maximum burnup of the PuO_2 fuel of 6.7% had been reached.

From 1965, BR-5 was operated with a 90% ^{235}U enriched uranium mono-carbide fuel. The maximum burnup was 6.2 at.%, and unsealed fuel elements were detected with 1.6 at.% owing to cladding carburization from the fuel side.

During 1971–1972, the BR-5 plant was updated to provide a power level of 10 MW(th), and was called BR-10. Operation of BR-10 started in March 1973 at a power level up to 7.5 MW(th).

From October 1979 until early 1983, BR-10 was extensively reconstructed, including the replacement of the reactor vessel with the new one. The reactor was brought up to a power of 8 MW(th) in November 1983. Two cores (~1300 fuel pins) have been irradiated with mono-nitride fuel and the maximum burnup reached beyond 10 at.%. All the fuel pins remain intact.

The problems in reactor component operation were almost entirely due to the relatively frequent pump repair: its life, determined by the ball bearings, averaged 10 000 h. Some operation and repair problems observed with the NaK secondary coolant were due to its very low freezing temperature, which was the reason for replacing it with sodium in 1963. Electromagnetic pumps (EMPs) were successfully operated for sodium pumping in auxiliary circuits. Therefore, it was decided to replace the primary and secondary mechanical pumps with EMPs.

The Soviet Union built a series of experimental fast reactors, beginning with the BR-1 critical assembly in 1955 (fuelled with plutonium metal), which was upgraded to a 100 kW plutonium fuelled mercury cooled reactor and renamed BR-2 in 1956. The world's first reactor fuelled with PuO_2 fuel, the BR-5, attained criticality in 1958. It was known as the BR-10 after a 1971–1972 modification and operated until December 2002 using 90% ^{235}U enriched mono-carbide fuel.

The working times of the plant components in sodium under nominal parameters are as follows: reactor vessel[1] — 150 000 h; primary piping — 300 000 h; electromagnetic sodium pump — 170 000 h: IHX — 300 000 h;

[1] This reactor vessel was replaced with a new one.

3300 PuO_2 fuel elements — maximum burnup of 14.2 at.%. The experience gained with the BR-5/BR-10 plant during 46 years (1958–2004) of successful operation was and is the most representative from the standpoint of sodium systems and components for future fast reactors; the reactor parameters were comparable in a future large scale plant [5.1–5.8].

5.2. DOUNREAY FAST REACTOR (DFR)

5.2.1. Heat transport system and balance of plant (BOP)

Since the early 1950s, much work on fast breeders has been done not only in the USA and in the Soviet Union, but also worldwide. Some European countries and Japan have shown interest in fast reactor programmes. Construction of the United Kingdom's Dounreay fast reactor (DFR) started in 1955.

The philosophy of the DFR was to have the experimental part of the system only inside the reactor vessel; in the outside zone, every effort was to be made to minimize the risk of breakdown of the cooling system. This explains the unusual number of coolant trains.

This reactor was fuelled with U–Mo, using a NaK eutectic as a coolant, and had a power of 72 MW(th)/15 MW(e). The developers believed at that time that the use of NaK would be an advantage in the early stages of commissioning and operation, when liquid metal could be circulated under varying temperature conditions without freezing. To this end, it was decided to operate the reactor with the NaK alloy as the coolant.

The primary objective of the DFR was a demonstration of the feasibility of fast reactor core operation; the heat transfer system was not designed as a suitable prototype of an economical system but rather as the most reliable combination of available components that would accomplish the purpose. The design objective was to reduce the risk of cooling system breakdown rather than to create an economical heat transport system.

The latter meant that some design problems that needed to be solved to build a fast reactor at low capital cost (e.g. economical liquid metal–water SGs) were bypassed in the interest of soundness and reliability of the project. It was assessed that a period of at least two years would have been required for the development and testing of shell and tube heat exchangers and electromagnetic pumps of a larger size. The 24 coolant loops were constructed of piping varying in diameter from 3/4 to 6 in. without the use of valves.

The United Kingdom Atomic Energy Authority (UKAEA) had considerable experience in the controlled fabrication of large plants made of stainless steel. Stainless steel made it easier to keep the circuit clean during erection, and hence no special cleaning of the system prior to its being filled with liquid metal was thought necessary. Components subjected to heavy working or welding stresses were stress relieved, and, in addition to being X rayed, all welds were pressure tested and leak tested with nitrous oxide or a halogen gas. Stainless steel was chosen for the material of construction because in the mid-1950s there was little information available on the behaviour of carbon steels in a liquid metal circuit.

Experience gained in the construction of the UK's chemical separation plants using stainless steel showed that it should be possible, given proper control of materials and fabrication techniques, to build a leaktight and completely drainable primary system, provided that it was welded throughout and the circuit was designed so that every weld could be radiographed and tested. The general arrangement of the DFR plant heat transport systems is shown in Figs 5.5 and 5.6.

A containment sphere contains the reactor vessel and the primary coolant system. Provision was made for shutdown heat removal by a natural convection loop which vents up the stack. No valves were used because of their potential weakness.

The heat removal system has two notable features: downward flow in the core and 24 primary loops. The downward flow of coolant through the core permits the various components at the top of the reactor to operate in cooler regions and simplifies the structural design of the core, since the coolant does not tend to lift the fuel elements.

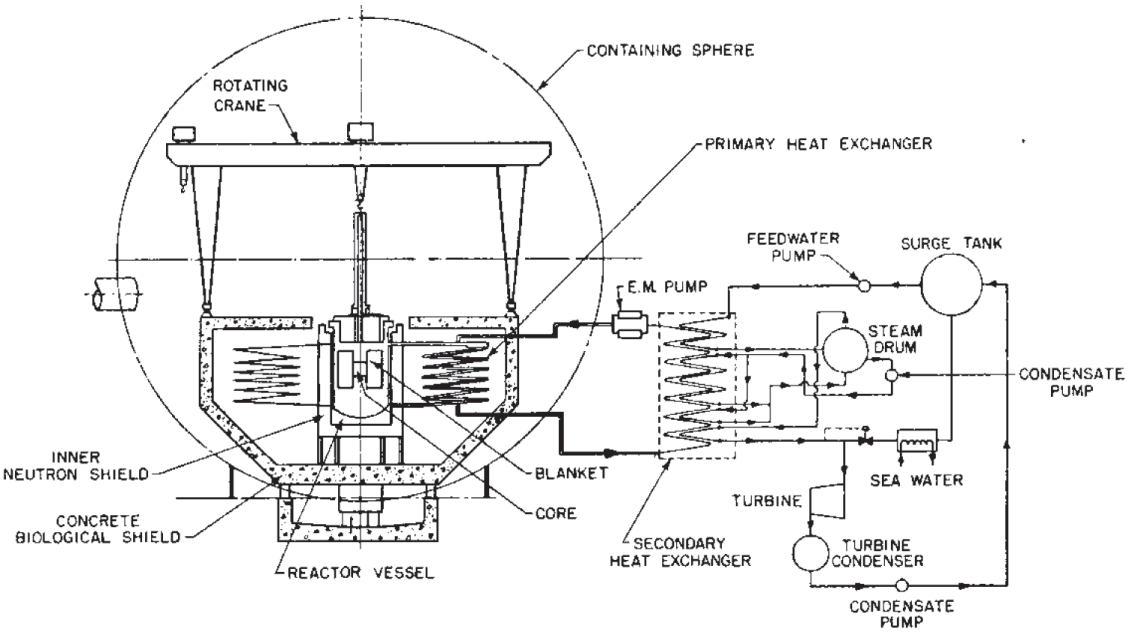

FIG. 5.5. DFR heat transport/conversion systems [5.9].

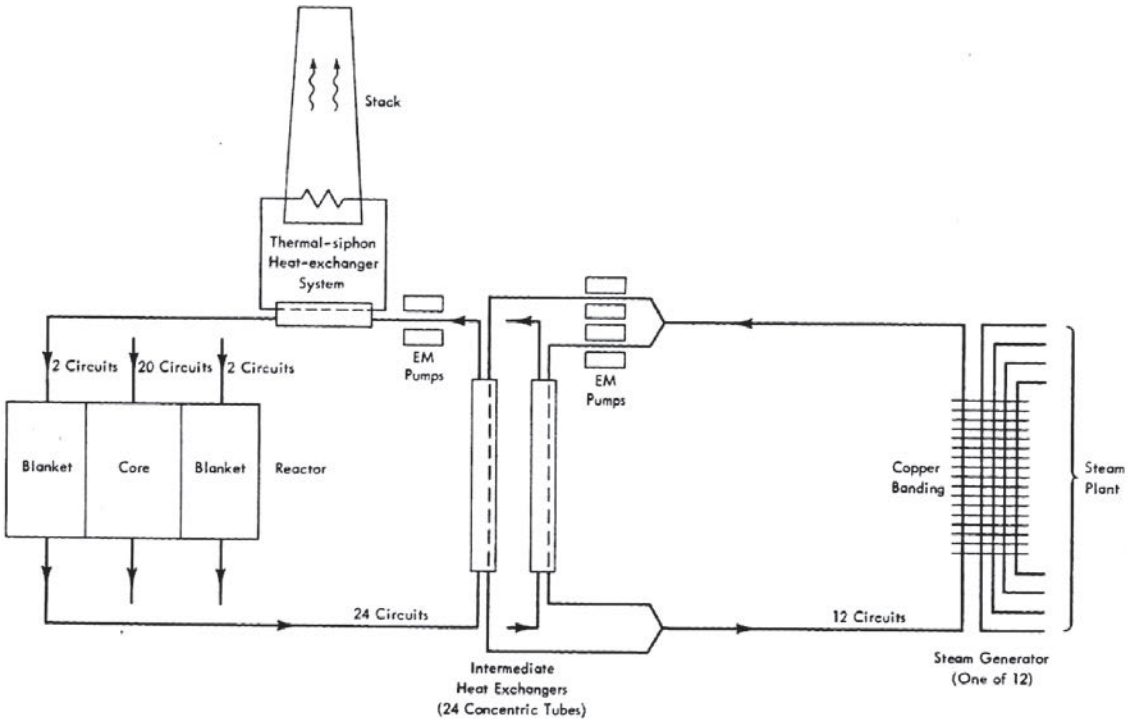

FIG. 5.6. DFR shutdown heat removal diagram [5.10].

The multiplicity of loops ensures continuous cooling. If the flow is normally downward and pumps fail, there is progressive changeover from downward to upward natural circulation flow.

A small liquid metal heat exchanger in each primary circuit is connected to a system that rejects its heat to air by a natural draft through a stack. This system was always in operation. In the event of total coolant pump failure, the reactor would be scrammed. Decay heat would then be removed by the thermal siphon heat exchanger system (Fig. 5.7).

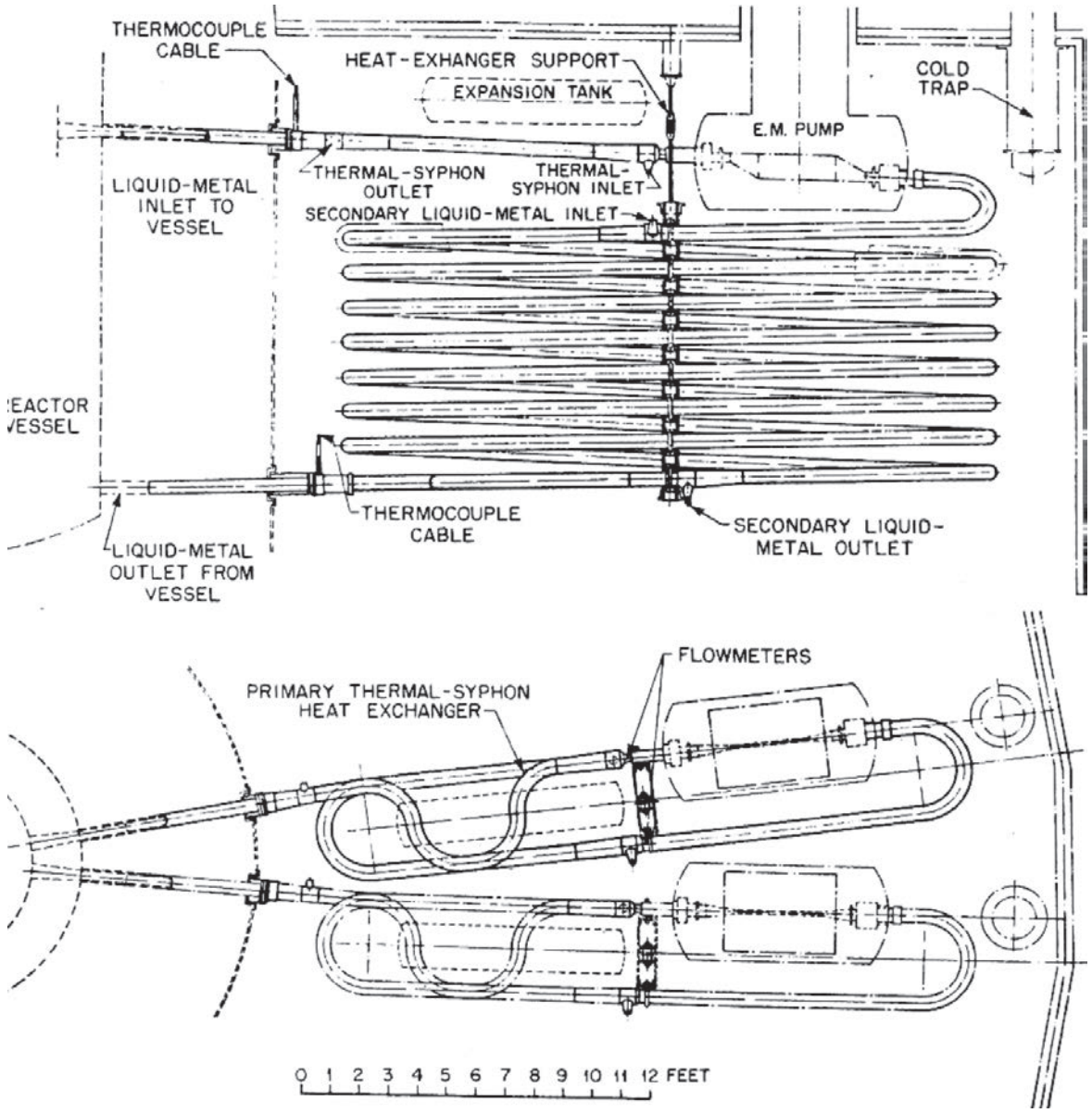

FIG. 5.7. DFR intermediate heat exchanger [5.9].

This system consists of 24 heat exchangers, of similar construction to the primary heat exchangers, situated between the EMPs and the reactor vessel. Owing to natural convection, coolant flow will reverse and decay heat will be transferred to the NaK on the secondary side of the siphon heat exchanger located at the base of a chimney (Fig. 5.7). The thermal siphon system will remove 2.24 MW(th) of heat on a complete pump failure.

The main primary heat exchangers consist of concentric tubes, each forming a separate heat transport circuit having its own EMP and flowmeter. This piping is so arranged that 20 of the circuits carry NaK to the core section of the reactor and four circuits feed the blanket section. The circuits are manually controlled, in pairs, with the flow regulated so that a constant inlet temperature is maintained. Primary coolant flow can be trimmed (the core circuits having a different flow rate than the breeder circuits, if required) to balance the heat outputs to the secondary liquid metal–water heat exchangers. Control of the EMPs is achieved by the manually regulated induction voltage regulators feeding the D-C rectifiers for the pumps. Adjacent pairs of secondary piping on the 24 primary heat exchangers are connected in parallel to form 12 NaK coolant circuits, ten of which extract heat from the primary core circuits and two from the blanket circuits.

There are 24 EMPs operating in pairs with control similar to the primary pumps. The 12 secondary liquid metal–water SGs transfer heat from the liquid metal coolant to the steam plant through copper banding of the stainless steel tubing, carrying the liquid metal and water.

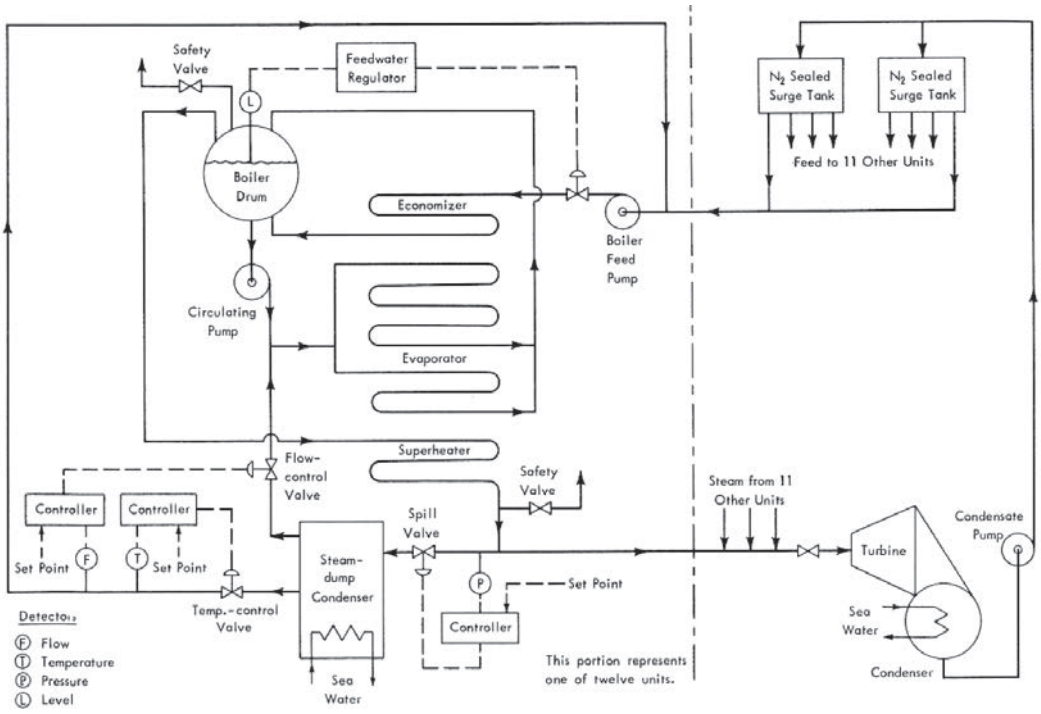

FIG. 5.8. DFR balance of plant diagram [5.10].

The heat transport system (Fig. 5.7) was designed to remove 60 MW(th) from the core and 12 MW(th) from the breeder blanket. The coolant leaves the bottom of the reactor vessel at 350°C, leaves the IMX at 200°C and then passes through the EMP and a thermal siphon heat exchanger before re-entering the vessel. The pump was installed in the cooler part of the circuit, since the coolant operating temperature was restricted to 200°C to prevent overheating of the windings.

Each secondary loop removes heat from two primary loops, necessitating 12 independent secondary units, each complete with a SG. The main IHXs, each designed for 3 MW(th), consist of an inner stainless steel pipe, 300 ft long and 4 in. in diameter, surrounded by an outer stainless steel pipe 6 in. in diameter which is formed into seven loops, as shown in Fig. 5.7. The inner and outer pipes are held concentric by means of spiders machined from solid stainless steel welded into the pipe. The secondary NaK coolant flows through the annulus of each leg of the exchanger, clamped to a steel framework that is supported by a hanger through a pin joint from the vault roof. The exchanger can move in a radial direction.

Each of the 12 secondary loops contains two EMPs installed in parallel in a cool return leg from the SG. The SGs, in turn, each of 6 MW(th) capacity, consist of 13 rows of 20 heat transfer elements each. These elements were constructed by spirally winding copper laminations to stainless steel tubes. Since the sodium-containing tubes are connected to the steam generating tube by copper laminations, heat transfer is by conduction from one tube to another via the copper. The possibility of leakage from the NaK to the water system is thereby minimized.

The structure of each of the 12 liquid metal–water SGs consists of economizer, evaporator and superheater sections, a boiler drum, a circulating pump, a feedwater pump and a steam dump condenser (Fig. 5.8).

Each SG is capable of producing 8000 lb/h at 185 psig and 275°C. The plant was designed so that the steam dump automatically accepts all the steam produced in excess of turbine requirements, up to 100% of steam production. If all the steam dump system should fail, the full reactor heat output can be extracted by exhausting steam to the atmosphere through the superheater safety valves as long as the supply of feedwater is maintained. Boiler drum safety valves act as a backup for the superheater safety valves. Condensate from the turbine feeds into two surge tanks. All 12 SGs are tied to common headers, which are connected to the turbine and the surge tanks.

The steam dump condenser can also be used for water dumping by dumping the evaporator water directly into the steam dump condenser. Greater flexibility was obtained in this manner for controlling temperature conditions in the core as well as increasing its total heat capacity to 50 MW(th).

The temperature at which the steam dump condenser outlet is controlled will determine the mean temperature at which the reactor core and breeder elements will operate. Control of the outlet of the steam dump condenser is

within the range of 32–392°F. Control is fully automatic, and adjustment of the desired level of control is effected by the operator through the control panel. Manual control is possible if the automatic system fails.

The temperature at the outlet of each steam dump condenser was measured by means of a temperature transmitter whose output signal feeds into a pneumatic controller. The output of the controller was 3–15 psig, corresponding to a temperature range of 32–392°F. The controller received its set point pressure through the control panel. During normal operation of the reactor, all 10 circuits extracting heat from the core were operated at the same temperature, and the local control panel was arranged for remote control. The two circuits extracting heat from the blanket were also operated at the same temperature, which may differ from the setting for the 10 circuits. The automatic system maintained the temperature to within ±3.6°F.

A further requirement of the steam plant was that the feedwater flow in each of the 12 circuits remain constant under all conditions of operation. Since the temperature control valve, installed in series with the respective steam dump condenser, will throttle the flow to the condenser and hence determine the amount of heat rejected, it was necessary to provide a further control system to meet the requirement that the feedwater flow be kept constant under all conditions of operation. A pneumatic control valve was installed in parallel with the temperature control valve and the steam dump condenser. This flow control valve was operated by a pneumatic flow recorder controller. If the temperature at the outlet of the heat exchangers should increase, the temperature controller would open the temperature control valve in series with the heat exchanger to increase the flow and hence increase the heat rejected by the steam dump condenser. The flow controller would therefore momentarily see an increase in flow and adjust (throttle) the flow control valve to produce the required flow. The flow was kept constant to within limits of +3%. Because of the thermal lag in the system, the series valve operated slowly; the shunt valve, however, responded very rapidly to a change in flow. Both series and shunt valves were arranged to lock into position should the air supply system fail during operation.

Delivery from the boiler feed pump is controlled by a regulator that maintains the water level in the boiler drum, which is fed from the evaporator section. Discharge from the boiler drum to the evaporator section is held constant for all loads by the circulating pump. A spill valve in the steam inlet to the steam dump condenser controls the pressure in the system. Steam generated in excess of turbine requirements causes a buildup of pressure until the valve opens and passes the surplus steam to the dump condenser.

The condensate is continuously returned to the suction of the feed pump by the pressure head in the steam dump condenser. Since the feed pump suction is connected directly to the surge tanks and the dump condenser, the system can be looked upon as forming the two legs of a U tube, the pressure in the steam dump condenser balancing the head of water in the surge tanks situated 25 ft above it. An increase in the rate at which steam enters the condenser causes a pressure rise that depresses the water level in the condenser and exposes more cooling surface until the steam is being condensed at the rate at which it is entering.

A spill valve can be set to lift at pressures ranging from 135 to 235 psig. A bypass is fitted which allows pressures below 135 psig to be obtained by hand control. The spill valve is a pneumatically controlled diaphragm valve of the pressure to close type. It receives air at pressure varying from 3 to 15 psig from a force balance type pneumatic controller that is actuated by steam pressure in the superheater outlet. Distribution of reactor heat among the individual units can be varied by these valves, since raising the pressure set point in one unit will reduce the temperature difference between steam and coolant and cause the heat transferred in the liquid metal–water heat exchanger to fall.

When the evaporator water circuit carries heat from the liquid metal to the seawater without raising and condensing steam, greater flexibility in the temperature conditions in the reactor core is obtained. This process is known as water dumping. Only the top part of the evaporator was used; the bottom part was closed off, drained and vented. The economizer and superheater were also shut off, drained and vented. The steam to, and condensate from, the dump condenser were closed off, and the condenser was used to cool the water in the evaporator circuit.

The temperature of the water in the evaporator circuit was controlled for any given reactor power level by a shunt across the dump condenser. A pneumatically operated diaphragm valve, called a series valve, controlled the flow through the dump condenser. The force balance pneumatic controller for this valve is situated in the unit control cubicle and is actuated by the temperature at the water inlet to the evaporator. Selection of the temperature was carried out locally or remotely from the reactor control room. A shunt valve of similar type was actuated by the flow in the main circuit, opening as the series valve closed, and vice versa, to keep the total flow constant.

The heat transport system included the usual array of accessory equipment, i.e. cold traps, hot traps, sampling equipment, filling stations and an inert gas (nitrogen) system. In the design of the heat transfer system,

considerable attention was devoted to a number of emergency and standby arrangements to ensure integrity of the system and the removal of decay heat during reactor shutdown for any reason. For example, a thermal siphon system was installed to remove the shutdown heat of the core from the primary circuits to a convection air cooled heat exchanger outside the containment sphere with no requirement for electrical power.

5.2.2. Liquid metal coolant system

The reactor went critical for the first time in November 1959 and operated at zero power until April 1960, when it was shut down for the installation of a second core, which reached a power level of 11 MW(th) in late 1961. A third fuel loading, made in mid-1962, reached criticality on 26 July 1962, and attained a power level of 30 MW shortly thereafter. A fourth loading completed in June 1963 was operated at levels as high as 60 MW(th).

The first DFR operated from 1959 to 1977; it came on-line in 1961. Electrical power was exported to the national grid from 14 October 1962 until the reactor was taken off-line for decommissioning in 1977. During its operational lifespan, the DFR produced over 600 million kW·h of electricity.

A number of problems were encountered during the initial start-up procedures. Contamination of the NaK with oxide proved to be much higher than anticipated and required a considerable cleanup effort. The cold traps installed in each of the coolant loops failed to operate effectively. The installation of a better cold trap system and more satisfactory impurity measurement instrumentation were found to be necessary. There was considerable stress corrosion in the 321 stainless steel superheaters and evaporators, starting in late 1961. The contributory causes were chlorides in the water, aerated conditions and carbide precipitation, particularly at the surface of the steel. Extensive repairs were made to the SGs, and careful control of water purity was instituted. Repairs were not completed until April 1963.

Niobium and vanadium fuel cladding failures occurred as a result of hydrogen embrittlement induced by hydride in the coolant. This contamination was believed to have been introduced with the first charge of fuel. It was understood that carbon in the system may also have contributed to the embrittlement of the cladding. Considerable work was done to determine this effect. Loops were in operation with a hot trap and specimens of zirconium, zircalloy, nimonic and three types of low carbon stainless steel. It was known that additional efforts were made in the other groups to determine the effects of carbon on the structural material. An extensive cold trap and hot trap system was installed to reduce oxygen, hydrogen, nitrogen and carbon concentrations in the coolant to very low levels. Excessive niobium corrosion was reported as late as March 1963. Considerable gas entrainment in the coolant circuit required a number of modifications. These included changes in the expansion tanks and a separate gas enclosure for the control rod mechanism.

Troubles encountered with the control rod thrust head were traced to the pickup of scum from the contaminated liquid metal surface. These problems were eliminated by the hermetically sealed drive. During the startup period, problems were also encountered with numerous components, such as the control units and the mercury seals on the rotating shield.

Low power experiments were concerned with the determination of physics parameters. The predicted critical mass, neutron flux and power distribution for the core region, and the neutron energy spectrum at the core centre were reasonably well confirmed.

The new core tube nest, designated as core B, was installed in April 1960. Many of the startup problems were subsequently solved, and a power level of 11 MW was reached in late 1961. The second charge of fuel of 345 elements was discharged in the period December 1961 to February 1962. After the discharge the primary system had four complete fills of sodium and 12 dumps. Only after cleanup operations were completed in June 1962 and the holdup of oxide in the clocked bypass circuits eliminated the plugging was the temperature reduced from 230 to about 140°C.

The third fuel loading was uranium-10 wt% molybdenum; it was completed in the period June to July 1962. During this loading the roller bearings on the charge machine were replaced with ball bearings to prevent the bearing seizure previously experienced. Criticality was reached in July 1962, and operation at 30 MW(th) was realized in August 1962. During this period the NaK content rose in the rotating plug, owing to unbalance in the gas lines, contaminating the mercury dip seal and requiring about 1300 lb of mercury to free the seal.

New balance lines were added to eliminate this problem. The plugging temperature was further reduced to 110°C by isolating the rotating plug graphite from the reactor cover gas. Testing of uranium-18 at.% molybdenum, uranium-20 at.% molybdenum, and uranium-25 at.% molybdenum indicated that the uranium-18 at.% molybdenum

transformation from gamma to gamma plus alpha phase started in 40–45 min at 890°F with completion of transformation in 150–250 h; uranium-20 at.% molybdenum at 800°F took 5–7 h to initiate the transformation and over 1000 h to complete it, whereas at 1020°F it took 1–2 h to initiate and 200–300 h to complete; and the uranium25 at.% molybdenum at 800°F took 50–70 h to initiate and was only 5% complete in 500 h.

Examination of the uranium–molybdenum alloy fuels indicated that fuel slugs irradiated to burnups of 0.3% had cracks that increased with fuel temperature up to 450°C. Cracking was greatest in the slugs having the large fuel–cladding clearances. An increase of molybdenum content from 20 to 25 at.% showed no improvement in irradiation behaviour at burnup of 0.48–0.6%. It is hypothesized that steep temperature gradients occur, as high as 2000°C per inch in the fuel. Centre swelling, produced by gas pressures in the high temperature centre of the fuel, acts against the restrained cooler outer layers. The combined action results in the cracks.

Modifications were made to the fuel handling system in early 1963 to include a 10 t hoist to move a fuel transfer cask from the canning station to the air lock trolley. A second carrier was added to the canning station trolley, permitting the refuelling machine to pick up a new subassembly immediately after releasing a spent fuel subassembly. These changes increased the rate of fuel changing from 14 to 20 per day with the possibility of increasing to 24 fuel subassemblies per day.

After a fourth loading of fuel, completed in June 1963, the operation of the reactor reached 55 MW(th) on 18 June 1963, with a subsequent increase to 60 MW(th) in July. The so called Mark-III fuel subassemblies with uranium–molybdenum fuel were designed to achieve this rating. The 60 MW(th) run achieved a fuel burnup of 1.12% of the heavy atoms. The condition of the fuel cans externally was good. The fuel, as expected, was cracked and swollen.

Operations through the autumn of 1963 were at a maximum burnup of the uranium–molybdenum of 1.2% of the heavy atoms. Electricity was first generated in October 1963, and a tie-in was made to the national grid in that month. The operating conditions for the 60 MW(th) run were as listed in Table 5.1.

TABLE 5.1. THE OPERATING PARAMETERS FOR THE 60 MW(th) [5.3]

Item	Value
Primary coolant flow through the core, lb/h	3.21×10^6
Primary coolant flow through the blanket, lb/h	0.64×10^6
Core pressure drop, psi	10.2
Inlet coolant temperature, °C	230
Mixed outlet temperature, °C	330
Maximum outlet temperature, °C	395
Maximum fuel temperature in standard element near core centre, °C	617
Maximum fuel temperature in pilot element in control rod, °C	649
Central neutron flux, neutrons · cm^{-2} · s^{-1}	2.64×10^{15}
Duration of run, days	37
Integrated power for run, MW·d	2015
Total integrated power, MW·d	4390

After several years of operation, the DFR was shut down in 1967–1968 for one year to locate and repair a small leak in one of the coolant outlet pipes inside the reactor vessel. The leak disappeared every time the reactor was shut down, making it very difficult to locate and assess. The DFR continued to operate until March 1977, when it was finally shut down. At its closure, MOX fuel experiments had reached a peak burnup of over 20%. Fuel pins with leaking cladding were irradiated following failure to a further 3 at.% burnup.

The Dounreay nuclear plant in northern Scotland was a reprocessing and fast reactor site requiring a complex range of decommissioning tasks, from the dismantling of contaminated areas to reacting volatile sodium coolant and removing fuel elements stuck in one of the site's fast reactors (DFR and PFR). A necessary step in removing this fuel and decommissioning the DFR containment sphere has now taken place with the sphere's being cut open

to connect it with a new breeder fuel removal building. A section of the DFR's steel sphere was removed in 2007 in preparation for the connection of the reactor and new plant. Since the closure of the DFR, most of the conventional non-nuclear equipment has been dismantled and disposed of together with the secondary circuit external to the sphere. Most of the fuel has been removed and methods for the removal of the remaining breeder have been decided.

The DFR was designed primarily to confirm the feasibility of the fast reactor concept, but it quickly assumed a more enduring role as a test bed for candidate fuel, cladding and structural materials. Until 1967, the major problem of damage to cladding materials was embrittlement. However, in 1967, evidence was announced of considerable void swelling taking place in austenitic stainless steels irradiated to high fluences in the DFR. This phenomenon has since tended to command the largest share of attention in the development of cladding and duct materials. A high nickel alloy was developed in the UK as reference cladding material.

During the final stages of normal power operation of the DFR, a series of experiments were performed with the objective of exposing bundles of typical MOX fuel pins to coolant boiling for prolonged periods. The series, known as the DFR special experiments programme, comprised eight separate experiments. They utilized both un-irradiated and previously irradiated fuel pins, and, in three experiments, included a thin steel plate simulating a local blockage in the heated section.

The information and experience gained from the DFR provided the necessary confidence that a commercial sized fast reactor could be successfully built and operated. However, because a large increase in size between the DFR and a commercial plant was necessary, the need for an intermediate plant incorporating the major steps in concept and scale was identified.

This power reactor was designed to produce 250 MW(e) from 600 MW(th) core power. In 1966, approval was given for building a prototype fast reactor (PFR) on adjacent land, to incorporate lessons learned from the operation of the DFR. The DFR had used a NaK alloy as coolant; the PFR used sodium, which was cheaper and easier to handle. Coolant flow was upward through the core (in the DFR the flow was downward) to avoid gas entrainment. The PFR fuel was a ceramic-a mixed plutonium–uranium oxide in sealed stainless steel clad pins (in the DFR the driver fuel was a vented enriched uranium metal alloy) to achieve higher burnup and to keep the coolant relatively clean. The sodium pumps were mechanical centrifugal pumps (EMPs were used in the DFR), to obtain higher capacity in compact units. Finally, the SGs were of an advanced highly rated tube in shell design (whereas those in the DFR were of a low rated, double walled design) [5.3, 5.8–5.13].

5.2.3. In-core coolant boiling experiments

5.2.3.1. Introduction and objectives of the experiment

This section presents the results of the DFR in-core coolant boiling experiments, including a brief description of the different rigs [5.14]. It summarizes the operating experience and a conclusion from post-irradiation examination (PIE) for each rig, and includes conclusions concerning the relevance of the programme and its results to ongoing LMFR safety studies. The work involved a large number of people at DNE and other centres, e.g. the intrinsic thermocouple was supplied by the Nuclear Research Centre, Karlsruhe, Germany.

In each experiment, coolant boiling was initiated by reducing the coolant flow through the rig using an inlet flow valve built into the experimental vehicle and controlled from the reactor control room. The coolant flow rate was reduced to a level which was 25% below that needed to induce boiling. Each experiment contained an array of thermal and acoustic sensors, with the precise complement of devices differing from rig to rig. The installed instrumentation served two purposes: first, it provided a means of monitoring conditions within the experiment; second, it enabled a comparison to be made between the efficacy of different types of technique for detecting the initiation and development of a subassembly incident.

In particular, the complementary and contrasting merits of the thermal and acoustic noise detection techniques were assessed at the Risley Nuclear Laboratories (RNL). Interpretation of the experiments was carried out using the subchannel boiling code that was specially developed for the DFR programme. As a further aid to interpretation, a replica of one of the rigs was studied, using electrical heaters, in a water rig at RNL. The range of tests carried out included both single and two phase behaviour, the influence of flow direction, the effect of different blockage porosities and the consequences of gas injection. The experiments were not

designed to study dry-out mechanisms, so the investigation did not attribute the encouraging behaviour to these mechanisms.

The experiments produced minimal interference with normal reactor operation; they were loaded as part of the normal reactor inventory and, with one exception, were not unloaded until the scheduled end of the run, some 65 d later. Therefore in most instances the fuel was subjected to significant periods of irradiation following exposure to boiling conditions.

PIE of the fuel pins provided insight into how fuel might behave in incident situations analogous to those modelled in this programme. Despite exposure to severe boiling conditions, the majority of the fuel pins examined to date showed either no damage or minor damage such as clad splitting; in one blockage experiment where conditions were severe enough to lead to clad melting there was no evidence of fuel melting.

In broad terms the experimental objectives were to investigate the consequences of local and inlet blockages in fuel pin bundles under reactor conditions, with the aim of demonstrating the pessimism inherent in safety analyses. More specifically, the results were expected to contribute to a more realistic understanding of the following aspects of LMFR safety arguments:

(1) Fuel failure characteristics and propagation under abnormal service conditions;
(2) The conditions for the initiation and stabilization of local boiling;
(3) The possibility of blockage growth through instability of the pin cluster under conditions of high temperature and high temperature gradient;
(4) Heat removal under bulk boiling conditions in a multi-pin geometry;
(5) The effectiveness of different instruments in detecting and distinguishing specific fault conditions;
(6) The time scales available for detection and for remedial action.

In addition, it may be possible to make qualitative comments upon:

— Fuel redistribution under escalating local incident conditions;
— The dynamics and extent of fuel–coolant chemical reactions.

The special experiments programme involved eight separate in-pile experiments using a total of 99 fuel pins. The coolant flow conditions were different in magnitude and direction from those in current LMFRs such as the PFR, but it is believed that these atypical conditions make the DFR experiments pessimistic and that the conditions experienced by the fuel were more severe than for the corresponding stages in a similar incident in a commercial LMFR. These experiments explored fresh ground by reducing the areas of speculation and by providing quantitative data, both supporting the development of theoretical methods used in safety analysis and providing pointers to the most appropriate areas for further development.

5.2.3.2. Design of the instrumented vehicles

The experiments were mounted in two different designs of instrumented vehicle: five experiments used a vehicle called a mini-subassembly containing 18 fuel pins and an unheated instrument probe; three experiments used a smaller vehicle, called a trefoil, involving only three fuel pins. The coolant flow through the eight experiments was determined by a valve located upstream of the fuel bundle in each vehicle and operated remotely from the reactor control room.

A typical mini-subassembly is shown schematically in Fig. 5.9; it contained 18 fuel pins within a pair of concentric cluster walls sitting inside a massive steel carrier. The cluster walls confined an argon gas layer which insulated the coolant flow in the rig from the comparatively cold bulk reactor flow. The five mini-subassemblies are divisible into two categories: the 523 series for bulk boiling and the 539 series for local blockage studies.

The fuel was MOX, either pelleted or vibro-compacted, with burnups ranging from zero to 10%, and cladding in cold worked M316 stainless steel. The nominal pin outside diameter (OD) was 5.3 mm and the pitch spacing similar to the PFR; the pins were spaced by honeycomb grids axially separated by approximately 100 mm. The fuelled length was comparatively short, being 505 mm in the 523 series and between 286 and 375 mm in the 539 experiments. Because of the low inlet temperature of 230°C and the short heated length, the axial temperature

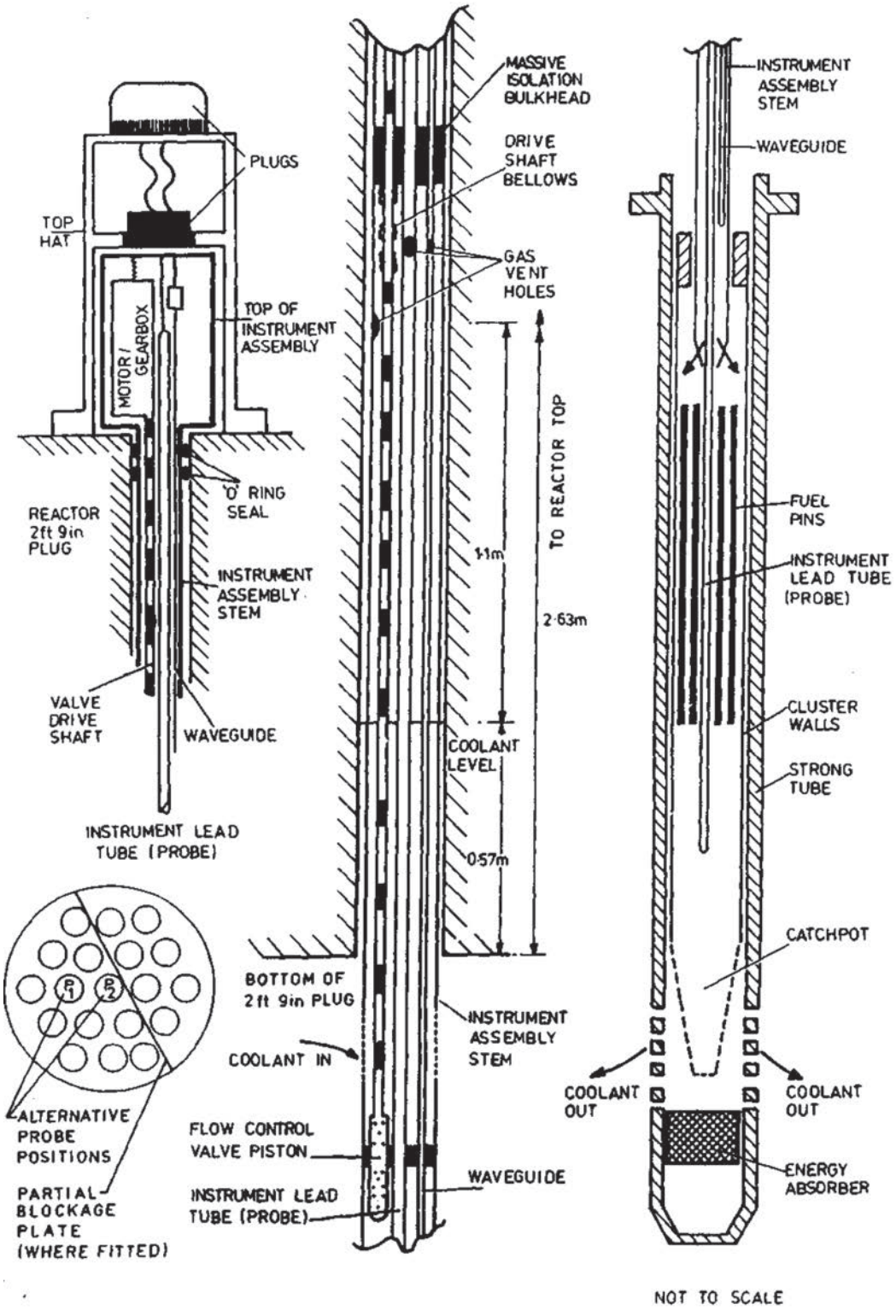

FIG. 5.9. Simplified sketch of mini-subassembly [5.14].

gradient under boiling conditions was between three and four times the gradient for a comparable incident in current LMFR designs. The typical peak linear rating for the fuel pins was 32 kW/m (280 W/g).

The local blockage in the 539 series was a thin steel plate mounted eccentrically and covering approximately 70% of the available flow area. The plate was welded to the downstream edge of a honeycomb grid and situated approximately midway along the heated length. There was a narrow, internally shaped, annular gap between the

blockage plate and each of the fuel pins which passed through the plate; the effect of the resulting small leakage flow upon the wake was examined in out-of-pile water tests.

The trefoil vehicle shown in Fig. 5.10 shared many features with the mini-subassemblies, e.g. the flow control valve design. The most distinct difference, apart from the number of fuel pins, was the introduction of instrumentation directly into and below the fuel cluster without the use of a separate instrument probe; this was

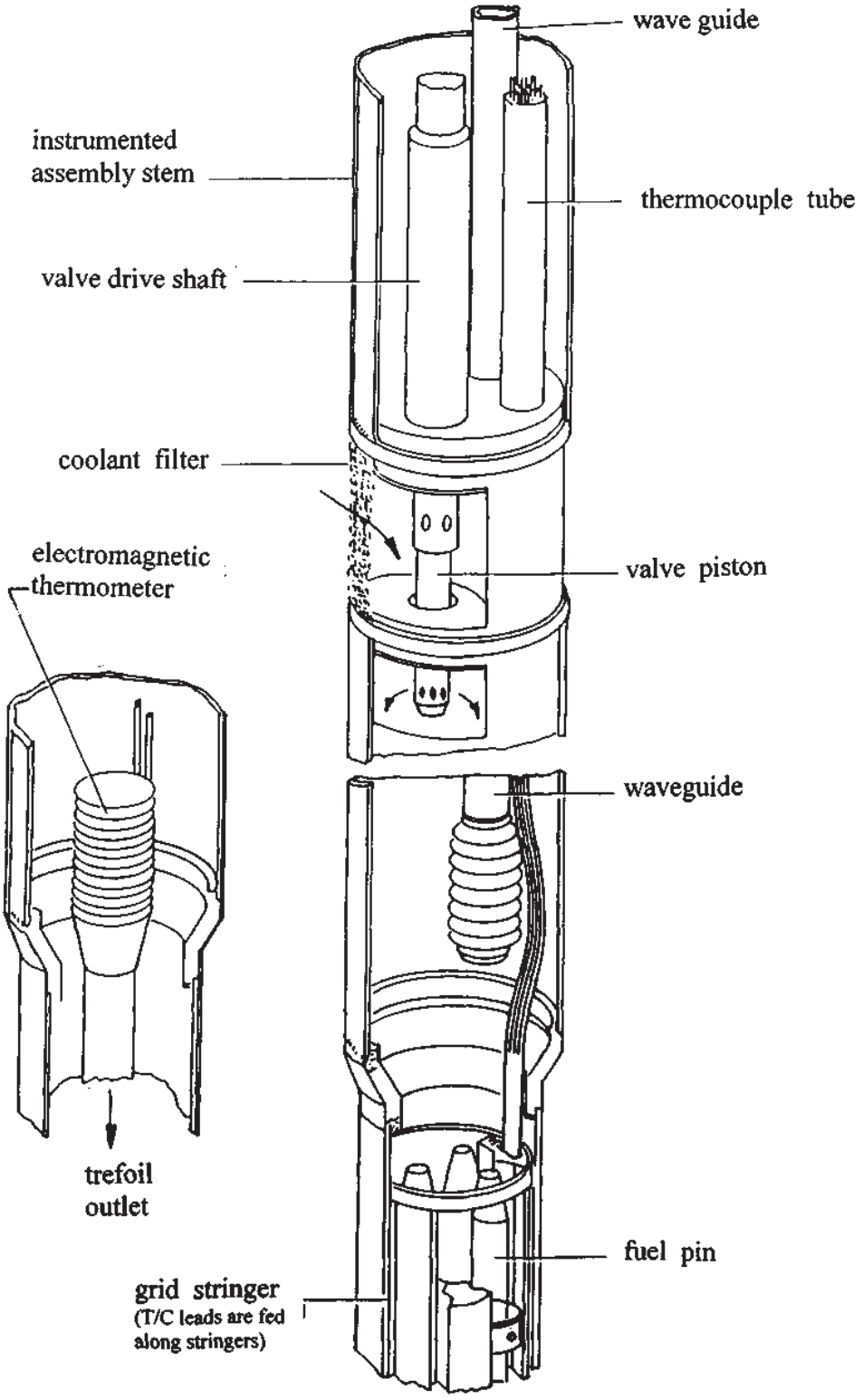

FIG. 5.10. Simplified sketch of the trefoil [5.14].

made possible by the use of unirradiated fuel, allowing the rigs to be assembled in one piece in the laboratory. Thus the trefoil experiments possessed thermocouple hot junctions sited in the main coolant flow, and, in the final trefoil experiment, an acoustic sensor positioned close to the boiling region.

All three trefoils contained irradiated MOX fuel; for two trefoil experiments, 522 and 540, the specification was similar to that used for the 523 series mini-subassemblies; for the remaining trefoil, 536, the fuel pins were 6.68 mm OD, spirally wrapped and containing vibro-compacted fuel at 80% theoretical density (TD) over a height of 569 mm.

In general, acoustic sensors were situated upstream of the fuel bundle and thermal sensors were positioned at inlet, midplane, outlet and, when appropriate, in the wake region downstream of the blockage. The instrument probe carrying the thermal sensors into the mini-subassembly fuel bundles passed centrally in the 523 series but was displaced to an off-central position in the local blockage experiments so as to provide a better guide to the wake temperatures.

Three types of thermocouple were used in the experiments: mineral insulated stainless steel sheath bifilar chromel/alumel 1 mm diameter conventional thermocouples; fast-response thermocouples consisting of filaments of chromel and alumel butt welded together inside mineral insulated stainless steel sheaths to form a single core coaxial cable, OD from 0.5 to 1 mm; and, in the last of the 528 mini-subassemblies only, an 'intrinsic thermocouple' based upon the principle described and allowing a very high frequency response. Experience with all three types of sensor was excellent throughout the programme, and of the many thermocouples used only one gave any sign of failure.

Three types of acoustic sensor were employed in the experiments, a conventional waveguide/accelerometer, a RNL high temperature microphone and a miniature capacitance microphone. Apart from the final trefoil experiment, all the acoustic sensors were situated approximately 300 mm upstream from the start of the fuel bundle. The RNL microphone was based around a lithium niobate crystal and was reduced in size especially for the DFR programme to an OD of 11 mm. The DNE miniature microphone was built from a 3 mm MISS single core cable and has a flattened 'sensitive' end of approximately 35 mm × 5 mm × 2 mm; because of its small size, it can be inserted into otherwise inaccessible locations. In the final trefoil experiment, a miniature microphone survived a temperature of nearly 1000°C for many hours.

In addition to the thermal and acoustic sensors described above, selected rigs also incorporated void detectors and electromagnetic devices designed to detect small, rapid changes in local coolant resistivity caused by temperature fluctuations or voids.

Throughout each experiment's in-pile life, the signals from the installed sensors were recorded visually on paper charts and, as a permanent record, on magnetic tape; on-line processing of thermal and acoustic noise data was provided by RNL during the majority of boiling runs. All these data have now been edited and a series of reference 'archive' magnetic tapes produced. The raw analogue data from the magnetic tapes have been normalized, to account for the amplification in the recording system and digitized to provide a computer data bank of temperatures for each boiling run of each rig.

5.2.3.3. Operation

The experiments were irradiated during the last three power runs of the DFR, i.e. in the period from December 1975 to March 1977; the experiments were loaded and discharged, with one exception, as part of the normal reactor loading schedule and were subject to the same stringent safety criteria as other rigs, with regard both to the safety of the core and to possible interference with other experiments.

To complement out-of-pile hydraulic tests, in-pile calibrations of the throttled rigs, i.e. curves of valve position against corresponding coolant temperature rise across the rig, were carried out during the period of low power operation at the beginning of each reactor run.

Additional calibrations were also carried out, if sufficient time was available, at the end of a reactor run and following any reduction in reactor power in an attempt to identify changes in the flow characteristics of the rigs as a result of boiling. Low power calibrations could be scaled to higher reactor powers and deviations between such scaled calibrations and data measured at the higher power attributed, in principle, to the presence of coolant boiling.

The simple intention behind the operation of each rig was to expose the fuel pins to periods of prolonged boiling; the mode of operation was straightforward. Because there was little previous experience to act as a guide,

coolant boiling was approached slowly in the early experiments and the periods of boiling kept relatively short; conditions were made more rigorous as confidence was gained. Thus, in the lead experiment, DFR 522, the outlet temperature was raised from 620°C to 900°C, at which subcooled boiling was first detected in slightly more than 3 h and boiling conditions were maintained for less than 1 h. For the final boiling run of an identical rig, the DFR 540, at the end of the programme, outlet temperatures in excess of 900°C were reached in less than an hour and boiling maintained for approximately 3.5 h.

The coolant flow rate was reduced to a level which was 25% below that needed to induce boiling. A typical boiling run proceeded by reducing flow through the rig using the control valve until coolant boiling was detected; the flow was reduced by a further 10–30% and the rig left for a predetermined period of time; finally, the valve was opened and the rig left until the next approach to boiling or the end of the reactor run. During their in-pile lifetime, the rigs were subjected to several boiling runs; e.g. in the local blockage experiments DFR 539/2 and 539/3 they boiled 5 and 11 times, respectively.

A summary of the overall programme is provided in Table 5.2. [5.14] and represents a total of 600 pin boiling hours; the longest total boiling time, 24 h, was experienced by 13 pins in DFR 539/3.

Three different indicators of boiling were recognized during the programme. Bulk boiling at the rig outlet was readily detected by the measured outlet temperature reaching the saturation temperature and by noting the invariance of the outlet temperature against a further decrease in coolant flow, as measured by the increase in midplane temperature.

Analysis of the lead experiment, DFR 522, showed that the inception of subcooled boiling within the bundle was accompanied by an increase in the thermal noise signal at the outlet thermocouples; the signal increased with further decrease in flow (i.e. increasing severity of boiling) until it reached a peak and thereafter decreased to a low value as bulk boiling was approached. For all subsequent rigs, thermal noise was monitored on-line by a team of experts from RNL; details of both this and the acoustic technique referred to in the next paragraph will be published elsewhere, and it is sufficient to say here that consistent and apparently reliable indications of the onset and development of boiling were made. Water tests in an electrically heated replica of the local blockage experiment confirmed that the thermal noise signal at the outlet thermocouple increased following the inception of fairly extensive nucleate boiling and increased further as the boiling developed.

In these experiments it was found that on-line examination of the RMS level and spectral content of the signals from the acoustic sensors sited upstream of the bundle was unable to provide any reliable indication of boiling inception.

A pulse technique developed by RNL and based on two separate detectors provided the only reliable acoustic indications of boiling and for the majority of rigs gave results consistent with those from the thermal noise analysis. In one rig, an acoustic detector was sited close to the boiling region and provided signals which have been interpreted as indicating subcooled nucleate boiling well before the outlet thermocouple showed any significant rise in thermal noise signal; this was consistent with signals from an electromagnetic sensor at the rig outlet and with observations from the water rig.

5.2.3.4. Analysis of the results and conclusions

The most important feature of the experiments is the behaviour of the fuel pins, and the first objective of the supporting analytical programme was to assist and complement the PIE of the fuel pins by specifying the thermohydraulic conditions experienced by each set of pins. A subsidiary objective is the determination of timescales at which significant points in the rig histories were reached, such as fuel failure, from changes in the measured thermal hydraulic data.

The CLAYMORE code was developed to help reach these objectives. CLAYMORE is a thermohydraulics subchannel code capable of describing local and bulk boiling; it includes a homogeneous two phase flow model with slip and reverse flow, i.e. it can represent the wake downstream of a local blockage. It is necessary to substantiate predictions from a code such as CLAYMORE, and to this end comparisons were made with:

— Measurements made in a water cooled replica of the local blockage rigs using electrically heated pins;
— Data from single pin and multipin out-of-pile sodium experiments.

TABLE 5.2. SUMMARY OF THE DFR IN-CORE COOLANT BOILING EXPERIMENTS [5.14]

Rig[a]	Brief rig description	Boiling history	Boiling duration	Comment
T522	Three unirradiated pre-pressurized MOX fuel pins. Maximum rating, 315 W/cm per pin.	One boiling run at end of run 79. This constituted a lead experiment for the series.	Approximately 1 h	Boiling was clearly detected at the time by the constant boiling temperature limiting at saturation temperature, and retrospectively by thermal noise analysis; examination of fuel pins showed no sign of damage.
M(b)539/l	18 reference design fuel pins, burnups in the range of 0–10%, vibro and pelleted fuel, different cladding types. Blockage plate covering approximately 70% of flow area.	One boiling run, but experiment terminated because of severe gas entrainment problems leading to extensive cladding failure in the wake region and self-induced boiling.		Despite the severity of the conditions to which the rig was subjected (failed pins exposed to hot coolant for the order of 10 d), there was no sign of fuel melting; nor was there any sign of rapid escalation of the fault condition.
T536	Three fat unirradiated spiral wrap MOX pins. Maximum rating 416 W/cm per pin.	Three boiling runs of approximately 1 h duration each. On two occasions a self-limiting temperature excursion was observed. First and second boiling runs approximately 1 week apart.	Approximately 4 h	Boiling detected by thermal noise and acoustics on-line. Examination of fuel pins showed no sign of damage.
M528/1	18 reference design fuel pins at 0.3% and 6% burnup. One pin contained an artificial defect at its hot end.	Two boiling runs; each run showed similar, steady and repeatable behaviour.	Approximately 2.5 h	Boiling detected by both thermal and acoustic noise techniques on-line at similar rig temperatures. Examination of bundle showed bowing of pins at the hot end and failure of one pin — no signs of clad melting or of any fuel loss.
M(b)539/2	As for 539/1.	Five boiling runs spread over 4 weeks. In the intervals between the first four boiling runs, the rig was left at approximately 100°C below saturation at hottest point.	Approximately 4 h	Boiling detected by thermal noise measurements on-line. Examination of rig showed marked bowing of pins at hot end. Six pins had failed with numerous longitudinal cracks. One also had a small zone of molten clad. No observable fuel loss.
M528/2	As for 523/1, proportion of pins at differing burnups changed.	Two boiling runs of approximately 3 h duration 10 d apart.	Approximately 6 h	Boiling clearly detected with thermal noise measurements and consistent results from acoustic noise. Evidence of coolant chugging for outlet temperatures exceeding 900°C. Nondestructive examination showed the pin array to be regular with no obvious pin failures. Swelling and distortion at hot end.
M(b)539/3	As for 539/1.	Eleven approaches to boiling spread over period of a month. For most runs the period of boiling lay between 2 and 3 h. A total of more than 7 h was spent with the rig outlet temp exceeding 900°C, with a significant fraction above 960°C.	Approximately 24 h	Increase in thermal noise signal with boiling less pronounced, although qualitatively the same as in previous rigs. Radiographs of the rig showed obvious signs of pin failures with possible fuel loss. During some of the later boiling runs, flows were reduced to 75% of their value at boiling inception.
T540	Similar to 522, but pins unpressurized and fuel in pelletted form.	Two boiling runs of approximately 1.5 and 3.5 h duration. Saturation temperature was kept steady at outlet and reached at the midplane.	Approximately 5 h	Thermal noise and acoustic noise both indicated boiling. Examination of pins showed distortion but no significant diameter change — no sign of failure of any description.

[a] M represents mini-subassembly; M(b) represents mini-subassembly with plate blockage; T represents trefoil.

The results of such comparisons showed there to be a broad measure of agreement between prediction and measurement, in particular the description of the development of local boiling appears to be qualitatively correct.

When applied to the DFR experiments, the code has adequately predicted the inception of boiling and such gross effects as the two phase pressure drop/flow curve, but detailed comparisons show that there are aspects of the rig behaviour which remained unexplained.

5.2.3.4.1. PIE, trefoil behaviour

PIE shows no signs of failure in any of the trefoil (previously unirradiated) fuel pins. Measured diameter changes are small, showing no apparent effect caused by prolonged high temperature operation: the DFR 540 coolant outlet temperature was above 800°C for more than 6 h, above 900°C for more than 5.6 h, and at a steady 960°C for just over 4 h. (The results with regard to PIE are summarized in Table 5.2.)

5.2.3.4.2. Mini-subassemblies without local blockage

The first of the DFR 528 series was radiographed and examined visually; the second experiment was only radiographed. Both bundles showed significant bowing of the pins and some swelling over the hottest region; otherwise, the pin arrays were regular. DFR 523/1 contained only one failure; there was no sign of fuel loss or of cladding or fuel melting.

5.2.3.4.3. Mini-subassemblies with local blockade

The first local blockage experiment inadvertently entrained gas into the wake region, causing fuel failure, including clad melting, soon after the first rise to full power. Boiling of the rig occurred after a further 10 d of irradiation and led to a further region of fuel failure downstream of the wake. Detailed PIE has been performed on the rig; there is no evidence of any fuel melting despite the severity of the incident; there are several examples of sintered fuel remaining intact despite removal of cladding from the failed region; there was no sign of any secondary blockage formation at the downstream grids despite the loss of complete sections of some fuel pins. The mechanism of gas entrainment into the wake and subsequent fuel failure has been demonstrated using the hot water rig.

The second blockage experiment has been examined visually. Six pin failures were found, including small regions of clad melting. There was some small observable fuel loss but no sign of steady blockage growth. The final blockage experiment was been examined radiographically, but there were obvious signs that at least three pins had failed extensively; however, the rig was boiled vigorously for nearly 24 h.

In the experiments, 600 pin-hours of detectable boiling were accumulated. No failures occurred in the pins with 3% burnup; seven failures arose among the 17 pins with greater than 6% burnup.

From the results obtained, it can be concluded that:

— DFR fuel pins were extremely durable, even when subjected to severe incident conditions.
— There was no sign that fuel failure, even when subjected to continuing irradiation and boiling, leads to a rapidly developing subassembly incident.
— The time available for the detection of the initial incident is long compared with the response times of all potential reactor monitoring systems.
— Thermal noise was an extremely effective and reliable method for detecting coolant boiling.

5.2.3.4.4. Relevance to safety studies

Because of the low, downward flow in these experiments, the effect of buoyancy upon boiling and entrained gas behaviour ensured that the experiments represented conditions that were more severe than the corresponding situation in a modern LMFR with high, upward coolant flow. In particular the results showed that:

— Boiling was detected at an early stage.
— Prolonged boiling was stable.

— Boiling did not necessarily lead to fuel failure.
— Fuel failure did not necessarily lead to fuel release.
— Fuel release did not lead to the formation of a local blockage.
— A local blockage did not lead to fuel melting.
— The combination of gas entrainment and a local blockage with consequent holdup of gas in the downstream wake did not lead to fuel melting.

Experimental studies on heat removal from the core by the boiling coolant carried out at the Obninsk, Russian Federation Institute of Physics and Power Engineering (fuel element simulators were tested in NaK coolant) have shown the possibility of the long term heat removal from the fuel elements by boiling coolant under conditions of natural circulation flow and heat flux up to 270 kW/m^2 (without fuel element simulator damage).

5.2.3.4.5. Relevance to sodium voiding reactivity

Historically, the desire to lower the amplitude of the positive sodium void worth in LMFR was driven by a concern about extremely high rates of sodium voiding. This concern had several origins. First, an observation in laboratory experiments showed that the onset of boiling in liquid sodium can occur at temperatures significantly higher than the boiling point before any vapour was formed. This would imply that once vapour began forming, the entire superheated coolant inventory in the core could void almost instantaneously without further heat addition. Second, there was the potential for vapour explosions wherein extremely high temperature fuel suddenly breached through cladding and mixed intimately with liquid sodium. Finally, any case of rapid voiding could result in high positive reactivity ramp rates which might act faster than the negative feedbacks could respond and would take the core into the super prompt critical range.

However, experimental data on boiling in tube bundles have shown that the in-core sodium boiling process in fact does not reach high superheat, but rather comprises a series of local pressurization and flow reversals which void part of an assembly for a short period of time. Detailed analyses have shown substantial spatial and temporal incoherence in the boiling process, with incoherent chugging and a few assemblies 'leading' the rest of core.

5.2.3.4.6. Relevance to reactor core acoustic instrumentation

Acoustic devices have been used successfully to detect boiling at the DFR. Therefore, acoustic detection of boiling can play an important part in the plant protective system, because it affords a means of detecting local overheating and allows protective action to be taken before damage spreads to otherwise unaffected parts of the structure.

The objective of the protective system is to intervene by shutting down the reactor — preferably soon enough to prevent fuel melting, and certainly soon enough to prevent the propagation of damage beyond the affected subassembly. Acoustic instrumentation has an important role in providing a signal that something is amiss, to initiate the protective action. Its importance lies in the fact that it may afford the only way of promptly detecting that the coolant is boiling.

As an example of the type of local fault against which acoustic boiling noise detection (ABND) provides protection, it is common to consider a complete instantaneous blockage of the coolant flow at the inlet to a core subassembly while the reactor is operating at full power. The performance of ABND systems was the subject of an IAEA coordinated research project aimed at determining whether boiling could be detected reliably, in the presence of background noise, with an acceptably low spurious detection rate. Background noise was recorded from the dummy cores of the PFR and Superphénix, from the operating cores of the PFR and KNK-2, and from various out-of-pile test rigs.

Various software methods for detecting boiling noise in the presence of background have been investigated. The use of filtration, pattern recognition techniques or a combination of both allows boiling to be detected in the presence of a background which is noisier than the boiling source.

The IAEA project showed that with a signal to noise ratio of -12dB (i.e. with the root mean square (RMS) method boiling signal power about a factor of 16 lower than the RMS background signal power), boiling can be detected with a reliability of less than one error in 10^6, and with less than one spurious indication in 10^6 a.

5.3. EXPERIMENTAL BREEDER REACTOR II (EBR-II)

5.3.1. Plant arrangement, heat cooling system

During 1950–1952, the US Atomic Energy Commission continued to develop various types of reactor, and in 1954, encouraged by the successful experience with EBR-I, it decided to build an advanced reactor plant at ANL. It was decided that the new breeder reactor, Experimental Breeder Reactor II (EBR-II), would use the pool type concept. The EBR-II, located at the National Reactor Testing Station in Idaho, was designed as a power plant for electricity generation and was to include an integrated fuel processing and refabrication facility.

EBR-II was designed to generate 62 MW(th) and about 19 MW(e), which met the electrical load of the Argonne National Laboratory–West (ANL-W) site (~ 5 MW), with the balance going to the utility grid. However, the main objective of the facility was to establish the feasibility of a fast power reactor system under operating conditions and to demonstrate the on-site fuel reprocessing and fabrication, a procedure believed to result in favourable fuel cycle costs for high power density FBRs. The design of the entire reactor system was affected by these requirements.

The driver fuel element consisted of uranium alloy about 4 mm in diameter, with 95% of uranium metal and with enrichment up to 50% ^{235}U for the MARK-I and 67% ^{235}U for the MARK-II. Reactivity was controlled by eight control rods with boron loaded followers and two fuelled safety rods.

A comparatively high enrichment leads to high power density, which, in turn, results in a high rate of fuel burnup. A finely divided fuel was necessary to achieve this high thermal performance. The fuel achieved a high specific activity after irradiation, with the resulting limitations on fission product separation processes.

Another feature is a high level of fission product decay heating; thus, there was a need for substantial cooling outside the reactor during fuel handling and in the fuel cycle. The fuel also has a high monetary value, and this provides the incentive to minimize total fuel inventory by reducing 'out-of-reactor' processing time requirements.

The fuel cycle utilizes pyrometallurgical processing, which, in the developer's opinion, can be accomplished with small equipment and requires a relatively short cooling time. However, incomplete decontamination associated with the process necessitates the use of remote control procedures for the fabrication of new fuel elements from the processed product. The fuel process itself has likewise affected the core design, specifically the composition of the metallic uranium–fissium alloy for the first core, 'fissium' being a mixture of noble metal fission products not easily removed by processing. Fissium contributes desirable characteristics to the fuel. Both the reactor and the associated fuel recycle facility were designed with the aim of providing a highly flexible installation that would permit the investigation and evaluation of various core configurations, types of fuel, fuel element designs and processing techniques.

The reactor was a test facility for fuel development, materials irradiation, system and control theory tests, and hardware development. The EBR-II core and blanket subassemblies were contained within the reactor vessel (Fig. 5.11). The 1.70 m (67 inch) diameter vessel and its shield were immersed in a sodium pool within the 7.9 m (26 feet) diameter by 7.9 m (26 feet) high primary tank.

The primary sodium contained within this tank represented the primary coolant for removal of the heat from the reactor core. Liquid sodium, with a boiling point of approximately 927°C (1700°F), has excellent thermal properties and was thus an optimum coolant. The primary system contained about 325 m^3 (86 000 gal) of sodium, and transferred heat to the secondary sodium system (which contained about 50 m^3 (13 000 gal) of sodium) through a sodium to sodium IHX.

A unique feature of this system was the primary tank, which, as noted, contains the reactor vessel and primary coolant system submerged in a large volume of bulk sodium. Sodium passes the heat from the core through a secondary circuit to a conventional steam plant that operated at 440°C and 90 bar.

Two identical, single stage centrifugal pumps, operating in parallel, force coolant from the bulk sodium in the primary tank through the reactor at a rate of about 8500 gal/min. Flow through the reactor itself totals 8200 gal/min, with 7000 gal/min flowing from a high pressure plenum through the core and inner blanket subassemblies, 700 gal/min flowing from a separate low pressure plenum through the outer radial blanket subassemblies, and 500 gal/min flowing through the clearance spaces between subassemblies. The remaining 300 gal/min represents leakage back to the primary tank through the pump ball seat disconnects and the subassembly hold-down devices at the bottom of the vessel.

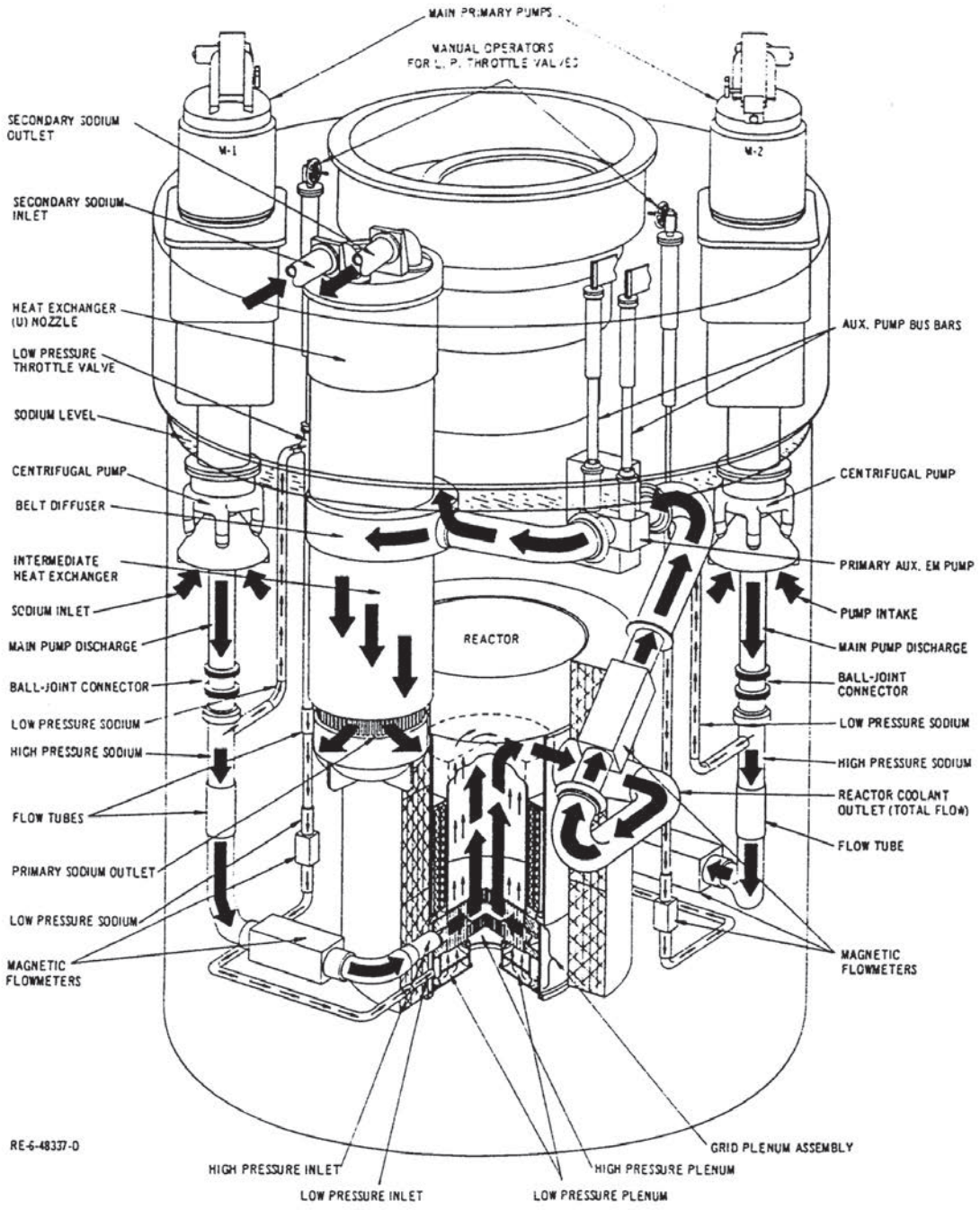

FIG. 5.11. EBR-II primary pipes and equipment [5.15].

In the EBR-II IHX there is no continuous shell, since the bundle is immersed in the primary vessel (Fig. 5.11). Flow from the reactor is directed by baffles to pass over the tubes and then return to the vessel. Secondary sodium flows in piping that penetrates the shield plug.

The coolant passes into a common outlet plenum chamber and then out of the reactor through a single outlet nozzle to the IHX. Finally, after passing through the IHX, the coolant returns to the bulk sodium supply at approximately 371°C (700°F), which is slightly above the bulk temperature since it is necessary to compensate for small heat losses from the primary system tank. For maintenance purposes, the pumps may be removed from the primary tank with ball seat type pipe disconnects provided. The heat exchanger shell is permanently attached to the cover of the primary tank, but the tube bundle and associated structure are removable as a unit.

The pumps, heat exchanger and connecting piping of the primary system are disposed around the reactor vessel; the equipment is at an elevation above the vessel (see Fig. 5.11). These items are immersed in sodium

contained in the primary sodium tank. The coolant flow path is as follows: the mechanical coolant pumps take in bulk sodium about 19 ft above the bottom of the primary tank; coolant flow from the pumps is downward to the connecting piping. The flow from each separates into two pipes; one enters the reactor high pressure plenum, and the second, the reactor low pressure plenum, with the smaller line supplying the low pressure plenum through an orifice and a valve. In all regions of the reactor vessel, coolant flows upward through the fuel and blanket subassemblies and into an upper plenum chamber, which has a single 14 in. outlet located on the opposite side of the reactor vessel from the IHX. The connecting pipe between these two components is designed to accommodate thermal expansion and contains an auxiliary pump. The coolant flows downward through the shell side of the heat exchanger and discharges into the bulk sodium in the primary tank. The heat exchanger outlet is approximately 7.5 ft above the centre line of the reactor to provide natural convection shutdown cooling.

Ball-seat pipe couplings are used in the lines between the main sodium pumps and the lower plenums of the reactor vessel. This allows for pump removal. The sodium line between the upper plenum of the reactor vessel and the heat exchanger shell is permanently attached to the cover of the primary tank. The IHX tube bundle, the secondary sodium inlet and outlet nozzles, and the shield plug can be lifted out as a unit.

When the reactor is in operation, coolant is supplied by the two primary sodium mechanical pumps. Flow to the low pressure plenum can be controlled by a valve in each circuit. During shutdown conditions, when the reactor power is 1% or less of the design value, sufficient coolant flow is established by thermal convection to remove fission product decay energy without exceeding the established fuel–alloy temperature limitations. For more drastic emergency shutdown conditions, including the case of complete failure of all pumps accompanied by reactor scram, analysis indicates that the fuel will overheat, but not dangerously. The relative elevations of the heat exchanger and the reactor were established to ensure natural circulation of the primary sodium.

The primary purpose of the auxiliary EMP (see Fig. 5.11) is to augment thermal convection under certain conditions of reactor shutdown. These conditions can result from any system malfunctions which destroy the normal temperature distributions which promote thermal convection.

Both the evaporator and the superheater shell were constructed of 2.25 wt% Cr, 1.0 wt% Mo steel. Four evaporators had mechanically bonded duplex tubes, and four evaporators and four superheaters had metallurgically bonded duplex tubes. Each duplex tube consisted of two single length seamless tubes. The units had double wall tube sheets at each end; the outer tube was welded to the sodium tube sheet, and the inner tube was welded to the steam tube sheet. The space between the tube sheets was open to the atmosphere. The EBR-II SG (Fig. 5.12) fabrication problems consisted in providing reliable welding of the bonded duplex tubes of chromium–molybdenum to the sodium tube sheets of the superheater without the introduction of real or potential defects.

The smaller tube diameter and thinner wall of the superheater tube required welding techniques superior to those used in welding the evaporator tubes. The welding development included a complete re-examination of all the welding parameters, including welding current, wire speed, voltage, welding speed, bead size and preheating temperature.

Two welding procedures were investigated: spray transfer and dip transfer. Both are modes of metal disposition. The principal difference between these methods is that the spray transfer technique produces sound and reliable welds most of the time, with only an occasional imperfect one. The imperfections usually consist of over-penetration and violation of the nickel–phosphorus bond line. The dip transfer method invariably incorporates a non-wetted area at the start of the weld cycle. Subsequent overlap of this area during the termination phase of the welding cycle does not wet the area. Defects of this type create a vertical leak path through the weld which allows the sodium to leak to the atmosphere. Other improved welding techniques include the use of two weld passes; about 75% of the first pass is machined off prior to the start of the second pass. A second technique used a substantial weld overlay applied to the outer tube end, which was then partially machined off; the tube was redrawn to the original outside diameter before the first joint weld pass was made.

Maximum integrity was obtained by controlling tube fabrication from preparation of the furnace heat to the installation of the finished tube. Some difficulty was experienced in obtaining the desired cleanliness of the furnace heat; however, the tubing as supplied was free of inclusion concentrations. Each tube was subjected to hydrostatic, due penetrant, eddy current and ultrasonic testing prior to duplexing. After assembly into duplex tubes, the mechanically bonded tubes were helium mass spectrometer leak tested, and the metallurgically bonded tubes were ultrasonically tested. A few millimetres had to be removed by surface grinding to ensure a good metallurgical bond.

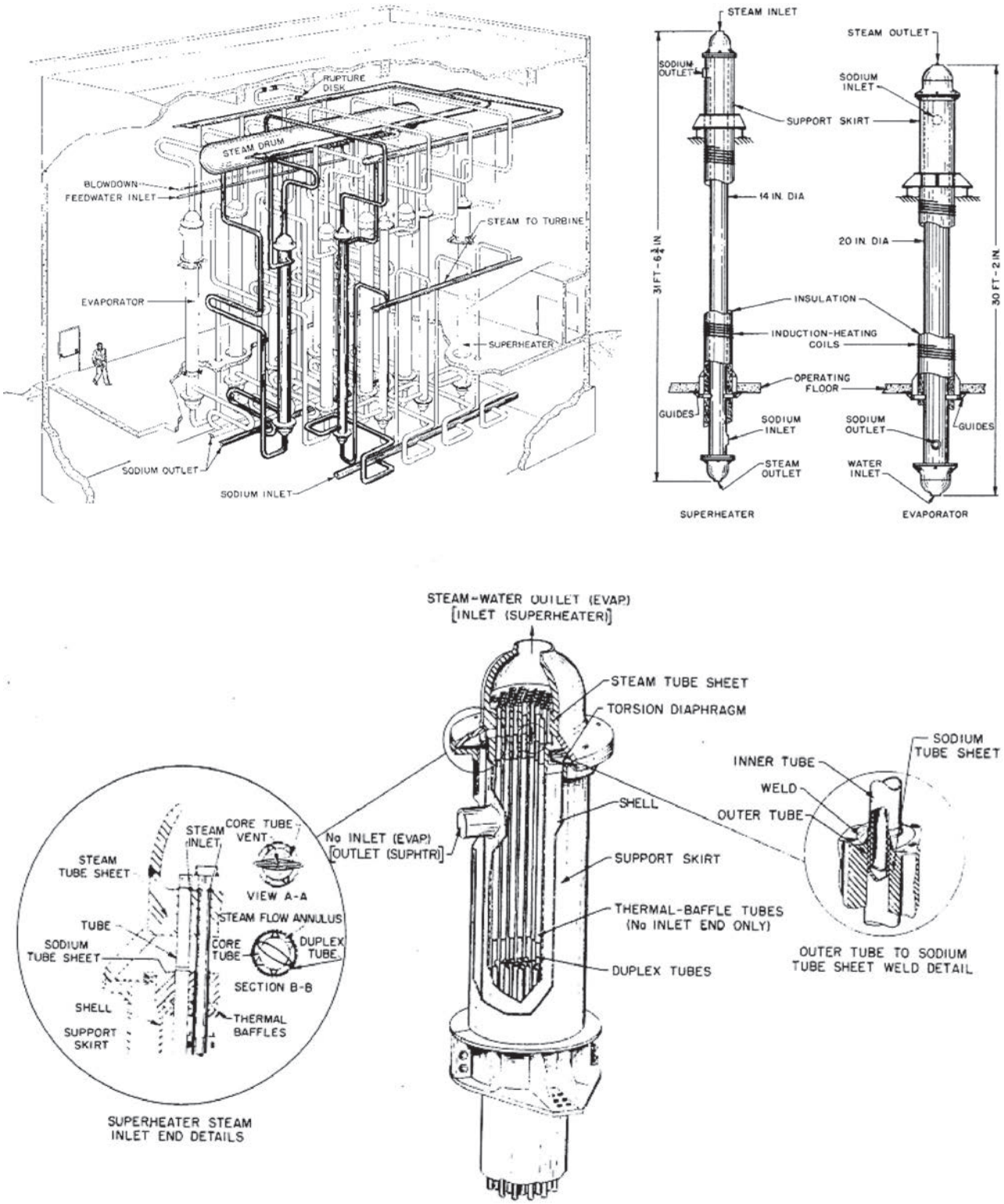

FIG. 5.12. EBR-II SG, superheater and evaporator details [5.9].

The welding procedure used to successfully attach the evaporator tubes to the sodium tube sheet did not produce consistently reliable welds to these criteria on the smaller and thinner superheater tubes. They have an OD of 0.596 in. and a 0.052 in. thick outer wall. The object was to weld the outer wall only to the sodium tube sheet. The fabrication of the four superheaters was not completed, and two evaporators were modified and substituted for them. A core tube was centred within each tube in the modified unit, and it provided 1/8 in. annuals for steam flow. These two modified evaporator units produce a steam temperature of about 820°F at 45 MW(th).

During the final tube to sodium tube sheet welding procedure, the tubes were cold sprung to reduce stress caused by differential expansion during severe over-temperature operation. During this process the shell was elongated about 1/8 in. relative to the tubes. The differential elongation was maintained during the tube to tube sheet welding and stress relieving operation.

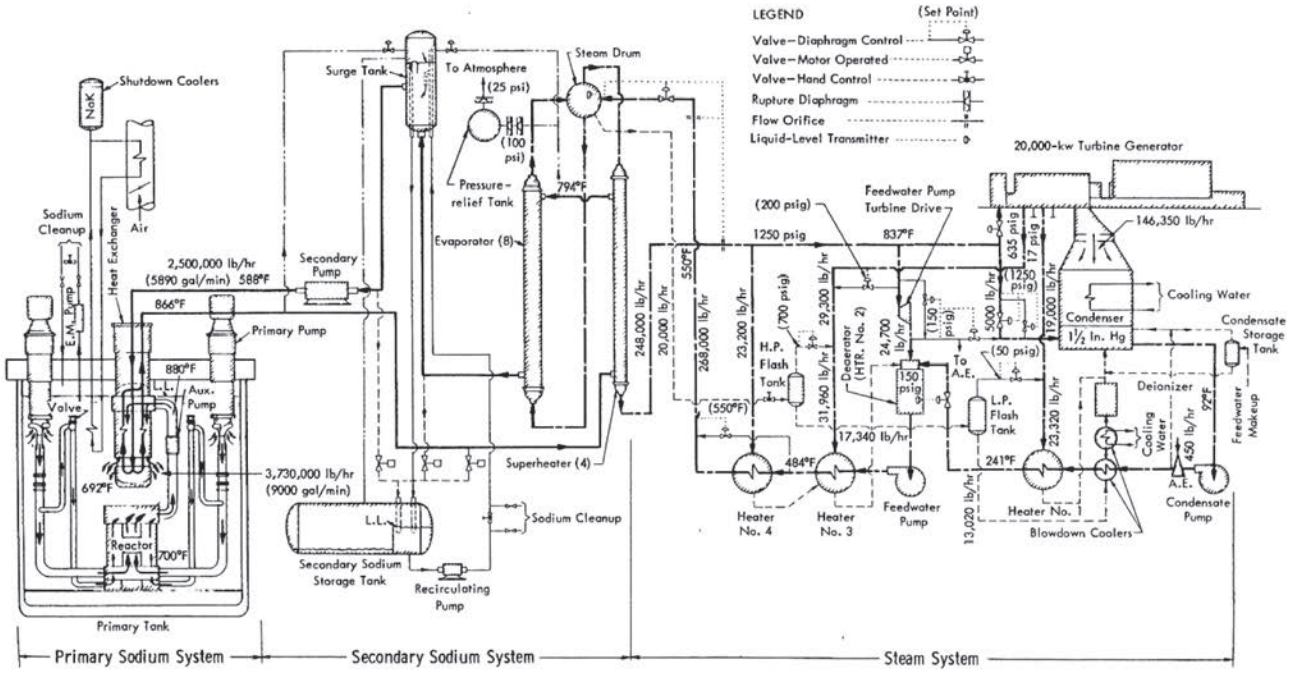

FIG. 5.13. EBR-II heat removal/transport and steam cycle system and BOP [5.3].

The heat transfer–steam cycle system is shown in Fig. 5.13. At full power (62 MW(th)) the generator produces 20 700 kW(e) gross; the steam system has a bypass. A full capacity automatic steam bypass system permits reactor operation without turbine generator operation or with turbine load at any fraction of reactor power. This bypass system prevents major load changes from effecting changes in the secondary system. Feedwater heating is accomplished by extraction from the main turbine, the exhaust from the feedwater pump turbine, and high pressure steam from the main steam line.

When the turbine control valves close, steam is admitted directly to the steam condenser through a pressure reducing valve and a de-superheating station. The damage in the condenser would be limited to the lower condenser structure if the source of de-superheating water were to fail.

Construction of the reactor began in 1957; dry criticality was achieved in the late autumn of 1961 including the check-out of necessary reactor instrumentation. In 1962, construction of the EBR-II complex was essentially completed with the exception of the fuel cycle facility, which was completed in 1963. In both facilities, however, some work was found to be inadequate and required correction.

After dry criticality in December 1961, operations were started to ready the reactor for wet criticality. The subassembly gripper and transfer arm were hung up in the early spring of 1962 during testing and required extensive repairs to the transfer arm drive shaft and transfer arm itself. Dry heat tests were conducted in March and April of 1962 at 350°F in the primary tank to ensure that the primary tank cover would operate successfully at the design differential temperatures. The rotating plug dip seals were filled in April 1962. In July 1962 the seals were sticking; both rotating plugs had to be removed. Extensive modifications were made; they were completed in October 1962. These modifications included installation of new cooling dampers, the reworking of some dampers, replacement of the lower dip seal rings, and a change in the method of operation of the dip seal to provide for freezing of only part of the dip seal during normal operation. In February 1963, 2100 lb of special alloy, 58% bismuth and 42% tin, was placed in the large rotating plug dip seal and 1300 lb of the alloy was placed in a small rotating plug dip seal.

Nitrogen purging of the primary tank in February 1963, with 90 000 cu ft of nitrogen, reduced the oxygen concentration to 0.56%. The primary tank was filled with 325 m^3 (86 000 gal) of sodium at 275°F. The primary

sodium was raised to 650°F in March 1963. Difficulty was experienced with all three reactor vessel cover locking mechanisms. The upper tie rod shaft bearings were galled; the bearing material was changed from stellite to aluminium bronze. In April 1963, pump No. 1 became difficult to rotate and had to be removed. The pump removal equipment utilized a transition section between the ellipsoidal nozzle of the primary tank and a cylindrical shell. The shell was 7 ft in diameter and 30 ft high, with a movable internal piston type seal attached to the crane. The pump was removed to a storage tank in the reactor building, where it was cleaned and disassembled. Inspection showed that the labyrinth was cocked with respect to the shaft centre line owing to the tilt of the bottom flange of the shield plug. The pump bowed, presumably owing to the high temperature caused by its rubbing on the aluminium–bronze labyrinth bushing. The shield plug bottom flange was remachined, and a new shaft and labyrinth bushing were installed.

The ascent to power began in July 1964, and from March 1965 EBR-II was operated at a power level of 45 MW(th), which was limited by the secondary (electromagnetic) sodium pump. An extensive irradiation test programme for fuels and structural materials was started in 1965. From September 1970, EBR-II was operated at a nominal power level of 62.5 MW(th).

The primary purpose of EBR-II was changed in the mid-1960s from demonstrating an integrated reactor fuel recycle system to the principal fast flux irradiation facility. An extensive irradiation test programme for the fuel and structural material was started in 1965 in order to obtain statistically valid data on LMFR MOX fuels and structural materials. This involved a gradual modification and enlargement of the reactor core, extensive changes in reactor operating conditions and modification of the fuel cycle facility. Several new facilities were added to the reactor plant, such as an instrumented subassembly, a radioactive chemistry sodium loop, an in-core instrument test facility and facilities for handling failed fuel.

Since that time, more than 10 000 individual specimens have been irradiated. The experiments have consisted of various fuel types (oxides, carbides, nitrides and metal). Peak burnup of 19 at.% for MOX fuel and 18.5 at.% for metal fuels, and peak fluences of 1.7×10^{23} n/cm^2 for structural materials have been reached. In 1975, EBR-II was upgraded in order to permit operation over the extended periods with failed (breached) fuel. This ‘run beyond cladding breach’ programme started in June 1977 and continued until 1982.

The first reprocessed fuel was recycled into the reactor in May 1965. Altogether, more than 35 000 fuel rods have been reprocessed from EBR-II. Experience showed that a fuel subassembly could be removed from the reactor, dismantled, reprocessed, fabricated and returned to the reactor within a total time about 30 d including a ~12 d cooling period.

5.3.2. Experiments with the EBR-II

The most dramatic safety tests were conducted on 3 April 3 1986, when it was demonstrated that a liquid metal reactor (LMR) with metallic fuel could safely accommodate loss of flow without scram (LOFWS).

The characteristics of these processes are depicted in Fig. 5.14. Experiments simulating the LOFWS were conducted at full power in the presence of different pump coast-down times: active rundown, by controlling the pump speed, pump stop time 300 s (Fig. 5.14) and 100 s, and passive coast down accompanied by the shutdown of the auxiliary electromagnetic sodium pump. The EBR-II pump system has small inertia, leading to a fast coast down. Therefore it was decided to use the stored energy in both the pumps and the motor–generator set, and to control the coast down with the magnetic clutch which couples the motor and generator.

A comparison of peak temperatures demonstrated the decisive influence exerted by the rundown time of the primary pumps on the fuel element cladding and reactor coolant temperature values. Experiments relating to the loss of heat sink without scram (LOHSWS) were also conducted at full power. The temperature placed at the reactor outlet was reduced, while the temperature placed at the reactor inlet was increased.

Owing to the experimental confirmation of the fact that safety properties are inherent in the fast reactors, design work has been undertaken aimed at ensuring the creation of conditions that favour, to the greatest extent possible, the utilization of inherent factors.

It is generally known that an increase in the reactor inlet temperature and the associated reactor coolant temperature rise are accompanied by the thermal expansion of the core diameter, the bending of the grid subassembly outward from the centre, and by the elongation of the control rod transfer bars, thereby resulting in the introduction of negative reactivity.

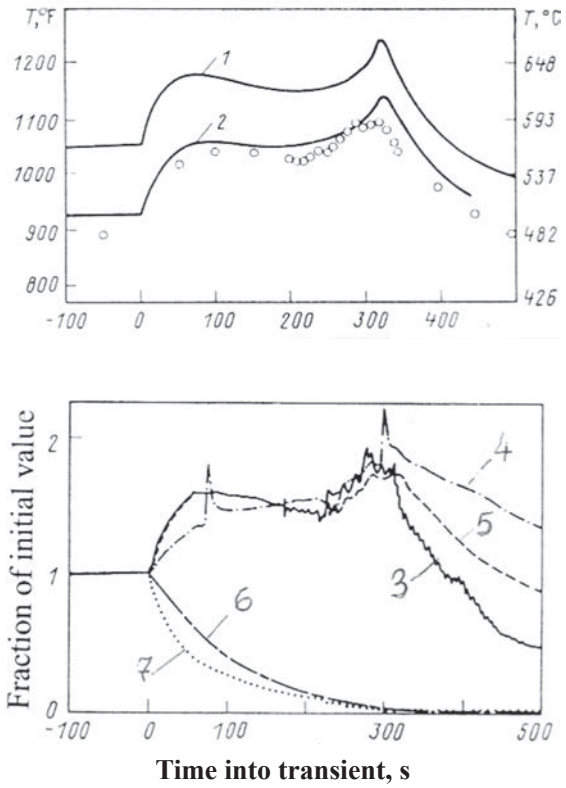

FIG. 5.14. Characteristics of EBR-II reactor during LOFWS transient [5.16]. 1, 2 — the maximum fuel cladding temperature and the coolant outlet temperature, respectively; thermocouple reading; 3 — power/flow; 4 — reactivity; 5 — sodium temperature rise; 6 — power; 7 — flow rate.

In order to reduce power, it is essential that the positive reactivity effects produced by the coolant density decrease associated with an increase in both the coolant temperature and the Doppler effect are overcome by the negative effects generated by heating up and the thermal expansion of the reactor inner structures, since the fuel temperature value is also necessarily reduced.

As previously mentioned, the most impressive results with respect to self-regulation were obtained on the EBR-II reactor when using metal fuel. During experiments involving pump shutdown in circuits I, II and III together with the safety rod failure, this reactor's output was spontaneously reduced to the decay heat level and the coolant temperature value at the outlet of the hottest core subassembly was increased from 520 to 720°C.

In summary, the EBR-II experiments carried out in April 1986 simulated both of the two major heat imbalance accidents that have happened in reality (pump failure which stopped coolant flow through the reactor, and the failure to transfer heat from the reactor coolant to steam system — essentially the Three Mile Island-2 accident). No operator or safety system action was taken in either case, and in neither case was the reactor or its fuel harmed in any way. Emergency heat removal from the reactor vessel was provided passively by a separate loop which included an intermediate NaK loop with a heat sink external to the building (Fig. 5.15).

The ability to passively accommodate anticipated transients without scram has resulted in significant benefits related to simplification of the reactor plant, primarily through less reliance on emergency power and by virtue of not requiring the secondary sodium or steam systems to be safety grade. These advantages have been quantified in a probabilistic risk assessment conducted for EBR-II that demonstrated considerable safety advantages over other reactor concepts. The US developers considered that uranium–plutonium–zirconium alloy metal fuel is fundamental to the superior safety and operating characteristics of the reactor; liquid sodium, with a boiling point of 927°C (at pressure in the core) has excellent thermal properties and is thus an optimum coolant for fast reactors.

From the results of assessments, analyses and tests in 1990, there were indications that the reasonable expected technical lifetime estimate for EBR-II was well beyond 30 years and possibly 50 years or more before approaching any ageing limits. An EBR-III of 200–300 MW(e) was proposed but not developed.

In January 1994, the US Department of Energy mandated the termination of the integral fast reactor programme, effective as of October 1994. To comply with this decision, ANL-W prepared a plan providing

detailed requirements to place the EBR-II in radiologically and industrially safe conditions, including removal of all irradiated fuel assemblies from the reactor plant, and removal and stabilization of the primary and secondary sodium used to transfer heat within the reactor plant.

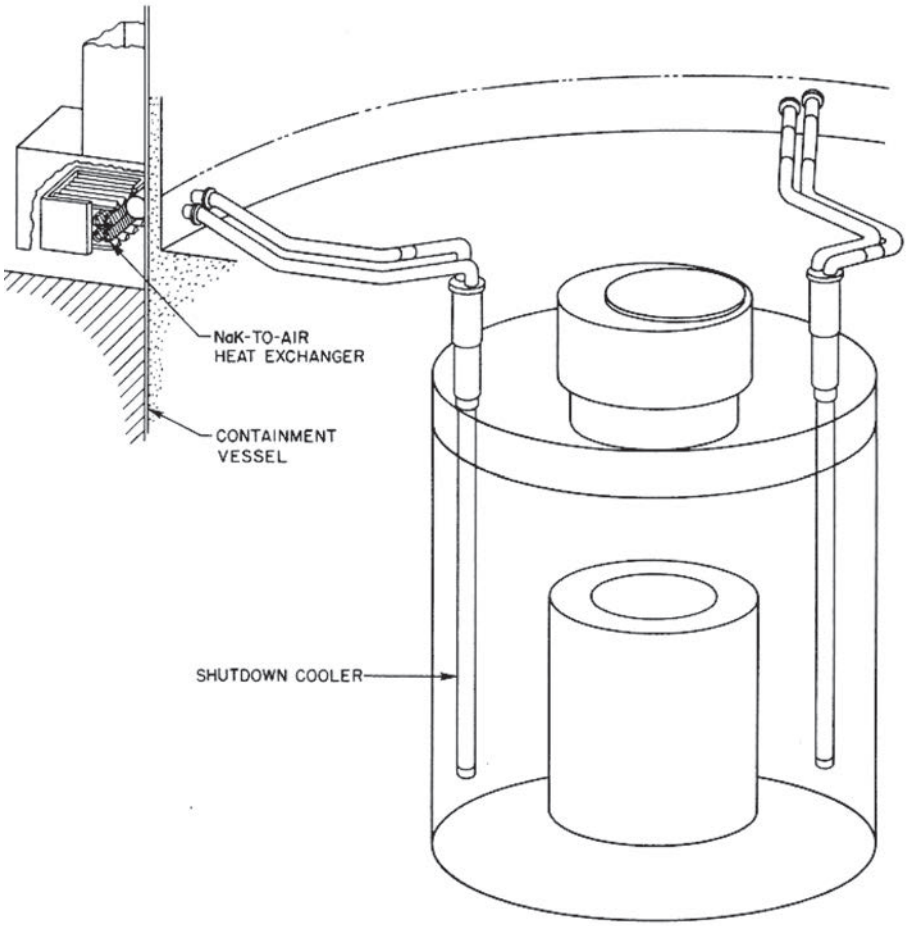

FIG. 5.15. EBR-II passive (NaK–air) emergency cooling system [5.9].

EBR-II's long, successful operating history provides an important source of information on the long term reliability of LMRs. Major programmes conducted in EBR-II included metal fuel irradiation testing and demonstration of the inherently safe response of a metal fuelled, pool type LMR. EBR-II also served as an important test bed for key features of innovative LMR designs, such as flexible pipe joints, materials, and improvements in the instrument and control systems. Other major tests conducted include those to determine the effects of running beyond cladding breach and the response of the oxide fuel to operational transients in a joint US–Japanese programme.

EBR-II was a demonstration reactor operated at 20 MW(e), providing heat and power to the Idaho facility. The objective of the programme was to use the full energy potential of uranium rather than only about one per cent of it. The important objective of EBR-II — the demonstration of an integrated fuel cycle of LMFR — was reached. EBR-II, before being closed, operated as the integral fast reactor prototype, demonstrating important innovations in safety, plant design, fuel design and actinide recycling.

The following key characteristics common to LMRs make reliable, extended life operation feasible: low pressure sodium coolant, limited thermal stress, limited corrosion of components, and simplicity of layout in both the primary and secondary sodium systems.

EBR-II was initially used to demonstrate a complete breeder reactor power plant and later used to test fuels and materials for larger LMRs. It operated for 30 years, longer than any other LMFR power plant in the world at the time (1994). Given the scope of what was developed and demonstrated over those years, it is arguably the

most successful test reactor operation ever. Tests were carried out on virtually every fast reactor fuel type, and the reactor itself was extensively characterized.

Perhaps the most significant feature of EBR-II was the operational track record that it achieved over its 30 year lifespan. With the consideration that EBR-II was a first of a kind engineering demonstration that operated with all new and unproven systems, components, fuel, etc., and also supported a wide variety of tests and experiments through most of its lifespan, its operational reliability record is quite remarkable.

EBR-II, a metal fuelled LMFR power plant, demonstrated capacity factors typically exceeding 70% and approaching 80%, even though the reactor supported an extensive testing programme while simultaneously producing electricity as a complete LMR power plant. Notably, even as some of the test programmes became more aggressive, the operational reliability continued to improve. The plant capacity factor bar chart is shown in Fig. 5.16.

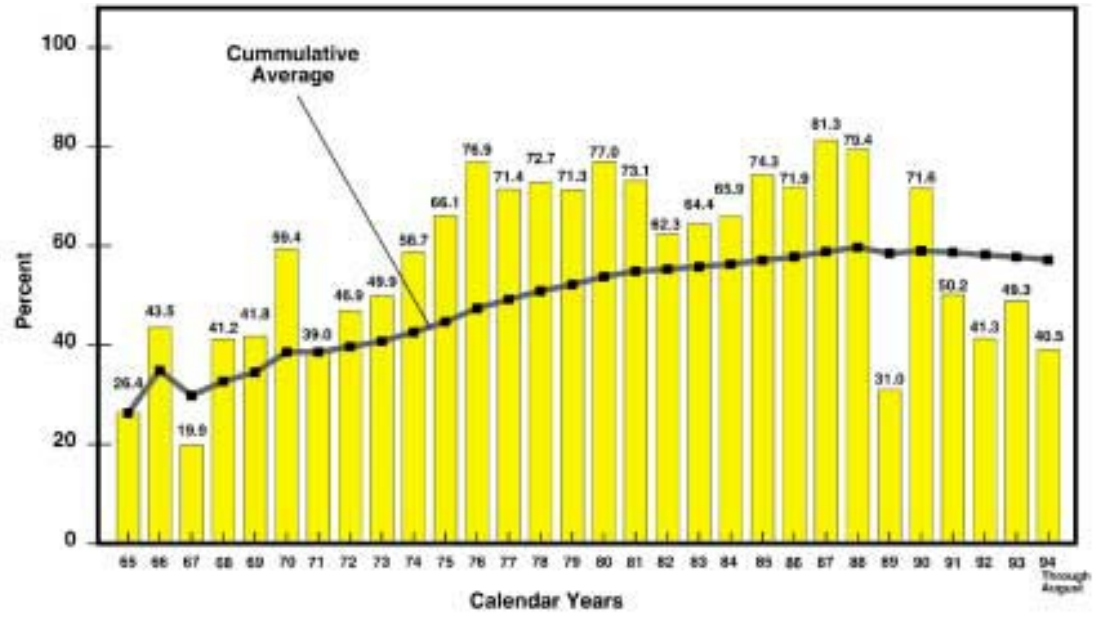

FIG. 5.16. EBR-II plant capacity factor [5.17].

The EBR-II pool design demonstrated the following advantages: (i) containment system as a single large cylindrical vessel rather than in several tanks with connecting pipes of loop design; (ii) only one free surface for which an inert cover gas was provided to prevent sodium–air reaction; (iii) the large sodium cold pool — at reactor inlet temperature — had a large heat capacity that served to minimize temperature transients and was an excellent heat sink during emergency cooling (while a completely separate cooling system could be utilized to cool the sodium tank); and (iv) thermal expansion in the piping was accommodated by bellows to provide axial and lateral movements.

The concept has two disadvantages: (i) shielding the primary tank filled with sodium requires increasingly greater steel consumption; and (ii) difficulties with components repair, inspection and testing.

5.3.3. Some decommissioning issues

The ultimate goal of the deactivation process was to place the EBR-II complex in a stable condition until a decontamination and decommissioning (D&D) plan had been prepared, thereby minimizing requirements for maintenance and surveillance and maximizing the amount of time for radioactive decay. The final closure state will be achieved in full compliance with federal, state and local environmental, safety and health regulations and requirements. The decision to delay the development of a detailed D&D plan necessitated this current action.

In order to properly dispose of the sodium in compliance with the Resource Conservation and Recovery Act (RCRA), a facility has been built to treat sodium with a dry carbonate powder in a two stage process.

ANL-W's plans for the deactivation of EBR-II provide for an industrially and radiologically safe complex, requiring minimal surveillance during the interim period prior to D&D. The deactivation of LMFRs presents unique concerns. Residual amounts of sodium remaining in the primary and secondary systems must be either reacted or made inert to preclude future concerns with sodium–air reactions that generate explosive mixtures of hydrogen and leave corrosive compounds. Residual amounts of sodium on components will effectively 'solder' components in place, making future operation or removal unfeasible.

The sequence of events used to 'lay up' sodium wetted systems is thus crucial in ensuring that these concerns are addressed. After removal of selected components, unique methods, potentially employing unique robotic applications, will be employed to ensure complete reaction of the residual sodium. Specialized components/systems exist within the primary system, including primary cold traps, cover gas condenser and miscellaneous systems containing a NaK alloy. The sodium or NaK alloy in these components must be reacted in place or the components must be physically removed in order to achieve a radiologically and industrially safe condition.

The sodium components maintenance shop, a facility at ANL-W, provides the capability for washing primary components and removing residual quantities of sodium or NaK while providing some decontamination capacity. The D&D procedures have been developed. Major primary components will be removed from the primary tank for cleaning and disposition. An integral part of the primary components removal provides the necessary access to primary tank internal components for D&D activities, removal of hazardous materials and removal of stored energy sources.

The sodium processing facility was designed to transform elemental sodium to sodium carbonate through two stages involving caustic process and carbonate process steps. The sodium is first reacted to sodium hydroxide in the caustic process step. The caustic process step involves the injection of sodium into a nickel reaction vessel filled with a 50 wt% solution of sodium hydroxide. Water is also injected, controlling the boiling point of the solution. In the carbonate process, the sodium hydroxide is reacted with carbon dioxide to form sodium carbonate. Its dry powder, similar in consistency to baking soda, is a waste form acceptable for burial in Idaho, USA, as a non-hazardous, radioactive waste.

Sodium will be processed in three separate and distinct campaigns: the 290 m^3 of Fermi primary sodium, the 50 m^3 of the EBR-II secondary sodium and the 330 m^3 of the EBRII primary sodium. The Fermi and the EBR-II secondary sodium contain only low levels of radiation, while the EBR-II primary radiation levels reach up to 0.5 mSv (50 mrem) per hour at 1 m. The EBR-II primary sodium will be processed last, allowing the operating experience to be gained with the less radioactive sodium prior to reacting the most radioactive sodium.

The sodium hydroxide will be disposed of in ~0.28 m^3 drums, four to a pallet. These drums are square in cross-section, allowing for maximum utilization of the space on a pallet and minimizing the required landfill space required for disposal.

Summing up, EBR-II was a reactor at the Materials and Fuels Complex of the Idaho National Laboratory. The original emphasis in the design and operation of EBR-II was on demonstrating a complete breeder reactor power plant with on-site reprocessing of metallic fuel. The demonstration was successfully carried out from 1964 to 1969. The emphasis was then shifted to testing fuels and materials for future, larger, liquid metal reactors in the radiation environment of the EBR-II reactor core. It operated as the Integral Fast Reactor prototype. Costing more than US$32 million, EBR-II ran more than 30 years [5.1, 5.3, 5.8, 5.9, 5.15–5.24].

5.4. ENRICO FERMI FAST BREEDER REACTOR (EFFBR)

5.4.1. Plant features

In the early 1950s, the US Atomic Energy Commission invited industry to submit proposals for constructing, with Commission assistance, power reactors. The Detroit Edison Company showed interest in participating in the US Atomic Energy Commission's civilian reactor programme and proposed to build a 100 MW(e) class liquid metal cooled FBR near Detroit. The reactor was named the Enrico Fermi Fast Breeder Reactor (EFFBR) in recognition of Fermi's many contributions to the development and control of nuclear energy and his early interest in FBRs.

The EFFBR was the first full scale, semi-industrial fast reactor power plant in the USA. The reactor plant was designed for a maximum capacity of 430 MW(th); however, the maximum reactor power with the first core

loading (Core A) was 200 MW(th). The design and development work was carried out under the auspices of a group of electrical utility companies and industrial firms, incorporated as the Atomic Power Development Associates (APDA). A separate corporation, consisting of group of electrical power companies and industrial firms, known as the Power Reactor Development Company (PRDC), provided funds for the actual construction of the reactor plant and the sodium heat transport systems. The Detroit Edison Company owned and operated the electricity and steam generating facilities of the plant.

The liquid metal cooled EFFBR was specifically designed, built and operated to evaluate the economics of operating a commercial prototype (at that time) FBR for electricity generation. The reactor was designed for an ultimate capacity of 156 MW(e), comparable to an average size conventionally fuelled unit.

EFFBR was fuelled with an enriched metallic alloy (U-10% Mo) with 25% ^{235}U enrichment. Zirconium was used as the cladding material. One hundred and forty fuel rods were clustered on a square lattice and encased in stainless steel wrapper tubes, thus forming a fuel subassembly. Each subassembly had an upper and lower axial blanket of depleted uranium alloy. Surrounding the core region were lattice positions normally filled with radial blanket subassemblies. Shutdown and control functions were based on the use of ten B_4C poison rods.

Sodium was used as the primary coolant, flowing upward through the core and radial blankets into a common plenum and from there to three IHXs. The pumps in the primary as well as in the secondary circuit were of the single stage centrifugal mechanical type. The SG was a vertical shell, once through unit having water and steam flow within the shell side and sodium on the outside. The steam produced had a temperature of 400°C and a pressure of 42 bar.

The arrangement of components within the primary reactor tank is illustrated in Figs 5.17–5.19. The reactor's central part, as well as the fuel transfer system, was contained within an irregularly shaped lower section of the reactor vessel.

There is an 'empty' region between the reactor vessel and the primary tank (Fig. 5.17), which is filled with graphite shielding. The upper section of the reactor vessel contains a large sodium pool above the core and blanket. Access to the core is accomplished by a rotating top shield plug arrangement.

The reactor vessel shell (Fig. 5.20) is composed of four parts: the lower vessel, upper vessel, transfer rotor container and rotating plug. The transition deck section connecting the lower reactor vessel and the transfer rotor container to the upper reactor vessel consists of a flat dished head with vertical ribs and a deck plate as shown in Fig. 5.20. Brackets for the reactor vessel support are welded under the transition section in line with the ribs. Eight flex-plate support columns, 2 in. thick and 7 ft long, made of carbon steel plates support the vessel and allow for free thermal expansion while holding the centre line of the upper reactor vessel in a fixed position. Some of the flex-plates are mounted on springs.

The lower reactor vessel, core and blanket shown in Figs 5.17–5.19 are located asymmetrically in the primary tank for fuel handling purposes and to permit decay heat removal by natural circulation during shutdown. The coolant flow is upward in this natural circulation system; the large supply of sodium in the primary system (~100 t) provides the heat capacity needed to reduce transients.

A cylindrical section in the lower reactor vessel, 80 in. in diameter and 70 in. high, contains the core and blanket square subassemblies. The central core region, which was surrounded by the breeder blanket, is in the form of a cylinder 31 in. in diameter and 31 in. high. Figure 5.19 shows a reactor cross-section plan view that illustrates the core and blanket subassembly arrangement. For 200 MW(th) power level operation, 105 central lattice positions contain fuel subassemblies. Within this region, ten positions are provided for control rods. Each of the core subassemblies contains an upper and lower axial blanket section in addition to the central fuel-bearing core region.

The upper reactor vessel section, at approximately atmospheric pressure, serves as a mixing pool for the hot sodium. This section contains a core hold-down device and offset fuel handling mechanism. The hold-down device maintains radial alignment of the upper ends of the core assembly and prevents subassembly movement induced by the uplift force of the sodium flow.

Spent fuel and blanket subassemblies are removed from the reactor vessel and deposited in a transfer rotor container by the offset handling mechanism. Each subassembly in a finned transfer pot can be transported by the transfer rotor container to the exit port; then the subassemblies are raised vertically into a cask car by the cask car gripper. Spent fuel is unloaded from the cask car in the fuel and repair building, where the fuel is placed in decay storage prior to shipping operations. Both the hold-down device and offset handling mechanism are mounted eccentrically on the rotating plug so that the hold-down device will be swung away when the handling mechanism is swung over the core.

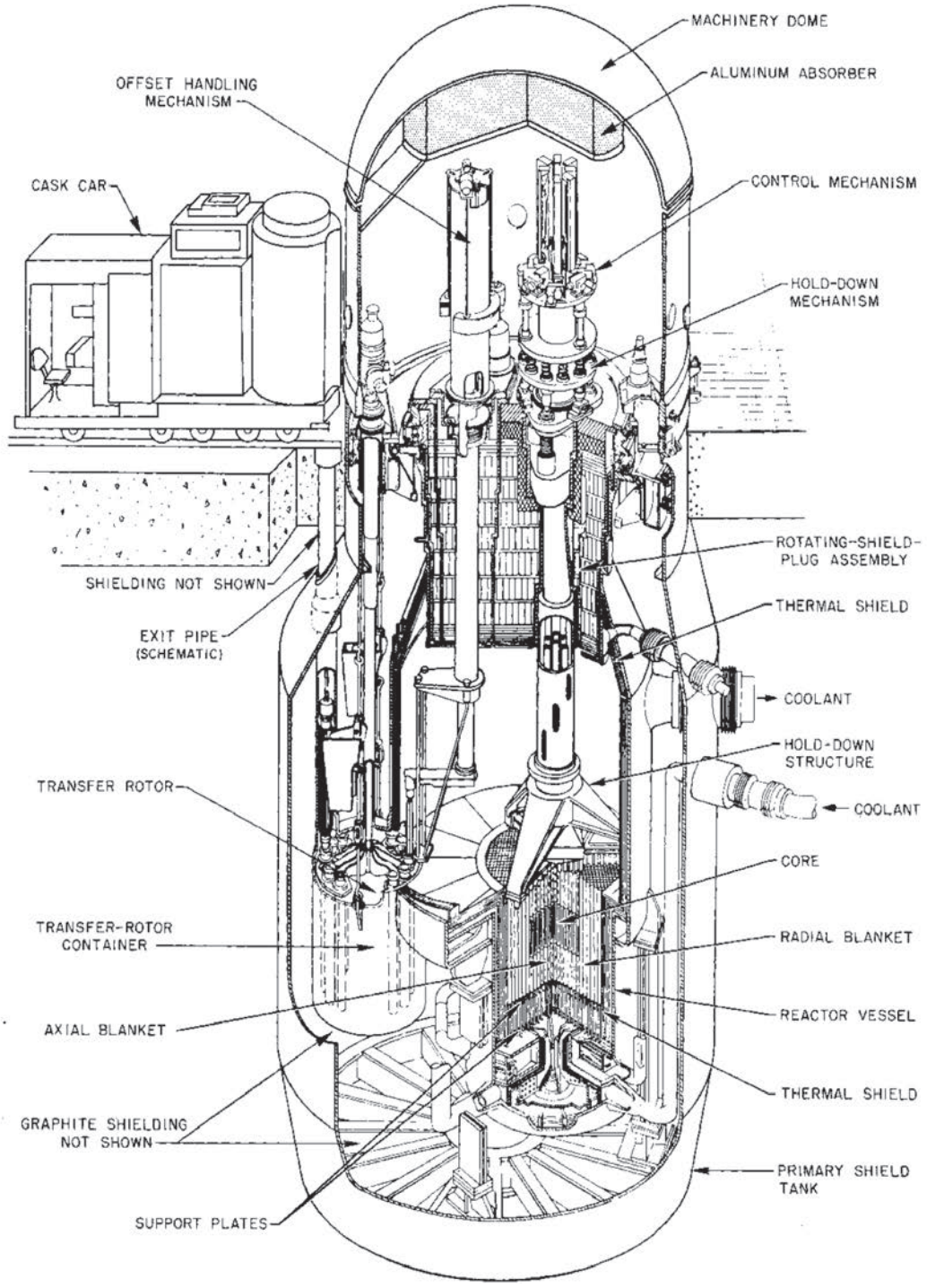

FIG. 5.17. EFFBR perspective view [5.1].

The lower reactor vessel includes provision for safe containment of molten fuel in the case of a core meltdown. This section, located in the inlet plenum, is arranged so that the thickness of the molten material in the region will be about 1¼ in. A conical flow guide is installed to prevent a build-up of fuel in the centre of the meltdown section by dispersing the molten fuel as it enters the plenum. The reactor vessel is surrounded by a graphite neutron shield located in a nitrogen atmosphere inside the primary shield tank, as indicated in Fig. 5.20.

The lower reactor vessel is cylindrical with a 111 in. inside diameter and with a dished elliptical 2 to 1 bottom head. The wall is 1½ in. thick in the plenum region and 2 in. thick above. The lower portion of the vessel has three 14 in. OD inlet nozzles supplying the core inlet plenum for core coolant flow and three 6 in. OD inlet

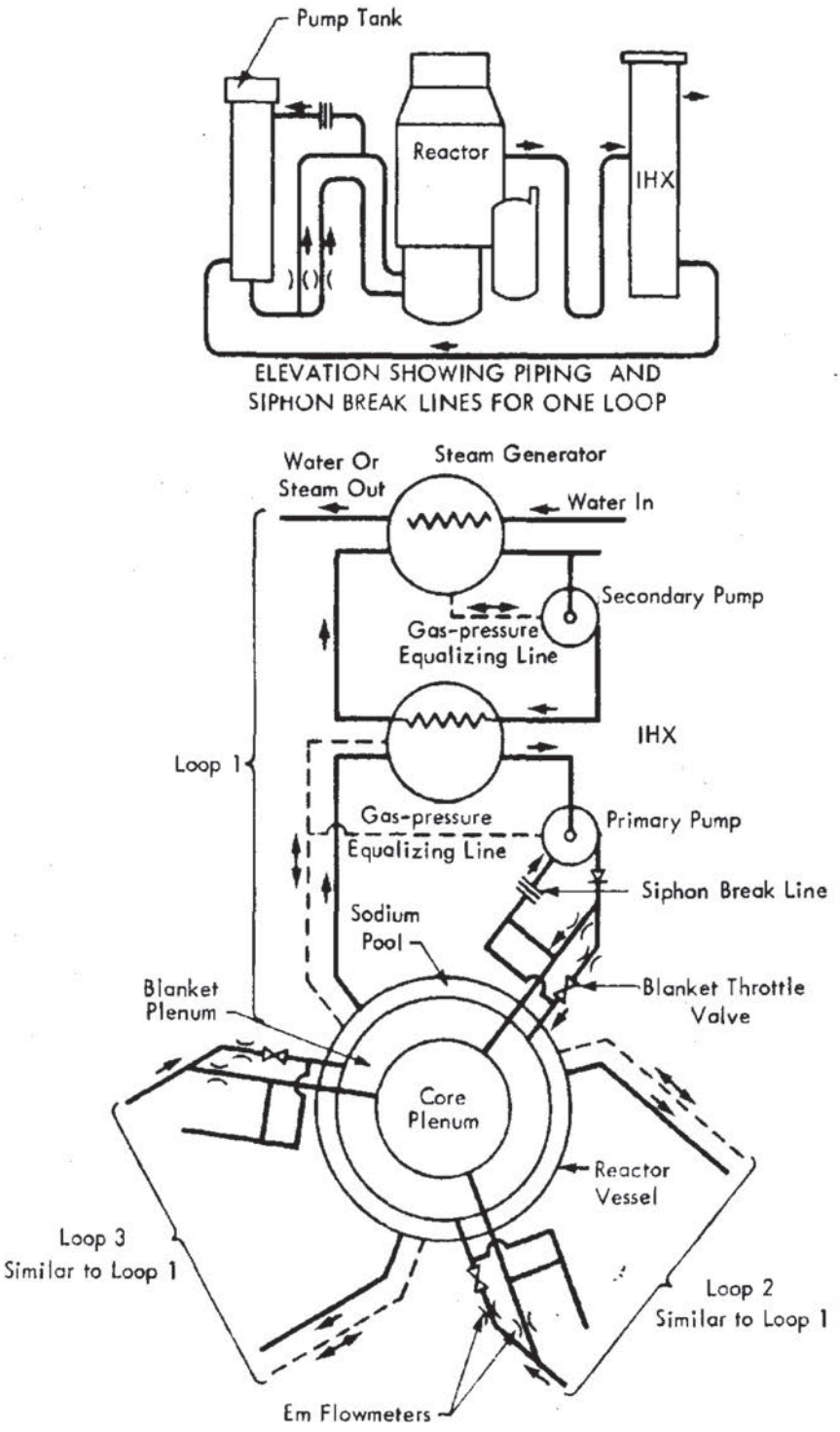

FIG. 5.18. EFFBR flow diagram [5.9].

nozzles for supplying the radial blanket inlet plenum. The blanket flow plenum also serves as the support structure for the core and the radial blanket support plates. The support plates rest on an outer ledger ring and an inner seal rail, which are welded to the top of the support structure.

The shield system also includes a 12 in. thick laminated steel thermal shield inside the reactor vessel wall. A secondary shield, consisting of a 30 in. thickness of concrete, surrounds the primary shield tank and prevents neutron activation of the secondary sodium system. A 5 ft thick biological shield outside the containment vessel completes the radial shielding system.

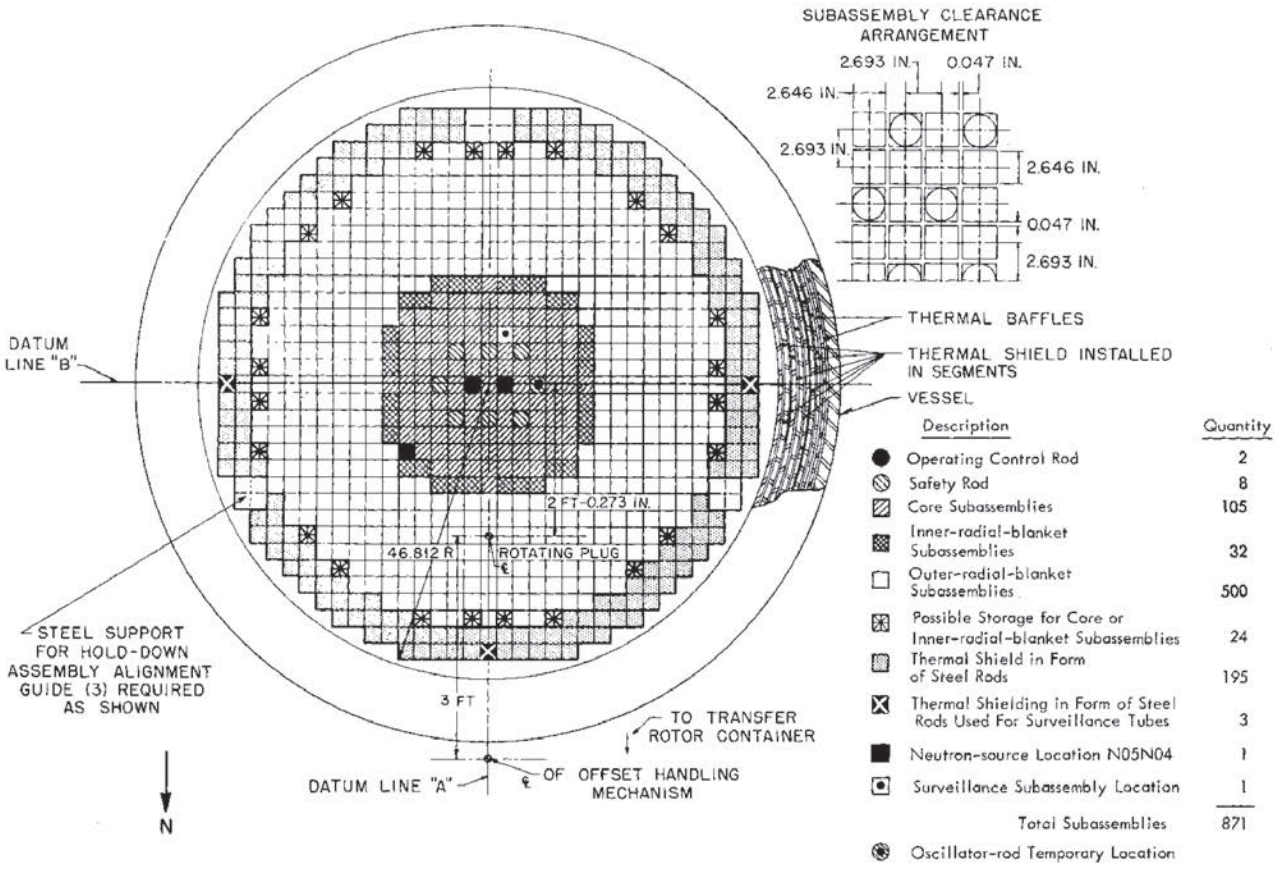

FIG. 5.19. EFFBR reactor cross-section [5.3].

The containment vessel (Fig. 5.21) was a vertical cylinder with hemispherical top head and semi-ellipsoidal bottom head. It houses the reactor and the primary system. The inside diameter is 72 ft, and the overall height is 120 ft, of which 51 ft is below grade. Design specifications, based on the containment of the sodium–air reaction, provide for the possibility of an internal pressure of 32 psig.

5.4.2. Heat transport system

The primary system is composed of three coolant loops having a common point in the reactor vessel (see Fig. 5.22). Each loop contains a sodium pump, a check valve, a blanket throttle valve, and the shell side of an IHX. Primary sodium flows by gravity from the upper reactor vessel through three 30 in. pipes. Each of the lines supplies the shell side of an IHX. The discharge of each IHX is connected to the pump suction by a 30 in. line. The discharge of each pump supplies a 16 in. line, which, in turn, supplies a 6 in. and a 14 in. line. The three 14 in. lines deliver approximately 87% of the flow to the plenum serving the reactor core. The three 6 in. lines deliver approximately 13% flow to the plenum serving the radial blanket. Flowmeters are located in both the 6 in. and the 14 in. lines. The flow of coolant to the blanket plenum can be adjusted by a throttle valve in each of the 6 in. lines.

The IHXs are counter-flow, shell and tube units, constructed of type 304 stainless steel. The primary sodium stream, at lower temperature, returns to the primary pump. A system of secondary containment for the primary system consists of a welded, leaktight enclosure for the reactor vessel, the primary system, the pump tanks and the IHX shells.

The core generates the fast flux greater than 10^{15} neutrons $\cdot$ cm^{-2} $\cdot$ s^{-1}. An important issue in the arrangement of IHXs and pumps is to minimize their neutron activation by locating them in fluxes less than 10^{14} neutrons $\cdot$ cm^{-2} $\cdot$ s^{-1}. Since liquid metal coolant has a high ratio of scattering to absorption, neutrons can scatter or stream along sodium pipes. The space required around loop reactor design pipes for clearance, expansion allowance and insulation provide gaps, down which neutrons may stream. Bends of the pipes can be used to eliminate direct streaming between the reactor and primary system components.

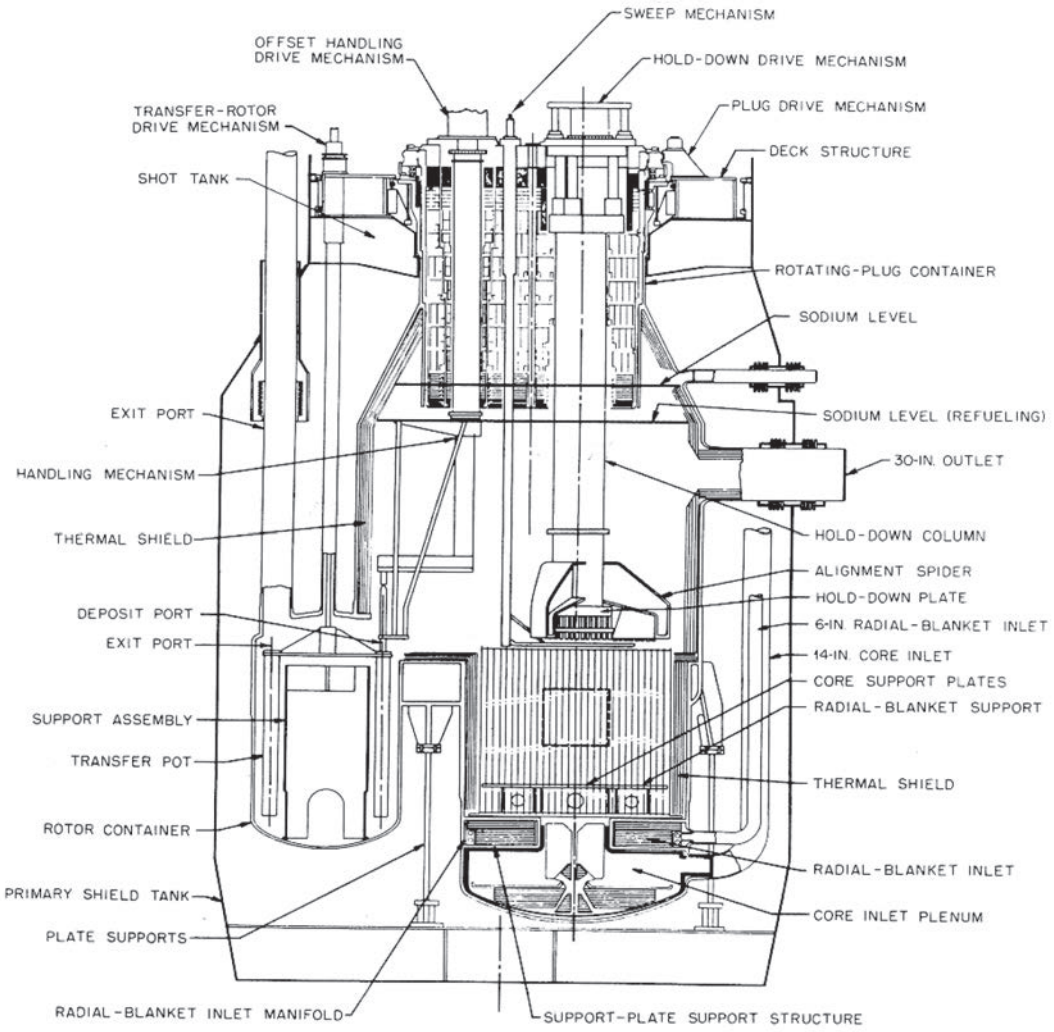

FIG. 5.20. EFFBR vertical cross-section of the reactor vessel [5.3, 5.9].

The primary sodium pipes, which pass through the primary shield tank, required special attention to decrease the neutron leakage. The problem of shielding was complicated because the shielding material had to withstand temperatures upwards of 1000°F in a radiation environment. A shield of calcium borate (Fig. 5.23) having a thickness of 9–11 in. is located around the 30 in. pipe loops within the reactor compartment. Ring or donut shields of the same material were installed directly to prevent the neutron streaming around the pipes.

The 30, 16 and 14 in. pipes are fabricated of 304 stainless steel plate. The wall thickness for all three of these pipe sizes is 3/8 in. The 6 in. piping is Schedule 40 seamless type 304 stainless steel pipe. The 30 in. piping is cold sprung 100% for 900°F operation, and the pump discharge piping is cold sprung 100% for 600°F operation.

All components of the primary coolant system are enclosed by secondary containment. Auxiliary 5 hp motors on each of the primary and secondary sodium pumps furnish the power to circulate primary coolant to remove decay heat from the reactor after shutdown.

The pump, a vertical shaft single stage centrifugal type, rated at 11 800 gal/min and driven by a 1000 hp motor, circulates sodium to the core through a 14 in. diameter pipe. About 13% of the total flow is pumped through a 6 in. pipe to the radial blanket, shown in Figs 5.20–5.22. Core coolant flows upward from the lower inlet plenum of the core, through the reactor core itself, and then to the upper reactor vessel, which serves as an exit plenum, as shown in Fig. 5.17. The hot sodium then flows by gravity from this ‘pool’ to the shell side of the IHX through a 30 in. line.

As mentioned above, EFFBR has three primary heat transport systems feeding the reactor. The major portion of the primary system pressure drop is in the reactor. Consequently, unless the head capacity curves at the various speeds of the primary pumps have sufficient slope, there is a tendency for a change in the speed of one pump to

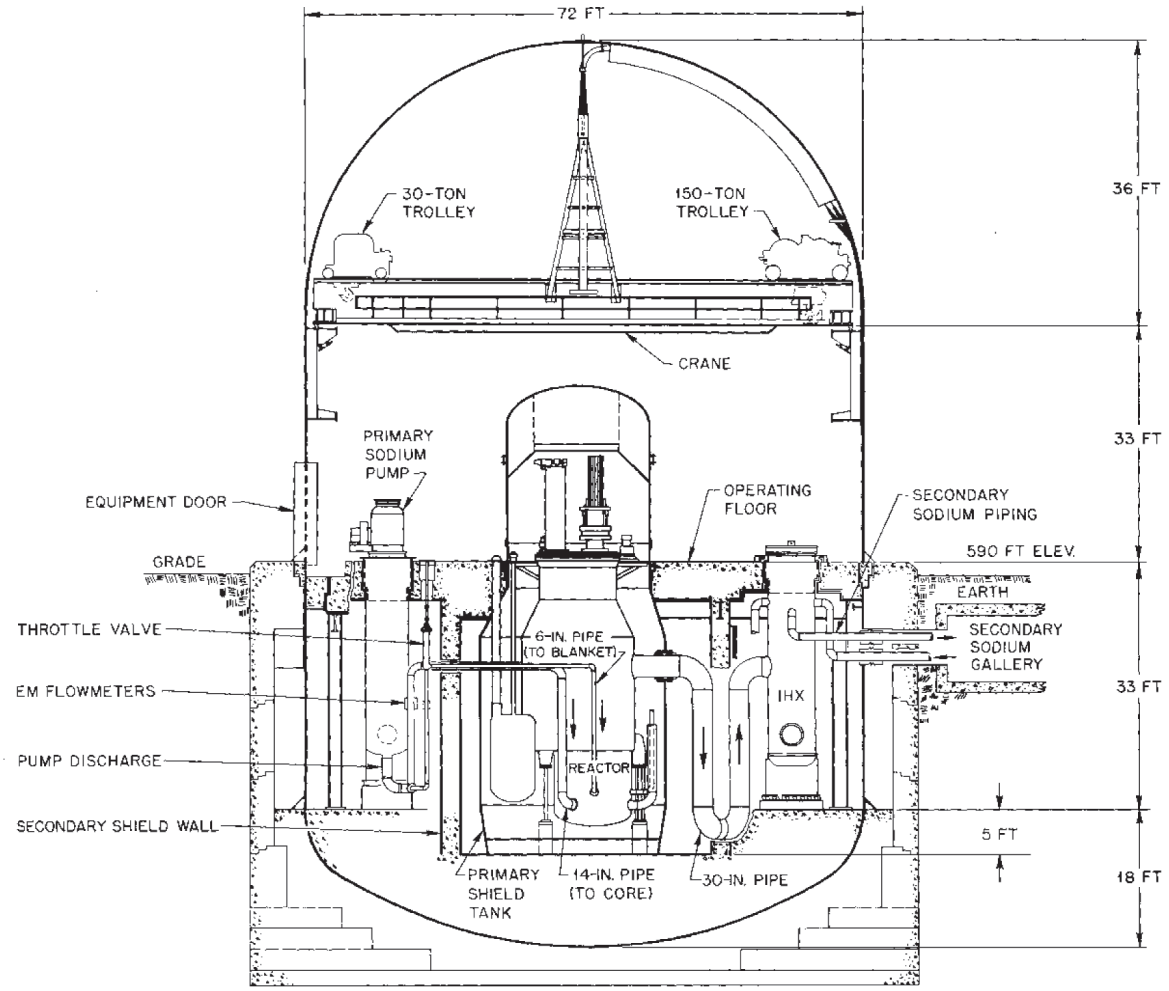

FIG. 5.21. EFFBR vertical cross-section of the reactor building [5.3, 5.9].

affect pumps in the other two systems as well. If one pump is increased in speed, its flow will increase, but the flow from the other two primary pumps will decrease.

The Fermi plant was equipped with variable speed drives for each of the three primary and three secondary pumps, but sodium flows (during the early years of operation) were kept constant for all power levels. There are some advantages to a constant coolant flow system. The operating control system is less complex because automatic control or manual manipulation of six pump speeds is eliminated during power operation. Scrams from any power level other than full power produce less severe thermal shocks with constant flow. In a prototype fast reactor plant, such as the Fermi reactor plant, there are other reasons for installing variable speed coolant pumps. The initial reactor core power rating was substantially less than the plant heat system power rating. At the lower power outputs, the pumps should be operated at reduced constant speeds to provide desired coolant temperature rises and steam temperatures. Increased pump speeds were planned for future cores of higher power ratings. Plans for reactivity oscillator tests for stability analyses of the initial core at EFFBR required reduced coolant flow rates to permit the study of temperature effects on nuclear properties at low power levels. Successive steps to higher powers and higher flow rates were planned as part of the stability tests.

An additional use for variable speed drives in plants using constant flow rates is to permit plant operation with one primary and one secondary heat transport system out of service, if necessary. The two primary pumps that are operating may need to be run at speeds other than that at which they are run when all primary pumps are operating. Flexibility was available to permit maximum permissible power to be obtained from the two heat transport systems. It was also possible with variable speed pumps to delay a plant shutdown until a more convenient time by continuing operation with the remaining circuits at reduced power when one of the systems was shut down because of equipment troubles.

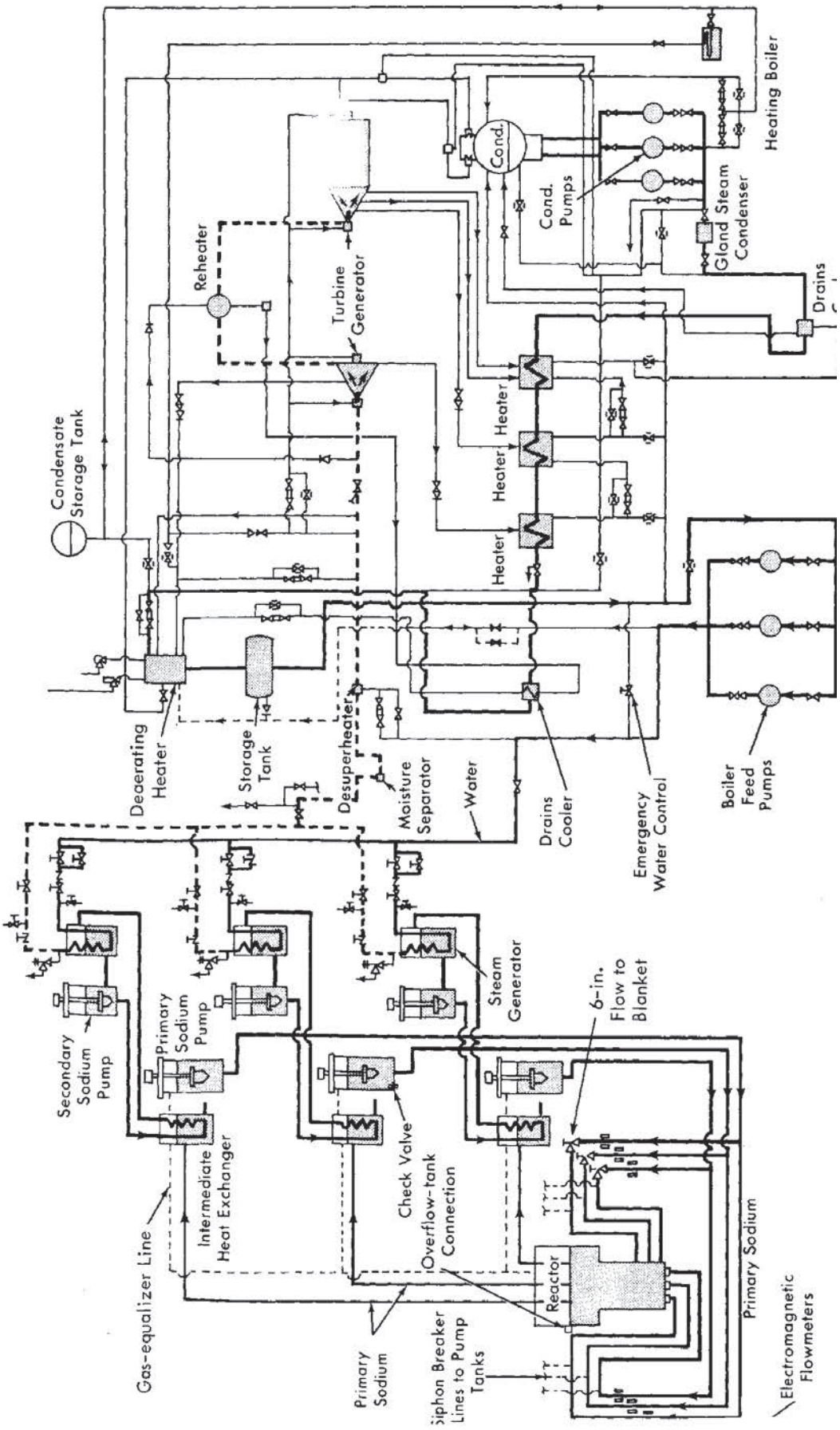

FIG. 5.22. EFFBR heat transport conversion system [5.3].

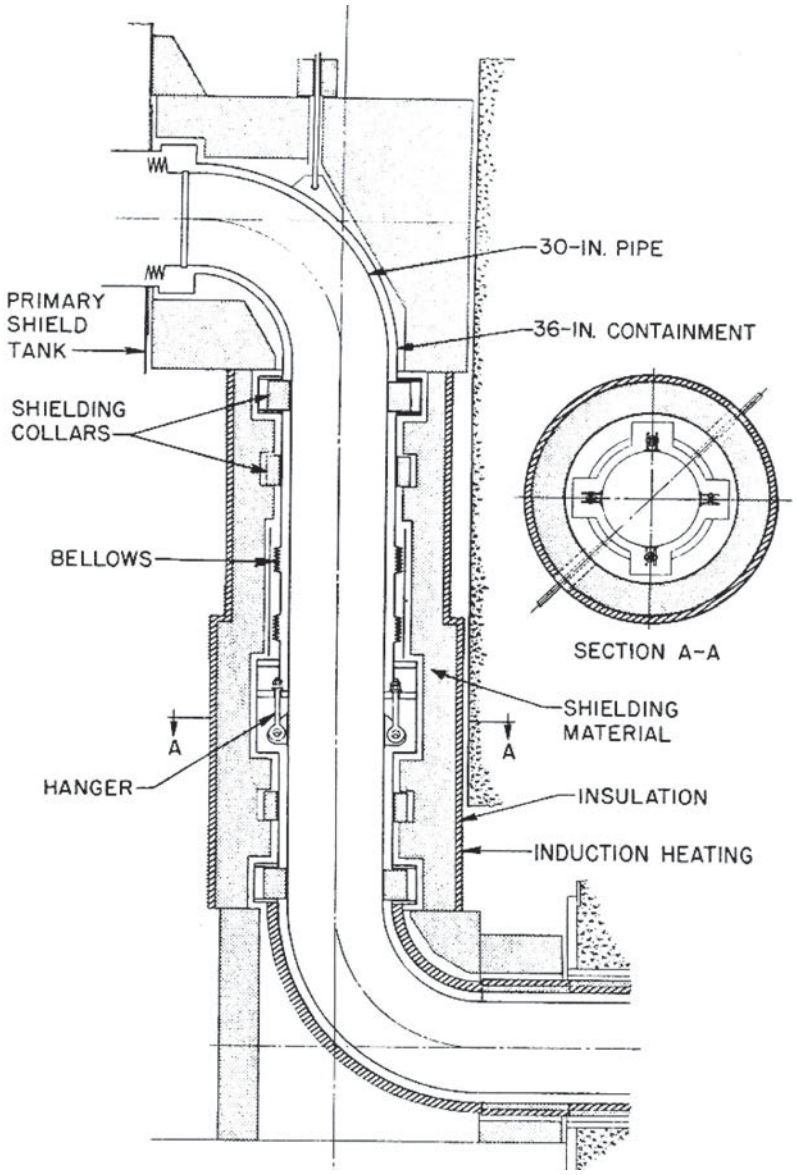

FIG. 5.23. EFFBR primary pipe shielding [5.25].

Heat is transferred from the IHX to the shell side of a SG by sodium circulated by a 13 000 gal/min pump driven by a 350 hp motor. The SGs (Fig. 5.24) were vertical shell and tube exchangers of a single wall tube design, arranged for a combination of cross- and counterflow. A number of design features provide protection against any leaks within the units. The tube to tube sheet joints were located in an inert gas space above the sodium to reduce thermal shocks.

During a cold hydraulic test at 850 psi, an unaccounted for leakage of 300 cm^3 over 1.5 h was observed. A hot hydraulic test was performed, and steam was observed at a shell side vent when the vent was opened. The bundle was then removed and examined. Metallographic examination of the cracked tubes disclosed that the tubes failed as a result of stress corrosion cracking. The tubes were stressed during cold formatting and were not stress relieved after bending.

It was concluded that some of alkaline cleaning agent was left in the tubes, since they were not flushed but were allowed to drip dry. The water analysis indicated the presence of an alkaline solution; the pH was considerably higher than was expected as a result of hydrazine, the only known addition.

The only cracks that were found occurred on the sides of the bend, not on the inside or outside radius of the bend. A considerable number of cracks that started on the inside surface but did not progress out of the tube was observed. Thus it appears that all cracks originated on the inside surface of the tubes. All cracks were intergranular.

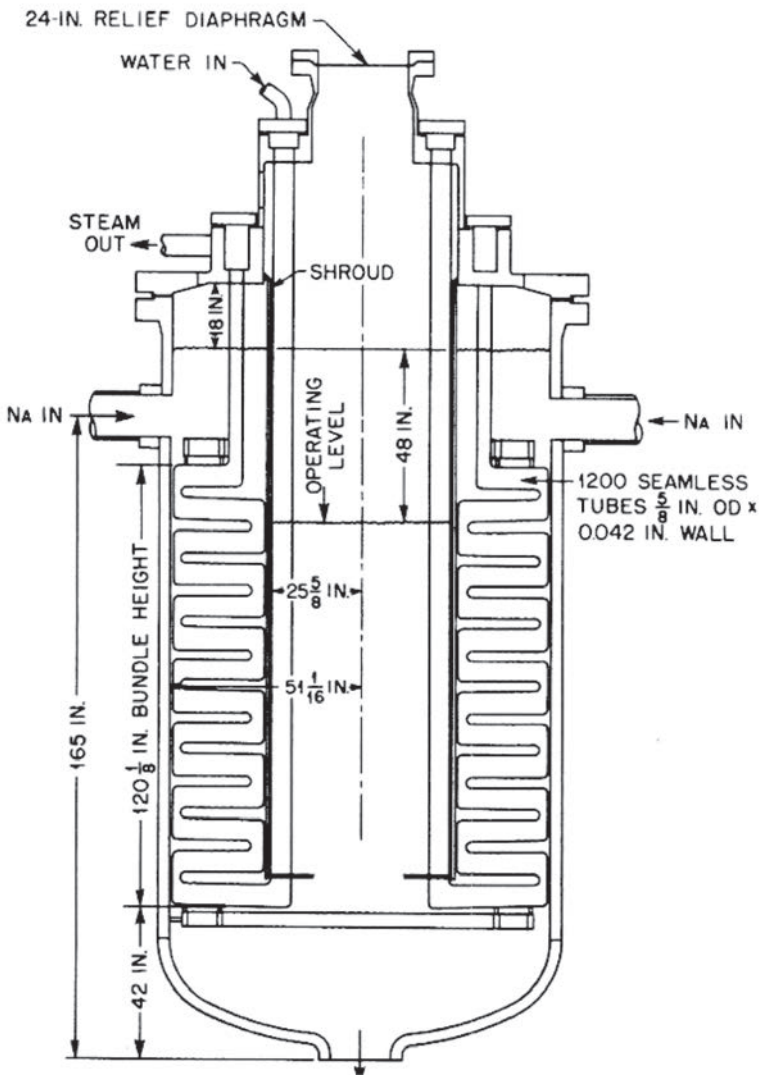

FIG. 5.24. EFFBR steam generator [5.9].

They showed distinct amounts of corrosion product in the network of the cracks. All indications pointed to stress corrosion cracking. Cracks were found in both the long and the short radius, but no cracks were found in the single straight section that was examined.

5.4.3. Operating experience

Starting in July 1959, a series of non-nuclear tests were performed at EFFBR on components in the reactor portion of the plant. The test facility included the reactor vessel, primary shield tank, rotating shield plug, fuel handling mechanisms, safety rod drives and one primary system sodium loop. These components, together with sodium purification, were used in conducting a full scale mechanical and hydraulic test of the reactor. The tests were isothermal up to temperatures of 1000°F. The overall results of the non-nuclear tests were satisfactory, although modifications were necessary.

Starting again on 1 July 1961, the Fermi plant was incorporated around the test facility and preoperational tests began preparatory to nuclear testing. The systems, in general, performed satisfactorily. Following the 1000°F test, tests of graphite directly around the reactor vessel (inside the insulation) indicated that the material failed to withstand the high temperature test. Tests indicated that the borated graphite did not conform to the design specifications and would have to be replaced. Tests on the remainder of the material outside the insulation in the primary shield tank indicated that this graphitic material also needed replacement. It was apparent that moisture

and oxygen control is a must in the use of high temperature graphite. All the graphite in the primary shield tank was replaced with high density, high temperature, reactor grade graphite. Any boron used was in the form of boron carbide. The reinstallation of the graphite shield was a primary factor in delaying completion of the reactor.

During the test of the offset fuel handling mechanism (OHM), it became jammed due to the malfunction. The OHM was bent when an attempt was made to move it laterally before it was fully declutched from a partially raised dummy subassembly. An interlock had been disconnected for the purpose of carrying out the test. The OHM was removed with a lightweight removal container in such a manner as not to violate the inert gas integrity of the reactor. After disassembly, it was found that the gripper and the stabilizer foot were not in the proper positions. After removal of the OHM and reduction of the sodium level, observation of the core and blanket subassemblies indicated a number of displaced subassemblies. Investigation showed that the subassembly heads had stuck to the hold-down plate fingers when the hold-down was raised. When the plug was rotated with the heads engaged with the fingers, the result was bending of the fingers and the subassemblies. Subsequent lowering of the hold-down resulted in further damage and in non-seating of some of the subassemblies in the support plate, which further resulted in flow erosion of the support-plate holes. For repairs, the reactor vessel was drained of sodium, and personnel in protective suits entered the reactor. They removed the centre support plate and the hold-down plate with its fingers. The hold-down finger sockets were redesigned.

Other modifications were made to the control and safety rod guide tubes. The centre support plate had stellite bushings inserted in the holes to prevent further possibility of erosion. The OHM was modified to strengthen the gripper linkage so that enough strength would be available to permit application of impact loads to force the gripper open. The stabilizer foot was redesigned to ensure that the OHM would not be locked over a partially raised subassembly. The stabilizer assembly and its attachment to the rotating tube were strengthened to withstand higher lateral loads. The possibility of obstructions interfering with future operations was avoided by the installation of a new mechanism called a sweep arm, which is used to check for obstructions in the upper plenum above the core and blanket. Approximately 2000 person-hours were expended in the vessel by personnel using protective suits within the argon atmosphere to accomplish repairs.

In July 1961, a series of hydrostatic water tests carried out at 850 psig on the No. 2 SG tubes indicated leaks. Subsequent checks indicated that 71 tubes were cracked through the tube wall. All these were located opposite one of the two sodium inlets. The tests of the tubes indicated that residual stresses, corrosion effects and elevated temperatures induced stress corrosion cracking. The entire tube bundle of the No. 2 SG was returned at the fabricator. All three units were stress relieved and inspected prior to reassembly.

In December 1962 a sodium–water reaction took place in the No. 1 SG, blowing the rupture disc installed for just such a possibility. The water was dumped manually by an operator to prevent further introduction of water. The No. 1 secondary loop was drained, and the tube bundle was removed and cleaned in approximately 800 gal of alcohol. The largest cleaning operation up to 1963 to remove sodium from one component was performed without incident. Examination showed extensive tube damage due to the vibration of the tubes against the support structures as well as erosion caused by the sodium–water reaction during the period between a reaction and the rupture disc blowout. Small and full scale models in the water of the tube bundle and its baffle indicated that the vibration of the tubes at the sodium inlet had been as high as 0.250 in. Baffling and lacing of the tubes was carried out to reduce this vibration to a negligible quantity.

A programme was initiated to modify the check valves in the primary system. The 16-in. check valves induced high pressure surges when one of the loops was shut down with either one or two of the loops operating. A programme was carried out to install new check valves, modified to include dashpots and springs to reduce the surge pressure to negligible values.

Each of more than 3000 cans in the rotating plug containing graphite was vented by three 1/16 in. holes to the argon cover gas above the sodium in the reactor. The primary system tests at 1000°F, and at lower temperatures, released material in the graphite binder to the primary system. This release resulted in carbon and other contamination of the primary system. Extensive programmes of sodium sampling, analysis and filtration were carried out to determine what contaminants were present and how they affected the system. Tests of the materials in the primary system indicated some degree of carburization, but not sufficient to affect operation of the reactor.

Preoperational tests prior to criticality on 23 August 1963 were successfully completed. Only minor modifications of the control and safety rods and control drives were required.

Under an extensive low power and high power test programme, the plant had up to 100 MW(th) from 1963 until 1966. On 5 October 1966, during start-up operation of the reactor plant, a fuel cooling problem occurred in

the core subassemblies at a power level of 34 MW(th). The operators manually shut down the reactor after the radioactivity level of the argon cover gas was observed to increase substantially owing to presence of gaseous fission products in the reactor. The reactor suffered a partial fuel meltdown. According to the US Nuclear Regulatory Commission, there was no abnormal radiation release to the environment. The main cause was a zirconium plate at the bottom of the reactor vessel (element A, Fig. 5.25) that became loose and blocked sodium coolant flow to some fuel subassemblies. The blockage caused an insufficient amount of coolant to enter and two subassemblies started to melt; this was not noticed by the operators until the core temperature alarms sounded.

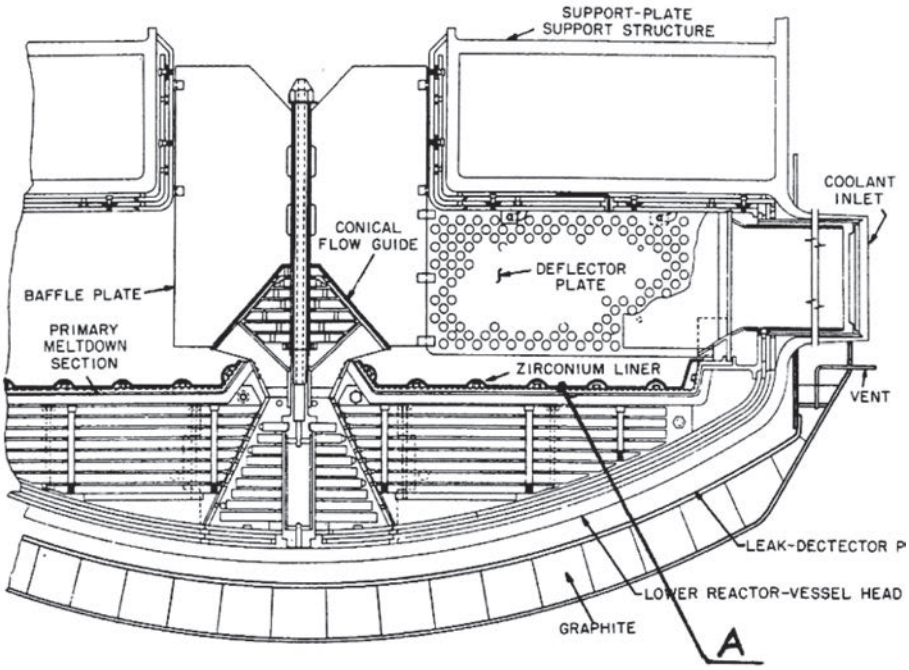

FIG. 5.25. EFFBR meltdown section [5.9].

In September 1967, a foreign body in the core inlet plenum was discovered to have blocked the coolant flow in several fuel channels and thus caused damage to six fuel subassemblies within the core. In March 1968, just before its removal after 16 months of investigation and modification, the foreign piece was identified. It was not, as had previously been assumed, a piece of construction debris left in the reactor, but one sixth pieces of zirconium sheet, used for cladding for a conical flow divider in the lower vessel (meltdown device in the core inlet plenum (Fig. 5.25)), which had unbolted and blocked the coolant flow in six fuel channels and thus caused the fuel melting.[2]

It consists of a flat 1/8 in. thick zirconium liner bolted to the top of a ½ in. thick baffle plate, which is a part of the shielding and baffling for the lower head of the vessel. The dimensions and geometry are such that material resulting from a meltdown can be collected in the shape of a flat circular subcritical slab, 7 ft in diameter. Three vertical baffles and a conical flow guide serve to direct coolant flow. The conical flow guide also serves, in the case of a meltdown, to disperse the molten fuel as it enters the plenum, and thus prevents a buildup of fuel in the centre of the meltdown section.

A secondary meltdown section was located immediately below the bottom head of the lower reactor vessel and follows the contour of the head. It consists of 6 in. cubes of 5% borated graphite bonded together with boron-containing cement to form a crucible capable of containing molten uranium.

Altogether, about two years were needed to define the details of the blockage, assess the damage and remove the dislodged zirconium piece. A third year was devoted to relicensing negotiations with the US Atomic Energy Commission and to preparing the plant for restart. The blockage and fuel melting revealed a design shortage — the axial coolant inlet port in the nozzle of the fuel subassembly (Fig. 5.26).

[2] This incident was the basis for a book by J.G. Fuller: We Almost Lost Detroit, Reader's Digest, New York (1975).

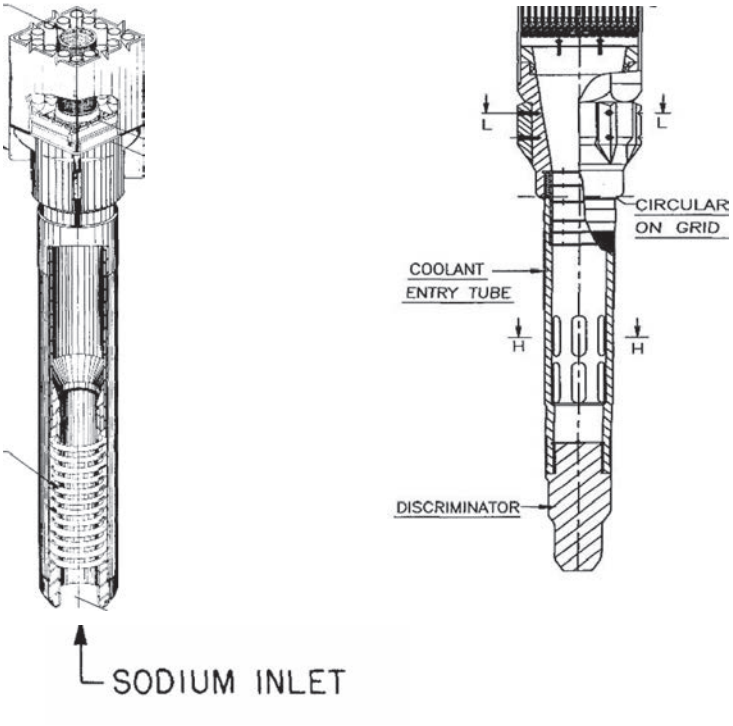

FIG. 5.26. Fuel subassembly nozzles: EFFBR (on the left, with one axial hole for the sodium inlet) and typical PFBR (on the right, with many radial holes for the coolant inlet) [5.8].

Several improvements were made at that time: installation of flow guards to prevent coolant blockage, improved control devices, a new fuel transport facility, modification of the SG, etc. After reloading with fresh fuel, the reactor was again brought to criticality in July 1970 and reached the designed power of 200 MW(th) for the first time in October 1970. The subsequent programme verified the stability and performance of a large liquid cooled fast reactor with metallic fuel. At that time the fuel supply was limited.

Fuel discharged as the result of the 1966 flow blockage was awaiting requalification. By the end of 1972 it was decided to decommission the EFFBR plant because of a lack of funding for a six year programme for operation with advanced MOX fuel and for use of the plant as an irradiation test facility.

Experience with the use of sodium was excellent. The operation of equipment in sodium and other environments presented no major difficulties and indicated that the high purity of large amounts of sodium (up to 130 t) in the system can be maintained without difficulty. The test indicated that the construction materials used in the system are compatible with sodium [5.1, 5.3, 5.8, 5.9, 5.25–5.29].

5.5. RAPSODIE

5.5.1. Main features of the installation

The French Atomic Energy Commission (CEA) started planning the experimental reactor Rapsodie (RAPide SODIum) in 1958. Start of construction was in 1962 within an association of CEA and Euratom; first criticality was reached in January 1967, and full power operation in March 1967. The time span to achieve full power with Rapsodie was comparatively short and was the result of an extensive out-of-plan pre-testing policy, a physical mock-up in MASURCA, and an engineering mock-up of the complete reactor cooling system in an oil fired 10 MW(th) rig.

The experimental FBR Rapsodie was designed, built and operated to obtain data on the physical behaviour of fast neutron reactors under static and dynamic conditions, to offer industrial information of direct use in the design of future liquid metal fast breeder reactors, and to supply a fast neutron flux for irradiation tests of fuels and

materials. Operating parameters were similar to those which would be used in a full scale reactor. Furthermore, a relatively high flux, 10^{15} neutrons · cm^{-2} · s^{-1}, provided the means for irradiating fuel for future reactors Phénix and Superphénix.

The use of plutonium for the first loading of the reactor, in the form of a mixed plutonium–uranium oxide element, was an example of the advanced philosophy utilized. A maximum power density of 700 kW/L was provided.

An extensive programme of fuel evaluation and development has been developed on a UO_2–PuO_2 MOX fuel and on various uranium–plutonium–molybdenum ternary alloys.

A poison type control system was utilized, with four safety rods, each containing about 100 g of ^{10}B in boron carbide. In addition, two regulating rods were provided, each containing about 100 g of ^{10}B. Each of the six rods located on the boundary between the core and the radial blanket in the high pressure coolant zone moved in a hexagonal guide tube similar to the hexagonal fuel subassembly cans for a distance of 45 cm. The rod boron carbide was enclosed in a cylindrical can, which was attached to a stellite nozzle and handling head for the drive shaft gripper.

Control rod drive mechanisms were located in six sections around the cover plate equipment. Removal of the control rods was accomplished by means similar to those used for refuelling a cask car.

The reactor core and blanket were cooled by two identical loops; each comprised a primary sodium circuit from which thermal power was transferred to a secondary sodium circuit through an intermediate (sodium–sodium) heat exchanger by means of a primary pump (Fig. 5.27).

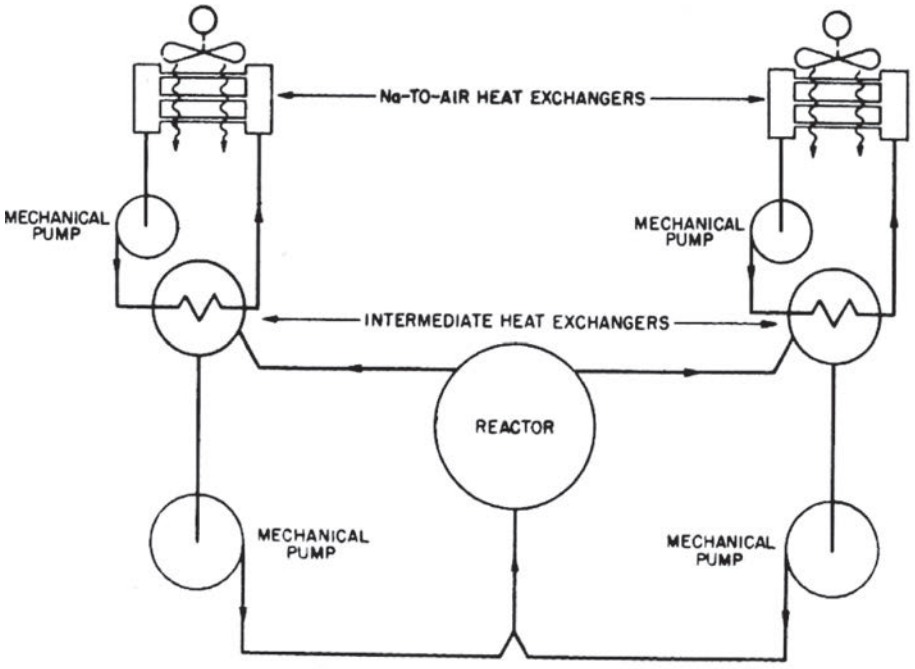

FIG. 5.27. Rapsodie primary and secondary system flow diagram [5.10].

The two loops had a common return line to the reactor and a common storage tank. The system lines were enclosed in concrete cells inside a double containment barrier. The principal geometric specifications of the primary pipe system were the following:

— Core to IHX: D = 300/314 mm, ~16 m long;
— IHX to pump: D = 300/314 mm, ~8.5 m long;
— Pump to Y junction: D = 200/208 mm, ~18 m long;
— IHX vessel dimensions: D = 884 mm, ~5.2 m high;
— Pump vessel dimensions: D = 850 mm, ~4.5 m high;
— Expansion tank: ~36 m^2 surface area.

The installation consisted of six main buildings, access to three of which was restricted; these were:

— The reactor building or secondary containment including the reactor vessel and its upper closures, as well as the two primary loops, each equipped with a mechanical pump and an IHX. All these components were enclosed in concrete cells to provide radiation shielding. The secondary, non-radioactive sodium was piped to a conventional building containing the components of the two secondary loops including a sodium–air heat exchanger in each.
— The active building comprising interim storage facilities for both fresh and used fuel, and various other facilities such as the washing cell for decontaminating components polluted with primary sodium, and a dismantling hot cell used for conditioning used, irradiated equipment for long term storage as waste.

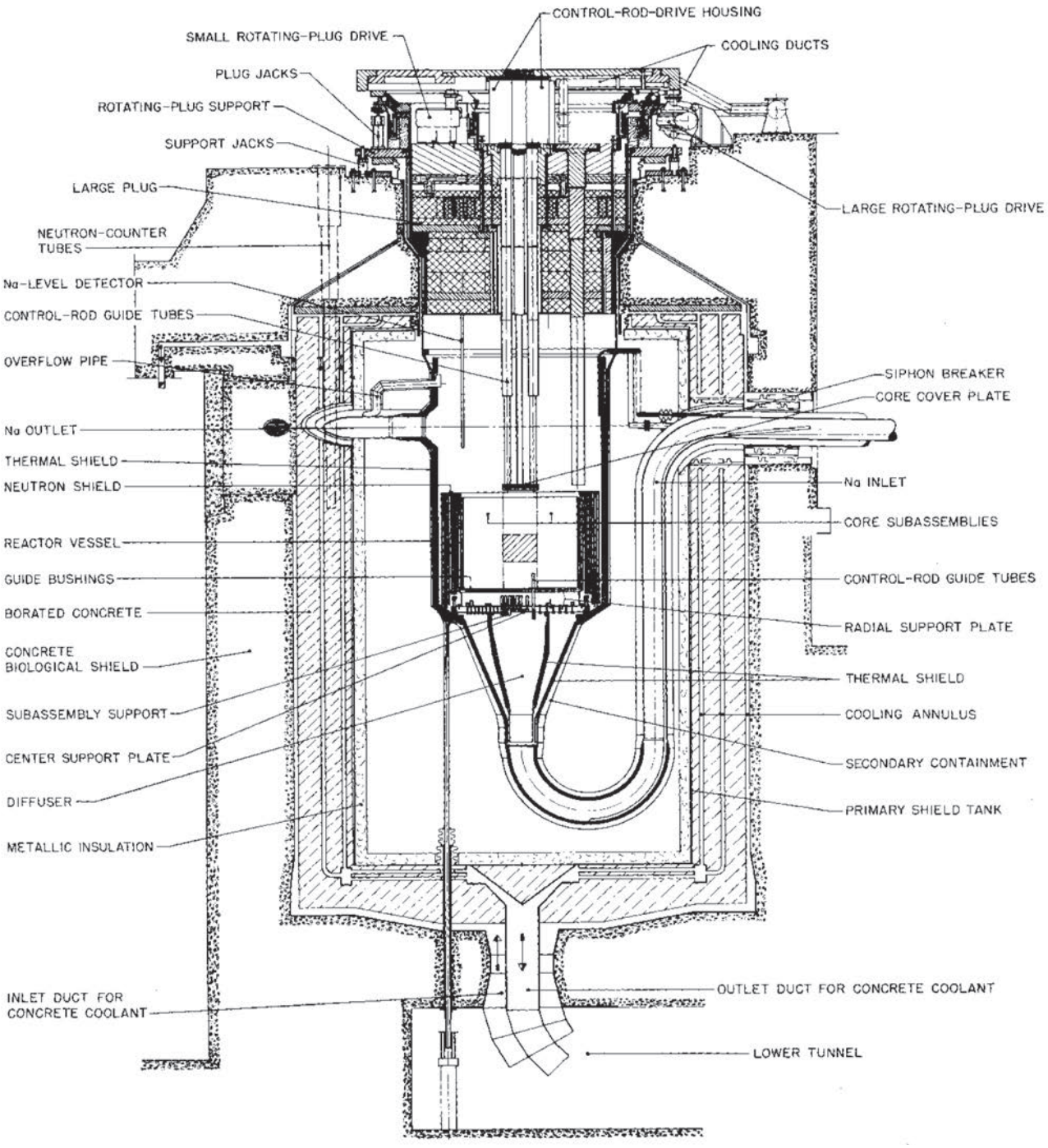

FIG. 5.28. Rapsodie reactor: vertical cross-section [5.3].

— The fuel assembly dismantling building comprising hot cells for non-destructive examination of fuel pins, and the assembly of experimental sub-assemblies.

All the circuits and components were made of austenitic stainless steel; the main pipes and vessels had a double wall. The reactor vessel was surrounded by special high density concrete, containing rare earth oxides. This was protected externally by a steel liner which was considered to constitute the second barrier when the decision was taken for dismantling to level 2 (of the IAEA scale), leaving the reactor block in place. A view of the reactor assembly is shown in Fig. 5.28.

The fuel subassemblies, which contained both a fuel section and an axial blanket section, were in a central region surrounded by radial blanket subassemblies. Removable subassemblies outside this region served as reflectors. The concentric steel cylinder assembly, as shown in Fig. 5.29, was used for both a non-removable reflector and thermal shield.

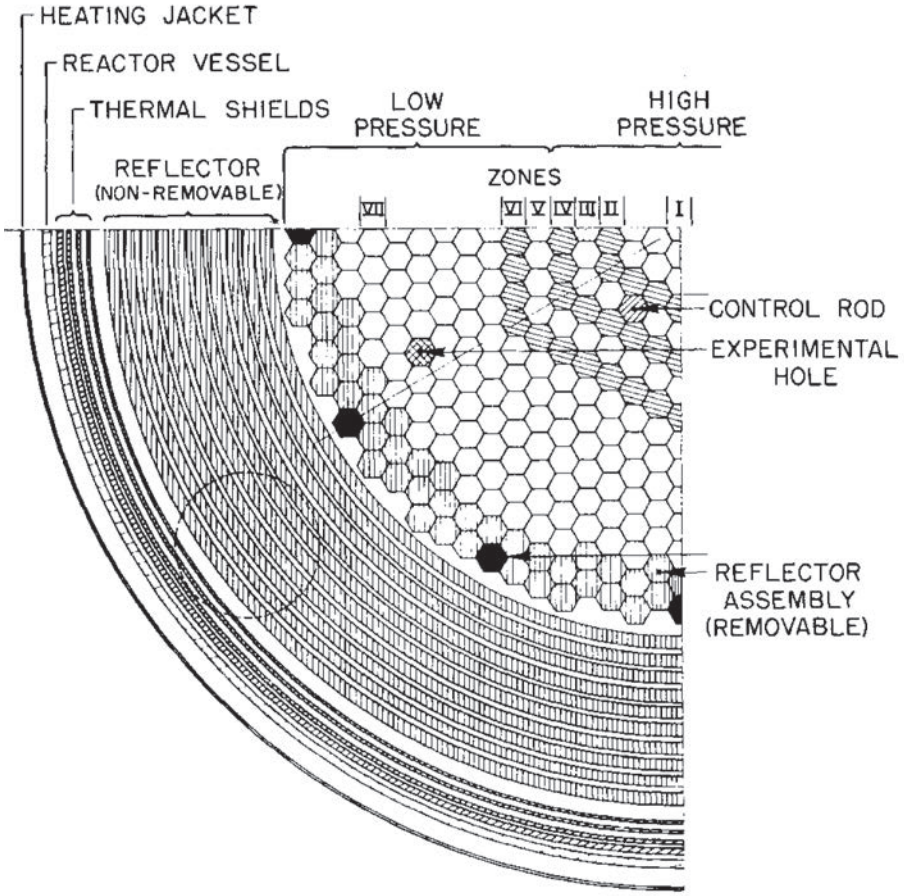

FIG. 5.29. Rapsodie reactor: horizontal cross-section [5.3].

A jacket located outside the reactor vessel served as a means for circulating gas for preheating. Eventually this space could serve for cooling the reactor during shutdown. Steel containers filled with thermal insulation were located outside the preheating jacket. Additional structures consisted of the containment tank and the biological shield. An outer blast shield consisted of three concentric layers: borated graphite, lightweight cellular concrete and reinforced concrete. A single sodium inlet pipe is shown with two sodium outlet pipes located in a vertical plane perpendicular to the plane of the inlet pipe. Within the reactor vessel, both the removable and non-removable reflector regions tended to reduce the neutron energy as well as attenuate the flux.

The non-removable portion of the reflector consisted of ten concentric cylindrical shields made of stainless steel, 24 mm thick, and separated by an 8 mm space. Outside this assembly was a thermal shield consisting of four

concentric cylinders having thicknesses of 4, 7, 10 and 10 mm, respectively. The reactor vessel, shown in Fig. 5.28, of type 316 stainless steel, consisted of a lower 12 mm thick elliptical cylinder, a main 15 mm thick plate section, and an upper section located between the fixed plug and a large rotating plug.

MOX was used as the reactor fuel. Although some researchers considered at that time that the metal fuel was attractive because of its good heat conductivity at high power densities, irradiation experiments indicated excessive swelling.

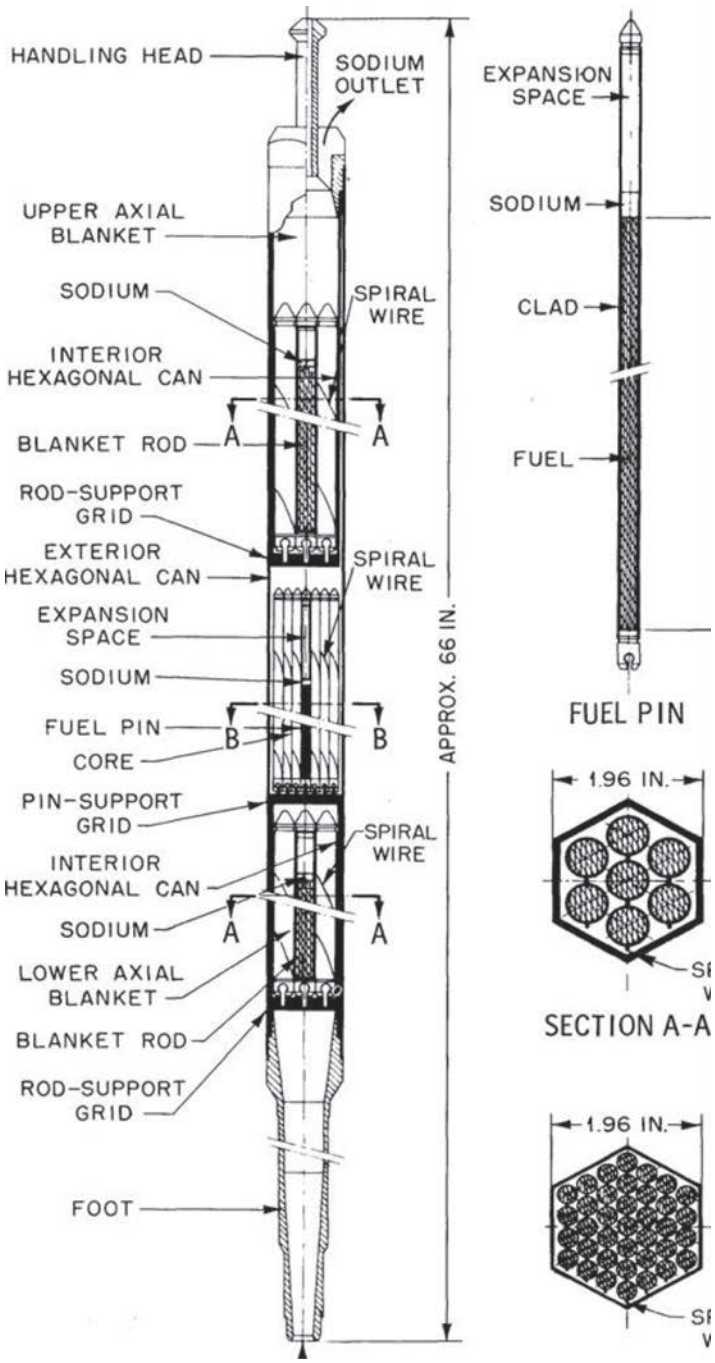

FIG. 5.30. Rapsodie fuel subassembly [5.3].

An additional disadvantage of the alloys was their poor compatibility with stainless steel: a double-cladding design would be necessary (at that time), consisting of an interior layer of niobium and an exterior layer of stainless steel with sodium bonding. The French CEA chose the MOX because it presented fewer fabrication problems than

the alloy and because there was a greater background of irradiation and production experience with the oxide. A fuel subassembly is illustrated in Fig. 5.30.

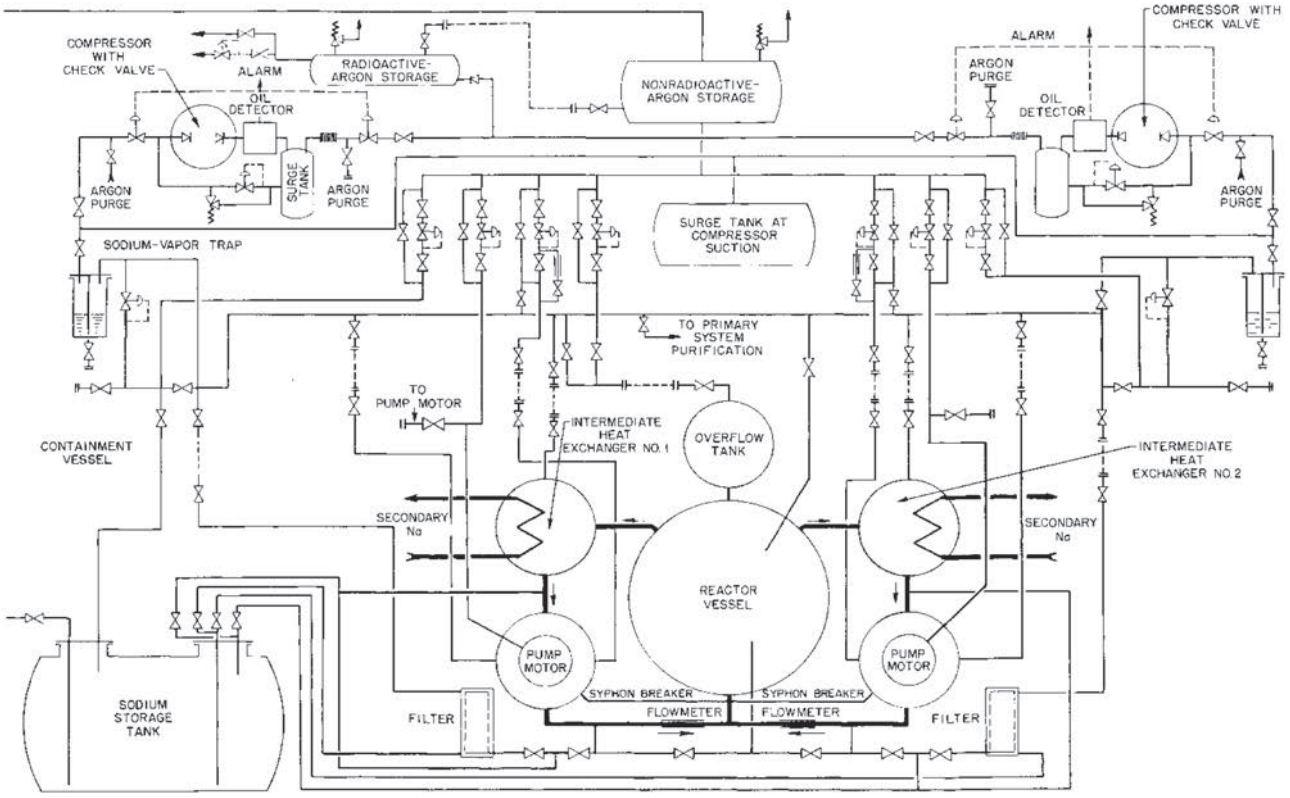

FIG. 5.31. Rapsodie heat transport system — primary circuit [5.3].

In the core region of the subassembly, 37 fuel rods were assembled in a stainless steel container with a hexagonal cross-section. Each individual element consisted of a number of sintered pellets of mixed uranium and plutonium oxide (25 wt% PuO_2) contained in the stainless steel tube. A spring arrangement maintained contact between the various pellets in the column, and provision was made in the upper region of the element to collect fission gases. Separation between pins was maintained by a wire spiral.

The ternary alloy (75 wt% uranium, 15 wt% plutonium and 10 wt% molybdenum) was under consideration as a possible alternative in the early stages. Its preliminary design was as follows (in accordance with the knowledge of that time): a double-cladding design was used to prevent the formation of a plutonium–iron eutectic, with the space between layers filled with sodium to ensure heat transmission; the wire spiral separation of pins was used in this case as well.

Both the upper and lower blanket sections consisted of a cluster of seven large-diameter elements of depleted uranium. A lower base plate was provided to distribute the coolant. The lower end of the subassemblies, shaped in the form of a nozzle with an internal Venturi section, reduced upward forces induced by the coolant flow and aided in positioning. The upper end of the subassembly was provided with a handling lug pierced with three holes for the sodium coolant outlet. The radial blanket subassemblies were similar to the fuel subassemblies, but they contained a continuous, seven rod internal structure of large-diameter depleted uranium elements. Removable stainless steel reflector subassemblies were available to provide flexibility of operation and fuel movement.

The primary coolant flow is shown in schematic form in Fig. 5.31. The reactor was a loop type and had two cooling trains, each designed for 12 MW(th). The 12 MW(th) loops used variable frequency motors driving mechanical pumps whose maximum speed was seven times greater than the minimum speed. Flow control for the sodium–air heat exchangers was accomplished by variable pitch of the fan blades.

The heat release in the core and blanket was removed by two parallel primary loops. The primary loops were placed symmetrically around the reactor. Each of them was located in a separate compartment, one with a tank

for expansion of the sodium from the reactor vessel. From this tank, the sodium passes through the purification system and then to the upper part of the reactor vessel. The two loops have a common return line (Fig. 5.27) to the reactor and a common coolant storage tank.

The joint to the return line was made just before it entered the primary shielding tank. The reactor, the IHX and the pump each had a free surface permitting maintenance. With a free surface, the shield plug of each piece of equipment was in a neutral atmosphere, and all the leakproof closures were at the level of the deck where they were easily accessible.

Closure was made with a tours seal except the reactor vessel, which used a tin–bismuth dip seal. The secondary coolant was sodium; the heat production was dumped to the atmosphere through sodium–air heat exchangers.

Sodium was used as the coolant in both the primary and secondary systems. Sodium was pumped by a vertical centrifugal pump rated at 1540 gal/min. Discharge from the pump tank entered the lower section of the reactor vessel and then flowed to the flow divider–diffuser assembly. The flow baffle separated the coolant into a high pressure zone, providing a coolant for the core and inner radial blanket, and a low pressure zone for the outer radial blanket. The diffuser assembly provided a non-critical geometry for the collection of fuel in the event of a meltdown accident. Primary sodium circulated through the shell of this vertical stainless steel tube exchanger, and secondary sodium circulated through the tubes. In the design the upper tube sheet was fixed, and the lower tube sheet was floating to permit thermal expansion of the tube bundle. The tubes themselves were located in 12 concentric sections.

The thermal transport system was provided with auxiliary components and equipment, i.e. necessary expansion tanks, purification loops and a variety of instrumentation. Preheating of the reactor vessel was made possible by a 4 mm thick jacket that allowed circulation of an inert gas at 150°C. This preheating prior to the introduction of sodium minimized thermal shock as well as provided for the heating of sodium in the event of freezing.

The first criticality was reached in January 1967, and full power operation was reached in March 1967. From August 1967 until February 1970, Rapsodie was in normal operation. From February 1970 until January 1971, the core and equipment were modified to increase the thermal power level from 24 to 40 MW(th) (Rapsodie-Fortissimo). The operating parameters were similar to those in large commercial size reactors.

During 16 years of operation, ~30,000 fuel pins of the driver core were irradiated, of which ~10 000 reached a burnup beyond 10%; 300 irradiation experiments and more than 1000 tests were performed. The maximum burnup of the test fuel pins was 27% (173 displacements per atom). In 1971, the irradiations performed in the core revealed a phenomenon of irradiation swelling in the stainless steel of the wrapper and the fuel cladding in the high neutron flux. An outstanding feature of Rapsodie operation was that the actual power output substantially exceeded the design level.

The decision to stop running the reactor was taken after two successive defects were detected in the primary system containment (double envelope of reactor vessel). The first defect, which appeared in 1978, consisted of a sodium micro-leak: radioactive sodium aerosols were found in the double wall reactor vessel. Investigations did not find any liquid sodium in the gap, nor was the defect located. The reactor was subsequently operated at a reduced power level (~0.6 P_N), which was high enough for irradiation needs but did not cause the leak to reappear. The second defect appeared in 1982 and consisted of a small leak from the nitrogen blanket surrounding the primary system. Repairs would have been long and costly. Since the reactor had fulfilled its aims, it was decided to finally shut down the plant in October 1982. Before the final shutdown of the reactor, a series of end-of-life tests were conducted in April 1983.

5.5.2. Experiments with the Rapsodie reactor

5.5.2.1. Natural circulation experiments

One experiment involved startup of natural circulation in the primary and secondary circuits from an isothermal reactor driven by the neutronic power rise up to 750 kW(th) (insufficient decay power data available) and kept constant thereafter. Following scram at nominal conditions of 22.4 MW(th), the transition to natural circulation in the whole installation including air coolers was analysed, simulating total loss of electric power supply.

5.5.2.2. High power fuel performance experiment

A short term irradiation programme was carried out with experiments concerning Superphénix geometry, fuel performance and pin behaviour under accident conditions. In the experiments the test pins showed perfect performance for a maximum linear power rating of 1000–1060 kW/cm kept constant for about 10 min, i.e. two times more than that normally used in commercial reactors. An evaluation showed a local fuel melt fraction up to 30% (Fig. 5.32).

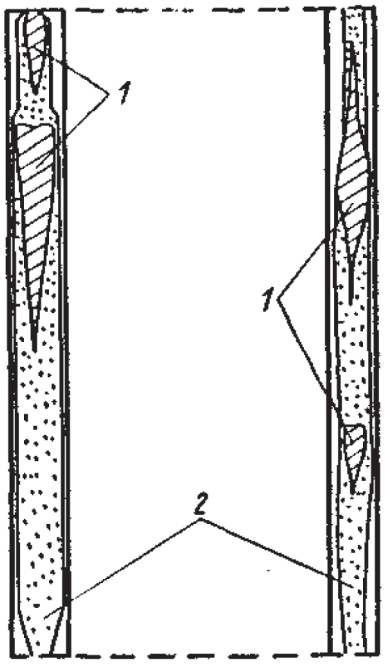

1 — empty space; 2 — molten fuel

FIG. 5.32. Fuel pin containing molten fuel of Rapsodie reactor.

5.5.2.3. Exceptional reactor transient without scram

The third series of experiments simulated the most serious accident — LOFWS, which consisted of the shutdown of the primary circuit and secondary circuit pumps, as well as the tertiary circuit fans, and the non-operation of the safety rods. Here, reactor output reached 21.2 MW (more than 50% of the rated value), while the mean coolant temperatures at the reactor inlet and outlet came to 402°C and 507°C, respectively. The principal characteristics of the subject process are depicted in Fig. 5.33. In this test, the maximum fissile sub-channel temperature rose to a maximum value of 800°C, whereas the nuclear power decreased continuously without any intervention from the reactor control.

A comparison of calculation results and experimental data demonstrated that the fuel residing in the core shared a state of coalescence with the fuel element cladding and expanded with the cladding upon heating up. It is of the utmost importance that good agreement is reached between the calculation results and the experimental data concerning the coolant temperature at the subassembly outlet. These experiments, performed in accordance with prediction, demonstrated the inherently stable reactor behaviour in a severe accident, including LOFWS.

5.5.3. Rapsodie decommissioning operations: Lessons learned

The decommissioning operations involved in the partial dismantling programme, which was finally adopted, were designed to eliminate the radioactivity as much as possible without exposing the operators excessively (the ALARA concept applies here, as everywhere), to confine the residual radioactivity and, as a result, to minimize

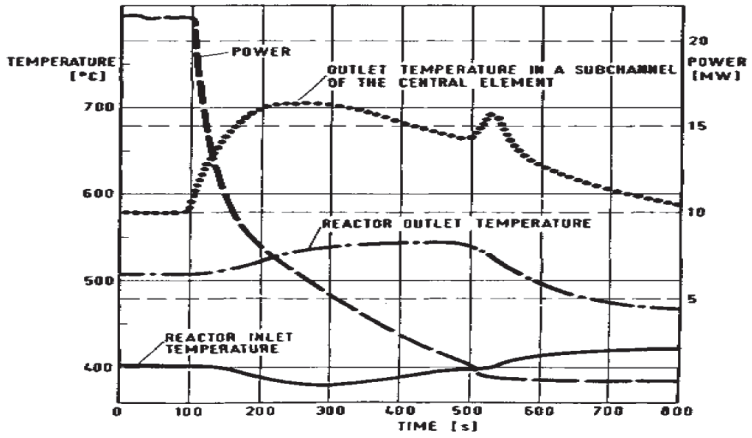

FIG. 5.33. Rapsodie end-of-life test: characteristics during a LOFWS transient[3] [5.30, 5.31].

monitoring and surveillance measures pending complete dismantling. In the Rapsodie case, the successive operations were:

— Removal and disposal of the steel and nickel reflector assemblies as waste;
— Washing and decontamination of the primary circuit;
— Dismantling of the primary circuit, one secondary circuit and the auxiliary systems of the reactor;
— Completion of the primary and secondary containment of the nuclear island;
— Dismantling of the auxiliary equipment used for handling, washing and storing nuclear materials or contaminated components;
— Disposal of the primary sodium (37 t) and cleaning of the active area.

At the end of 1986, the reactor vessel evaluation programme having been dropped, there was no longer any need for its immediate washing and decontamination. The vessel was isolated from all the circuits and the main and auxiliary pipes were disconnected and blocked off.

The subsequent Rapsodie decommissioning operations were as follows:

— A cleaning period from 2004 to 2008 for:
  (i) Dismantling of auxiliary systems;
  (ii) Receiving permissions from the safety authorities for the full dismantling of the reactor block and cleaning of the building.
— The period from 2009 to 2017: the dismantling of the reactor block and cleaning of the building; the carbonating of the remaining primary sodium, the dismantling under water of the reactor vessel internals, using specific plasma cutting and handling tools. After water drainage, the dismantling of the primary and safety vessel and the building itself will be carried out and the remnants will be sent to long term storage.

After draining the primary sodium, washing and decontamination of the circuits was essential before any further action was taken for the following reasons:

— Removal of any sodium remaining in the system improves the safety of future operations;
— Removal of a large part of the radioactive contamination of the circuit walls, due mainly to ^{137}Cs, allows the dose accumulated by the operators during dismantling work to be reduced.

The decision to proceed with washing and decontamination of the primary cooling system was aimed at reducing radiation dose to the dismantling personnel. The decontamination of the primary system, on the other

[3] The pump stop time was about 400 s; the halving time appears to be about 45 s.

side, would reduce the cost of dismantling by decreasing its duration, because it would be possible to use high speed cutting devices such as a plasma torch. Dismantling without washing and decontamination would require ten months of work by five persons including two waste conditioning specialists. The washing and decontamination of the primary system should leave only a few localized deposits whose harmful effects can easily be limited.

The overall integrated dose should thus be limited to a maximum of 10^{-2} man Sv due to the shortening of the work period and reduction of the contamination level by a factor of 300. At the French and other LMFRs, methods for washing experimental devices such as large components using either water mist or vapour have been developed and used for years. The washing of a complex circuit, comprising pipes of different diameters and capacities, in which relatively large amounts of sodium may persist as oxide deposits adhering to the walls or as puddles trapped in undrainable areas, requires special attention.

It was estimated that around 100–150 kg of sodium remained in the plant tanks. As a result, it was judged preferable to take a more straightforward approach by using a 'heavy' alcohol (ethylcarbitol, or EC) instead of water for neutralizing the sodium. Neutralization was achieved by changing the sodium into a caustic-free alcoholate that is inert from the corrosion point of view. Of course, hydrogen is produced and there is some risk of explosion, but several tests showed that it was easier to control sodium destruction in this manner. As the alcoholate becomes viscous at high concentrations, an excess of alcohol has to be maintained at all times and the waste volume consequently increases. It is considered that 1 m^3 of sodium results in 4 m^3 of alcoholate + alcohol with the same content of radioactive contamination.

The first washing operations took place in 1986. They began with the washing of the normal dump tank RENa 300 that was assumed to contain about 100 kg of sodium forming a large 3 m^2 puddle. The process consisted in introducing small quantities of ethylcarbitol into the tank, which was kept unheated and under an internal nitrogen atmosphere. The total destruction of the sodium took about two days without any noticeable difficulty.

A few weeks later, an attempt to wash some auxiliary circuits, including the purification system (without the cold traps that had been previously disconnected) and the filling–draining lines, by using the 2500 L of ethylcarbitol and alcoholate left in the dump tank failed. Plugs of solid or viscous alcoholate formed at some lower points. It was then decided to cut these circuits into pieces and to wash them by standard means.

The washing of the primary system was performed during the second quarter of 1988. It was done in several steps by making up a series of loops, each including a portion of the system. Ethylcarbitol was circulated in the pipes and sprayed into the cavities simultaneously. After that, rinsing with demineralized water and then flooding of the whole system completed the process. In all, 4200 L of alcohol and 11 m^3 of water were used for the various rinsing procedures. In total, the washing operations involved the destruction of 125 kg of sodium with 0.4 TBq of ^{137}Cs content, most of it removed from the system walls. This caesium was partially trapped on the ion exchanging resins during the subsequent regeneration of the alcohol. As a result, the dose rates in the concrete cells were generally reduced by a factor of 10, and even 100 locally.

In March 1994 it was decided to wash the sodium storage tank RENa 302 (located in a peripheral gallery beside the reactor building) using ethylcarbitol as was done eight years earlier with the RENa 300 storage tank. The amount of sodium left in the tank had been estimated, at that time, at ~100 kg. Several days after the beginning of this operation, a violent explosion took place, causing casualties and heavy damage to the gallery. Only slight radioactive contamination was detected on the scene of the accident resulting from the caesium content of the tank. The accident was due to the tank's pneumatic bursting under an internal pressure of ~15 bars, eight days after its cleaning started. Investigation of the circumstances and possible causes of this accident were completed in May 1999.

5.5.4. Accident interpretation with current knowledge

5.5.4.1. First injection

During the first two days (24 and 25 March 1994), 1000 L of alcohol were injected. The temperature measured on the operation thermocouples rose up to 150°C, i.e. a temperature of about 200°C in the tank's centre. A successive formation of ethylcarbitolate and ethylcarbitol–ethylcarbitol–Na octahedral complexes took place, with the production of hydrogen and trapping of this 'produced' hydrogen by the sodium, with formation of hydrides retained in the complexes, then partial decomposition of the formed alcoholate (at the interface between the alcohol and the sodium, the temperature can easily reach 240°C).

5.5.4.2. Reaction medium ageing

During the period without injections, the temperature achieved by electrical heating increased to the same level as the first days and amplified the same phenomena: slow dissolution of the remaining sodium with formation of ethylcarbitol–ethylcarbitol lNa–NaH complexes favoured by the absence of agitation (no new injections), ECNa decomposition, formation of oxalate, ethanol, ethylate soda, sodium carbonate, and trapping of some ethylcarbitolate decomposition hydrogen with a new formation of hydride. This ethylcarbiytolate decomposition process also 'freed' some of the hydride retained by the complexes.

5.5.4.3. Final injection

After five days without any 'fresh' alcohol, the tank's centre contained a mixture mainly constituted of partially decomposed ethylcarbitol–ethylcarbitol lNa–NaH complexes, 'freed' hydride, oxalate, ethylate and soda. The fresh ethylcarbitol injected on this medium briskly reacted with the 'free' hydride, thus contributing to the reactions' divergence by producing over 900 m^3 of gas, thus causing the tank's pneumatic bursting.

It is also interesting to note that, although a high temperature was reached (180–250°C) during the morning of 31 March, the runaway only occurred in the afternoon, as the heat released by the miscellaneous chemical reactions (ethylcarbitolate decomposition, ethylcarbitol decomposition) was 'consumed' by the tank's thermal losses, by increases in the temperature of the cold injected ethylcarbitol and by the evaporation of the volatile components. Throughout the day, the thermal balance of the medium was therefore very unstable, and the 'runaway' only prevailed over the 'damping' process after a long period of thermal oscillations.

Currently, it is considered that the only cause of the accident was a considerable and sudden discharge of gas, due to a runaway of exothermal chemical reactions, which could not have been forecast in 1994 owing to the lack of knowledge. Indeed, until this accident, ethylcarbitolate was considered a stable final product of the sodium dissolving reaction, on the same grounds as soda, due to the analogy between the following reactions:

$$ROH + Na \rightarrow NaOR + 1/2\ H_2 \text{ and}$$

$$HOH + Na \rightarrow NaOH + 1/2\ H_2$$

However, the studies performed after the accident highlighted that:

— The EC–ECNa–NaH mixture, resulting from the EC + Na reaction, is very unstable: minor instability under 150°C, but major instability above. If it is maintained at 180°C for more than 24 h, the ECNa fully disappears and an ethylcarbitol decomposition process may start.
— This thermal instability results from decomposition reactions, which are exothermal themselves. Above 150°C the EC–ECNa–NaH decomposition product system enters in a self-heating initiation range, which, according to the experimental conditions (notably, thermal leaks), can either gradually reduce (the reaction then stops between 250 and 300°C), or increase (the reaction then changes into a runaway reaction at about 220–270°C), with a considerable production of gas.
— These extremely sudden decompositions of the medium EC–ECNa–NaH mixtures produced by the reaction, with test cell pneumatic bursting, can occur without external medium heating. If the reaction runaway does not occur, it is often possible to trigger it simply by adding some 'fresh' ethylcarbitol in the medium.

The incident occurred in the process of decommissioning (removal of sodium residues from the drain tanks using heavy alcohol) and resulted in the extensive local damage of the auxiliary building structures. Appropriate studies of the use of alcohol together with sodium have been performed. Based on this new knowledge, the prohibition regarding cleaning sodium puddles with alcohol was confirmed for all CEA facilities.

The International Working Group on Fast Reactors, at its meeting in May 1999, summarizing results of the discussions, took note of a presentation of the French delegation on the above mentioned accident, and made the following conclusion: under certain circumstances (e.g. closed geometries, sodium puddles), the use of alcohol to clean components or to destroy sodium can be dangerous. This is proven for ethylcarbitol, but can at present not be

excluded completely for other alcohols. It was strongly recommended to perform appropriate studies prior to the use of alcohol together with sodium [5.3, 5.10, 5.30–5.38].

REFERENCES TO CHAPTER 5

[5.1] INTERNATIONAL ATOMIC ENERGY AGENCY, Status of Liquid Metal Cooled Fast Breeder Reactors, Technical Reports Series No. 246, IAEA, Vienna (1985).

[5.2] KHOMYAKOV. Y.S., "Substantiation of physical concepts of fast reactors in Russia: experience and prospects", Proc. of the International Conference on the Physics of Reactors "Nuclear Power: A Sustainable Resource", PHYSOR '08, Casino-Kursaal Conference Canter, Interlaken, Switzerland, September 14–19, 2008.

[5.3] SESONKE, A., YEVICK, J.G., "Description of fast reactors", in: "Fast reactor technology: plant design", edited by Yevick, J.G. and Amorosi, A., The M.I.T. PRESS, the Massachusetts Institute of Technology (1966).

[5.4] LEIPUNSKIY, A.I., et al., "Experimental fast reactors (BR-2, BR-5) in the Soviet Union", in Proceedings of the Second United Nations International Conference on the Peaceful Uses of Atomic Energy, Geneva, 1958, Vol. 9, United Nations, New York (1959).

[5.5] INTERNATIONAL ATOMIC ENERGY AGENCY, "Experimental fast reactors in the Soviet Union", in Physics of fast and intermediate reactors, Vol. III (Proc. of a Sem. Held in Vienna Aug. 3–11, 1961), Proceedings Series No. 2, IAEA, Vienna (1962).

[5.6] PINCHASIK, M.C., et al., "Operating experience with the BR-5 reactor, in Power Reactor Experiments", Proceedings of the IAEA Symposium in Vienna, STI/PUB-51, Vienna (1962).

[5.7] LEYPUNSKIY, A.I., "Fast Neutron Systems", in Book: A.I. Leypunskiy, Selected Papers. Reminiscence, Naukova Dumka, Kiev (1990).

[5.8] INTERNATIONAL ATOMIC ENERGY AGENCY, Fast Reactor Database, 2006 Update, IAEA-TECDOC-1531, IAEA, Vienna (2006).

[5.9] CHASE, W.L., "Heat-transport systems", Fast Reactor Technology: Plant Design, (YEVICK, J.G., AMOROSI, A. (Eds)), The M.I.T. Press, Cambridge, MA (1966).

[5.10] SCOTT, C.C., "Plant instrumentation and control", Fast reactor technology: plant design, YEVICK, J.G., AMOROSI, A. (Eds), The M.I.T. Press, Cambridge, MA (1966).

[5.11] GARTWRIGHT, H., et al., "The Dounreay fast reactor — basic problems in design", in Proceedings of the Second United Nations International Conference on the Peaceful Uses of Atomic Energy, Geneva, 1958, Vol. 9, United Nations, New York (1959).

[5.12] PHILIPS, J.L., "Operating experience with the Dounreay fast reactor", Nuclear Power (August 1962).

[5.13] Proceedings of the Symposium on the Dounreay fast reactor, December 1960, BNEC, London (1961).

[5.14] INTERNATIONAL ATOMIC ENERGY AGENCY, "Design, construction, and operating experience of demonstration LMFRs" (Proc. of a Symp., Bologna, Italy, 10–14 April 1978) IAEA, Vienna (1978).

[5.15] MICHELBACHER, J.A., et al., "Shutdown and closure of the Experimental Breeder Reactor-II", Proc. of the 10th International Conference on Nuclear Engineering, ICONE10, April 14–18, 2002, Arlington, Virginia.

[5.16] "The Experimental Breeder Reactor-II inherent safety demonstration", Stanley H. FISTERS, Ed., North-Holland-Amsterdam, 1987.

[5.17] KING, R.W., PORTER, D.L., et al., "Performance of key features of EBR-II and the implications for next generation systems", Proc. of the 10th International Conference on Nuclear Engineering, ICONE10, April 14–18, 2002, Arlington, Virginia.

[5.18] LINDSAY, R.W., "Application of advanced technology to LMR control", Proc. of the Seventh Power Plant Dynamics, Control and Testing Symposium, May 15–17, 1989, Knoxville, Tennessee.

[5.19] CHRISTENSEN, L.J., "Experimental Breeder Reactor II (EBR-II), instrumentation for core surveillance", paper presented at the IWG-FR Int. Meeting, December 12–15, 1989, Kalpakkam, India.

[5.20] MESSICK, N.C., et al., "Modification of EBR-II plant to conduct loss-of-flow-without scram test", Nuclear Engineering and Design, **101** (1987) 13.

[5.21] INTERNATIONAL ATOMIC ENERGY AGENCY, "The physics design of EBR-II", in Physics of Fast and Intermediate Reactors, Vol. III, (Proc. of a Sem. held in Vienna Aug. 3–11, 1961), IAEA, Vienna (1962).

[5.22] SACKETT, J., "Operating and test experience with EBR-II, the IFR prototype", Progress in Nuclear Energy, Vol. **31**, No. ½, 1997.

[5.23] MICHELBACHER, J.A., et al., "Deactivation of the EBR-II complex", paper presented at the IAEA Consultants Meeting on Technical Options for the Decommissioning of the BN-350 LMFR, Obninsk, Russian Federation, 23–27 February, 1998.

[5.24] McDERMOTT, M.D., et al., "Completion of Experimental Breeder Reactor-II sodium processing at Argonne National Laboratory", ICONE10, April 14–18, 2002, Arlington, Virginia.

[5.25] HUNGERFORD, H.E., “Shielding in fast reactor technology”, Fast reactor technology: plant design, YEVICK, J.G., AMOROSI, A. (Eds), The M.I.T. Press, Cambridge, MA (1966).
[5.26] AMOROSI, A.A., YEVICK, J.G., “An appraisal of the Enrico Fermi Fast Reactor”, Proceedings of the Second United Nations International Conference on the Peaceful Uses of Atomic Energy, Geneva, 1958, Vol. 9, United Nations, New York (1959).
[5.27] McCARTHY, W.J., et al., “Recent operating experience at the Enrico Fermi Atomic power plant”, (Proc. BNES Conf. London, 1966), Pergamon Press, Oxford (1967).
[5.28] ALEXANDERSON, E.L., et al., “Enrico Fermi Atomic power plant – operating experience through 100 MW(th), Fast Reactors”, Topical Meeting, American Nuclear Society, Report ANS-101, 1967.
[5.29] DUFFY, J.G., et al., “Investigation of the fuel melting incident at the Enrico Fermi Atomic power plant”, ibid.
[5.30] MARTH, W., “The story of the European fast reactor cooperation”, KfK, 5255, Kernforsscugszentrum, Karlsruhe GmbH, Germany, 1993.
[5.31] ESSIG, C., “Dynamic behaviour of Rapsodie in exceptional transient experiments”. In: Proc. ANS International Topical Meeting on Reactor Safety, Knoxville, 1985.
[5.32] ZALESKI, C.P., VAUTREY, L., “Le Reacteur Rapide Surregenerator”, Vols 1, 2, CEA, France, 1961.
[5.33] SEBILLEAU, F., ZALESKI, C.P., “Plutonium as a fuel for the fast reactor Rapsodie”, ANS Topical Meeting, Richland, Washington, 1962.
[5.34] VENDRIES, G., “RAPSODIE”, Proceedings of the 3rd United Nations International Conference on the Peaceful Uses of Atomic Energy, Geneva, 1964, Vol. 6, United Nations, New York (1965).
[5.35] DENILOU, G., et al., “A technical problem raised by the construction and testing of Rapsodie, Fast Reactors”, Topical Meeting, American Nuclear Society, Report ANS-101, 1967.
[5.36] VAUTREY, L., ZALESKI, C.P., “Design studies of fast reactor in France”, Proc. of the London Conference on Fast breeder Reactors, organized by the British Nuclear Energy Society, London, 17-19 May, 1966.
[5.37] ROGER, J., “Stage 2 dismantling of reactor, case of the experimental FBR Rapsodie”, paper presented at the International symposium on Decontamination and Decommissioning, Knoxville, 1985.
[5.38] INTERNATIONAL ATOMIC ENERGY AGENCY, Status of Liquid Metal Cooled Fast Reactor Technology, IAEA-TECDOC-1083, IAEA, Vienna (1999).

6. HEAVY METAL COOLANT SUBMARINE REACTORS AND LAND BASED POWER PLANT PROJECTS

6.1. SUBMARINE LIQUID METAL COOLED REACTORS: ESTABLISHING THE ENGINEERING FEASIBILITY OF HEAVY METAL COOLANTS

In the earlier 1950s, nearly simultaneously, the USA and USSR launched the development of power reactors for nuclear submarines. In both countries, the work was carried out for two types of reactor: pressurized water reactors and reactors cooled by liquid metal coolant. In the USA, sodium was chosen, as it possessed the better thermohydraulic characteristics; use of lead/lead–bismuth was dismissed early, mainly owing to high pumping power requirements.

The sodium cooled submarine reactor 'Sea Wolf' is shown cruising at sea in Fig. 6.1. Sodium was chosen as the coolant for three reasons: low operating pressure, excellent heat transferability and increased outlet temperature to produce improved power cycle efficiency. At that time, such luminaries as Fermi, Szilard, Zinn and others favoured liquid metal fast reactors which used fissions at energies of several hundred thousand electron volts to reduce non-fission capture and to produce more fissile material than was consumed. A sodium intermediate reactor (SIR) was selected to give priority to safety over increased fissile resources.

FIG. 6.1. USS Sea Wolf (SSN 575) submarine at sea [6.1].

The ground based test facility prototype of the nuclear power installations and the nuclear submarine 'Sea Wolf' were constructed. The operating experience showed that the choice of liquid metal was not justified in such types of reactor.

A programme for studying the compatibility of lead, bismuth and their alloys with structural materials existed at BNL (UK) between 1950 and 1962 as part of the liquid metal fuel reactor programme. The focus was on the development and testing of a natural U–Bi liquid metal fuel. An in-pile liquid metal fuel loop was constructed and tested in the 1950s.

The only lead–bismuth cooled reactors are those developed for the Soviet Union's Project 705 (Alfa Class) submarines: a modified version (Project 645) commissioned in 1963 to test reactors intended for Alfa Class submarines and an initial prototype (Project 661/Papa Class) commissioned in 1969. Production started in 1974, with the first commissioning in 1977.

The thermohydraulic features of lead–bismuth and lead coolants are high boiling temperatures and relative inertness to water compared with sodium. The melting and boiling points of sodium are respectively 98°C and 883°C at atmospheric pressure. For lead–bismuth eutectic the respective values are 123.5°C and 1670°C, and those for lead are 327°C and 1740°C at atmospheric pressure. It should be stressed that the heavy metal boiling points are well above cladding failure temperatures. The specific heat per unit volume of lead–bismuth and lead are similar to those of sodium but the conductivities are about a factor of four smaller.

A great deal of experience has been accumulated in the course of the development and operation of submarine propulsion reactors (Fig. 6.2) cooled by lead–bismuth eutectic. Eight submarines with lead–bismuth reactors were constructed in the USSR.

FIG. 6.2. The USSR's Alfa Class (Project 705) submarine at sea.

Detailed information on the results of Russian lead–bismuth testing is published in the literature. The first vessel was decommissioned in 1987, with four more by 1992. At least one vessel was refitted with a PWR and used for training. Reactors were comparatively low temperature designs with high enriched uranium and a long core lifetime (up to 15 years).

One of the difficulties of reactor plant servicing and refuelling at the submarine bases was the need for continuous steam ingress into the steam heating system of the primary circuit in order to provide the liquid form of coolant, and the need to periodically join up the reactor with the base installation to perform the maintenance work on the coolant circuits. In the course of operation of reactor plants with lead–bismuth reactors, there were accidents on three units that resulted in the early termination of the programme.

6.1.1. Water–steam leaks into heavy coolant

In the first lead–bismuth cooled reactor plant, the formation of deposits of heavy metal oxide and other impurities posed problems. As was understood from the first reactor operating experience, an uncontrollable accumulation of significant masses of oxides in the primary circuit could occur when the pipelines of the primary circuit gas system were depressurized and thus the air penetrated into the primary circuit. Moreover, the primary circuit was contaminated by the products of the pyrolysis of the oil used as a lubricant for the pump shaft seal.

When the SG leakage occurred and increased suddenly (it had started some time before the accident), the oxides accumulated and other impurities filled the core, which was the cause of the violent deterioration of heat removal. A negative temperature reactivity effect was the cause of transfer of the automatic power control rod to the upper switch terminal and spontaneous power reduction to 7% of rated value. This was the first symptom of the accident that happened in May 1968.

However, operational documentation did not include any necessary instructions for the operator regarding how to act when that kind of situation arose. Instead of resetting the emergency protection at the left side reactor, the operator followed the commander's directions (it occurred in the course of naval training) and tried to maintain the given power level by continuous removal of shim control rods out of the core.

All reactivity reserve for 12 safety control rods was released in about 30 min, although it was intended to provide power generation for about 4000 efficient hours. When the safety control rods were pulled out, the fuel in the core area, where heat removal had deteriorated, melted and left the core together with the coolant flow. Radiation hazard alarms in the compartment signalling the need to shut down the reactor and remove the crew were located far from the reactor and were not taken into account.

After this accident, the work on the coolant technology problem was launched. For many years, this work was carried out at a number of organizations under the scientific supervision of the Russian Institute of Physics and Power Engineering. As a result, the problem was solved and the solution has been corroborated by the many years of experience of further nuclear steam supply system (NSSS) operation.

The following main technical measures have been developed for eliminating the causes of such accidents:

— To eliminate the accumulation of oxides, excess inert gas pressure was maintained in the primary gas system during equipment repair and reactor refuelling.
— To eliminate the possibility of air penetration into the primary circuit and radioactivity release to the environment, the primary circuit has been made leaktight. For this purpose, special repair and refuelling equipment has been developed.
— Thermodynamic oxygen activity sensors enabling control of the content of oxygen dissolved in LBC and detection of alloy oxidation at the very early stages have been designed and introduced.
— The use of oil seals for the pump shafts has been rejected and water seals or gas-tight electric drives for the primary pumps have been adopted. This eliminates oil penetration into the primary circuit and contamination of lead–bismuth by the products of oil pyrolysis.
— Use of an ejection system for high temperature hydrogen regeneration (built into the NSSS) to ensure chemical recovery of the lead oxides by hydrogen (the explosion proof compound of helium and hydrogen is used) enables purification of even strongly contaminated circuits from lead oxides.
— Use of a continuously operated system of coolant purification from irreducible impurities on the glass fabric filters.
— Use of an automatic system of coolant quality control (equipped with sensors of continuous control of coolant and cover gas quality) ensures preservation of oxide films on the surface of the primary circuit structural materials, contacting with the coolant, eliminates their corrosion deterioration, and ensures the early diagnostics of the abnormal conditions.

6.1.2. Coolant leaks caused by damage to the primary pipelines

Since the beginning of the NSSS tests in 1970 and further operations in 1971 and 1972, the operation has been accompanied by a higher content of moisture in the air of the compartment where the reactor was installed. Tests showed that the causes of moisture content increase were poor air-tightness of the seal of one SG cover

because of a flaw in the nickel gasket (which was later replaced) and a steam leak through the steam heating system welds, which were made unsoundly, with no possibility to eliminate this leakage because of tight assembly.

As a result of cold surface sweating inside the compartment, water drops caused the wetting of the thermal insulation and 'dry' protection materials containing chlorides. The drops of water saturated with chlorides touched the primary circuit hot auxiliary pipelines made of austenitic steel and gave rise to their corrosion cracking on the outer surface, as has been fully verified by the results of the reactor plant inspection performed.

Corrosion damage of the primary circuit auxiliary pipelines at two of three loops and the impossibility of their repair because of compact assembly led to the decision to remove this unit from use and to carry out the NSSS inspection. The engineering measures eliminating the causes of such accidents are described below.

In the designed advanced plant, a pool type primary circuit arrangement has been used. This fully eliminates any primary circuit pipelines extending from the unit vessel, including comparatively thin wall auxiliary pipelines of small diameter, and no valves. Therefore, a ramified steam heating system was eliminated. Manufacturing the power plant monoblock unit under the plant conditions ensured high quality and delivery of the reactor unit available for operation. The integral (pool) arrangement almost completely eliminated the possibility of coolant leakage.

6.1.3. Coolant leaks owing to corrosion damage of the steam generator

Global corrosion damage of the evaporator section tubes made of perlitic steel occurred as a result of disregard of requirements concerning the water–chemical regime for SG feedwater. Under real operating conditions, the means of reducing oxygen content in the feedwater by electron ion exchanging filter with copper-containing charge, provided for in the design, caused copper release to the secondary circuit that resulted in severe electrochemical corrosion of the piping system of the evaporator sections.

As a result of punctures in the piping, steam from the secondary circuit began to penetrate into the primary circuit, where, after separation from the coolant, it condensed in the emergency condenser specially provided in the gas system for the case of leakage in the SG. As the emergency condenser's internal cavity had been filled, step by step, with the condensate, a signal was given to the operator, who repeatedly drained the emergency condenser by removing the accumulated condensate to the appropriate reservoir, thus eliminating the essential pressure increase in the primary circuit gas system.

However, the emergency condenser drainage was stopped for reasons that were unclear. The heat transfer surface of the condenser was completely flooded by water, and the condensation of the penetrating steam stopped. The pressure began to increase in the primary gas system. The gas system and primary circuit were able to bear the full working pressure of the secondary circuit. This is why, in that case, there could not be any loss of integrity of the primary circuit.

The gas pocket in the leakage re-injection pump (LRP) located in the pump tank below the coolant level had an adjustable manometer with an ultimate pressure of 4 kg/cm^2. According to the instructions, if the reactor plants were in operation, this manometer had to be shut off using the valve. This requirement was violated, and the valve was open. For this reason, when steam pressure in the gas pocket of the LRP tank reached ~6 kg/cm^2, and the coolant level in the internal pocket of the LRP increased with the increase of gas pressure, the sensitive manometer element was destroyed and gas escaped from the pump pocket. This caused the LRP gas pocket to be filled up with lead–bismuth alloy, which then leaked through the damaged manometer into the inhabited section of the reactor compartment (Fig. 6.3).

Air contamination by ^{210}Po aerosols reached ten times the maximum allowable concentration. Due to the appropriate corrective actions, the crew irradiation and radioactive contamination were within the permissible limits. The analyses of crew bio-samples performed by the medical service demonstrated that none of the crew had a content of ^{210}Po more than 10% of the maximum permissible value.

The reactor installation examination showed that it could be reconditioned. However, it was decided to replace the whole reactor compartment of this unit with a new one manufactured earlier. This decision was taken because in the course of fabricating the reactor, piping that was to be made of high nickel, corrosion resistant steel was replaced with the same size piping made of common stainless steel. This error was found out after the plant had been fabricated, and it was impossible to change the piping. Since the service lifetime of the stainless steel piping was restricted by corrosion, a decision was made to limit the service lifetime of the reactor unit by 25 000 h and to fabricate a reserve reactor unit in order to use it for the replacement of the off-specification unit in

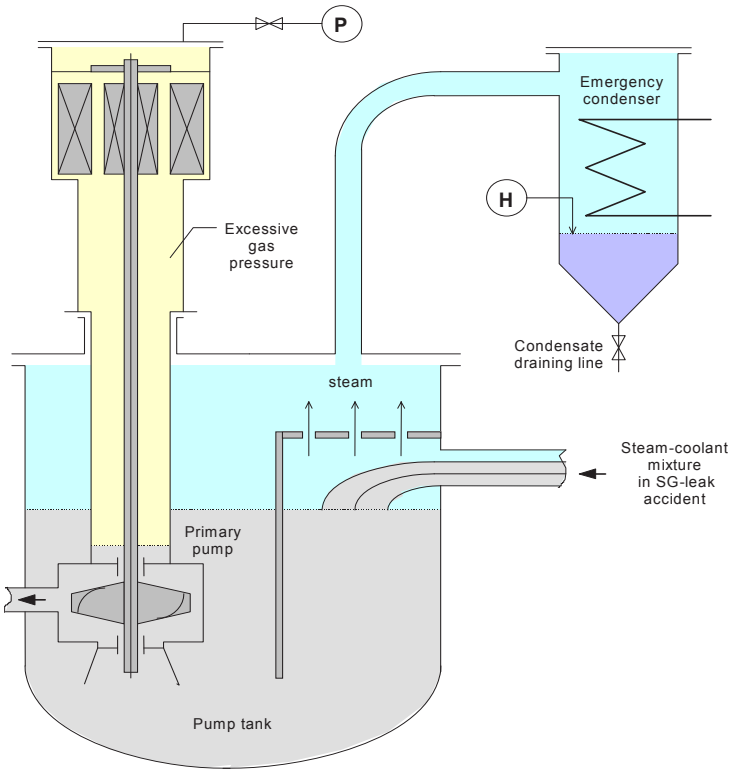

FIG. 6.3. Primary pump with auxiliary system: flow diagram [6.2].

the course of the submarine overhaul period. In 1982, the service life of the stainless steel piping expired, which was the motive for replacing the whole reactor compartment. The analysis performed showed that the cause of the accident discussed in the previous section did not relate to the use of lead–bismuth. The following technical measures ensure the elimination of such accidents in new generation plants:

— Elimination of use of copper-containing materials in the water–steam circuit;
— Preferable use of corrosion resistant steel for SG water–steam tubes instead of low alloyed perlitic steel;
— Provision of passive drainage of the emergency condenser when filled up by the condensate to the given level;
— Uniting gas volume inside the pump electric motor with the total gas volume above the free coolant surface;
— Provision of a greater extent of plant maintainability.

In summary, the following characteristics were ascertained in the course of reactor plant tests and operation: power parameters of installation, core lifetime, reactivity margin, reactivity coefficients, poisoning effects, temperature distribution, dynamic parameters, coolant radioactivity, and dose rates caused by neutron and γ radiation behind the shield. The data were in reasonably good agreement with calculation results.

Among the positive properties of the reactor plant using heavy coolant that have been discovered in the course of operation are the following: the simplicity of control, high manoeuvrability and short time required to reach the power regime from the sub-critical reactor state, the possibility of power plant operation even if there is small leakage in the SG pipe system, high repair fitness of the SG by plugging the depressurized pipes, the possibility of stable reactor plant operation at any low power level, the possibility of quickly changing the circulation regime of coolant with an essential change of its flow rate, and almost complete generation of designed power by cores under normal and acceptable conditions of tightness of fuel rod cladding.

In the early stages of development, the formation of deposits of heavy metal oxide and other impurities posed problems. Careful control of coolant purity is required to avoid the formation of such deposits. It was necessary to improve corrosion resistant steels and to pretreat the surface of the components, and also to use special inhibitors in the lead–bismuth coolant.

Lead–bismuth alloy is inflammable in either air or water. In principle, a lead–bismuth cooled reactor would not have to have an intermediate circuit separating the primary coolant and water–steam. However, as is mentioned above, there have been incidents with lead–bismuth cooled reactors. Some areas of the reactor core were plugged by lead oxides and other impurities as well as by the products of water and lead–bismuth interaction due to SG leaks, causing meltdown of the core. Therefore, the elimination of the intermediate circuit requires additional R&D efforts.

The design and operating experience of the propulsion NSSS using lead–bismuth coolant has been used to develop the SVBR-75/100 reactor design.

6.2. ADVANCED POWER PLANT SVBR-75/100 WITH LEAD–BISMUTH COOLANT

The principal technical parameters of NSSS SVBR-75 are presented in Table 6.1.

TABLE 6.1. PRINCIPAL TECHNICAL PARAMETERS OF NSSS SVBR-75 [6.3]

Item	Value
Rated heat power, MW(th)	268
Electric power, MW(e)	75
Steam capacity, t/h	487
Steam pressure, MPa/temperature,°C	3.24/238
Feed water temperature, °C	192
Primary coolant flow rate, kg/s	11 180
Primary coolant core outlet/inlet temperature, °C	439/275
Core dimensions, D × H, m	1.65 × 0.9
Average value of fuel element linear power, kW/m	~22
Fuel: ^{235}U inventory, kg Average ^{235}U-enrichment, %	UO_2 1476 15.6
Steam generator (SG) number	2
Evaporator numbers in SG	6
Evaporator dimensions D × H, m	~0.6 × 4
Number of primary main pumps (PCMPs)	2
Pump electric driver power rate, kW	400
Pump head, MPa	~0.5
Primary circuit coolant volume, m^3	18
Reactor vessel dimensions, D × H, m	4.53 × 6.92

The design of the SVBR-75 (Svinets (lead)–Vismut (bismuth) Bystryi (fast) Reactor) with a power output of 75 MW(e) has a two circuit arrangement with lead–bismuth in the primary circuit and steam–water in the secondary circuit. The integral (pool type) design is used for the reactor plant (Fig. 6.4). This enables the primary circuit components to be mounted inside one vessel.

The SVBR-75 reactor plant includes a removable part with the core, 12 SG modules with forced circulation in the primary circuit and natural circulation in the secondary circuit, two main circulation pumps for coolant circulation in the primary circuit, devices for controlling lead–bismuth quality, an in-vessel radiation protection system and buffer reservoir, which are part of the main circuit.

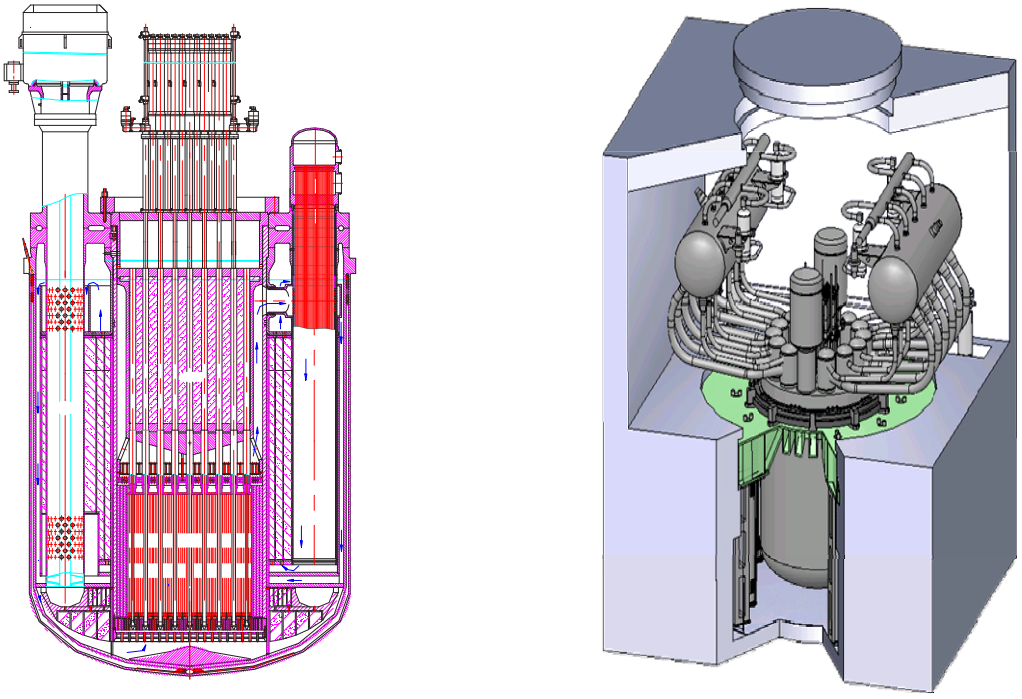

FIG. 6.4. Reactor and NSSS SVBR 75/100 [6.3, 6.4].

The adopted flow path, with free levels of lead–bismuth existing in the monoblock upper part and SG module channels contacting cover gas, ensures reliable separation of the steam–water mixture from the coolant flow should an accidental integrity loss of the SG tube system occur, and the presence of a gas medium ensures the possibility of coolant temperature change.

The monoblock is placed and mounted in the tank. The tank is filled with water and designed for cooling reactor installation in the case of a beyond design basis accident. The gap between the main vessel and the protective vessel is chosen to ensure the circuit 'rupture' in the case of accidents related to the loss of the monoblock main vessel integrity.

Coolant heated in the core flows through the windows of the reactor outlet chamber to the inlet of 12 SG modules connected in parallel. It flows downwards, being cooled on the shell side of modules. Then the coolant enters the intermediate chamber, from which it flows to the channels of the in-vessel shielding, removing its heat. The coolant enters the monoblock upper part and forms the free level of 'cold' coolant (peripheral buffer chamber). Then the coolant flows to the pump suction inlet.

The secondary system is designed to operate the SG, producing saturated steam with multiple natural flows through the evaporator–separator, as well as to provide scheduled and emergency reactor plant cooling by the SG.

The SVBR-75 reactor plant is designed to operate for eight years without core refuelling. In the initial stage, uranium oxide fuel mastered in the uranium fuel cycle is provided. Further, the use of high density uranium and plutonium nitride fuel is possible. In this case, the core breeding ratio is 1.0 and in the plutonium closed fuel cycle the reactor would operate using only depleted waste pile uranium [6.1–6.5].

REFERENCES TO CHAPTER 6

[6.1] LEVY, S., "Sodium fast reactors (SFRs) and recyclers", Proc. of the International Congress on Advanced Nuclear Power Plants, ICAPP '08, Anaheim, CA, USA, 8–12 June 2008.

[6.2] GROMOV, B.F., SUBBOTIN, V.I., TOSHINSKY, G.I., "Application of Lead-Bismuth eutectic and Lead melts as nuclear power plant coolant", Atomnaya Energiya, **73** 1 (1992) 19 (in Russian).

[6.3] INTERNATIONAL ATOMIC ENERGY AGENCY, Fast Reactor Database: 2006 Update, IAEA-TECDOC-1530, IAEA, Vienna (2006).

[6.4] INTERNATIONAL ATOMIC ENERGY AGENCY, Comparative Assessment of Thermophysical and Thermohydraulic Characteristics of Lead, Lead–Bismuth and Sodium Coolants for Fast Reactors, IAEA-TECDOC-1289, IAEA, Vienna (2002).
[6.5] INTERNATIONAL ATOMIC ENERGY AGENCY, Small Power and Heat Generation Systems on the Basis of Propulsion and Innovative Reactor Technologies, IAEA-TECDOC-1172, IAEA, Vienna (2000).

7. IMPORTANT ISSUES OF SODIUM AND HEAVY METAL COOLANT TECHNOLOGY

7.1. SODIUM PURIFICATION, IMPURITY SOURCES AND MONITORING

Sodium of high purity has a lower corrosion effect on the materials used in the primary coolant system. The sodium purification system should maintain the sodium oxide content at or below the prescribed value.

A comparatively large number of impurities are present in liquid metals as trace quantities only and are, therefore, of little consequence to the design of the coolant system of a fast reactor. Nevertheless, the designer should include in the specifications limits on the allowable concentration of those impurities that may be deleterious to the system or that may affect the nuclear control characteristics of the reactor.

Among the permanent contributors of impurities under normal operating conditions are corrosion related hydrogen from SGs, tritium from the reactor core, oxygen and hydrogen from the cover gas and corrosion products. Sources of impurities in liquid sodium determined in the BN-350 and BN-600 reactors under operating conditions are shown in Table 7.1 [7.1, 7.2].

TABLE 7.1. SOURCES OF IMPURITIES IN LIQUID SODIUM

Sources	Oxygen	Water, kg/year	Hydrogen	Corrosion products, kg/year	Tritium from the core, g/h
Cover gas	1 kg/year[a]	0.1 – 0.5	(3÷6) 10^{-2} g/h[b]	20[b]	6.3×10^{-5}[a]
Repair works	6 kg/year[a]	0.6	0.5–1 g/h[b]	60[a]	
Steel (Cr18Ni10Ti)	0.01 g/m^2	—	4.4×10^{-3} g/kg		
Steel (11/4 Cr2Mo)	0.01 g/m^2	—	6.4×10^{-3} g/kg		

[a] BN-600 reactor.
[b] BN-350 reactor [7.2].

They have the following characteristics:

(1) Initial impurity content due to oxygen absorption on the circuit surface is 3.4 g/m^2 (primary circuit) and 2.2 g/m^2 (secondary circuit); this is in a good agreement with the experimental data (1.4–2.4 g/m^2). The total amount of oxygen absorbed is about 30 kg.
(2) Impurities introduced during repair operation are Na_2O, NaOH and Na_2CO_3. Assessments have shown that during operation (20 years) about 200 kg of the aforementioned substances is introduced [7.1, 7.2].
(3) Impurities added during subassembly loading. Assuming 2 g/m^2 specific content, the total amount is equal to about 200 kg.
(4) Impurities caused by diffusion from other sources. Diffusion rate is evaluated to be about 50 g O_2/d. The total amount of impurities is about 720 kg. The primary and secondary circuit sodium must be continuously purified to impurity levels such as:

Oxygen <5 ppm;
Hydrogen <0.5 ppm;
Carbon <10 ppm.

Such low impurity levels are necessary to minimize corrosion and mass transport effects and to avoid sodium plugging while flowing through the small holes in the core or coolant circuits. Purification is achieved by operating cold traps and plugging meters in a bypass of the main circuits.

The principal objective of the purification system is to maintain the coolant relatively free from chemical and radioactive contaminants. The function of the impurity monitoring system is to measure the existing amount of contamination. Several elements contained in core structural materials are continuously dissolved by the liquid sodium. In addition, oxygen (usually as sodium oxide), carbon, hydrogen and nitrogen are always present.

Different equipment is used for purification and for control procedures; the most important items are the following:

— Filters can be used for gross purification between the storage/drain tank and the sodium system. Usually, stainless steel microfilters are used and sodium is cooled below the oxide saturation temperature to remove precipitated solids. Problems arise from the tendency of the filters to plug. Therefore removable filters should be designed to allow for periodic cleaning.
— Plugging indicators (control of initial temperature of impurity crystallization) are used for the determination of the oxygen content in the coolant. This is an in-line device with which the saturation temperature can be determined by lowering the sodium temperature until sodium oxide is precipitated and plugs the flow rate by a break. Super-saturation is achieved by decreasing the temperature of the coolant flowing through the indicator.
— As the temperature becomes lower than the saturation point, the flow rate through the indicator decreases, this being registered by the indicator. Actually, the indicator measures the temperature at which the rate of impurity deposition or solubility is sufficient to detect a change in the flow rate. The presence of different impurities in the coolant makes it possible to detect several 'plugging temperature' values. It should be noted that saturation temperature is determined within an accuracy of about 3°C. The principle of the function can be seen from Fig. 7.1. Oxygen contents ranging from 10 to 200 ppm can be determined by this device.
— Cold traps are the most commonly used device for removing impurities. Cold traps are crystallizers or precipitating chambers connected to a bypass line of the main circuit. In this bypass the temperature is kept significantly below the saturation temperature of sodium oxide or other impurities (below 150°C). A requirement for design is that the cold trap must provide sufficient surface area for grain growth of the material being removed. It must have sufficient capacity for the volume of expected impurities and sufficient residence time for precipitation. Cold traps are designed to operate with either natural or forced circulation. An important feature in some cold trap systems is an economizer. This is a heat exchanger in which the hot sodium entering into the trap is cooled by reheating the cold sodium leaving the trap to return to the main stream. Figure 7.2 shows a typical sodium cold trap.
— At the present time, the sodium purification technique with the use of cold traps based on decreasing solubility of the majority of impurities in sodium with temperature decrease has found the most widespread practical application [7.3, 7.4]. In the cold trap, sodium is cooled within the settling tank and the section upstream of the filter. This results in reduction of oxygen and hydrogen concentrations to 1 and 0.05 ppm, respectively. A cold trap is capable of retaining impurities in amounts up to ~30% of its volume [7.5].
— A fraction of the coolant flow, often ~5%, is circulated through the cold trap, which is typically operated in the range of 120–135°C with the intent of keeping oxygen below ~10 ppm. The cold trap precipitates oxygen impurities as Na_2O, hydrogen as NaH, and other species as well such as Fe, Cr, N, C, etc.
— Carbon is confined in the cold trap as suspension, the purification process being ten times longer than that for oxygen. In order to trap caesium, a graphite based purification technique was developed [7.6, 7.7]. After ten years of operation of the BN-350 reactor, the capacity of the secondary traps was exhausted and their hydrogenation was carried out. The basic amount of sodium transformed to caustic phase was removed at 420°C. Thus, normal operation of traps was restored [7.3].
— Before the primary coolant system is filled, the sodium charge is purified by circulating the sodium through the cold trap system.
— Hot traps are used to getter contaminants which are not or are only partly removed by cold traps, i.e. oxygen and carbon. Oxygen hot traps use the selective absorption of oxygen on a high temperature zirconium surface. This gettering process is temperature dependent; typical operating conditions of oxygen hot traps are between 700 and 900°C. The carbon hot traps are similar to the oxide type; the main difference is the packing material, which is stainless steel. Operating temperatures of carbon hot traps are in the range of 900–1050°C.
— Argon and in some cases also helium are used as cover gas in LMFRs. Impurities such as oxygen, hydrogen, nitrogen, and carbon in the cover gas are not to exceed certain upper limits. Therefore, the impurity level is continuously verified by gas chromatography. If the impurity level exceeds the upper limits, or if the cover

gas contains too high a content of gases, it can be purified by filling in clean argon and releasing the waste argon into a cover gas waste tank. There, any radioactivity (e.g. $^{133, 135}$Xe and $^{85, 87, 88}$Kr, the short term total activity of which reached 6.7×10^9 Bq/L in the BN-600 reactor) can decay, and, after a sufficient time, the waste argon can be released to the environment after having been passed through special filters with activated coal as an absorbent [7.1, 7.3].

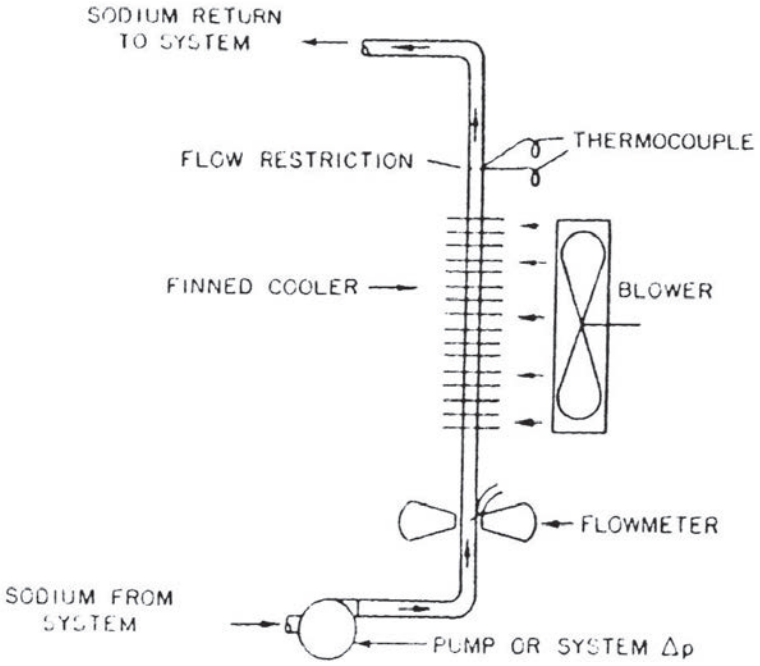

FIG. 7.1. Plugging indicator.

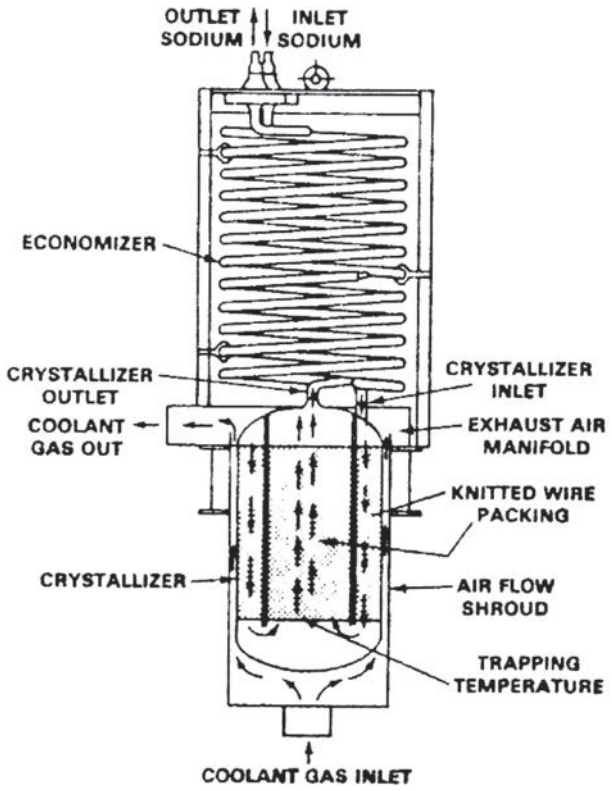

FIG. 7.2. Cold trap.

7.2. SODIUM AND COVER GAS: CONTROL OF IMPURITIES CONTENT

Monitoring the content of non-metal impurities in the coolant (O_2, H_2 and C) and cover gas (H_2O, CH_4 and N_2), as well as ^{90}Sr, ^{131}J, ^{137}Cs, ^{54}Mn and $^{58, 60}Co$ in the primary circuit is most important [7.1].

7.2.1. Oxygen monitoring

Oxygen is usually present in liquid sodium as sodium oxide. In order to make measurements of oxygen activity in sodium, the electrochemical control technique based on a galvanic cell has been mastered with sodium flowing over an electrolytic pellet of thorium and yttrium sealed into the metal tube. The reference electrode is located inside the tube. The electromagnetic force (EMF) generated depends on the temperature and oxygen concentration: EMF = f (T, CO_2). The service life of such a device is over 10^4 h.

7.2.2. Hydrogen monitoring

The need for hydrogen monitoring was caused by the need for detection of water leaks into sodium resulting in the following reaction:

$$Na + H_2O \rightarrow Na_2O + H_2$$

The diffusion technique that has found the widest application is the method using metal membrane permeable to hydrogen in combination with different secondary devices (mass spectrometer, magnetic discharge pump, etc.). The flow rate of hydrogen passing through the nickel membrane into a vacuum cavity is measured by the system equipped with a magnetic discharge pump, where gas ionization takes place. The automatic hydrogen detector is capable of detecting a 10–30 g water leak to 100 t of secondary sodium. A description of other techniques can be found in Ref. [7.3].

7.2.3. Carbon monitoring

Carbon needs to be controlled for evaluating carburization of structural materials because of the possible impact on their mechanical properties. Diffusion and electrochemical cells similar to those mentioned above are used for carbon control, with the salt mixtures Na_2CO_3–Li_2CO_3 and CaC_2–LiCl used as electrolytes.

7.3. BASIC ISSUES OF HEAVY COOLANT TECHNOLOGY

The basic technological challenge of using lead as a reactor coolant is ensuring that the quality of the coolant (as well as that of the surfaces contacting coolant) is such that the following conditions are realized:

— Sufficient corrosion resistance of structural materials;
— Stable hydrodynamics and heat transfer during lifetime.

The presence of impurities in the lead coolant is problematic for at least two reasons, namely:

— Possible partial or total plugging of the coolant flow cross-section area that disturbs the hydrodynamics and hence heat transfer;
— Formation of deposits on the heat transfer surfaces (especially on the fuel elements of the reactor core causing rise of cladding temperature).

7.3.1. Heavy coolant impurity contributors

The following impurities are present at the initial stage of circuit filling [7.1]:

— Residual oxygen and water vapours remaining after evacuation;
— Gas adsorbed on the inner surfaces;
— Steel corrosion products;
— Casual impurities (chip, welding hail, etc.).

Under operating conditions, the basic factors causing an increase of impurity contents in the lead circuit are:

— Structural material corrosion;
— Erosion and abrasion of materials;
— Penetration of grease from pump seals and bearings;
— Cover gas entrainment by the coolant;
— Admixtures to the coolant aimed at forming protective films.

Impurities can be located in such parts of the circuit as cover gas plenum and stagnant sections, as well as on the free surface of molten lead (since the density of practically all impurities is lower than that of lead) and structures (as deposits). During facility operation the impurities are transported along the circuit. The methods of impurity control in lead and cover gas are shown in Table 7.2.

TABLE 7.2. METHODS OF IMPURITY CONTROL IN LEAD AND COVER GAS

Impurities	Methods of monitoring
Water vapour in cover gas	(1) Condensation of vapour from cover gas (2) Permanent chromatography control of cover gas
Hydrogen in cover gas	Measurement of hydrogen content in cover gas: – Thermal conductivity method – Chromatography
Oxygen in lead	Galvanic cell (measurement of EMF induced in solid electrolyte with ion conductivity)

7.3.2. Heavy coolant cleaning from slag

Oxide based slag (PbO) can be removed from the coolant by settling and reducing with hydrogen. Slag originating from dispersed impurities, caused by lead interaction with structural materials (Fe, Cr and Ni), is removed by mechanical filter or by settling. Oil and pyrolysis products can be removed using organic solvents or water vapour injected into the circuit.

It has been observed that an unusual property of lead–bismuth eutectic (LBE) is that it has virtually zero volumetric change going through the freezing or melting transition. This could be an important advantage of this coolant for some applications where melting/freezing transitions are unavoidable or where it is not possible to apply the normal rules of freezing to a free surface and melting from a free surface [7.1].

7.3.3. Heavy coolant freezing

One of the most dangerous events resulting in coolant freezing is secondary steam header depressurization. The rarefaction wave propagates at sound velocity in the secondary circuit in the initial stage of such an accident [7.8].

Secondary circuit water boiling and an abrupt increase of heat removal from the primary coolant occur, probably resulting in its freezing. Steam turbine drive of the feedwater pump and bypass pipelines connecting the SG inlet and steam header through orifices are provided in the secondary circuit to decrease the consequences of such accidents.

Engineering features are provided in the reactor design to prevent lead freezing due to malfunctions or human errors in the startup and transient modes.

The relatively low melting temperature of LBE (125°C) required that research be carried out on the primary circuit components and reactor as a whole in the case of a change of phase state of the coolant under conditions of accident or scheduled cooling down and the posterior primary circuit heating up ('freezing' and 'unfreezing' conditions).

Research has been carried out at the Russian Institute of Physics and Power Engineering on the change in LBE density within the limits of possible deviation from eutectic within the temperature interval from –50°C to +130°C. It has been demonstrated, in particular, that in the case of a lead content deviation of +5% from that of the eutectic composition, the volumetric effect of fusion neither varies significantly nor deviates from the corresponding value for eutectic by more than +0.17%.

The experimental studies have shown that due to the limited solubility of components in the solid state, lead–bismuth alloy is subject to phase structural transformations, in the course of which its properties change. It has turned out that it is possible to describe these changes using kinetic relationships that have been determined for the most significant properties such as density, elasticity and creep.

Experimental studies of features of the alloy–structure interaction were carried out by tests of mock-ups, models and real primary components. Fuel subassemblies, control and safety system components, primary pumps, SGs, sections of main and auxiliary pipelines and their valves have been tested. In the course of tests, requirements have been worked out for the temperature conditions of the heating up and cooling down modes, as well as for separate structures designed for avoiding damage at multiple condition changes.

On the basis of experimental and analytical studies, algorithms have been developed to implement the required conditions at particular plants.

The research work carried out and the experience gained in the field of realizing freezing–unfreezing conditions facilitate solution of the problem of different types of plant to be applied for various purposes and to realize the conditions repeatedly according to the schedule.

7.3.4. Lead–bismuth purification from polonium

Some studies in this field have been carried out at the Russian Institute of Physics and Power Engineering in Obninsk, Russian Federation. In particular, the possibility of polonium alkaline extraction from lead–bismuth was studied, with a coolant flow rate of ~0.1% being sufficient to decrease the polonium activity in the circuit by over four orders of magnitude and transform extracted polonium into non-volatile compounds. Periodic polonium removal from the circuit is possible, for example, before a scheduled repair.

Where polonium is present it is important to assess the evaporation rate of the media. Polonium can be either in elementary form or in chemical compounds such as oxide (Po-O), inter-metalloid (PbPo), hydride (Po-H), etc. The evaporation rate depends on the composition, its temperature, density, gas content and other parameters. The rate of evaporation into vacuum follows the Lenghmure law:

$$G_o = kP\sqrt{M/T}$$

where P is pressure, k = 0.0044, M is molecular mass and T is temperature. If the substance is in a solution, the evaporation rate is proportional to the mole part *m*:

$$G=mG$$

Experiments [7.9, 7.10] on polonium evaporation from eutectic polonium–lithium have shown that within the 300–800°C temperature range, evaporation rate of polonium into vacuum is 10^3 times lower than that of elementary polonium. Inert gas atmosphere (Ar, Ne) reduces the evaporation rate by 10^3 times more. Similar data were obtained in experiments on polonium evaporation from lead–bismuth [7.1, 7.11].

Thus, polonium may be thought of as evaporated from lead–bismuth in the form of PbPo or BiPo. Saturation pressure for polonium vapour follows the relationship:

$$lgP = 6.94 - (7270/T)$$

Calculations made using the relationships presented give the following polonium yield rates:

— From PbBi with activity of 1.85×10^{13} Bq/L at 300°C: 6.7×10^5 Bq/kg;
— From Pb with activity of 1.85×10^{10} Bq/L at 500°C: 1.15×10^6 Bq/kg.

Although Po activity in lead is 1000 times lower than that in PbBi, polonium yield from lead is approximately the same due to higher temperature.

7.3.5. Polonium and reactor engineering

In Refs [7.11, 7.12], the general conclusion was reached that ^{210}Po activity cannot be considered as the main barrier preventing the use of lead–bismuth coolant. The conclusion was mainly based on the operating experience of nuclear power plants, nuclear submarines and their ground based prototypes. Some data on an accident with a lead–bismuth cooled submarine reactor are presented in Ref. [7.13].

Experience gained on LOCA studies has shown that application of protective coating makes it possible to confine polonium by preventing its release to the environment. This coating effect is based on sorption and dissolution of impurities in dispersed medium and fixing in the coating.

In the case of SG tube failure and depressurization of the secondary circuit, lead–bismuth alloy can find its way into the secondary circuit and water can be contaminated by polonium. In this case, a basic amount of polonium is kept in the alloy, condensate saturation activity of $10 \div 10^4$ Bq/kg is reached, and SG inner surfaces become contaminated owing to polonium sorption from the water. Water evaporation determines the radioactivity level in the turbine hall.

Contamination of the inner surface of the secondary circuit gives rise to danger in the case of equipment repair, since the alloy kept in the secondary circuit is a permanent source of water contamination. Water replacement and SG inner surface decontamination without any alloy removal would not give the desired result. The secondary circuit decontamination turns out to be possible only after complete removal of the alloy from the secondary circuit. Obviously, this cannot be ensured.

If SG tube failure is assumed to be possible, the alloy penetration to the secondary circuit should not be neglected. Experiments [7.11] have shown that lead–bismuth evaporation rate is within the limits given by Raoult's law. Lead contained in the air may produce the same danger for health as ^{210}Po does.

Polonium activity is one of the important operational problems in case of lead–bismuth used as a coolant.

REFERENCES TO CHAPTER 7

[7.1] INTERNATIONAL ATOMIC ENERGY AGENCY, Comparative Assessment of Thermophysical and Thermohydraulics of Lead, Lead–Bismuth and Sodium Coolants for Fast Reactors, IAEA-TECDOC-1289, IAEA, Vienna (2002).
[7.2] KOZLOV, F.A., IVANENKO, V.N., Atomnaja Energia, **80** 5 (1996) 337–345.
[7.3] BAKLUSCHIN, R.P., KOZLOV, F.A., Atomnaja Energia, **44** 3 (1978)224–228.
[7.4] KOZLOV, F.A., et al., "Liquid Metal Coolants for NPP: Purification and Control", Moscow, Energoatomizdat (1983).
[7.5] KOZLOV, F.A., KARABASCH, A.G., BOGDANOVITCH, N.G., "Sodium Technology for NPP", Report on the Meeting "Chemistry of Sodium", Dimitrovgrad, March (1989).
[7.6] SARAEV, O.M., et al., Atomnaja Energia **80** 5 (1996) 330–337.
[7.7] POLYAKOV, V.I., CHECHETKIN, Yu.V., Atomnaja Energia **38** 3 (1975) 171–172.
[7.8] KAZACHKOVSKIY, O.D., et al., Atomnaja Energia **38** 3 (1975) 131–134.
[7.9] SPENCER, B.W., "The rush to heavy liquid metal reactor coolants-gimmick or reasoned", Proc. of ICONE-8th International Conference on Nuclear Engineering, 2-6 April 2000, Baltimore, MD, USA.
[7.10] FEUERSTEIN, H., et al., Fusion Eng. Design **17** (1991) 203–207.
[7.11] FEUERSTEIN, H., et al., J Nucl. Mat. **191–194** (1992) 288–291.

[7.12] GROMOV, B.F., et al., Proc. ARS'94 Int. Topical Meeting on Adv. Reactor Safety, Pittsburgh, USA, 17–21 April 1994, Vol. 1, 530–537.
[7.13] PANKRATOV, V.D., et al., paper presented at Conf. on Heavy Liquid Metal Coolant, Obninsk, 5–9 October (1998).

8. CONCUSIONS

(1) The operation of experimental facilities and fast reactors has demonstrated that breeding is a technically achievable objective and that the use of liquid–metal coolant (sodium, sodium–potassium) is compatible with breeding economy and is metallurgically and mechanically feasible.

After capsule failure and the plutonium–iron fuel entered into the coolant in the LAMPRE facility, the liquid plutonium fuel programme was cancelled by the US Government in 1965 in view of the foreseeable breakthrough of MOX fast reactor fuel.

One of the notable achievements of the Clementine facility included measurements for the total neutron cross-sections of 41 elements to a 10% accuracy. Additionally, Clementine provided invaluable experience in the control of fast neutron reactors. It was also determined that mercury was not an ideal cooling medium for this type of reactor due to its poor heat transfer characteristics and other concerns.

Using experimental fast reactors, measurements were made of the critical mass, effectiveness of reactor control, temperature coefficient, neutron spectrum and general behaviour. The information obtained was valuable in establishing the feasibility of fast reactor operation, including the demonstration of control by delayed neutrons.

In September 1967, a foreign body was indicated in the EFFBR core inlet plenum which had blocked the coolant flow in several fuel channels and thus caused damage to six fuel subassemblies within the core. The blockage and melting of some of the fuel subassemblies revealed a design shortage — the axial coolant inlet port in the nozzle of the fuel subassembly.

(2) Sodium production meeting reactor standard requirements was developed and mastered in industry; and measuring/control instruments and devices were developed for controlling sodium quality and operational parameters required for reactor systems.

(3) For the most vulnerable element of the nuclear power plant, i.e. the SG heated by sodium, special systems were developed for detection of water to sodium leaks and protection of the SG against consequences of sodium–water reaction. Issues related to the design of pumps with bearings lubricated by the pumped liquid (sodium) were successfully solved.

(4) The complicated and labour intensive operation and maintenance technology for the repair of sodium components and the absence of a guarantee that components will function after removal of sodium residues (washing) and decontamination necessitate conducting tests of forerunners or representative models of reactor mechanisms and components on sodium facilities under designed operating conditions. All components manufactured without defects and tested have been operated in LMFRs for decades owing to the corrosion inertness of sodium and the low pressure.

(5) Serious incidents occurred during the cleaning of sodium residues from components because complete sodium draining had not been developed at the design stage. This approach was justified in the initial stage of mastering fast reactors in order to eliminate the probability of coolant leakage from the drain tanks and component vessels. The presence of non-drained cavities in the components can be explained by insufficient understanding of the problem at that stage. The accumulated technological experience provides the basis for studying the possibility of draining the tanks and the vessels of advanced reactor facilities with deterministic elimination of emergency draining by design.

(6) Excellent thermophysical properties of sodium were demonstrated at the first test facilities as early as the 1950s, and promised its large scale application in the power area. In this context, sodium's attractive properties should be recalled, namely, compatibility with traditional structural materials and all fuel compounds up to high temperatures owing to its corrosion inertness and pressure close to atmospheric value, and excellent thermohydraulic characteristics, thus ensuring effective heat removal under conditions of either nominal flow rate or natural circulation flow rate at the reactor. Therefore, on condition of proper design and manufacture of components, there are no physical factors provoking failures. Consequently, in most countries involved in fast reactor R&D activities, a sodium cooled reactor line is considered to show promise.

(7) Emergency cooling can be provided in several ways. One way is to provide a separate loop. This arrangement requires an auxiliary heat exchanger and either a gravity flow or a pumped cooling loop separate from the normal cooling loops for the plant. An intermediate coolant loop, together with a heat sink external to the

building, could be used to remove heat from the heat exchanger. Any pumps used in this scheme should be powered by a special emergency power supply with high reliability.

Another method involves auxiliary pony motors attached to the main pump shafts. These motors, connected to an emergency power supply, turn the pumps at a low speed sufficient to supply the flow needed to remove decay heat.

Finally, natural circulation can be provided, and, unless the power supply is guaranteed for the period of emergency cooling, the heat transport system should be operable by natural circulation. The proper selection of relative elevations of the reactor, the IHX and the SG ensures emergency cooling by natural circulation. Careful determination should be made of the relative elevations and the system pressure drops to be sure that the sodium will circulate under the available thermal driving head.

There are two advantages to using a separate loop to handle the decay heat:

(i) The loop is independent of normal operating requirements, allowing the normal operating loops to be designed for their main function.

(ii) The check valve for the loop can be designed for low pressure drop requirements.

There are some disadvantages to a separate loop, e.g. increased heat losses, increased number of reactor vessel nozzles, and increased costs and space requirements.

(8) The pool type design offers the following advantages:

(i) The containment system can be provided in a single large cylindrical vessel rather than in several tanks with connecting pipes.

(ii) There is only one free surface for which an inert cover gas must be provided.

(iii) The large sodium pool has a large heat capacity that serves to minimize temperature transients and is an excellent heat sink during emergency cooling.

(iv) Thermal expansion in the piping can be accommodated by leaky joints, such as slip-fit unions.

The pool type concept has the disadvantage that shielding within the primary tank becomes increasingly expensive owing to larger weight and very high requirements to surface finishes for structural materials in contact with sodium.

(9) The specific feature of lead–bismuth and lead reactor cooling are high boiling temperatures and the relative inertness to water as compared with sodium. The melting and boiling points of sodium are 98 and 883°C, respectively, at atmospheric pressure. For LBE, these values are 123.5 and 1670°C, respectively; and for lead they are 327 and 1740°C, respectively. However, the boiling points are well above cladding failure temperatures. The specific heat per unit volume of lead–bismuth and lead are similar to that of sodium, but the latent heat and conductivities are lower by about a factor of more than four to that of sodium.

Techniques to counter the heavy metal coolant disadvantages are being developed, but in spite of this work and the apparent disadvantages of sodium, the consensus in favour of sodium remains strong. In the past few years, sodium has been chosen for fast reactor development projects. This is a significant endorsement for sodium as a fast reactor coolant.

(10) Design, development and operation of experimental fast reactors led to the physical and technological substantiation of fast reactor designs (from the first experimental reactor BR-5 with plutonium oxide as a fuel and sodium as a coolant to the EFFBR semi-industrial experimental power plant). Of the numerous design developments and mastering that form the basis of the fast reactor technology and design, the cornerstones are the following:

— Liquid metal coolant: technology, thermohydraulics, and reactor core structure materials;
— System of heat removal from reactor to SG and its conversion to electric energy;
— Experience gained during the development and operation indicating that neither micro modular (EBR-I), macro modular (DFR), nor double wall (EBR-II) SGs meet all operating and economic criteria;
— Structure materials facilitating increasing fuel burnup.

(11) The fuel technology foundation for future fast reactor development (metallic fuel — EBRII; ceramics: PuO_2, (U-Pu) N, (U-Pu) C — BR-5/10 and MOX — Rapsodie) was prepared in the 20th century.

ACRONYMS

ABND	acoustic boiling noise detection
APWR	advanced pressurized water reactor
DFR	Dounreay Experimental Fast Reactor
EBR	experimental breeder reactor
EFFBR	Enrico Fermi Fast Breeder Reactor
FBR	fast breeder reactor
FBTR	fast breeder test reactor
GFR	gas cooled fast reactor
GIF	Generation IV International Forum
IHTS	intermediate heat transport system
IHX	intermediate heat exchanger
JSFR	Japan Sodium Fast Reactor
LAMPRE	Los Alamos Molten Plutonium Reactor Experiment
LMFR	liquid metal cooled fast reactor
LOHSWS	loss of heat sink without scram
LRP	leakage re-injection pump
LWR	light water reactor
MOX	mixed oxide
NSSS	nuclear steam supply system
PFBR	Prototype Fast Breeder Reactor (India)
PFR	Prototype Fast Reactor
PHTS	primary heat transport system
PIE	post-irradiation examination
RCRA	Resource Conservation and Recovery Act
RNL	Risley Nuclear Laboratories
SPP	Solar Power Plant (Spain)
SG	steam generator
SGS	steam generator system
SIR	sodium intermediate reactor
SVBR	Svinets-Vismut Bystryi Reactor
SVRE	sodium void reactivity effect
TWG-FR	Technical Working Group on Fast Reactors (IAEA)
ZPR	Zero Power Reactor

CONTRIBUTORS TO DRAFTING AND REVIEW

Ashurko, Y.	Institute of Physics and Power Engineering, Russian Federation
Astegiano, J.C.	Centre d'études de Cadarache, France
Chetal, S.C.	Indira Gandhi Center for Atomic Research, India
Fujita, E.	Argonne National Laboratory, United States of America
Hahn, D.	Korea Atomic Energy Research Institute, Republic of Korea
Monti, S.	International Atomic Energy Agency
Pryakhin, A.	International Atomic Energy Agency
Rineyskiy, A.	International Atomic Energy Agency
Stanculescu, A.	International Atomic Energy Agency
Stogov, V.	Institute of Physics and Power Engineering, Russian Federation
Toti, A.	International Atomic Energy Agency
Yamaguchi, K.	Japan Nuclear Cycle Development Institute, Japan
Yarovitsin, V.	Institute of Physics and Power Engineering, Russian Federation
Zhang, D.	China Institute of Atomic Energy, China

Structure of the IAEA Nuclear Energy Series

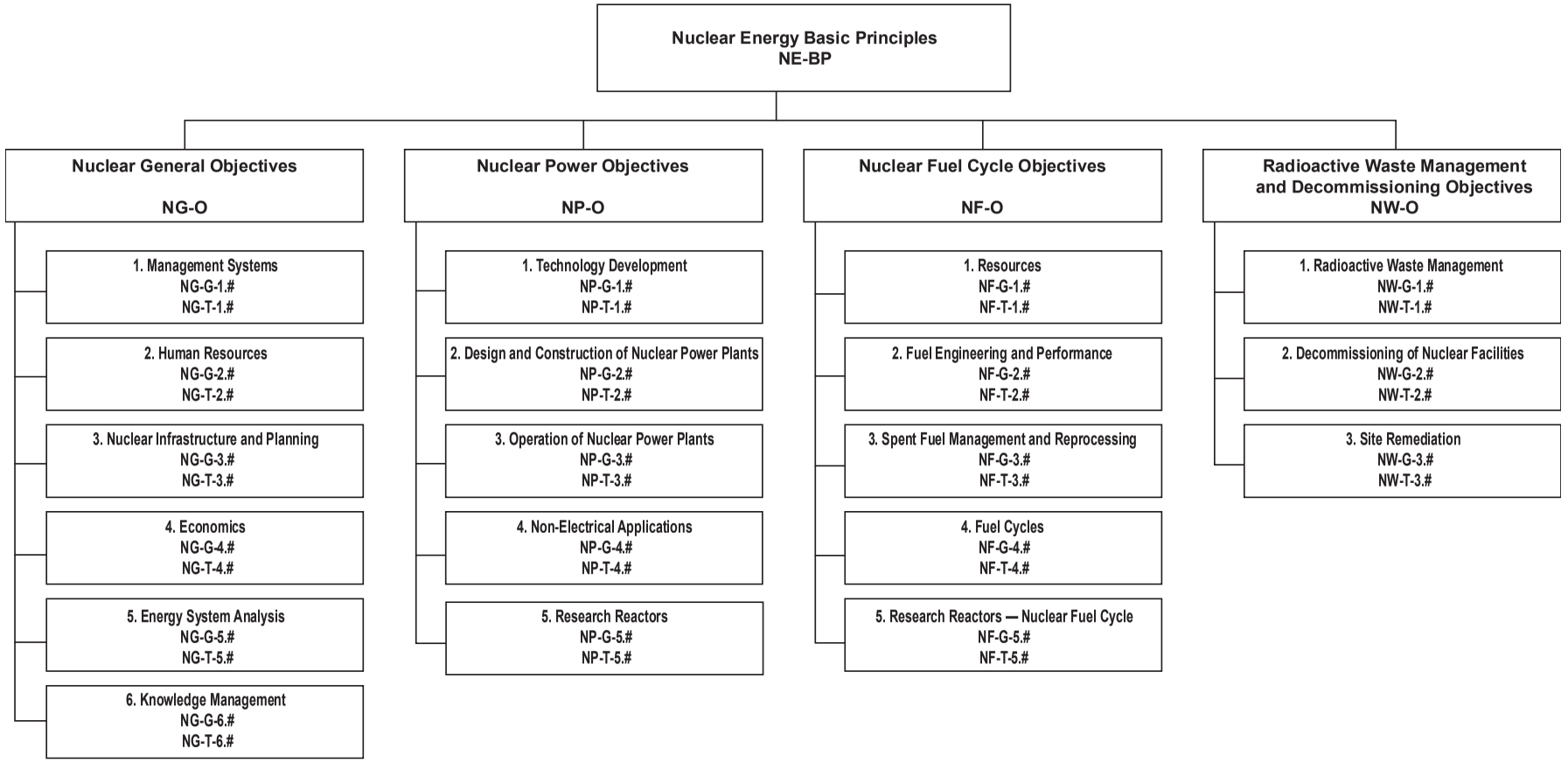

Key

BP: Basic Principles
O: Objectives
G: Guides
T: Technical Reports
Nos. 1-6: Topic designations
#: Guide or Report number (1, 2, 3, 4, etc.)

Examples

NG-G-3.1: Nuclear General (**NG**), **G**uide, Nuclear Infrastructure and Planning (topic **3**), **#1**
NP-T-5.4: Nuclear Power (**NP**), Report (**T**), Research Reactors (topic **5**), **#4**
NF-T-3.6: Nuclear Fuel (**NF**), Report (**T**), Spent Fuel Management and Reprocessing, **#6**
NW-G-1.1: Radioactive Waste Management and Decommissioning (**NW**), **G**uide, Radioactive Waste (topic **1**), **#1**

IAEA
International Atomic Energy Agency

No. 23

ORDERING LOCALLY

In the following countries, IAEA priced publications may be purchased from the sources listed below, or from major local booksellers.

Orders for unpriced publications should be made directly to the IAEA. The contact details are given at the end of this list.

AUSTRALIA
DA Information Services
648 Whitehorse Road, Mitcham, VIC 3132, AUSTRALIA
Telephone: +61 3 9210 7777 • Fax: +61 3 9210 7788
Email: books@dadirect.com.au • Web site: http://www.dadirect.com.au

BELGIUM
Jean de Lannoy
Avenue du Roi 202, 1190 Brussels, BELGIUM
Telephone: +32 2 5384 308 • Fax: +32 2 5380 841
Email: jean.de.lannoy@euronet.be • Web site: http://www.jean-de-lannoy.be

CANADA
Renouf Publishing Co. Ltd.
Telephone: +1 613 745 2665 • Fax: +1 643 745 7660
5369 Canotek Road, Ottawa, ON K1J 9J3, CANADA
Email: order@renoufbooks.com • Web site: http://www.renoufbooks.com

Bernan Associates
4501 Forbes Blvd., Suite 200, Lanham, MD 20706-4391, USA
Telephone: +1 800 865 3457 • Fax: +1 800 865 3450
Email: orders@bernan.com • Web site: http://www.bernan.com

CZECH REPUBLIC
Suweco CZ, spol. S.r.o.
Klecakova 347, 180 21 Prague 9, CZECH REPUBLIC
Telephone: +420 242 459 202 • Fax: +420 242 459 203
Email: nakup@suweco.cz • Web site: http://www.suweco.cz

FINLAND
Akateeminen Kirjakauppa
PO Box 128 (Keskuskatu 1), 00101 Helsinki, FINLAND
Telephone: +358 9 121 41 • Fax: +358 9 121 4450
Email: akatilaus@akateeminen.com • Web site: http://www.akateeminen.com

FRANCE
Form-Edit
5, rue Janssen, PO Box 25, 75921 Paris CEDEX, FRANCE
Telephone: +33 1 42 01 49 49 • Fax: +33 1 42 01 90 90
Email: fabien.boucard@formedit.fr • Web site: http://www.formedit.fr

Lavoisier SAS
14, rue de Provigny, 94236 Cachan CEDEX, FRANCE
Telephone: +33 1 47 40 67 00 • Fax: +33 1 47 40 67 02
Email: livres@lavoisier.fr • Web site: http://www.lavoisier.fr

L'Appel du livre
99, rue de Charonne, 75011 Paris, FRANCE
Telephone: +33 1 43 07 50 80 • Fax: +33 1 43 07 50 80
Email: livres@appeldulivre.fr • Web site: http://www.appeldulivre.fr

GERMANY
Goethe Buchhandlung Teubig GmbH
Schweitzer Fachinformationen
Willstaetterstrasse 15, 40549 Duesseldorf, GERMANY
Telephone: +49 (0) 211 49 8740 • Fax: +49 (0) 211 49
Email: s.dehaan@schweitzer-online.de • Web site: http://www.goethebuch.de/

HUNGARY
Librotade Ltd., Book Import
PF 126, 1656 Budapest, HUNGARY
Telephone: +36 1 257 7777 • Fax: +36 1 257 7472
Email: books@librotade.hu • Web site: http://www.librotade.hu

INDIA
Allied Publishers Pvt. Ltd.
1st Floor, Dubash House, 15, J.N. Heredi Marg
Ballard Estate, Mumbai 400001, INDIA
Telephone: +91 22 42126969/31 • Fax: +91 22 2261 7928
Email: arjunsachdev@alliedpublishers.com • Web site: http://www.alliedpublishers.com

Bookwell
3/79 Nirankari, Dehli 110009, INDIA
Tel.: +91 11 2760 1283 • +91 11 27604536
Email: bkwell@nde.vsnl.net.in • Web site: http://www.bookwellindia.com/

ITALY
Libreria Scientifica "AEIOU"
Via Vincenzo Maria Coronelli 6, 20146 Milan, ITALY
Tel.: +39 02 48 95 45 52 • Fax: +39 02 48 95 45 48
Email: info@libreriaaeiou.eu • Web site: http://www.libreriaaeiou.eu/

JAPAN
Maruzen Co., Ltd.
1-9-18 Kaigan, Minato-ku, Tokyo 105-0022, JAPAN
Tel.: +81 3 6367 6047 • Fax: +81 3 6367 6160
Email: journal@maruzen.co.jp • Web site: http://maruzen.co.jp

NETHERLANDS
Martinus Nijhoff International
Koraalrood 50, Postbus 1853, 2700 CZ Zoetermeer, NETHERLANDS
Tel.: +31 793 684 400 • Fax: +31 793 615 698
Email: info@nijhoff.nl • Web site: http://www.nijhoff.nl

Swets
PO Box 26, 2300 AA Leiden
Dellaertweg 9b, 2316 WZ Leiden, NETHERLANDS
Telephone: +31 88 4679 263 • Fax: +31 88 4679 388
Email: tbeysens@nl.swets.com • Web site: www.swets.com

SLOVENIA
Cankarjeva Zalozba dd
Kopitarjeva 2, 1515 Ljubljana, SLOVENIA
Tel.: +386 1 432 31 44 • Fax: +386 1 230 14 35
Email: import.books@cankarjeva-z.si • Web site: http://www.mladinska.com/cankarjeva_zalozba

SPAIN
Diaz de Santos, S.A.
Librerias Bookshop • Departamento de pedidos
Calle Albasanz 2, esquina Hermanos Garcia Noblejas 21, 28037 Madrid, SPAIN
Telephone: +34 917 43 48 90
Email: compras@diazdesantos.es • Web site: http://www.diazdesantos.es/

UNITED KINGDOM
The Stationery Office Ltd. (TSO)
PO Box 29, Norwich, Norfolk, NR3 1PD, UNITED KINGDOM
Telephone: +44 870 600 5552
Email (orders): books.orders@tso.co.uk • (enquiries): book.enquiries@tso.co.uk • Web site: http://www.tso.co.uk

On-line orders:
DELTA International Ltd.
39, Alexandra Road, Addlestone, Surrey, KT15 2PQ, UNITED KINGDOM
Email: info@profbooks.com • Web site: http://www.profbooks.com

United Nations (UN)
300 East 42nd Street, IN-919J, New York, NY 1001, USA
Telephone: +1 212 963 8302 • Fax: +1 212 963 3489
Email: publications@un.org • Web site: http://www.unp.un.org

UNITED STATES OF AMERICA
Bernan Associates
4501 Forbes Blvd., Suite 200, Lanham, MD 20706-4391, USA
Tel.: +1 800 865 3457 • Fax: +1 800 865 3450
Email: orders@bernan.com • Web site: http://www.bernan.com

Renouf Publishing Co. Ltd.
812 Proctor Avenue, Ogdensburg, NY 13669, USA
Tel.: +800 551 7470 (toll free) • +800 568 8546 (toll free)
Email: orders@renoufbooks.com • Web site: http://www.renoufbooks.com

Orders for both priced and unpriced publications may be addressed directly to:

IAEA Publishing Section, Marketing and Sales Unit, International Atomic Energy Agency
Vienna International Centre, PO Box 100, 1400 Vienna, Austria
Telephone: +43 1 2600 22529 or 22488 • Fax: +43 1 2600 29302
Email: sales.publications@iaea.org • Web site: http://www.iaea.org/books

INTERNATIONAL ATOMIC ENERGY AGENCY
VIENNA
ISBN 978–92–0–136410–4
ISSN 1995–7807